

UNDERSTANDING THE MODE OF ACTION OF COMPOUNDS THAT ARE SUGGESTED TO POSSESS EFFLUX INHIBITORY PROPERTIES

By

ELIZABETH MARY GRIMSEY

A thesis submitted to the University of Birmingham for the degree of
DOCTOR OF PHILOSOPHY

Antimicrobials Research Group
Institute of Microbiology and Infection
College of Medical and Dental Sciences
University of Birmingham
February 2021

UNIVERSITY OF
BIRMINGHAM

University of Birmingham Research Archive

e-theses repository

This unpublished thesis/dissertation is copyright of the author and/or third parties. The intellectual property rights of the author or third parties in respect of this work are as defined by The Copyright Designs and Patents Act 1988 or as modified by any successor legislation.

Any use made of information contained in this thesis/dissertation must be in accordance with that legislation and must be properly acknowledged. Further distribution or reproduction in any format is prohibited without the permission of the copyright holder.

Abstract

In Gram-negative bacteria, efflux is an important mechanism conferring multidrug resistance and the inhibition of efflux is one strategy to restore the antibacterial activity of antibiotics. Chlorpromazine and amitriptyline have been shown to behave as efflux inhibitors. However, their mode of action was poorly understood. Here, these compounds potentiated the activities and increased the intracellular concentrations of AcrB substrates against *S. Typhimurium* and *E. coli*. This inhibitory activity of chlorpromazine and amitriptyline was a result of their activity as competitive inhibitors of AcrB. Both compounds bound AcrB within the distal binding pocket and clashed with the binding of the AcrB substrates ethidium bromide and norfloxacin.

Further investigation into the mechanism of chlorpromazine resistance revealed that exposure to this drug resulted in the mutation of *ramR* and *marR*. These conferred chlorpromazine resistance though the increased expression of *ramA* and *marA* by *S. Typhimurium* and *E. coli*, respectively, and a resulting increase in *acrB* expression and the efflux of AcrB substrates from these strains. In *S. Typhimurium* this was as a result of an inability of the mutant RamR protein to bind the promoter of *ramA*. The mutations were proposed to reflect the role of chlorpromazine as an AcrB substrate, whereby mutation of *marR* and *ramR* occurred to increase the efflux of chlorpromazine. Further experiments with *S. Typhimurium* further supported that chlorpromazine and amitriptyline are AcrB substrates; exposure to chlorpromazine resulted in the upregulation of *acrB* and its regulatory genes and chlorpromazine and amitriptyline exposure resulted in the reversion of a strain of *S. Typhimurium* containing AcrB D408A (a non-functional efflux pump) from the mutant *acrB* allele to the wild type.

This research has revealed that chlorpromazine and amitriptyline exert their efflux inhibitory activity against *S. Typhimurium* and *E. coli* as competitive substrates of AcrB.

This thesis is dedicated to the memory

of

Stewart Angus Lough

(1984-2019)

Who is forever in the hearts of those who knew and loved him

Acknowledgments

Firstly, I would like to say a massive thank you to my supervisor Laura Piddock for your constant support over the last four years. I would also like to say thank you to all current and past members of the ARG laboratory for making my PhD experience so enjoyable. In particular, I would like to thank Vito Ricci for helping me with all my inane questions and helping me with all my ridiculous mistakes. Even if it was accompanied by too many jokes at my expense. Quite simply I would not have managed even half of my PhD without you. I would also like to thank Chiara Fais and Dr Atillio Vargiu and the rest of the team at the University of Cagliari for providing the molecular dynamics simulations that were vital for the conclusions drawn throughout this thesis. I would also like to thank Professor John Marriott for providing information regarding the pharmacology of phenothiazines.

Thank you to Chris, Xuan, Hannah, Sarah, Jamie and everyone else in T102 for always being around to cheer me up and provide coffee and cake on long lab days or when I have tantrums over my EMSA assays. I would also like to say the biggest of thanks to Michelle Buckner for being an unwavering support in times of crisis. If I listed all the ways in which you have helped me this would be several pages long.

I would like to say a thank you to my parents for constantly supporting me, in whatever way I need, and always being just a phone call or a drive away. Will, I'm sure you did something and I acknowledge that.

Duncan and Jack! I would say thanks for keeping me sane but I'm not sure that is strictly accurate. Regardless, I am so thankful for having you both around to prevent me from completely losing my mind. Frankie... I'm not sure what to say... there is too much. Thank you for everything. But specifically, thanks for keeping me fed and watered.

Contents

	Page
1 Introduction	1
1.1 Antibiotic resistance	1
1.1.1 Intrinsic and adaptive resistance	2
1.1.2 Antibiotic resistance evolution	2
1.1.3 Appearance of mutations	3
1.1.4 Mutation supply	3
1.1.5 Mutation rate and frequency in the context of antibiotic resistance . .	5
1.1.6 Selection of antibiotic-resistant bacteria	9
1.1.7 Mutations can incur fitness costs	11
1.1.8 Mutation reversion	11
1.2 Mechanisms of antibiotic resistance	13
1.2.1 Reduced intracellular accumulation of an antibiotic	13
1.3 The outer membrane	13
1.4 The role of efflux pumps in MDR	16
1.4.1 The resistance nodulation division family	17
1.4.2 The AcrAB-TolC efflux system	18
1.4.3 AcrB	18
1.4.4 AcrA	22
1.4.5 TolC	23
1.4.6 Assembly of the AcrAB-TolC complex	23
1.4.7 Mechanism of substrate extrusion by AcrAB-TolC	24
1.5 Local regulation of expression of <i>acrAB</i> expression	26
1.6 Global regulation of <i>acrAB</i> expression	26

1.6.1	Mar	26
1.6.2	MarR	28
1.6.3	Ram	30
1.6.4	RamR	30
1.6.5	Sox and Rob	32
1.7	Inhibition of efflux pumps	32
1.7.1	Deciphering the mode of action of efflux pump inhibitors	34
1.7.2	What is known about competitive efflux inhibitors?	35
1.7.3	Phenothiazines	41
1.7.4	Antibacterial activity of phenothiazines	42
1.7.5	Proposed mechanisms of the antibacterial activity of phenothiazines	44
1.7.6	Effects on Bacterial Cellular Replication	44
1.7.7	Membrane Damaging Effects	44
1.7.8	Effects on Energy Generation	45
1.7.9	Use of phenothiazines as antibiotic adjuvants	46
1.7.10	Chlorpromazine as an Efflux Inhibitor	47
1.7.11	The efflux inhibitory activity of other phenothiazines	48
1.7.12	Non-selectivity of chlorpromazine as an efflux inhibitor	49
1.7.13	Clinical usefulness of phenothiazines	49
1.7.14	Efflux inhibitory activity of amitripytline	50
2	Materials and Methods	52
2.1	Bacterial strains, growth and identification	52
2.2	Molecular biology techniques	56
2.2.1	Polymerase chain reaction (PCR)	56
2.2.2	DNA sequencing of PCR amplimers	61
2.2.3	Isolation of plasmids	62

2.2.4	Preparation of electrocompetant cells	62
2.2.5	Electroporation	63
2.3	Susceptibility of strains to AcrB substrates in the presence and absence of efflux inhibitors	64
2.3.1	Determination of the minimal inhibitory activity (MIC) of antimicrobials on agar	64
2.3.2	Chequerboard assay to determine potentiation of antibiotic activity .	66
2.3.3	Disk diffusion assay	67
2.3.4	Well diffusion assay	68
2.4	Characterisation of the efflux inhibitory profiles of inhibitors	68
2.4.1	Hoechst 33342 accumulation assay	68
2.4.2	Ethidium bromide accumulation assay	70
2.4.3	Norfloxacin accumulation assay	71
2.5	Determination of damage to the outer membrane	72
2.5.1	ATP luciferin-luciferase membrane permeability assay	72
2.5.2	DisC3(5) membrane depolarisation assay	74
2.6	Selection of antimicrobial or putative efflux inhibitor-resistant mutants and identification of mutations conferring resistance	75
2.6.1	Mutant selection experiments	75
2.6.2	Isolation of DNA for whole genome sequencing	76
2.6.3	Whole genome sequencing and data analysis	77
2.6.4	Confirmation of mutations identified by WGS	78
2.7	Homology modelling of SL1344 AcrB and SL1344 RamR and MG1655 MarR mutant proteins	78
2.8	Characterisation of <i>ramR</i> and <i>marR</i> mutants	80
2.8.1	Growth kinetics	80

2.8.2	Fluorescence reporting assays measuring the expression of <i>ramA</i> , <i>marA</i> and <i>acrAB</i>	80
2.9	Construction of <i>E. coli</i> MG1655 <i>marR::aph</i>	81
2.10	Construction of mutant and wild type RamR and MarR on pTrc-His	82
2.10.1	Design of primers for TA cloning	84
2.10.2	Producing PCR products for TA cloning	84
2.10.3	TA cloning reaction and transformation	85
2.11	Purification of mutant and wild type RamR	86
2.11.1	Pilot expression	86
2.11.2	SDS-PAGE	86
2.11.3	Staining of SDS PAGE	87
2.11.4	Full scale expression	87
2.11.5	Purification by Ni-NTA chromatography	88
2.11.6	Protein concentration quantification	89
2.11.7	Western blot	89
2.12	Determination of protein DNA binding	90
2.13	Transcriptomic analysis	92
2.13.1	RNA sequencing	92
2.13.2	Bioinformatic analysis	92
2.14	RT-PCR to determine <i>acrB</i> expression post exposure to chlorpromazine	93
2.15	Allele specific quantitative PCR	94
2.16	Statistical analysis	95
3	Are antipsychotics efflux inhibitors?	97
3.1	Hypothesis	98
3.2	Aims and objectives	98
3.3	Synergy/potential of antibiotic activity by chlorpromazine and amitriptyline	99

3.3.1	The use of strains overexpressing efflux pumps in synergy assays . . .	99
3.3.2	Chequerboard assays to determine potentiation of the activity of AcrB substrates by chlorpromazine and amitriptyline	100
3.3.3	Disk diffusion assays to determine whether chlorpromazine and amitriptyline potentiated the activity of AcrB substrates	105
3.3.4	Well diffusion assays to determine potentiation of the activity of norfloxacin and ethidium bromide by chlorpromazine and amitriptyline	105
3.4	The impact of chlorpromazine and amitriptyline on the accumulation of AcrB substrates	107
3.4.1	Chlorpromazine and amitriptyline increase the accumulation of ethidium bromide	109
3.4.2	Chlorpromazine and amitriptyline increase the accumulation of Hoechst H33342	111
3.4.3	Chlorpromazine and amitriptyline inhibit the efflux of norfloxacin only in strains overexpressing AcrAB-TolC	111
3.5	<i>In silico</i> experiments to elicit the interaction, if any, of chlorpromazine and amitriptyline with AcrB	114
3.5.1	Chlorpromazine and amitriptyline bind to a well-characterised substrate/inhibitor binding region of AcrB	114
3.5.2	Molecular dynamics simulations confirm the binding of chlorpromazine and amitriptyline to the hydrophobic trap	115
3.6	Is the observed synergistic phenotype due to membrane damage by chlorpromazine?	117
3.6.1	ATP leakage from Gram-negative bacteria following exposure to chlorpromazine	117
3.6.2	Ability of chlorpromazine and amitriptyline to depolarise the inner membrane	121

3.7	Discussion	124
3.8	Key finding	134
4	Resistance to efflux inhibitors can evolve and description of mutants selected in the laboratory	135
4.1	Background	135
4.2	Hypothesis	136
4.3	Aims and Objectives	136
4.4	Post exposure of <i>Salmonella</i> to chlorpromazine with ciprofloxacin gives rise to fluoroquinolone-resistant colonies only	136
4.5	Exposure to inhibitor alone selects for colonies of <i>S. Typhimurium</i> SL1344 and <i>E. coli</i> MG1655 that are able withstand chlorpromazine	140
4.5.1	Resistance to chlorpromazine is conferred by mutations within genes that regulate expression of <i>acrAB</i> and <i>tolC</i>	141
4.6	Mutants resistant to the efflux inhibitor Pa β N can be selected	150
4.6.1	Susceptibility of single <i>barA</i> , <i>recN</i> and <i>bamE</i> <i>E. coli</i> Keio Collection knockouts	156
4.7	Discussion	160
4.8	Key findings	171
5	Phenotypic characterisation of chlorpromazine-selected <i>E. coli</i> MG1655 <i>marR</i> and <i>S. Typhimurium ramR</i> mutants	173
5.1	Background	173
5.2	Hypothesis	173
5.3	Aims	174
5.4	Phenotype of <i>S. Typhimurium</i> SL1344 and <i>E. coli</i> MG1655 and their respective chlorpromazine resistant mutants	174
5.5	Growth kinetics	174

5.6	Antimicrobial susceptibility	176
5.7	Construction of <i>E. coli</i> MG1655 <i>marR::aph</i>	176
5.8	Effect of mutations within <i>ramR</i> and <i>marR</i> on the expression of <i>acrAB</i> and its regulatory genes	179
5.8.1	Transformation of promoter-GFP constructs into the <i>S. Typhimurium</i> and <i>E. coli</i> mutants.	179
5.8.2	The substitution L158P in RamR of <i>S. Typhimurium</i> increased the basal expression of <i>ramA</i> and <i>acrAB</i>	181
5.8.3	Deletions within MarR of <i>E. coli</i> MG1655 increase the basal expression of <i>marA</i> and <i>acrAB</i>	183
5.8.4	Exposure of <i>S. Typhimurium</i> to chlorpromazine increases the expression of <i>acrB</i>	183
5.9	Impact of mutations within <i>ramR</i> and <i>marR</i> on the intracellular accumulation of AcrB substrates	186
5.9.1	A substitution within RamR results in a decrease in the intracellular accumulation of Hoechst H33342	186
5.9.2	Deletions within MarR result in a decrease in the intracellular accumulation of Hoechst H33342	189
5.9.3	Mutations within <i>ramR</i> but not <i>marR</i> result in a decrease in the intracellular accumulation of ethidium bromide from <i>S. Typhimurium</i> and <i>E. coli</i>	192
5.10	Do mutations within <i>ramR</i> and <i>marR</i> impact on the ability of chlorpromazine to damage the outer and inner membrane of <i>S. Typhimurium</i> SL1344 and <i>E. coli</i> MG1655?	195
5.10.1	The presence of mutations within <i>ramR</i> and <i>marR</i> impair the ability of chlorpromazine to permeabilise the outer membrane of <i>S. Typhimurium</i> SL1344 and <i>E. coli</i> MG1655	195

5.10.2	The presence of mutations within <i>ramR</i> and <i>marR</i> impair the ability of chlorpromazine to depolarise the inner membrane of <i>S. Typhimurium</i> SL1344 and <i>E. coli</i> MG1655	198
5.11	Construction of vectors for overexpression of RamR and MarR	202
5.12	Purification of wild type SL1344 RamR and SL1344 RamR L158P	207
5.12.1	Determination of optimal expression conditions	207
5.12.2	Purification of RamR wild type and RamR L158P by nickel affinity chromatography	207
5.13	Binding to the <i>ramA</i> promoter is ablated in the RamR L158P-6xHis mutant	210
5.14	Discussion	215
5.15	Key findings	222
6	Chlorpromazine and amitriptyline may elicit their activity through interactions with AcrB	224
6.1	Background	224
6.2	Hypothesis	225
6.3	Aims	225
6.4	Impact of chlorpromazine on the transcriptomic profile of <i>S. Typhimurium</i> SL1344	226
6.5	Impact of Pa β N on the transcriptomic profile of <i>S. Typhimurium</i> SL1344 . .	232
6.6	Comparison of the transcriptome of <i>S. Typhimurium</i> SL1344 post exposure to chlorpromazine and Pa β N	237
6.7	Comparison of the transcriptome of <i>S. Typhimurium</i> SL1344 post exposure to chlorpromazine and Pa β N against <i>S. Typhimurium</i> SL1344 AcrB D408A. .	237
6.8	Selection of chlorpromazine-resistant mutants for strains lacking a functional AcrB protein	241

6.8.1	Chlorpromazine-resistant <i>S. Typhimurium</i> SL1344 AcrB D408A mutants were selected	241
6.8.2	The mutated gene conferring AcrB D408A in <i>S. Typhimurium</i> consistently reverts to the wild type allele upon exposure to chlorpromazine and amitriptyline	244
6.8.3	Exposure to chlorpromazine does not result in reversion of <i>E. coli</i> MG1655 D408A to the wild type sequence	247
6.9	Discussion	251
6.10	Key findings	268
7	Overall discussion and conclusions	269
	Publications resulting from this study	281
	Conference presentations resulting from this study	282
	Appendices	284
	Appendix Figures	290
	References	294

List of Figures

1.1	Plot showing the mutational events that can cause drug-resistance in relation to fitness, level of resistance conferred, selective pressure and rate of appearance of drug resistance.	4
1.2	Classical mutant accumulation experiment.	7
1.3	Schematic overview of a fluctuation analysis experiment.	8
1.4	Methods and their equations used to calculate mutation rate.	10
1.5	Representation of the selective windows for antibiotic-resistant bacteria. . . .	12
1.6	Cell envelope of Gram-negative bacteria.	15
1.7	The structure of AcrB in ribbon representation.	20
1.8	Scheme showing the proposed transport mechanism of substrates through AcrB.	25
1.9	Schematic representation of the known regulatory pathways for expression of AcrAB-TolC efflux pump in <i>S. Typhimurium</i>	27
1.10	The structure of <i>E. coli</i> MarR in ribbon format	29
1.11	Crystal structure of <i>S. Typhimurium</i> RamR in ribbon representation.	31
1.12	Structures of the efflux inhibitors Pa β N, NMP, D13-9001 and MBX-3132. . . .	36
1.13	Chemical structure of the core unit of phenothiazines.	42
1.14	Chemical structures of the phenothiazines that possess antimicrobial activities.	43
1.15	Structure of amitriptyline	51
2.1	pTrcHis vector map.	83
3.1	Comparisons of the zone of inhibition obtained for disks containing chloramphenicol, ciprofloxacin, amitriptyline, tetracycline and nalidixic acid, when used in combination with chlorpromazine, amitriptyline and the positive control Pa β N.	106

3.2	Comparisons of the zone of inhibition obtained for well diffusion assay with ethidium bromide and norfloxacin when used in combination with chlorpromazine and amitriptyline.	108
3.3	Accumulation of ethidium bromide in the presence of chlorpromazine or amitriptyline.	110
3.4	Accumulation of Hoechst H33342 in the presence of chlorpromazine or amitriptyline.	112
3.5	Accumulation of norfloxacin in the presence of chlorpromazine or amitriptyline.	113
3.6	Representative conformations obtained from molecular dynamics simulations showing the most stable binding poses of chlorpromazine and amitriptyline within the DP of AcrB _{EC} and AcrB _{ST}	116
3.7	An example of a standard curve showing luminescence in relation to the concentration of ATP for one biological replicate.	119
3.8	ATP leakage from <i>E. coli</i> MG1655 and <i>S. Typhimurium</i> SL1344 upon exposure to increasing concentrations of chlorpromazine.	120
3.9	Effect of chlorpromazine on the membrane potential sensitive fluorescent dye DiSC ₃₅ in <i>S. Typhimurium</i> SL1344.	122
3.10	Effect of chlorpromazine on the membrane potential sensitive fluorescent dye DiSC ₃₅ in <i>E. coli</i>	123
4.1	Artemis 18.0.2 analysis of the mutant <i>S. Typhimurium</i> SL1344 sequence and subsequent translation of the sequenced DNA to confirm the presence of the GyrA (S83F) substitution	139
4.2	Artemis 18.0.2 analysis of the mutant <i>S. Typhimurium</i> SL1344 sequence and subsequent translation of the sequenced DNA to confirm the presence of the RamR L158P substitution	143

4.3	Homology model of SL1344 RamR L158P.	144
4.4	Artemis 18.0.2 analysis of the mutant <i>E. coli</i> MG1655 sequence and subsequent translation of the sequenced DNA to confirm the presence of the MarR K141Sfs*150 frameshift	146
4.5	Artemis 18.0.2 analysis of the mutant <i>E. coli</i> MG1655 sequence and subsequent translation of the sequenced DNA to confirm the presence of the MarR A105Rfs*114 frameshift	147
4.6	Homology model of MG1655 MarR K141Sfs*150.	148
4.7	Homology model of MG1655 MarR A105Rfs*114.	149
4.8	Artemis 18.0.2 analysis of the resistant mutant <i>S. Typhimurium</i> SL1344 sequence and subsequent translation of the sequenced DNA to confirm the presence of the GyrA (S83F) substitution	153
4.9	Artemis 18.0.2 analysis of the resistant mutant <i>S. Typhimurium</i> SL1344 sequence and subsequent translation of the sequenced DNA to confirm the presence of the BarA R9Afs*10 frameshift	154
4.10	Artemis analysis of the resistant mutant <i>S. Typhimurium</i> SL1344 sequence and subsequent translation of the sequenced DNA to confirm the presence of the RecN R78H substitution	155
4.11	Artemis 18.0.2 analysis of the mutant <i>S. Typhimurium</i> SL1344 sequence and subsequent translation of the sequenced DNA to confirm the presence of the BamE W73STOP substitution	158
4.12	Artemis 18.0.2 analysis of the mutant <i>S. Typhimurium</i> SL1344 sequence and subsequent translation of the sequenced DNA to confirm the presence of the BamE V26Gfs*50 frameshift	159
5.1	Growth curves and generation times of (A) <i>S. Typhimurium</i> SL1344, (B) <i>E. coli</i> MG1655 and their respective chlorpromazine-resistant mutants.	175

5.2	Comparison of the zones of inhibition obtained against <i>S. Typhimurium</i> SL1344, <i>E. coli</i> MG1655 and their respective chlorpromazine-resistant mutants using antibiotic-containing disks.	177
5.3	PCR amplification of <i>marR::aph</i> from <i>E. coli marR::aph</i> BW25113.	178
5.4	PCR amplification of <i>marR</i> from <i>E. coli</i> MG1655 and the three <i>marR::aph</i> mutant candidates	180
5.5	Effect of the RamR L158P substitution on (A) <i>ramA</i> and (B) <i>acrAB</i> expression compared to wild type <i>S. Typhimurium</i> SL1344 and SL1344 <i>ramR::aph</i> in the presence and absence of 25 µg/ml of chlorpromazine. . . .	182
5.6	Effect of deletions within MarR on (A) <i>marA</i> and (B) <i>acrAB</i> expression compared to wild type <i>E. coli</i> MG1655 and MG1655 <i>marR::aph</i> in the presence and absence of 25 µg/ml of chlorpromazine.	184
5.7	Fold change in normalised <i>acrB</i> expression in SL1344 +/- chlorpromazine at 50, 100 and 200 µg/mL.	185
5.8	Accumulation of Hoechst H33342 within <i>S. Typhimurium</i> SL1344 RamR WT, RamR L158P and <i>ramR::aph</i> in the presence and absence of chlorpromazine, relative to unexposed wild type SL1344.	187
5.9	Accumulation of Hoechst H33342 within <i>S. Typhimurium</i> SL1344 RamR WT, RamR L158P and <i>ramR::aph</i> in the presence and absence of chlorpromazine, relative to the unexposed wild type of each respective strain.	188
5.10	Accumulation of Hoechst H33342 within <i>E. coli</i> MG1655 MarR and the mutants MarR K141Sfs*150, MarR A105Rfs*114 and <i>marR::aph</i> in the presence and absence of chlorpromazine, relative to unexposed wild type MG1655.	190

5.11 Accumulation of Hoechst H33342 within <i>E. coli</i> MG1655 MarR and the mutants MarR K141Sfs*150, MarR A105Rfs*114 and <i>marR::aph</i> in the presence and absence of chlorpromazine, relative to the unexposed wild type of each respective strain.	191
5.12 Accumulation of ethidium bromide within <i>S. Typhimurium</i> SL1344 RamR WT, RamR L158P and <i>ramR::aph</i> in the presence and absence of chlorpromazine.	193
5.13 Accumulation of ethidium bromide within <i>E. coli</i> MG1655 MarR and the mutants MarR K141Sfs*150, MarR A105Rfs*114 and <i>marR::aph</i> in the presence and absence of chlorpromazine	194
5.14 ATP leakage from <i>S. Typhimurium</i> SL1344 wild type and RamR L158P upon exposure to increasing concentrations of chlorpromazine.	196
5.15 ATP leakage from <i>E. coli</i> MG1655, MarR K141Sfs*150 and MarR A105Rfs*114 upon exposure to increasing concentrations of chlorpromazine.	197
5.16 Effect of chlorpromazine on the membrane potential sensitive fluorescent dye DiSC ₃ 5 in <i>S. Typhimurium</i> SL1344 wild type and RamR L158P.	199
5.17 Effect of chlorpromazine on the membrane potential sensitive fluorescent dye DiSC ₃ 5 in <i>E. coli</i> MG1655, MarR K141Sfs*150 and MarR A105Rfs*114	200
5.18 Effect of chlorpromazine on the membrane potential sensitive fluorescent dye DiSC ₃ 5 in <i>S. Typhimurium</i> SL1344 and <i>E. coli</i> MG1655 and their respective chlorpromazine resistant mutants.	201
5.19 Amplification of <i>ramR</i> (wild type and mutant) and <i>marR</i> (wild type and mutant) for cloning into pTrcHis.	203
5.20 Amplification of <i>ramR</i> WT and <i>ramR</i> L158P from the recombinant pTrc vector backbone.	204
5.21 Amplification of <i>marR</i> WT, <i>marR</i> A105Rfs*114 and <i>marR</i> K141Sfs*150 from recombinant pTrc vector backbone.	205

5.22	DNA sequencing to confirm correct cloning of wild type and mutant and <i>marR</i> and <i>ramR</i> into pTrcHis.	206
5.23	Coomassie staining of an SDS-PAGE gel containing pTrc RamR WT-6xHis and pTrc RamR L158P-6xHis samples post induction with 10 μ M IPTG at varying time points.	208
5.24	Coomassie staining of an SDS-PAGE gel containing pTrc RamR WT-6xHis or pTrc RamR L158P-6xHis purified by nickel affinity chromatography.	209
5.25	Western blot using anti-His antibodies of an SDS-PAGE gel containing pTrc RamR WT-6xHis or pTrc RamR L158P-6xHis purified by nickel affinity chromatography.	211
5.26	Amplification of <i>ramR-ramA</i> intergenic region from wild type <i>S. Typhimurium</i> SL1344.	212
5.27	Electrophoretic mobility shift assay showing the interaction of RamR WT-6xHis and RamR L158P-6xHis with the <i>ramR-ramA</i> intergenic region including <i>pramA</i>	213
5.28	Electrophoretic mobility shift assay, post gel extraction, showing the interaction of RamR WT-6xHis and RamR L158P-6xHis with the <i>ramR-ramA</i> intergenic region including <i>pramA</i>	214
6.1	Percentage of <i>S. Typhimurium</i> SL1344 genes that were significantly changed upon exposure to chlorpromazine compared to unexposed SL1344 and classification of the significantly changed genes into COG categories.	227
6.2	Transcriptional landscape of <i>S. Typhimurium</i> SL1344 post 60 minute exposure to 50 μ g/ml of chlorpromazine.	228
6.3	Percentage genes within each COG class that were significantly altered upon exposure to chlorpromazine.	231

6.4	Percentage of <i>S. Typhimurium</i> SL1344 genes that were significantly changed upon exposure to PaβN compared to unexposed SL1344 and classification of significantly changed genes into COG categories.	233
6.5	Transcriptional landscape of <i>S. Typhimurium</i> SL1344 post 60 minute exposure to 100 µg/ml of PaβN.	234
6.6	Percentage of genes within each COG class that were significantly altered upon exposure to PaβN.	236
6.7	Comparison of the Log2FC values between <i>S. Typhimurium</i> SL1344 exposed to chlorpromazine or PaβN for each significantly transcribed gene.	238
6.8	Comparison of the percentage of genes within each COG class for chlorpromazine and PaβN.	239
6.9	Comparison of the Log2FC values of SL1344 exposed to (A) chlorpromazine or (B) PaβN for each significantly transcribed gene against SL1344 AcrB D408A.240	
6.10	Artemis analysis of the whole genome sequence of mutant <i>S. Typhimurium</i> SL1344 AcrB D408A and the translation of the subsequent DNA sequencing to confirm the absence of the AcrB (D408A) mutation	243
6.11	Artemis analysis of the WGS of mutant <i>E. coli</i> MG1655 AcrB D408A and subsequent translation of the DNA sequencing to confirm the presence of the AcrB (D408A) mutation.	249
6.12	Artemis analysis of the WGS of mutant <i>E. coli</i> MG1655 AcrB D408A and subsequent translation of the DNA sequencing to confirm the presence of the PitB (A38V) substitution.	250
A3.1	Top docking poses of chlorpromazine, amitriptyline, norfloxacin and ethidium bromide with AcrB _{EC} (A) and AcrB _{ST} (B).	290

A3.2 Docking poses of chlorpromazine (CPZ) against norfloxacin (NOR) (A) and ethidium bromide (EtBr) (B) at the CH3 entry gate of AcrB _{EC} and AcrB _{ST} (monomers L and T).	291
Transcriptional landscape of <i>S. Typhimurium</i> SL1344 AcrB D408A relative to wild type <i>S. Typhimurium</i> SL1344	292
Percentage of significantly altered genes of <i>S. Typhimurium</i> SL1344 AcrB D408A within each COG class	293

List of Tables

2.1 Bacterial strains used throughout this project.	54
2.2 Primers used throughout this project.	57
2.3 Generic PCR cycling conditions when using the MyTaq TM Red master mix .	61
2.4 Plasmids used in this study.	62
2.5 Antibiotics used throughout this study	65
2.6 Conditions used to select for efflux inhibitor resistance	77
2.7 RT-PCR cycling conditions for the amplification of <i>acrB</i>	93
2.8 Quantitative PCR cycling conditions for amplifying the D408A allele	94
3.1 MIC of chlorpromazine and amitriptyline against a variety of Gram-negative organisms.	100
3.2 MIC of compounds alone, and with amitriptyline, against <i>S. Typhimurium</i> SL1344 <i>ramR::aph</i> , <i>E. coli</i> BW25113 <i>marR::aph</i> , <i>A. baumannii</i> AB211 and <i>P. aeruginosa</i> K1454.	102
3.3 MIC of compounds alone and with CPZ against <i>S. Typhimurium</i> SL1344 <i>ramR::aph</i> , <i>E. coli</i> BW25113 <i>marR::aph</i> , <i>A. baumannii</i> AB211 and <i>P. aeruginosa</i> K1454.	102
3.4 MIC of compounds alone, and with Pa β N, against <i>S. Typhimurium</i> SL1344 <i>ramR::aph</i> , <i>E. coli</i> BW25113 <i>marR::aph</i> , <i>A. baumannii</i> AB211 and <i>P. aeruginosa</i> K1454.	103
4.1 Frequency and rate of mutation upon exposure to <i>S. Typhimurium</i> and <i>E. coli</i> MG1655 to efflux inhibitors in the presence and absence of ciprofloxacin.	137
4.2 Susceptibility of <i>S. Typhimurium</i> mutants selected with chlorpromazine in combination with ciprofloxacin.	138

4.3	Mutations identified in the <i>S. Typhimurium</i> SL1344 mutant selected upon exposure to chlorpromazine (50 µg/ml) and ciprofloxacin (0.03 µg/ml). . . .	138
4.4	Susceptibility of chlorpromazine-resistant <i>S. Typhimurium</i> SL1344 and <i>E. coli</i> MG1655 mutants.	141
4.5	Mutations and subsequent substitutions conferring chlorpromazine resistance identified by whole genome sequencing of a representative mutant from each MIC phenotype group.	142
4.6	Susceptibility of <i>S. Typhimurium</i> mutants selected with PaβN in the presence and absence of ciprofloxacin.	151
4.7	Mutations and substitutions identified in the <i>S. Typhimurium</i> SL1344 mutant selected upon exposure to PaβN and ciprofloxacin.	152
4.8	Mutations identified in the <i>S. Typhimurium</i> SL1344 mutants selected upon exposure to PaβN.	157
6.1	COG classes	230
6.2	Minimal inhibitory profiles (MIC) of chlorpromazine-resistant <i>S. Typhimurium</i> SL1344 AcrB D408A.	242
6.3	Frequency and rate of mutation and reversion rate of the D408A mutation when <i>S. Typhimurium</i> AcrB (D408A) was exposed to chlorpromazine, amitriptyline, minocycline, spectinomycin and ethidium bromide.	245
6.4	Minimal inhibitory profiles (MIC) of chlorpromazine-resistant <i>E. coli</i> MG1655 AcrB D408A.	248
A3.1	FIC of compounds +/- amitriptyline against <i>S. Typhimurium</i> SL1344 <i>ramR::aph</i> , <i>E. coli</i> BW25113 <i>marR::aph</i> , <i>A. baumannii</i> AB211 and <i>P. aeruginosa</i> K1454.	285

A3.2 FIC of compounds +/- chlorpromazine against <i>S. Typhimurium</i> SL1344 <i>ramR::aph</i> , <i>E. coli</i> BW25113 <i>marR::aph</i> , <i>A. baumannii</i> AB211 and <i>P.</i> <i>aeruginosa</i> K1454.	286
A3.3 FIC of compounds +/- PaβN against <i>S. Typhimurium</i> SL1344 <i>ramR::aph</i> , <i>E.</i> <i>coli</i> BW25113 <i>marR::aph</i> , <i>A. baumannii</i> AB211 and <i>P. aeruginosa</i> K1454. . .	287
A3.4 (Pseudo) binding free energies evaluated through the scoring function of AutoDock VINA for the top ranked poses of both amitriptyline and chlorpromazine on AcrB _{EC} and AcrB _{ST}	287
A3.5 The residues of AcrB that interact with chlorpromazine and amitriptyline at their polar tail	288
A3.6 Binding free energies (ΔG – Kcal/ml) of chlorpromazine (CPZ), amitriptyline (AMI), norfloxacin (NOR) and ethidium bromide (EtBr) to AcrB _{EC} and AcrB _{ST}	289

Abbreviations

ABC; ATP binding cassette

Acr; Acriflavin

AcrB_{EC}; AcrB_{*E. coli*}

AcrB_{ST}; AcrB_{*S. Typhimurium*}

AMI; Amitriptyline

AMP; Ampicillin

AMR; Antimicrobial resistance

ANOVA; Analysis of variance

aph; Aminoglycoside aminotransferase

ATP; Adenosine triphosphate

bp; Base pair

BGI; Beijing Genomics Institute

BSAC; British Society of Antimicrobial Chemotherapy

CCCP; Carbonyl cyanide 3-chlorophenylhydrazone

CFU; Colony forming units

CHL; Chloramphenicol

CIP; Ciprofloxacin

COG; Cluster of orthologous genes

CPZ; Chlorpromazine

DISC3(5); 3,3'-Dipropylthiadicarbocyanine iodide

DMSO; Dimethyl sulfoxide

DP; Distal pocket

DPBS; Dulbecco's phosphate buffered saline

dsDNA; Double stranded DNA

DTT; 1,4-Dithiothreitol
 EDTA; Ethylenediaminetetraacetic acid
 EMSA; Electrophoretic mobility shift assay
 EtBr; Ethidium bromide
 EUCAST; European Committee of Antimicrobial Susceptibility Testing
 FIC; Fractional inhibitory concentration
 GFP; Green fluorescent protein
 HEPES; N-(2-Hydroxyethyl)piperazine-N'-(2-ethanesulfonic acid)
 HGR; Hygromycin
 Hoescht 33342; H33342
 HRP; Horseradish peroxidase
 HT; Hydrophobic trap
 HTH; Helix turn helix
 INDELS; Insertions and deletions
 IM; Inner membrane
 IPTG; Isopropyl β -D-1-thiogalactopyranoside
 KAN; Kanamycin
 Kb; Kilobase
 LB; Lysogeny medium
 LPS; Lipopolysaccharide
m; Number of mutations per culture
mar; Multiple antibiotic resistance
 MATE; Multidrug and toxic extrusion
 MDR; Multidrug resistant
 MFS; Major facilitator superfamily
 MIC; Minimal inhibitory concentration
 MIN; Minocycline
 MSS maximum likelihood; Ma Sandri Sarkar maximum likelihood

MOPS; 3-(N-Morpholino)propanesulfonic acid
 NAL; Nalidixic acid
 NI-NTA; Nickel nitrilotriacetic acid
 NMP; N-methyl-2-pyrrolidone
 NOR; Norfloxacin
Nt; Viable count
 OD_{xx}; Optical density at X nm
 OM; Outer membrane
 OMP; Outer membrane protein
 PaβN; Phe-arg-beta naphthylamide
 PACE; Proteobacterial antimicrobial compound efflux
 PAGE; Polyacrylamide gel electrophoresis
 PBS; Phosphate buffered saline
 PCR; Polymerase chain reaction
 PDB; Protein databank
 PMF; Proton motive force
 PolyP; Polyphosphate
 PPB; Ppotassium phosphate buffer
 QPCR; Quantitative polymerase chain reaction
r; Observed mutations
 R&D; Research and development
 RMSD; Root-mean-square deviation
 RND; Resistance nodulation division
 ROS; Reactive oxygen species
 RPM; Revolutions per minute
 RT-PCR; Reverse transcription polymerase chain reaction
 SDS; Dodecyl sodium sulfate
 SMR; Small multidrug resistance

SPC; Spectinomycin

SPI; *Salmonella* pathogenicity island

ssDNA; Single stranded DNA

SPR; Surface plasmon resonance

TBE; Tris-borate-EDTA

TET; Tetracycline

TM; Transmembrane

TTSS; Type two secretion system

xg; G force

XLD; Xylose lysine deoxycholate

μ; Mutation rate

Chapter One

Introduction

1.1 Antibiotic resistance

The discovery of the sulfonamide prontosil in 1932 was one of the most substantial milestones in modern medicine, creating a platform from which the subsequent development of a diverse range of antibiotic classes was built (Lobanovska et al., 2017). Without access to these drugs, numerous medical fields including surgery, chemotherapy, paediatric care and organ transplantation would be severely disadvantaged, entailing high, if not prohibitive risk (Piddock, 2012). Unfortunately, bacteria have evolved a plethora of mechanisms to circumvent inhibition by antibiotics thus compromising the effectiveness of these drugs. Resistance can occur against one or many antibiotics; an isolate is considered to be “multi-drug resistant” (MDR) when it is resistant to at least one drug in three or more antibiotic classes (Magiorakos et al., 2012).

A review commissioned by the UK government highlighted the burden that antimicrobial resistance (AMR) places on public health, in terms of morbidity and mortality and estimated that AMR would cause 10 million annual deaths by 2050; this is 18% higher than the current mortality rate for all cancers (O’Neill, 2016). Whilst there is contention regarding the reliability of this estimate (Kraker et al., 2016; Tillotson, 2017),

this report allowed many outside of the field of AMR to acknowledge antimicrobial resistance as a global public health concern.

This AMR crisis is not limited to one cause; the use of large amounts of antibiotics in human and animal health, agriculture and industry, coupled with poor public health and access to clean water in low and medium income countries has allowed the evolution and spread of numerous transmissible antibiotic-resistance genes and drug-resistant bacteria (Lee et al., 2013). Until the 2000s, antibiotic discovery, and research and development (R&D) efforts were able to contain the threat of drug-resistant infections. But, unfortunately, very few compounds with novel modes of action have been developed in recent years and despite programmes offering economic incentives to develop novel antibiotics, most large pharmaceutical companies have withdrawn their anti-infective programmes (Edwards, Morel, et al., 2018).

1.1.1 Intrinsic and adaptive resistance

AMR can be intrinsic or acquired. Intrinsic resistance is defined as the physiological properties of the bacterium that provide high tolerance to the presence of an antibiotic and is a feature that is largely conserved amongst all members of a given bacterial species (Blair, Webber, et al., 2015).

Adaptive resistance arises when a previously drug-sensitive bacterium becomes resistant. This acquisition of resistance can occur via the horizontal transfer of genes and/or evolution via spontaneous genetic mutations that can be transferred vertically and horizontally between bacteria (Blair, Webber, et al., 2015).

1.1.2 Antibiotic resistance evolution

It has been proposed that the original biological role of many resistance genes was unrelated to AMR (Hughes et al., 2017). However, these roles provided low-level resistance to

naturally occurring antibiotics in the environment. Over time, the survival and propagation of bacteria with these ‘drug-resistance’ genes allowed for evolution that conferred high-level resistance. For example, it has been suggested that acetylate-modifying enzymes, which confer resistance to aminoglycosides, fluoroquinolones and chloramphenicol, had an original role in the metabolism and modification of sugars (Hughes et al., 2017; Ramirez et al., 2010).

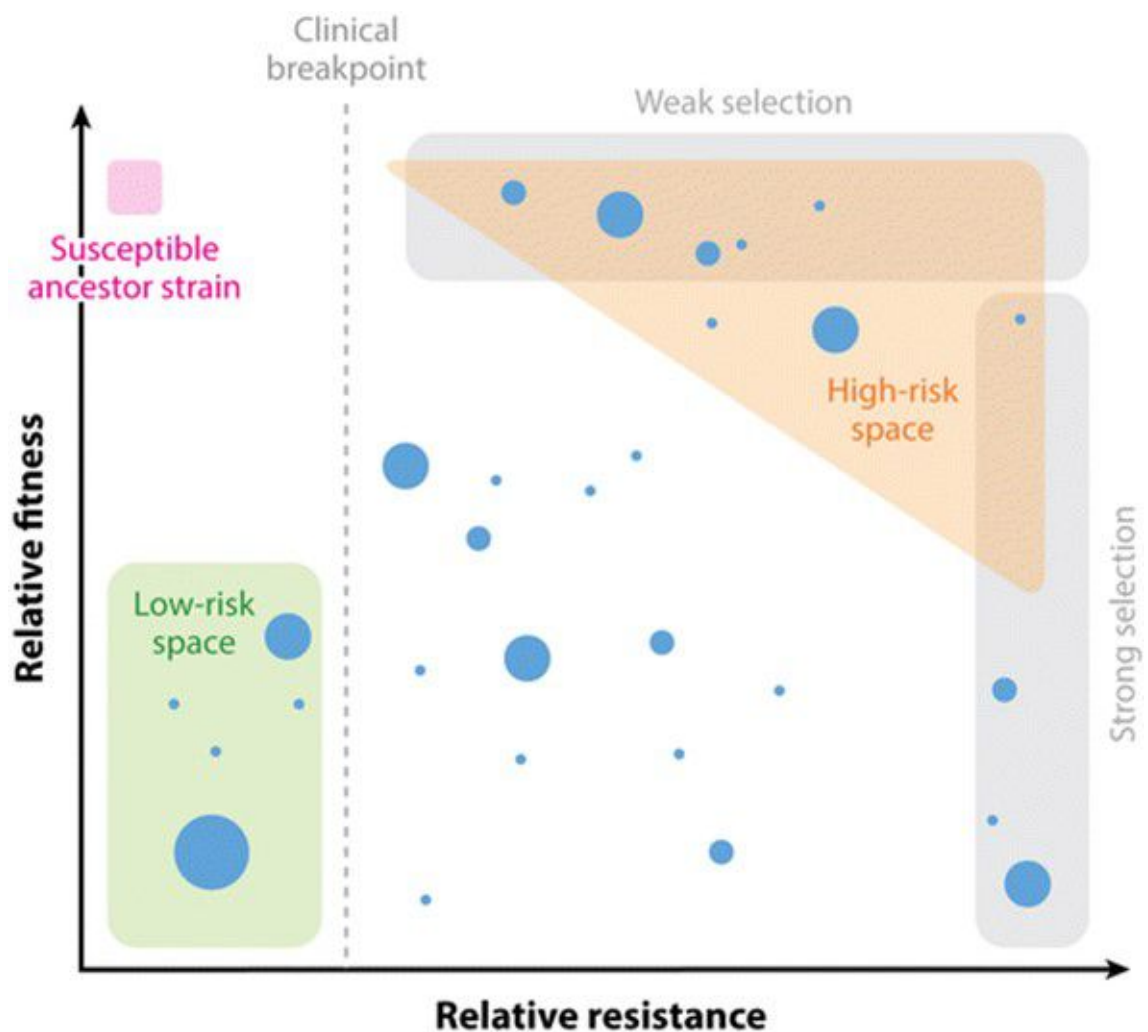
1.1.3 Appearance of mutations

Mutations can occur spontaneously as a result of errors in DNA replication and DNA repair pathways or can be induced by the presence of mutagens (e.g. UV, chemicals and reactive oxygen species (ROS)). Given that the antibiotics in clinical use are not typically mutagens the evolution of antibiotic resistance is often assumed to follow Darwin’s view of evolution that spontaneous DNA mutations occur randomly, uninfluenced by adaptive forces (MacPhee et al., 1996). Under this view, mutations pre-exist in a population and the presence of an antibiotic kills all bacteria except those with genes that confer resistance to the given antibiotic, allowing for the propagation of the resistant mutants. However, the reality is that the evolution of resistance and its maintenance within a bacterial population is complex and unpredictable; influenced by a number of biotic and abiotic factors. These include: mutation rates and frequency, population size, level of resistance, fitness of the resistant mutants, potential epistatic interactions and the type and strength of the selective pressure (Figure 1.1) (Hughes et al., 2017).

1.1.4 Mutation supply

Mutation supply is the frequency of beneficial mutations, a factor that is strongly influenced by the population size (Hall, Griffiths, et al., 2010). Large and small bacterial populations often have very different evolutionary trajectories. Smaller bacterial populations have a smaller degree of genetic drift and consequently a smaller mutational supply. If beneficial mutations are present they are likely to be fixed in the population rapidly

Figure 1.1: Plot showing the mutational events that can cause drug-resistance in relation to fitness, level of resistance conferred, selective pressure and rate of appearance of drug resistance.



The rate of mutation appearance is shown as blue circles; the larger the circle the higher the mutation rate. The higher the fitness advantage and level of resistance conferred by an individual mutation the higher the probability of selection. Figure from Hughes et al., 2017.

(Van Dijk et al., 2017). Conversely, larger populations are likely to contain multiple beneficial mutations. However, because bacteria are asexual these mutations are only present in the daughter cells of the parent with the original mutation (mutation A). This means in a large population, the relative frequency of this mutation increases very slowly over time. In the time it takes for mutation A to become fixed in the population an additional beneficial mutation (mutation B) can arise independently. The subsequent competition (clonal interference) between mutation A and mutation B slows the propagation of one mutation and may lead to its elimination (Van Dijk et al., 2017; Gerrish et al., 1998).

1.1.5 Mutation rate and frequency in the context of antibiotic resistance

Mutation frequency is simply a measurement of all the mutants in a given population and does not take into consideration whether a mutational event occurred early or late in the growth of a population; a mutation appearing earlier in the growth period would be represented by a higher mutation frequency. For this reason, mutation frequency is an unreliable estimation of mutation probability (Rosche et al., 2000; Pope et al., 2008).

Mutation rate is an estimate of the probability of a mutation occurring per cell per generation. The rate of beneficial, neutral and costly mutations are assumed to occur at the same frequency (Pope et al., 2008). In terms of antibiotic resistance, the mutation rate is calculated based on the number of detectable drug-resistant mutants that arise upon exposure to a given antibiotic. It is important to note that only beneficial mutations which lead to an observable resistance phenotype are detected, not the number of individual mutational events (Martinez et al., 2000). Calculating mutation rates is difficult and is complicated in that mutations in different genes can produce identical drug-resistance phenotypes. Thus, calculations produce a phenotypic mutation rate that is the result of one or more genotypic changes (Martinez et al., 2000). Generally, there are two methods for calculating mutation

rates (i) mutant accumulation and (ii) fluctuation analysis.

Mutant accumulation method

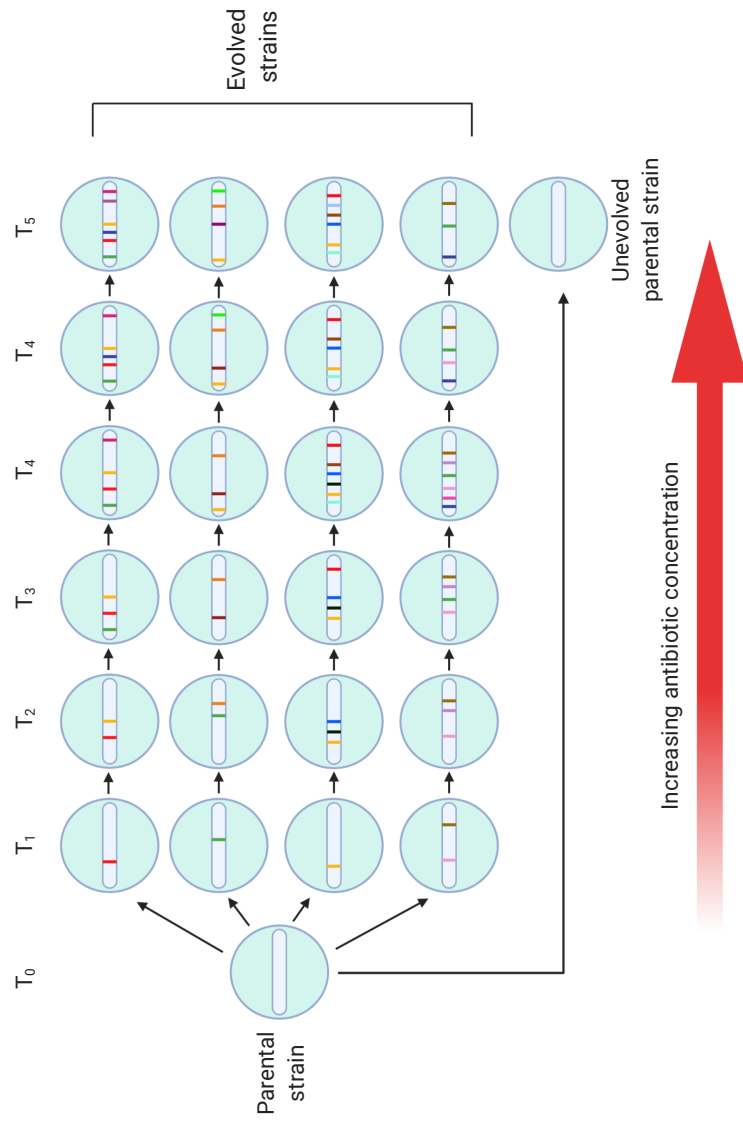
The mutant accumulation method is dependent on exponentially growing bacterial cultures and is an extremely accurate method of calculating mutation rate (Pope et al., 2008). Simply, parallel cultures derived from the same parental strain are allowed to evolve independently and each generation is subjected to bottlenecking to allow evolution by genetic drift (e.g. increasing antibiotic concentrations) (Figure 1.2). This bottlenecking severely reduces the population size and enables the accumulation of spontaneous mutations; a reduction in the bacterial fitness of the population over time is common with mutant accumulation methods (Katju et al., 2019; Pope et al., 2008). Unfortunately, mutant accumulation experiments are extremely complicated and time-consuming to perform.

Fluctuation assays

The fluctuation assay was first used in 1943 (Luria et al., 1943). Luria and Delbrück observed that mutants resistant to bacteriophages arose from a population of phage-sensitive *Escherichia coli*. Originally assuming that the phage was required to force evolution, they discovered that the mutations conferring phage resistance were present in some bacteria in the population before exposure to the bacteriophages and that there is a small, but fixed, chance that a mutation arises in a given period of time; the size of the mutant population depends on how early during growth the mutation arises (Luria et al., 1943; Pope et al., 2008).

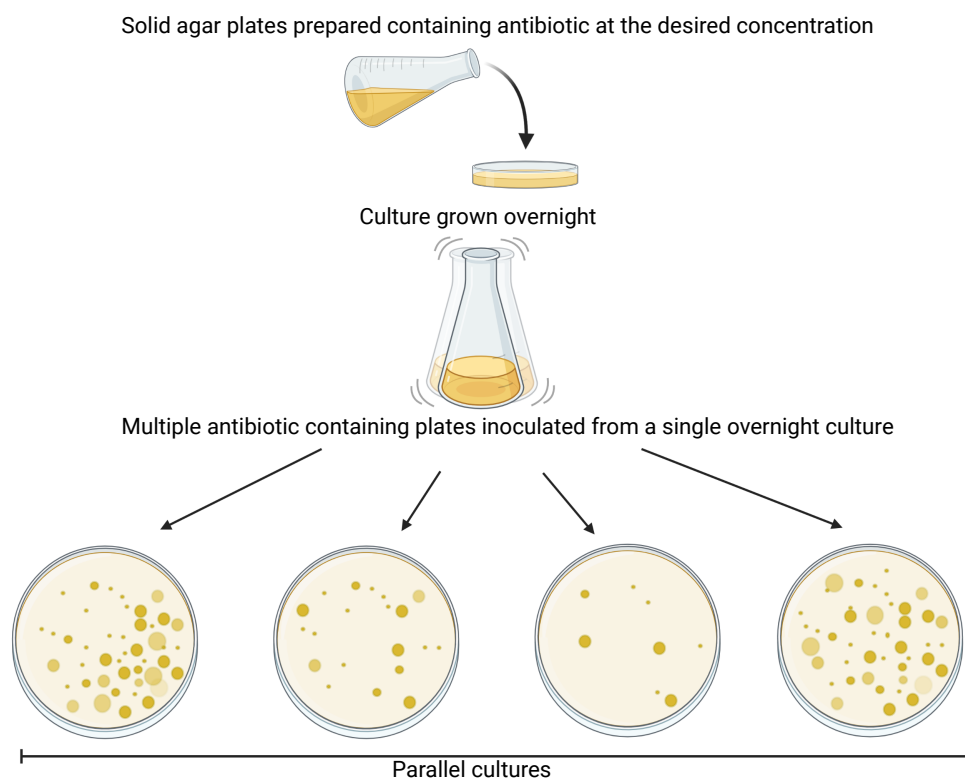
Mutation rates calculated from fluctuation analysis experiments rely on an estimation of m (the number of mutations per culture) from multiple parallel cultures (Figure 1.3). In short, cultures grown in the absence of selective pressure are used to inoculate an antibiotic

Figure 1.2: Classical mutant accumulation experiment.



Multiple parallel cultures are independently evolved for T_n generations. Increasing antibiotic concentration serves as the bottleneck for each generation. New spontaneous mutations are denoted by a coloured line on a chromosome. These mutations can be lost over time. Figure modified from Katju et al., 2019. Drawn using BioRender.

Figure 1.3: Schematic overview of a fluctuation analysis experiment.



Agar plates are made containing compound to apply selective pressure to inhibit the growth of susceptible cells and allow the propagation of resistant mutants. Each plate is inoculated with a single culture of the desired organism. Drawn using BioRender.

containing solid medium. The antibiotic provides a selective pressure that inhibits the growth of drug-susceptible cells and allow for the growth of drug-resistant mutants. In parallel, the number of bacterial cells in the initial culture is determined (viable count) (Pope et al., 2008). Several factors need to be taken into consideration when designing a mutation rate experiment, these are: (i) m , (ii) the number of cells in the initial inoculum, (iii) the final number of cells, (iv) the volume of culture plated and (v) the number of parallel cultures (Rosche et al., 2000).

There are many methods available to calculate mutation rate and the method chosen is dependent on the value of m (Figure 1.4); the most commonly used methods are the p_0 method, the Lea-Coulson method of the median and the Ma-Sandri-Sarkar (MSS)-maximum-likelihood methods which are used for low, low-medium and higher m values, respectively. Currently, the MSS-maximum likelihood calculation is the most robust method to estimate m and although is optimised for higher values of m , it can be used across all values (Rosche et al., 2000).

Regardless of the method the following assumptions are made: (i) all the cells within a population are growing exponentially with the same growth rates, (ii) the probability of mutation is constant and not influenced by previous mutations, (iii) the mutant population is small (iv) reversion rates and cell death is negligible, (v) all mutants are detected and (vi) selective pressure does not cause mutation (Rosche et al., 2000; Foster, 2006).

1.1.6 Selection of antibiotic-resistant bacteria

The mutant selective window hypothesis relies on the assumption that antibiotic resistance can only be selected within a certain antibiotic concentration window (Figure 4); between the minimal inhibitory concentration (MIC) of the drug-susceptible and drug-resistant population (Drlica, 2003). However, many studies have shown that sub-MIC

Figure 1.4: Methods and their equations used to calculate mutation rate.

Method	Valid over which values of m	Equation (s)
The $p0$ method	$0.3 \leq m \leq 2.3$	$p0 = e^{-m}$ $m = -\ln(p0)$
The Lea-Coulson method of the median	$1.5 \leq m \leq 15$	$\frac{\bar{r}}{m} \ln(m) - 1.24 = 0$
The MSS-maximum likelihood method	Any	$p0 = e^{-m}, Pr = \frac{m}{r} \sum_{i=0}^{r-1} \frac{P_i}{(r-i+1)}$ $f(r/m)^* = \prod_{i=1}^c f(r_i \setminus m)$ $*_f \left(\frac{r}{m} \right) = Pr$
The Luria-Delbrück method of the mean	Any	$m \ln(mC) - \bar{r} = 0$
The Drake Formula	≤ 30	$\frac{\bar{r}}{m} - \ln(m) = 0$
The Jones median	$1.5 \leq m \leq 10$	$m - \frac{\bar{r} - \ln(2)}{\ln(\bar{r}) - \ln(\ln(2))}$
Koch's quartile's method	$2 \leq m \leq 14$	$m1 = 1.7335 + 0.4474 Q1 - 0.002755(Q1)^2$ $m2 = 1.1580 + 0.2730 Q2 - 0.000761(Q2)^2$ $m3 = 0.6658 + 0.1497(Q3) - 0.0001387(Q3)^2$
The Lea-Coulson maximal likelihood method	$4 \leq m \leq 15$	$x = \frac{a}{\frac{r}{m} - \ln m + b} - c$

m ; number of mutations per culture. r ; number of mutants. \bar{r} ; mean number of mutants. \tilde{r} ; median number of mutants. $P0$; proportion of no mutants. Pr ; proportion of r mutants. C ; number of parallel cultures. $Q1$; first quartile of r . $Q2$; median of r . $Q3$; third quartile of r . f ; mutant frequency. Adapted from (Rosche et al., 2000).

concentrations of antibiotics (up to hundreds-fold below the MIC) can select for drug-resistant mutants (Liu, Fong, et al., 2011; Gullberg et al., 2011; Wistrand-Yuen et al., 2018).

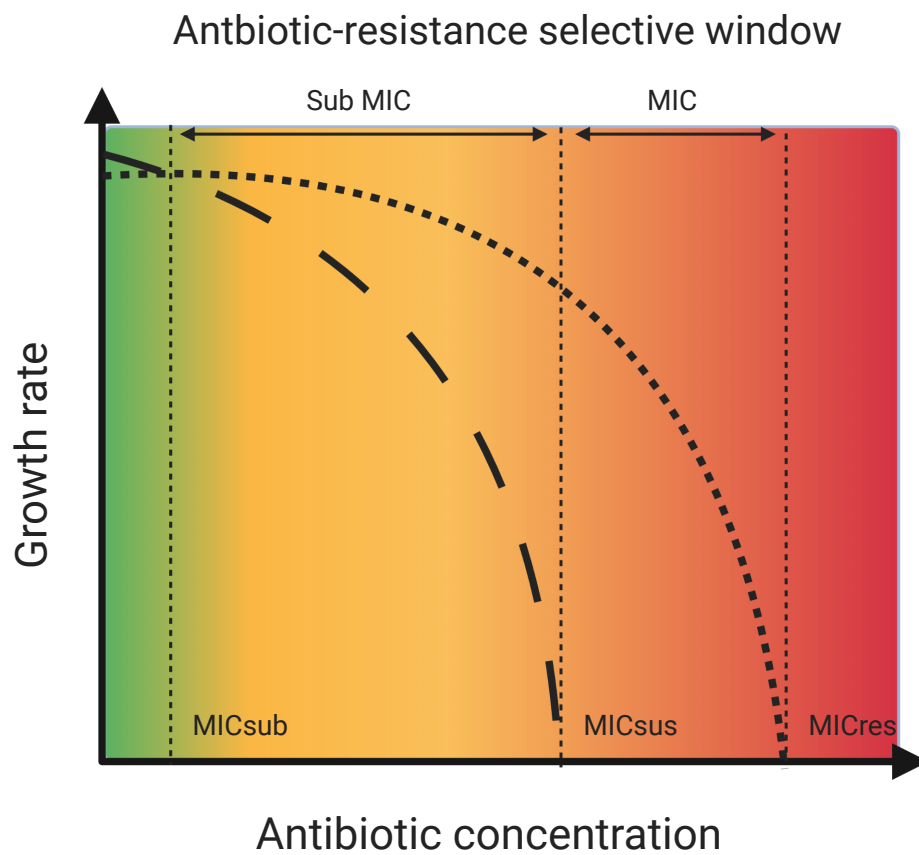
1.1.7 Mutations can incur fitness costs

Many mutations present within a population are deleterious, incurring a bacterial fitness cost that often reduces their growth rate and subsequent survival. In particular, mutations that provide resistance to antibiotics are often deleterious, unsurprising given that antibiotics target essential cellular functions including cell wall synthesis, RNA transcription and protein synthesis (Andersson et al., 2010). As a result, these mutants are outcompeted by high-fitness strains and the mutation is often lost from the population. However, this isn't always the case; the high-level drug-resistance benefit provided by certain mutations may offset any fitness disadvantage in the presence of a selective pressure. Additionally, epistatic interactions can emerge that compensate for fitness defects allowing for mutant survival; this further complicates predictions regarding resistance evolution (Knopp et al., 2015; Cowperthwaite et al., 2006).

1.1.8 Mutation reversion

Compensatory mutations occur to ameliorate the fitness cost of a given mutation. One particular type of compensation is reversion in which the mutant DNA sequence is reverted back to the wild type sequence (Durão et al., 2018). This usually occurs in the absence of antibiotic selective pressure where the mutation is no longer an advantage to the strain; this is important in the context of AMR as the bacteria regain their antibiotic susceptibility. When revertants occur in the presence of selective pressure, this is usually due to genetic drift or clonal interference (Andersson et al., 2010). However, it is important to note that reversion is much less common than compensation by the acquisition of additional mutations that reduce any fitness impact of drug-resistance mutations; *fusA* mutations

Figure 1.5: Representation of the selective windows for antibiotic-resistant bacteria.



At sub-MIC concentrations susceptible strains (dashed lines) outcompete resistant strains (green zone). As the antibiotic concentration increases (orange and red zones) the growth of the susceptible strains is inhibited and that of the resistant population dominate (dotted lined). MSC; sub-MIC. MIC_{sus} ; MIC of the susceptible population. MIC_{res} ; MIC of the resistant population. Adapted from (Wistrand-Yuen et al., 2018)

and *rpsL* mutations conferring resistance to fusidic acid and streptomycin in *Salmonella enterica* serovar Typhimurium, respectively were 20 times more likely to be compensated for by additional mutation than by reversion (Björkman, Hughes, et al., 1998; Björkman and Andersson, 2000).

1.2 Mechanisms of antibiotic resistance

The mechanisms by which bacteria have evolved resistance to antibiotics include: (i) antibiotic modification/inactivation, (ii) modification/protection of antibiotic targets, (iii) metabolic bypass and (iv) reduced intracellular accumulation of an antibiotic (Blair, Webber, et al., 2015).

1.2.1 Reduced intracellular accumulation of an antibiotic

Decreased susceptibility to antibiotics can occur via a reduction in the intracellular accumulation of a given antibiotic (Blair, Webber, et al., 2015). This can occur in two ways.

- i. Entry of the antibiotic to the intracellular environment may be restricted. The outer membrane (OM) of Gram-negative bacteria provides a permeability barrier to prevent the entry of molecules.
- ii. Antibiotics may be exported from the internal to the external cellular environment by efflux pumps.

1.3 The outer membrane

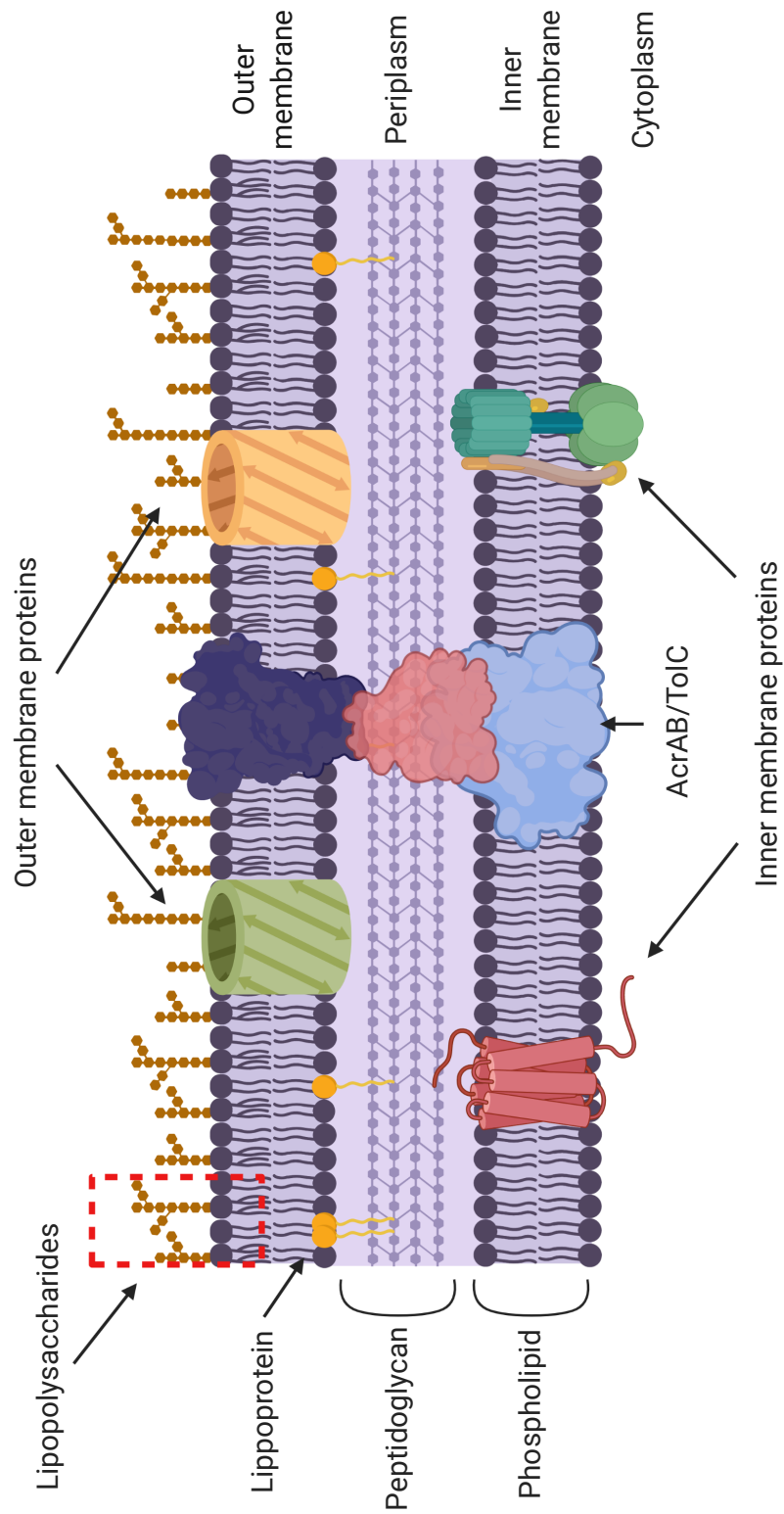
Gram-negative bacteria are surrounded by an OM that is absent in Gram-positive bacteria (Figure 1.6). Connected to the underlying peptidoglycan layer by Braun's lipoprotein, the OM performs the critical function of protecting the organism from the harsh environments in which they reside (Silhavy, Kahne, et al., 2010). The OM is an

asymmetric bilayer composed of phospholipids and glycolipids (predominantly lipopolysaccharides (LPS)), respectively (Bos et al., 2007). In addition, the OM of *E. coli* possesses pore forming proteins including OmpC, OmpF and OmpX. These outer membrane proteins (OMPs) confer a selective permeability barrier that prevents the entry of many toxic molecules whilst allowing for the entry and removal of nutrients and waste products (May et al., 2017).

The presence of LPS in the OM enables Gram-negative bacteria to survive their harsh environments. LPS is composed of lipid A, a core oligosaccharide and an O-antigen polysaccharide which varies in length (Raetz et al., 2002). The core oligosaccharide consists of a short chain of sugars and is divided into a highly conserved inner core (which binds lipid A) and an outer core that is attached to the O-antigen. The core oligosaccharide is crucial for the structural integrity of the OM (Heinrichs et al., 1998). The heptose region of the core oligosaccharide is of particular importance to the OM stability of *Enterobacteriales*; this region facilitates the cross-linking of adjacent LPS and enables interactions with the positively charged groups of proteins. Changes in the heptose region produces a “deep-rough” phenotype characterised by an increased phospholipid to protein ratio, that causes the OM to become more permeable and thus susceptible to the action of hydrophobic compounds (Parker et al., 1992; Heinrichs et al., 1998).

LPS is anchored to the membrane by lipid A. Lipid A is composed of a long chain of fatty acids linked to an acylated glucosamine disaccharide backbone and is the feature of LPS that confers to the OM a very effective barrier to prevent the diffusion of lipophilic compounds (Nikaido, 2003). This important protective role for Gram-negative bacteria is mediated through the phosphate group of Lipid A which confers a negative charge to the membrane surface (Stock et al., 1977). Bridging of the negative charges by electrostatic interactions with divalent cations in the environment, and from neighbouring LPS molecules, reduces the fluidity of the membrane and creates a barrier for excluding lipophilic and

Figure 1.6: Cell envelope of Gram-negative bacteria.



Adapted from Maldonado et al., 2016. Drawn using Biorender

hydrophilic molecules (May et al., 2017). Disruptions to the lipid A component of LPS can cause phospholipids to flip from the inner to the outer leaflet. As a result, regions of the bilayer are compromised and allow toxic molecules to penetrate the membrane more easily (Nikaido, 2003).

1.4 The role of efflux pumps in MDR

Located in the cell membrane of Gram-positive and Gram-negative bacteria, efflux pumps recognise toxic substances that have breached the bacterial cell wall entering the cytoplasm or the periplasm. Once recognised, efflux pumps extrude substrates to the external environment. Efflux pumps may be specific for a single substrate, or they may export a wide variety of structurally unrelated compounds. Substrates include antibiotics, dyes, biocides, detergents and degradation products from cellular metabolism (Nikaido, 2003).

Chromosomally encoded MDR efflux systems are highly conserved across all members of a given species and have existed and evolved within the core of the bacterial genome for millions of years, long before the advent of traditional antibiotics (Saier, Paulsen, et al., 1998). Efflux pumps are classified by their structure, the number of transmembrane (TM) domains they contain and their substrates. In prokaryotes, there are six major super-families: the major facilitator superfamily (MFS), the resistance nodulation division (RND) family, the small multidrug resistance (SMR) family, the ATP binding cassette superfamily (ABC), the proteobacterial antimicrobial compound efflux (PACE) family and the multidrug and toxic compound extrusion (MATE) family. These six families are grouped into two classes dependent on their energetic requirements; primary transporters that utilise the energy of ATP hydrolysis (ABC) and secondary transporters (RND, MATE, MFS, PACE and SMR) that rely on the energy produced from TM electrochemical gradients (Li and Nikaido, 2009).

Overexpression of efflux pumps, conferring clinically relevant drug resistance, is a problem. For example, 80% of *Pseudomonas aeruginosa* strains resistant to the β -lactam

carbenicillin were found to be MDR, mediated by overexpression of *mexAB-oprM* (Williams et al., 1984). In addition, overexpression of *acrAB-tolC* has been implicated in MDR amongst the *Enterobacteriales* including *E. coli* and *S. Typhimurium* (Baucheron, Tyler, et al., 2004; Giraud, Cloeckert, Kerboeuf, et al., 2000; Mazzariol et al., 2000; Piddock et al., 2000), this resistance is often conferred by mutation in *acrR* or other regulators of the efflux pump (e.g. *marR* and *ramR*) (Abouzeed et al., 2008; Vinué et al., 2016; Wang, Dzink-Fox, et al., 2001). Clinically relevant MDR, mediated by overexpression of efflux systems, has also been found for many other Gram-negative species including *Klebsiella pneumoniae* (Deguchi et al., 1997), *Proteus vulgaris* (Ishii et al. 1991), *Shigella dysenteriae* (Ghosh et al., 1998), *Enterobacter cloacae* (Notka et al., 2002), *Campylobacter jejuni* (Charvalos et al., 1995), *Acinetobacter baumannii* (Magnet et al., 2001), *Helicobacter pylori* (Van Amsterdam et al., 2005) and *Haemophilus influenzae* (Sanchez, Pan, et al., 1997).

1.4.1 The resistance nodulation division family

The RND superfamily is ubiquitous across all major phylogenetic kingdoms and is divided into seven subfamilies, of which four are found in Gram-negative bacteria. These are the heavy metal efflux family, the hydrophobic and amphiphilic family, the nodulation factor exporter family and the SecDF-protein-secretion accessory protein family (Tseng et al., 1999).

There are certain unusual structural features common to all members of the RND superfamily that resulted from tandem duplications early in their evolution (Saier, Paulsen, et al., 1998). This includes the presence of 12 α -helical TM domains and two hydrophilic extra-cytoplasmic loops located between TM domains one and two and seven and eight (Gotoh et al., 1999). Another common trait of RND efflux pumps is their organisation; they are tripartite systems formed of an inner membrane (IM) protein complexed with an OM channel and a periplasmic adaptor protein (Nikaido and Takatsuka, 2009). This structure

allows efflux pumps to traverse the inner and outer membranes allowing substrates to be extruded from the cytoplasm to the external environment. This confers a very effective drug-resistance mechanism as to re-enter the intracellular environment antibiotics have to pass through the OM (Zgurskaya et al., 2000).

1.4.2 The AcrAB-TolC efflux system

The RND pump AcrAB-TolC is highly conserved amongst *Enterobacteriales* and is the most extensively studied efflux pump in the context of MDR. Like other RND pumps, AcrAB-TolC is a tripartite structure consisting of a periplasmic adaptor protein (AcrA), an IM protein (AcrB) and an OMP (TolC); high-resolution X-ray crystallography structures for each component of the *E. coli* complex have been obtained (Koronakis, Sharff, et al., 2000; Mikolosko et al., 2006; Murakami, Nakashima, Yamashita, and Yamaguchi, 2002).

The substrates exported by AcrAB-TolC are so diverse in their structure it has been difficult to identify common features. However, there are some shared properties including that they are usually lipophilic, amphiphilic and carry a net positive charge (although some substrates are negatively charged). Of these, lipophilicity is suggested to be the most important determinant for AcrB substrates and is due, in part, to the hydrophobic nature of the binding pockets of AcrB (Nikaido, Basina, et al., 1998; Ramaswamy et al., 2017). This observation is reflected by the common features amongst compounds that are not exported by *E. coli* AcrAB-TolC which includes very hydrophilic compounds (e.g. aminoglycosides and β -lactams with hydrophilic side chains) (Nikaido, Basina, et al., 1998; Nikaido, 1996).

1.4.3 AcrB

Distributed in the periplasmic and TM domains, the crystal structure of AcrB was solved at 3.5 Å in three-fold symmetry (Murakami, Nakashima, Yamashita, and

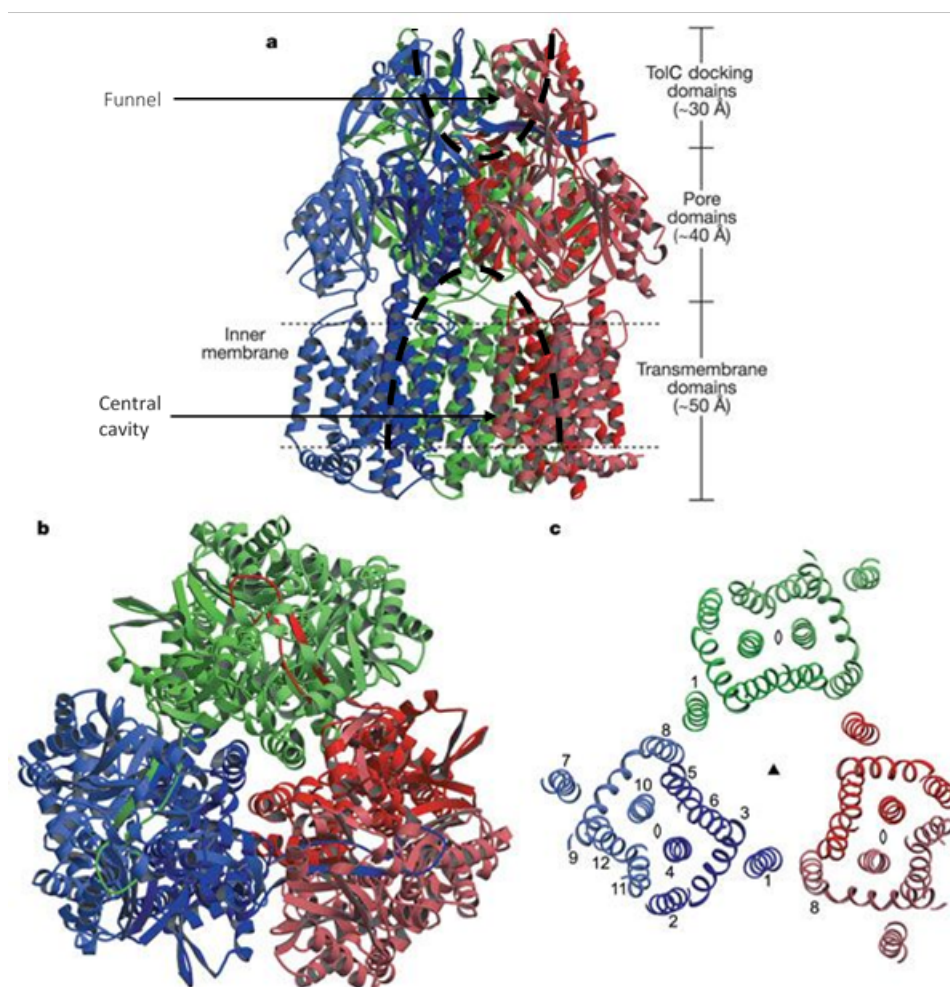
Yamaguchi, 2002) and later in an asymmetric conformation (Murakami, Nakashima, Yamashita, Matsumoto, et al., 2006; Seeger et al., 2006; Sennhauser et al., 2007). Simply, AcrB is homotrimer comprised of three identical protomers (1,049 amino acids apiece); each protomer is formed of a 50 Å thick TM domain and a 70 Å thick periplasmic headpiece (Figure 1.7) (Murakami, Nakashima, Yamashita, and Yamaguchi, 2002; Du et al., 2014; Shi et al., 2019). The periplasmic headpiece of AcrB consists of two large periplasmic loops located between helices 1-2 and 7-8, each of which contain a porter (40 Å thick) and a TolC docking domain (30 Å thick) and as such resembles a trapezoid (Eicher, Cha, et al., 2012; Nakashima, Sakurai, Yamasaki, Nishino, et al., 2011; Cha et al., 2014; Sjuts et al., 2016). From the bottom up, the TM domain forms a vestibule in which substrates can enter the central cavity of AcrB. The TM domain connects to the porter domain which contains a pore at the centre of the headpiece that opens up into a funnel shape within the TolC docking domain through which substrates can exit AcrB (Das et al., 2007; Murakami, Nakashima, Yamashita, and Yamaguchi, 2002; Du et al., 2014; Shi et al., 2019). The pore is closed in the absence of a substrate.

The transmembrane domain

AcrB is a proton/substrate antiporter, meaning the efflux of substrates is coupled with the transport of protons across the IM. Mutagenesis experiments have identified key residues of AcrB found within the TM domain that are essential for proton translocation, the so called proton relay network; Asp407 and Asp408 found within TM4, Lys940 within TM10 and Thr978 within TM11 (Guan et al., 2001; Takatsuka and Nikaido, 2006; Eicher, Seeger, et al., 2014; Matsunaga et al., 2018; Zhang et al., 2017).

In addition to containing residues that are essential for proton translocation, Yu et al., 2003 revealed that the TM domain also contains residues within the central cavity that play a role in the binding of the structurally diverse ligands ethidium, rhodamine 6G, dequalinium

Figure 1.7: The structure of AcrB in ribbon representation.



(A) Side view of AcrB in which the three protomers are differently coloured. The TolC docking domain has a funnel like shape which narrows into a pore in the centre of the porter (pore) domain and leads to the central cavity within the TM domain. (B) Top view of AcrB. (C) Structure of the TM domain, the numbers indicate the TM helix number. Figure from Murakami, Nakashima, Yamashita, and Yamaguchi, 2002.

and ciprofloxacin (Yu et al., 2003). These include Phe386, Phe388, Phe458 and Phe459, Ala385, Leu25, Val382 and Lys29.

Porter domain

The porter domain is essential for substrate specificity and is characterised into four subdomains; PN1, PN2, PC1 and PC2, which are organised such that the β -sheets of each form a substrate binding domain ((Murakami, Nakashima, Yamashita, and Yamaguchi, 2002; Seeger et al., 2006; Eicher, Cha, et al., 2012). This substrate domain has been shown to be rich in hydrophobic residues, namely phenylalanine's, that form hydrophobic interactions or aromatic stacking interactions with AcrB substrates, other charged and polar residues are also present that can form hydrogen bonds with substrates (Murakami, Nakashima, Yamashita, Matsumoto, et al., 2006; Vargiu and Nikaido, 2012). The wide variety of residues that participate in substrate binding underlies the polyspecificity of AcrB. The binding domain is further divided into proximal (access) and distal (deep) binding pockets, separated by a flexible glycine rich G-loop. These two binding pockets play a major role in the discrimination and export of AcrB substrates; high molecular weight substrates initially bind to the access pocket before moving to the deep binding pocket, whereas low molecular weight substrates are able to pass through the access pocket and bind immediately to the deep binding pocket (Eicher, Cha, et al., 2012; Nakashima, Sakurai, Yamasaki, Nishino, et al., 2011).

It is well understood that the access and deep binding pockets of the porter domain are the primary substrate binding sites of AcrB and largely contribute to the substrate specificity of AcrB. However, less is known about the mechanism by which substrates enter AcrB. Generally, there is considered to be three pathways designated the CH1, CH2 and CH3 channels. The CH1 channel, previously called the vestibule pathway, is located next to the vestibule between TM8 and TM9 of AcrB and allows substrates to be translocated from the

outer leaflet of the IM (Murakami, Nakashima, Yamashita, Matsumoto, et al., 2006; Zwama et al., 2018). The CH2 channel, previously called the cleft pathway, allows substrates to enter AcrB from the periplasm between the PC1 and PC2 subdomains (Sennhauser et al., 2007; Zwama et al., 2018; Schuster, Vavra, et al., 2016). Only very recently characterised, the CH3 channel is open to the central cavity of AcrB and allows substrates to pass directly to the deep binding pocket without any initial interaction with the access pocket (Zwama et al., 2018). The discovery of these three channels of AcrB shows that not only do different substrates bind to different locations of AcrB but they also enter the protein through different pathways. In general it is not well known which substrates utilise which pathway. However, compounds which pass through CH1 and CH2 are generally those for which the access binding pocket is the initial preferred binding site while compounds that pass through CH3 tend to be smaller, planar, aromatic compounds that initially bypass the access binding pocket and bind the distal binding pocket (Zwama et al., 2018; Schuster, Vavra, et al., 2016).

1.4.4 AcrA

AcrA interacts with both AcrB and TolC forming the tripartite structure (Du et al., 2014; Shi et al., 2019). Crystal structures have revealed AcrA is a hexamer composed of two conformationally distinct protomers (Wang, Fan, et al., 2017). The membrane proximal domain, the β -barrel domains and the hairpin domain of each AcrA protomer are responsible for forming interactions with AcrB and TolC, respectively. The lipoyl domain makes no contact with either AcrB or TolC, but instead interacts with the lipoyl domains of the adjacent protomers forming a channel that is closed to the periplasm (Du et al., 2014; Wang, Fan, et al., 2017). In addition to interacting in the tripartite structure, evidence shows that AcrA can be independently cross-linked to AcrB in the absence of TolC and to TolC in the absence of AcrB (Tikhonova et al., 2004; Touzé et al., 2004).

1.4.5 TolC

While the OMP of many other efflux pumps can only interact with a particular pump, TolC is promiscuous forming the OM constituent of many RND, MFS and ABC efflux systems in *E. coli* including AcrD, AcrEF, MdtABC, EmrAB, EmrKY and MacAB (Elkins et al., 2002; Horiyama et al., 2010). A 51.5 kDa trimer, TolC possesses a β -barrel domain (channel domain) that anchors the protein to the OM, an α -helical barrel structure (tunnel domain) that confers a tunnel through the periplasm and a mixed α/β structure that wraps around the tunnel domain (Koronakis, Sharff, et al., 2000; Koronakis, Eswaran, et al., 2004). In the presence of a substrate the top of the protein is open to the environment allowing for a large access area through which substrates can pass and tapers to a close at the bottom of the protein (Koronakis, Sharff, et al., 2000). It is important to note that in the absence of substrate the TolC exit channel is kept closed to keep the periplasm closed to the extracellular environment (Shi et al., 2019).

1.4.6 Assembly of the AcrAB-TolC complex

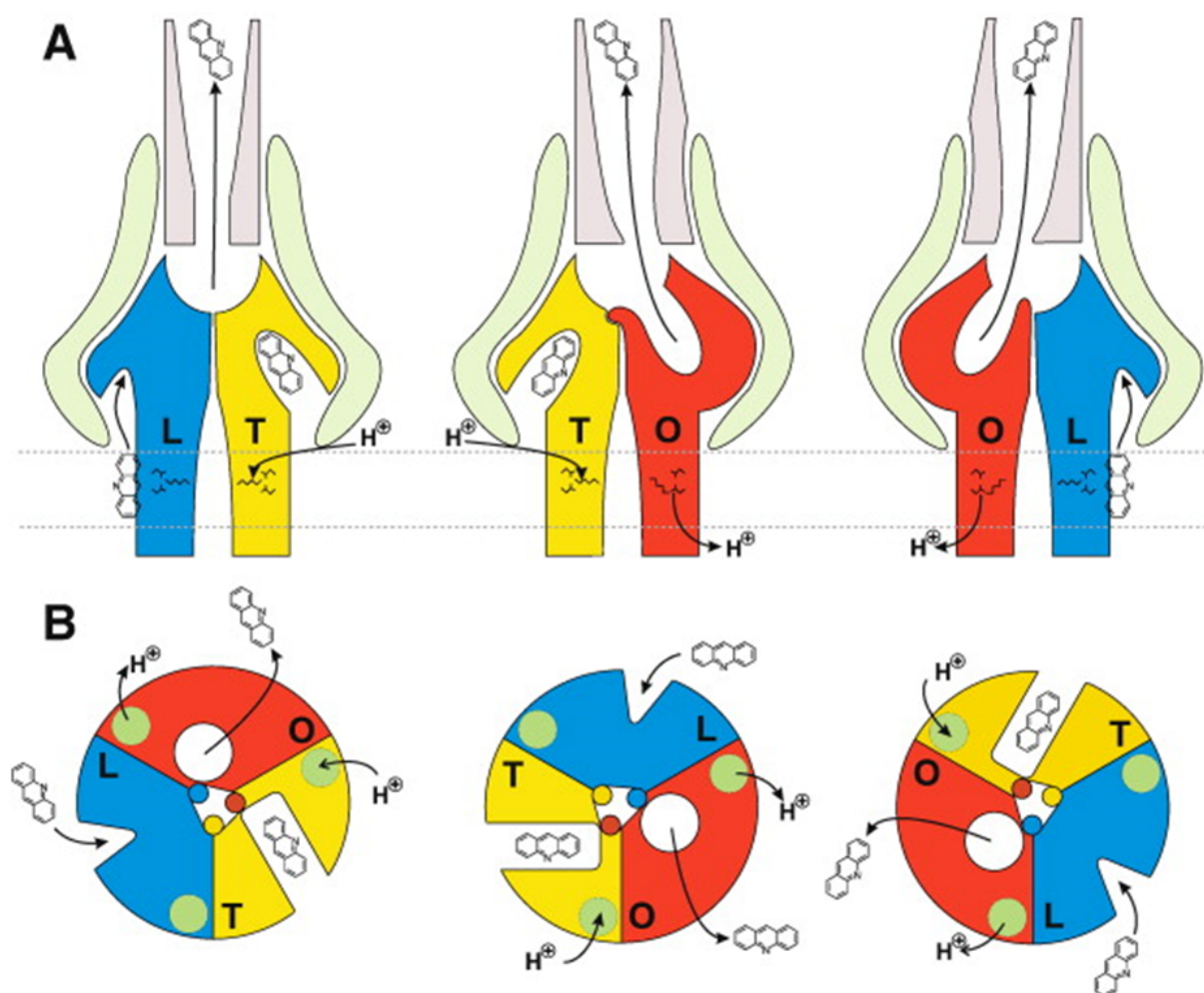
There has been contention regarding the stoichiometry of and the mechanism of assembly of the AcrAB-TolC efflux pump. However, in recent years a general consensus regarding the assembly of AcrAB-TolC has been reached in the community. This model was largely influenced by a cryo electron microscopy structure produced in 2014 (Du et al., 2014) and is as follows: AcrAB-TolC is formed of a 3:6:3 ratio of AcrB:AcrA:TolC (Du et al., 2014) in which AcrB and TolC (located in the IM and OM, respectively) are unable to touch and instead are bridged across the periplasm by AcrA (Du et al., 2014; Wang, Fan, et al., 2017; Shi et al., 2019). This complex appears to form in a multistep fashion by which AcrB and AcrA first form a dipartite complex in a 3:6 AcrB:AcrA ratio through interactions of the β -barrel and membrane proximal domains of AcrA with AcrB (Du et al., 2014; Shi et al., 2019). This dipartite structure is stabilised through interactions of the α -hairpin domain

of AcrA with the peptidoglycan layer of the membrane (Shi et al., 2019). The proposed hypothesis is that this interaction with the peptidoglycan layer enables the AcrAB complex to 'walk' across the IM until it encounters TolC in the OM and forms the tripartite structure by way of interactions of the hairpin domain of AcrA with TolC (Du et al., 2014; Shi et al., 2019; Wang, Fan, et al., 2017).

1.4.7 Mechanism of substrate extrusion by AcrAB-TolC

The three monomers of AcrB are asymmetric and exist in one, of three, different conformations: access (L), binding (T) and extrusion (O), each representing a consecutive stage of the transport cycle (Wang, Fan, et al., 2017) (Figure 1.8). The proposed transport mechanism is as follows: (i) binding of a substrate to the L monomer and protonation of the proton relay network, (ii) a conformational change to the T monomer during which the substrate moves deeper into the binding pocket of AcrB, (iii) a shift to the O monomer allowing the extrusion of the substrate into TolC and (iv) relaxation of the O monomer to the L state to restart the cycle (Pos, 2009). It is important to note that the energy dependent conformational change from the T to the O monomer requires the binding of a second substrate to another monomer in the L state (Pos, 2009). Despite the extensive conformational changes in AcrB that accompany drug extrusion, little is observed in the TolC docking domain (Murakami, Nakashima, Yamashita, Matsumoto, et al., 2006). The functional rotation of AcrB requires an external source of energy driven by the proton motive force (PMF). As previously mentioned, AcrB possesses a protonation site within its TM domain consisting of the following residues: Asp407, Asp408, Lys940 and Thr978 (Pos, 2009; Takatsuka and Nikaido, 2006; Zhang et al., 2017; Eicher, Seeger, et al., 2014; Matsunaga et al., 2018). The exact protonation states of these residues has been disputed. However, it has been suggested that in the absence of a substrate Lys940 is protonated and the positive charge of this residue lies over Asp407 and Asp408 preventing them from being protonated. Upon substrate binding there is a slight conformational change that pushes the positive

Figure 1.8: Scheme showing the proposed transport mechanism of substrates through AcrB.



The L, T and O monomers conformational states are shown in blue, yellow and red, respectively. (A) Side view of the AcrB trimer. (B) The top view of AcrB in which the binding sites are shown as a triangle, a rectangle and a circle and represent low, high and no binding affinity for a given substrate. The substrate here is acridine which binds in the L state and upon a conformational change moves to the T state and finally the O state where it can be released to TolC. Figure from Pos, 2009.

charge of Lys940 away from Asp407 and As408 allowing them to be protonated. Consequently, the salt-bridges and hydrogen bonds that hold the network of residues together is disturbed resulting in a series of conformational changes that allow for substrate transport (Pos, 2009; Takatsuka and Nikaido, 2006; Su, Li, et al., 2006; Matsunaga et al., 2018; Zhang et al., 2017).

1.5 Local regulation of expression of *acrAB* expression

In 1993, Ma et al cloned the *E. coli* *acr* locus, revealing the presence of three genes within a single operon *acrR*, *acrA* and *acrB* (Figure 1.9). Of these, *acrA* and *acrB*, encoding the efflux proteins AcrA and AcrB, are co-located, while *acrR* is found 141bp upstream encoding the local repressor AcrR (Ma, Cook, et al., 1993; Ma, Alberti, et al., 1996), a member of the Tet family of repressors (Su, Rutherford, et al., 2007).

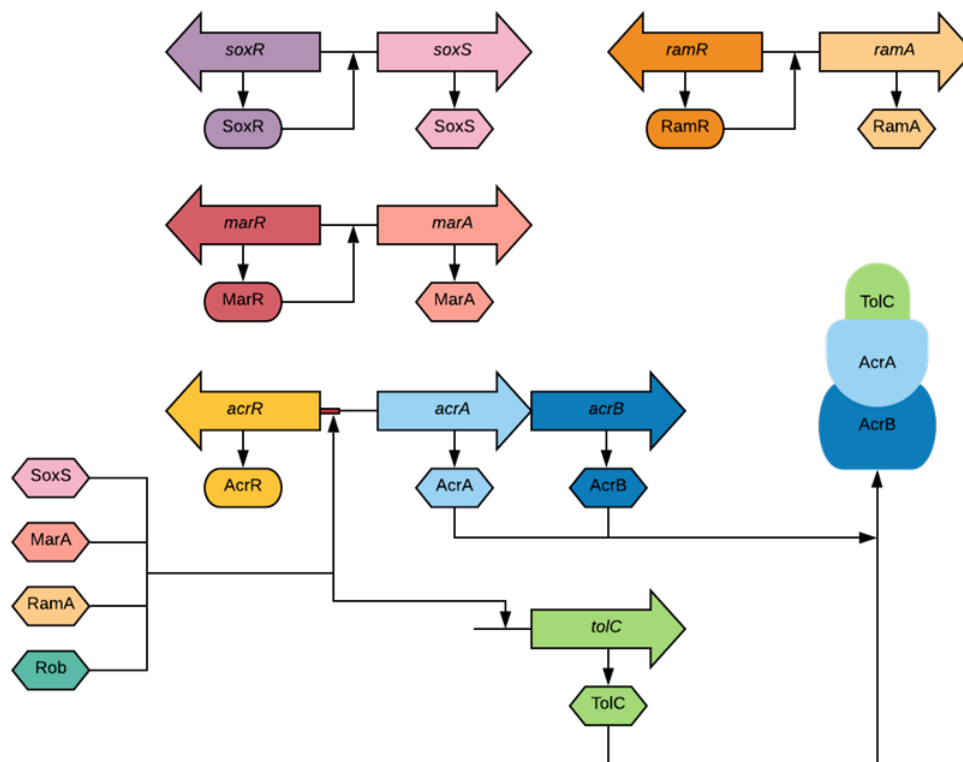
In *E. coli*, AcrR binds to the *acr* promoter via a 24bp palindrome operator site located between *acrR* and *acrAB*. This operator site is contained within a 28bp sequence of DNA that intersects the *acrAB* promoter and thus, AcrR prevents transcription of *acrAB* (Ma, Cook, et al., 1993; Ma, Alberti, et al., 1996). Upon binding of a substrate (e.g. ethidium) to the C-terminal binding domain of AcrR, a conformational change occurs in its N-terminal helix-turn-helix (HTH) motif enabling AcrR to dissociate from its operator site allowing transcription of *acrAB* (Su, Rutherford, et al., 2007).

1.6 Global regulation of *acrAB* expression

1.6.1 Mar

The *E. coli* *mar* (multiple antibiotic resistance) locus consists of two divergent operons, *marC* and *marRAB*, controlled by the promoters *p_{marI}* and *p_{marII}*. *marRAB* encodes the *mar* repressor (MarR) and activator (MarA) (Aleksun and Levy, 1999). In the absence of stimulus (salicylate acid, antibiotics, dyes, disinfectants, biocides and

Figure 1.9: Schematic representation of the known regulatory pathways for expression of AcrAB-TolC efflux pump in *S. Typhimurium*



The genes are represented as arrows and their translated proteins are represented as ovals (transcriptional repressors) and hexagons (transcriptional activators). The AcrAB-TolC pump extrudes drugs across the cytoplasmic and outer membranes. Excessive production of AcrA and AcrB is prevented by the local repressor AcrR. Activation of *acrA*, *acrB* and *tolC* transcription occurs primarily due to the global regulatory protein RamA by binding to the rambox (shown in red) upstream of these genes. RamA expression is controlled by RamR which represses activation of *ramA*. The regulatory protein SoxS and Rob can also activate *acrAB-tolC* transcription. SoxR controls expression of both *soxR* and *soxS*. In *E. coli*, MarA is the primary activator of *acrAB-tolC* transcription. Likewise, MarA expression is regulated by MarR which represses activation of *marA*.

oxidative stress agents) MarR binds to *pmarI* and *pmarII* within *marRAB* and *marC*, preventing *marA* transcription (Alekshun and Levy, 1999). Upon exposure to a stimulus, MarR undergoes extensive conformational changes and dissociates from the *marRAB* operon allowing for the overexpression of *marA* (Alekshun and Levy, 1997). MarA binds to the 20bp marbox binding site located within the promoters of certain genes within the *mar* regulon (Gillette et al., 2000). Chip-seq has revealed that the *mar* regulon of *E. coli* K-12 is vast with 28 identified MarA binding sites, 15 of which are within 150 bp of a σ^{70} binding site (Sharma, Gupta, et al., 2019). Other MarA binding sites include the promoter regions of the *mlaFEDCB* operon, *xseA*, *micF* and *acrAB* (Sharma, Gupta, et al., 2019). MarA is able to regulate the expresison of a large number of genes, the vast majority of which are involved in a stress response mediated by σ^{70} (Sharma, Gupta, et al., 2019). However, drug resistance results from the ability of MarA to decrease synthesis of the OmpF porin and overexpress AcrAB-TolC (Cohen, McMurry, et al., 1988).

1.6.2 MarR

MarR is a homodimeric DNA binding protein with a winged HTH structure (Figure 1.10) (Alekshun, Levy, et al., 2001). Each subunit of MarR consists of a mixed α -helical β -sheet structure and possesses the following distinct domains: an N-/C-terminal domain and a globular domain. The N-terminal domain (residues 10-21) and the C-terminal domain (residues 123-144) of one monomer intertwine with the equivalent regions of the second monomer forming a single domain (Alekshun, Levy, et al., 2001). Two long antiparallel helices (residue 103-126) link this domain to the rest of the protein. The globular domain (residues 55-100) is known as the DNA binding domain and limited contact is established between the globular domains of each monomer (Prajapat et al., 2015; Martin, Rosner, et al., 1995; Seoane et al., 1995; Alekshun, Levy, et al., 2001). The ligand binding domain

Figure 1.10: The structure of *E. coli* MarR in ribbon format



One of the MarR dimers is coloured and the other is shown in grey. Image from Alekshun, Levy, et al., 2001.

is suggested to be located within $\alpha 1$ and $\alpha 2$ helices at the interface of the dimerization and DNA binding domains (McMurry et al., 2013; Perera et al., 2010). Mutations within *marR* have been well described in antibiotic-resistant clinical isolates of *E. coli* and *S. Typhimurium* and usually results from structural changes in MarR that prevent the interaction of MarR with the promoter of *marA*, allowing for overexpression of *marA* and consequently *acrAB* (Duval et al., 2013; Alekshun, Levy, et al., 2001; Notka et al., 2002; Alekshun and Levy, 1997; Seoane et al., 1995; Linde et al., 2000; Watanabe et al., 2012).

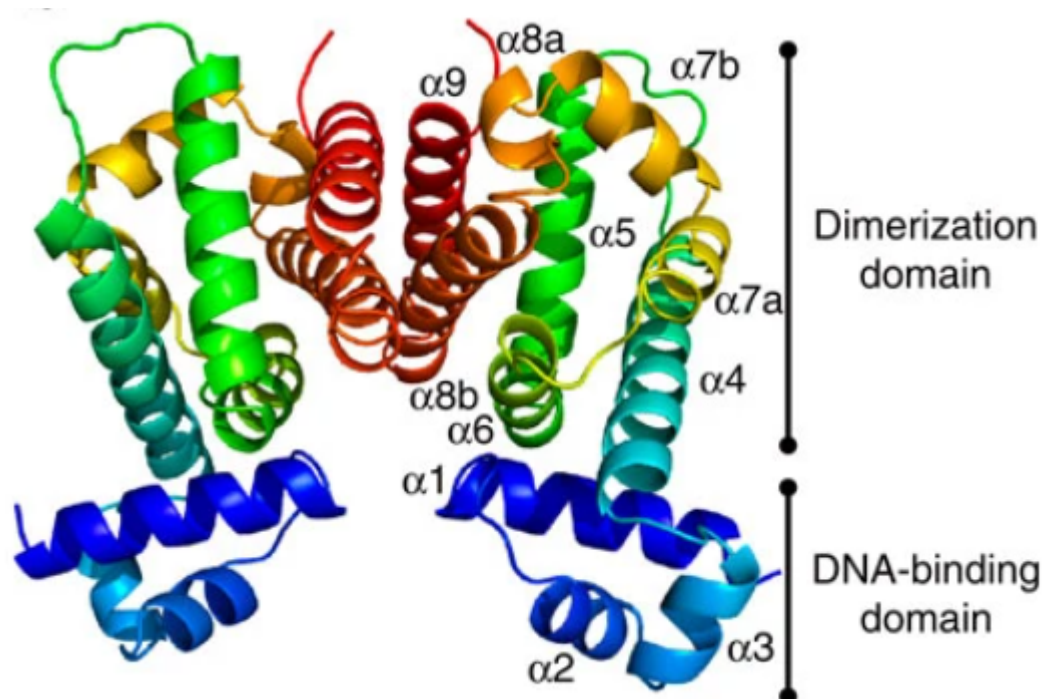
1.6.3 Ram

Absent in *E. coli*, but present in *S. Typhimurium*, RamA is encoded by the gene *ramA*, which is under the direct control of RamR, another Tet-like repressor (Baucheron, Coste, et al., 2012; Ricci, Blair, et al., 2014; Bailey et al., 2008). RamR represses the expression of *ramA*. Repression of *ramA* results in decreased expression of *acrAB*. Upon binding of a ligand, RamR undergoes extensive conformational changes and dissociates from *ramA* (Yamasaki, Nikaido, et al., 2013a; Liu and Chen, 2017; Yamasaki, Nikaido, et al., 2013b). This results in the expression of *ramA* and drug resistance as a result of the concomitant overexpression of *acrAB* (Ricci, Blair, et al., 2014; Yamasaki, Nikaido, et al., 2013a).

1.6.4 RamR

RamR is a homologue of MarR that has been implicated in MDR by *S. Typhimurium* (Figure 1.11). Like MarR, RamR is a transcriptional repressor that negatively regulates the expression of its transcriptional activator RamA. RamR is a homodimeric DNA binding protein consisting of nine α -helices. The N-terminus consists of $\alpha 1$ - $\alpha 3$ (residue 9-49) and forms the DNA-binding region. The C-terminus consists of $\alpha 4$ - $\alpha 9$ (residue 51-189) and is

Figure 1.11: Crystal structure of *S. Typhimurium* RamR in ribbon representation.



The alpha helices of one monomer is displayed alongside a division of the docking and DNA binding domains. Image from Yamasaki, Nikaido, et al., 2013a.

known as the dimerization domain. Dimerization of RamR occurs via hydrogen bonding and hydrophobic interactions within α -helices 8 and 9 (residue 139-189). The crystal structure of ligand-complexed RamR showed that all complexed ligands interact via π - π interactions with Phe155 within α 8a. Mutations within *ramR* have been well described in antibiotic-resistant clinical isolates of *S. Typhimurium*. These mutations overwhelmingly occur within the dimerisation domain resulting in structural changes in RamR that prevent the interaction of RamR with the promoter of *ramA*, allowing for overexpression of *ramA* and consequently *acrAB* (Yamasaki, Nikaido, et al., 2013a; Ricci, Blair, et al., 2014; Yamasaki, Nikaido, et al., 2013b; Baucheron, Tyler, et al., 2004; Abouzeed et al., 2008; Baucheron, Coste, et al., 2012).

1.6.5 Sox and Rob

Sharing 42% sequence homology with MarA (Cohen, Hachler, et al., 1993; Ma, Alberti, et al., 1996), SoxS is a transcriptional activator under the control of SoxR. Found co-located with *soxS* (Wu et al., 1991), *soxR* encodes the homodimer SoxR. SoxR is activated upon exposure to oxidative stress (paraquat and some antibiotics) (Nunoshiba et al., 1992) and nitrosylation. Upon activation, transcription of *soxS* is stimulated resulting in the upregulation of the expression of ≥ 20 genes associated with increased AcrAB-TolC expression. In the absence of this stress, SoxR binds to *soxS* preventing its transcription (Duval et al., 2013; Wu et al., 1991). Containing 289 amino acids and a C-terminal domain, Rob (encoded by *rob*) is a larger homologue of SoxS and MarA (Aleksun and Levy, 1997) and unlike MarA, RamA and SoxS, which are synthesised in response to a stimulus, Rob is constitutively expressed but sequestered until needed (Duval et al., 2013).

1.7 Inhibition of efflux pumps

In the relative absence of novel clinically approved antibiotics, attention has turned to the inhibition of efflux pumps as a strategy to reduce the impact of efflux-mediated bacterial

resistance. In addition to increasing the intracellular accumulation and thus potency of a given antibiotic, inhibition of efflux also has the potential to slow down the evolution of further antibiotic resistance by reducing the selective window during which target site mutations conferring resistance to an antibiotic can appear (Fange et al., 2009; Markham et al., 1999; Ricci, Tzakas, et al., 2006).

The following have been proposed as potential strategies to inhibit efflux by AcrAB-TolC:

- i. Disruption of the proton gradient that is essential to drive the rotation of the pump.
- ii. Modification of existing antibiotics so that they are not efflux pump substrates.
- iii. Prevention of protein assembly into a functional tripartite pump.
- iv. Inhibitors of AcrA which interact directly with the protein to disrupt assembly of the tripartite pump or disrupt AcrA functionality.
- v. Blocking the exit channel of TolC.
- vi. Prevention of antibiotic binding to AcrB by an inhibitor. This may be competitive or non-competitive. Non-competitive in that the compound induces changes in the conformation of the pump preventing substrate binding and/or restricts protein movement preventing substrate transport and extrusion. Or competitive, where the inhibitor is a preferential substrate and either occupies the same binding site blocking their binding, or is a preferential substrate and is extruded into the extracellular environment instead of, or before, the antibiotic.

This thesis focuses on the last category; the use of efflux inhibitors to prevent substrate binding and extrusion by AcrB. To qualify as an efflux inhibitor a compound should meet

the following criteria, it must (i) potentiate the activity of pump substrates, (ii) increase the accumulation and decrease the extrusion of pump substrates, (iii) not potentiate the activity of non-pump substrates, (iv) not potentiate the activity of antimicrobials in strains lacking an efflux pump and (v) not permeabilise the OM or interfere with the IM proton gradient (Lomovskaya, Warren, et al., 2001). These criteria were proposed to eliminate compounds with non-specific efflux activity as a result of off-target effects on the bacterial membrane. However, it is important to note that a compound failing to meet at least one of criteria i-v does not necessarily limit their use as an efflux inhibitor, but it is a strong indicator that this compound would also damage eukaryotic cells and exhibit cytotoxicity.

To date there are many compounds that have been shown to possess efflux inhibitory activities. The first of these were verapamil and reserpine (both anti-hypertensive drugs), capable of inhibiting efflux of fluoroquinolones by NorA of *S. aureus* (Aeschlimann et al., 1999; Ng et al., 1994). In subsequent years, a large effort has been made to identify additional inhibitors with greater potency. Broadly, these efflux inhibitors fall into one of two classes based on their origin: plant derived and synthetic inhibitors. In addition, a small number of inhibitors have been identified that are produced by microbial fermentation (Seukep et al., 2020; Sharma, Gupta, et al., 2019). Unfortunately, despite many of these inhibitors having vastly improved potency none have reached clinical development, largely due to their toxicity.

1.7.1 Deciphering the mode of action of efflux pump inhibitors

In order to develop efflux inhibitors with increased potency and reduced toxicity, it is important to understand their mode of action. Unfortunately, due to the structural complexity of tripartite efflux pumps it is difficult to undertake mode of action studies for efflux inhibitors.

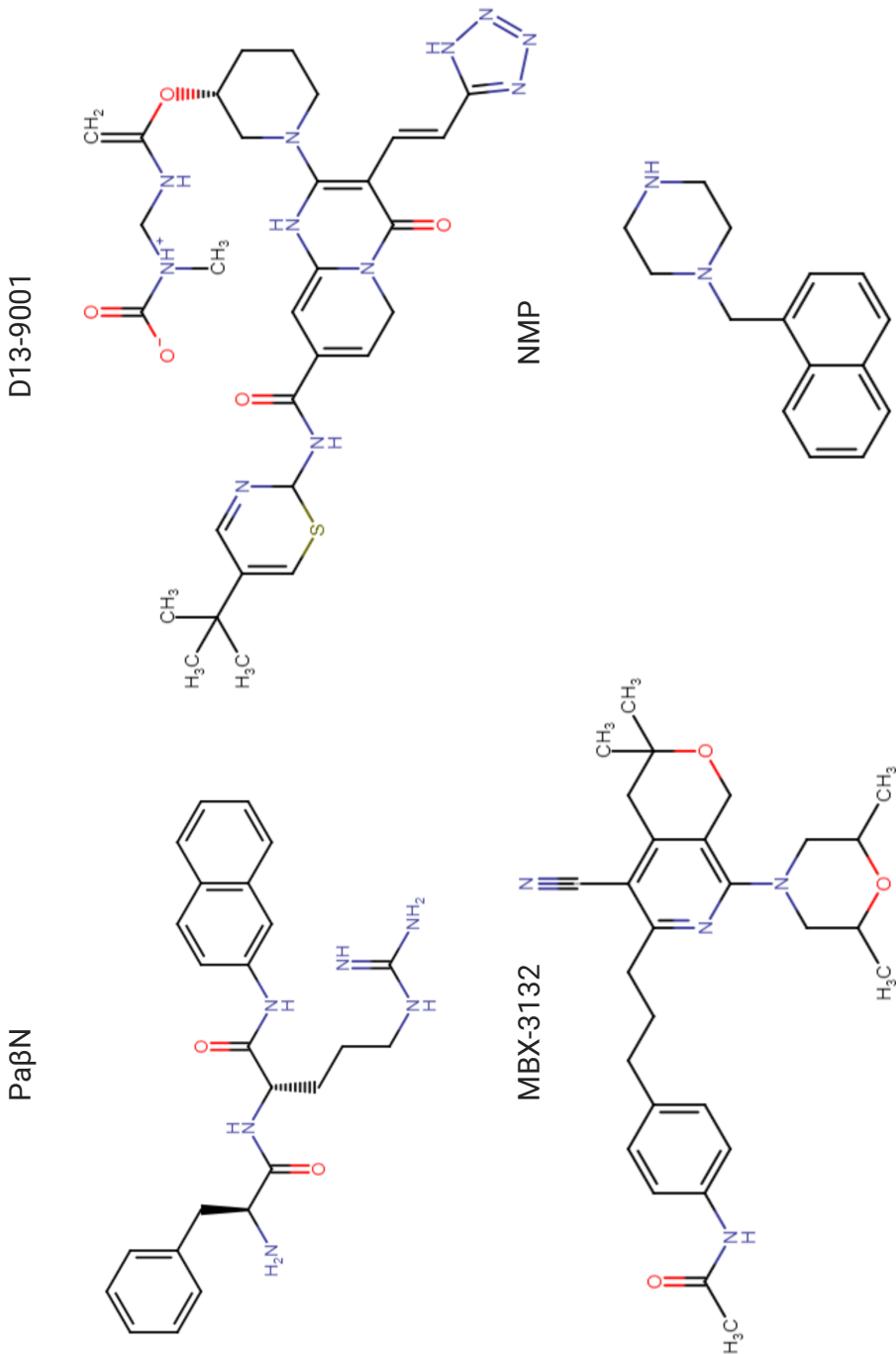
Classically, mutant selection experiments have been used to identify the molecular target of antibacterial agents. Unfortunately, this approach has not been very successful for

efflux inhibitors. This is predominantly because the majority of efflux inhibitors have very low antibacterial activity. This means it is difficult to directly select for mutants resistant to the inhibitors. Instead, mutants must be selected using an inhibitor in combination with an antibiotic substrate to provide the required selective pressure. Unfortunately, the selective pressure of the antibiotic typically selects for target site mutations, or mutations in resistance mechanisms such as porins, or efflux pump regulatory proteins, that result in resistance to the antibiotic rather than the inhibitor (Opperman and Nguyen, 2015). In addition, given that the binding sites of inhibitors and antibiotics within RND efflux pumps often overlap, mutations may arise that reduce the affinity for both agents alike rather than being specific for the efflux inhibitor (Lomovskaya and Bostian, 2006; Opperman and Nguyen, 2015). It is also difficult to select for spontaneous binding site mutations within RND pumps for both substrates and efflux inhibitors given the high plasticity of the substrate binding site; single point mutations within this region often do not significantly alter the MIC of pump substrates as the binding of substrates is not restricted to a single residue or amino acid region (Bohnert et al., 2008; Lomovskaya and Bostian, 2006; Opperman and Nguyen, 2015).

1.7.2 What is known about competitive efflux inhibitors?

Mutant selection experiments have been utilised in studies assessing the activity of efflux inhibitors. However, these have been of little use due to the reasons listed above. In 2014, Schuster et al undertook a serial passage experiment with the efflux inhibitors N-Methyl-2-pyrrolidone (NMP) and phe-arg beta naphthylamide (Pa β N) (Figure 1.12) in the presence of linezolid or clarithromycin. Exposure of *E. coli* to NMP resulted in the selection of the G288S mutation within the switch loop region of AcrB. No Pa β N-resistant mutants were produced with mutations in *acrAB-tolC*. The authors then used error-prone PCR to generate mutations within the two periplasmic loops of AcrB. Selection on agar

Figure 1.12: Structures of the efflux inhibitors PaßN, NMP, D13-9001 and MBX-3132.



Drawn using Biorender.

plates containing NMP and Pa β N in combination with clarithromycin revealed which mutations resulted in resistance to these inhibitors. While no mutants resistant to Pa β N were isolated, mutations conferring resistance towards NMP were found. The most frequently altered residues (G288, G141, A279 and N282) were all found near the phenylalanine rich binding pocket in close proximity to F610, a key residue in the substrate translocation process (Opperman and Nguyen, 2015; Schuster, Kohler, et al., 2014). Unfortunately, the mechanism of inhibition by NMP could not be deciphered from this mutational experiment as the substituted residues were not near the predicted binding site of this drug (Vargiu, Ruggerone, et al., 2014; Schuster, Kohler, et al., 2014).

Outside of genetic studies, the mode of action of efflux pump inhibitors has been assessed by a variety of different methods including antibiotic susceptibility assays, measurements of accumulation and efflux, ligand binding assays and X-ray crystallography. However, due to the complexity of RND efflux pumps and the difficulty producing co-crystals with efflux inhibitors, the use of computational methods have been used widely to study the interactions of efflux inhibitors and substrates with efflux proteins (Sjuts et al., 2016; Vargiu and Nikaido, 2012; Jewel et al., 2020; Ruggerone et al., 2013; Kinana et al., 2016; Tam et al., 2020; Vargiu, Collu, et al., 2011; Vargiu, Ramaswamy, et al., 2018).

The most commonplace method to determine a compounds ability to inhibit efflux is by the use of drug-susceptibility assays. i.e. determining the MIC of an antimicrobial in the presence and absence of an efflux inhibitor. Unfortunately, for some inhibitors, this approach is of limited use. This is because traditional chequerboard style synergy assays identify only large changes in MIC and subtle differences can be difficult to detect. Of greater use, is the utilisation of assays that measure efflux. Typically, these assays are divided into efflux (how much substrate is pumped out) and accumulation assays (how much substrate is kept in) in which the relative concentration of a fluorometric efflux substrate can be measured over time (Blair and Piddock, 2016). Fluorometric substrates commonly used include: ethidium

bromide (Paixão et al., 2009; Whittle et al., 2019), Rhodamine 6G (Coldham et al., 2010; Whittle et al., 2019), Nile Red (Whittle et al., 2019; Bohnert et al., 2008; Kern et al., 2006), nitrocefin (Misra et al., 2015; Nagano et al., 2009), Hoescht H33342 (Seigel et al., 2004) and fluoroquinolones (Coldham et al., 2010; Mortimer et al., 1993).

The nitrocefin (a β -lactam) efflux assay is a method that utilises the spectrophotometric change that occurs when nitrocefin is hydrolysed by β -lactamases within the periplasm. The kinetic parameters of this hydrolysis can be calculated and used to determine the affinity of substrates for AcrAB-TolC (Nagano et al., 2009; Lim et al., 2010). As a result, this assay has proved to be of particular use to characterise the activity of competitive efflux inhibitors of β -lactams.

Opperman et al (2014) assessed the effect of the efflux inhibitors MBX-2319 and Pa β N on the efflux of nitrocefin by AcrAB-TolC in *E. coli* (Opperman, Kwasny, et al., 2014). This study revealed that MBX-2319 inhibited the efflux of nitrocefin by causing a decrease in its K_m (the affinity of an enzyme for its substrate). From this data it was suggested that MBX-2319 behaves as a competitive efflux inhibitor inhibiting efflux by decreasing the access of nitrocefin for its binding sites. In this study, Pa β N did not affect the efflux of nitrocefin at the low concentrations assessed (0.2 to 10 μ M) (Opperman, Kwasny, et al., 2014; Opperman and Nguyen, 2015). However, Kinana (2016) showed that at a higher concentration of Pa β N (20 μ M) the efflux of nitrocefin was inhibited by competitive binding of Pa β N to the nitrocefin binding site of AcrB (Kinana et al., 2016). Unfortunately, the nitrocefin assay is also used to determine membrane permeabilisation (Misra et al., 2015; Reens et al., 2018; Misra et al., 2015). The greater the degree of membrane permeabilisation the more nitrocefin can cross the membrane and be hydrolysed in the intracellular environment. Therefore, it can be difficult to determine between true efflux inhibition and membrane permeabilisation using this assay.

Another method for determining the mode of action of efflux inhibitors relies on the use of ligand binding assays. Mowla et al (2018) assessed the interaction of the efflux inhibitors D13-9001, Pa β N and NMP with purified AcrB by surface plasmon resonance (SPR). It was revealed that all inhibitors bound AcrB with differing affinities. NMP and D13-9001 bound with a higher affinity than the substrates minocycline, doxorubicin and novobiocin, this is in agreement with their proposed mechanism of action as competitive efflux inhibitors. On the other hand, Pa β N (also suggested to be a competitive inhibitor) bound with a low affinity relative to the substrates. This suggests the potent activity of Pa β N as an efflux inhibitor may, in part, be a result of the ability of Pa β N to permeabilise the OM (Mowla et al., 2018).

The first X-ray crystal structure of an efflux inhibitor with AcrB was solved in 2013 (Nakashima, Sakurai, Yamasaki, Hayashi, et al., 2013). D13-9001 was found to bind via π - π interactions with F178 and F628 of the hydrophobic trap within the distal binding pocket of AcrB from *E.coli*. D13-9001 also interacted via its hydrophilic portion to polar residues within the upper groove of the distal binding pocket. It was suggested that the efflux inhibitory action of D13-9001 was that of a competitive efflux inhibitor; by binding to the groove region of AcrB of *E. coli*, D13-9001 was predicted to interfere with the binding of other substrates to this region. In addition, tight binding to the hydrophobic trap prevented the conformational changes that are essential for efflux activity (Nakashima, Sakurai, Yamasaki, Hayashi, et al., 2013; Opperman and Nguyen, 2015; Aron et al., 2018). The importance of the hydrophobic trap to the mechanism of competitive efflux inhibitors was confirmed when the crystal structure of AcrB was solved with the MBX series of pyranopyridines. Each compound was found to bind via hydrophobic interactions with residues lining the distal binding pocket, namely the hydrophobic trap (Sjuts et al., 2016). This was in agreement with the binding location of D13-9001 (Nakashima, Sakurai, Yamasaki, Hayashi, et al., 2013). Superimposition of the MBX-3132 binding sites overlapped with the binding sites of AcrB

substrates. This suggested a mechanism of competitive inhibition where binding of MBX-3132 hindered the binding of substrates to the distal binding pocket (Aron et al., 2018). Further work showed that MBX-3132 bound with very high affinity to AcrB and locked it in an inactive TTT conformation (Pos, 2009; Wang, Fan, et al., 2017).

Given the difficulty producing co-crystals of AcrB with efflux inhibitors much of the work regarding their mode of action has been undertaken using molecular docking and molecular dynamics simulations. Using computer docking, Takatsuka et al (2010) predicted that Pa β N and NMP are competitive inhibitors of AcrB, binding tightly to the groove and cave (Pa β N) and cave (NMP) regions of the AcrB distal binding pocket (Takatsuka, Chen, et al., 2010). Molecular dynamics simulations provided further evidence that Pa β N and NMP bound the lower (cave) region of the distal binding pocket at the hydrophobic trap, the same region as the AcrB substrates modelled. Unlike typical AcrB substrates, once bound Pa β N and NMP moved out of the distal pocket and partially contacted the switch loop that separates the distal from the access binding pocket (Vargiu and Nikaido, 2012; Nakashima, Sakurai, Yamasaki, Nishino, et al., 2011; Eicher, Cha, et al., 2012; Vargiu, Ruggerone, et al., 2014; Cha et al., 2014). By interacting with the G-loop, Pa β N and NMP can reduce the flexibility of this region and thus inhibit the peristaltic action by which the G-loop moves substrates from the access to the distal binding pocket (Vargiu, Ruggerone, et al., 2014).

Vargiu et al (2014) undertook a comprehensive study comparing the mechanism of AcrB inhibition of NMP, Pa β N, MBX-2319 and D13-9001 in the presence and absence of the AcrB substrate minocycline. All inhibitors bound to the upper groove of the distal binding pocket. The relative binding affinities of each inhibitor was from the highest to lowest affinity: D13-9001, MBX-2319, NMP and Pa β N, consistent with their potency as efflux inhibitors (Vargiu, Ruggerone, et al., 2014). All inhibitors, with the exception of D13-9001 were shown to induce conformational changes in the binding site of minocycline,

thereby reducing the affinity of this and other substrates for AcrB. This provided support to the hypothesis that many of these compounds are competitive efflux inhibitors (Vargiu, Ruggerone, et al., 2014; Ramaswamy et al., 2017; Opperman and Nguyen, 2015).

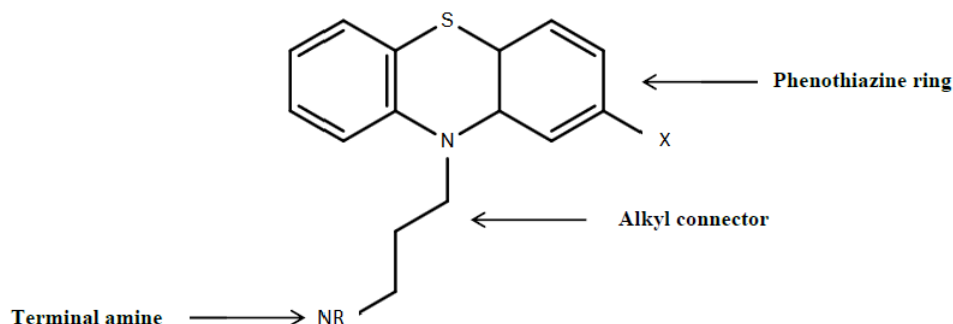
In terms of the differences between each inhibitor the binding positions of NMP, Pa β N, MBX-2319 and D13-9001 are similar. Although each compound interacts with the upper groove of the distal binding pocket, MBX-2319 and D13-9001 almost exclusively interact with the hydrophobic trap (D13-9001 does extend further into the upper groove than MBX-2319). Conversely, NMP and Pa β N occupy a smaller fraction of the groove region of the distal binding pocket as they are able to make contact with the switch loop (Vargiu, Ruggerone, et al., 2014).

1.7.3 Phenothiazines

In 1876 methylene blue was synthesised (Varga et al., 2017) and its derivatives have since amassed significant therapeutic importance due to their wide functional diversity (Taurand, 2000). The first of these derivatives, phenothiazine (synthesised in 1883), (Bernthsen et al., 1883) was found, in the 1930's to be antibacterial (Deeds et al., 1939). However, this was overshadowed when the sedative properties of the phenothiazine derivatives promethazine and chlorpromazine were observed in 1949. For many years the usefulness of phenothiazines in psychiatry was disputed and it wasn't until Elkes and Elkes undertook a successful, randomised and placebo controlled, clinical trial at The University of Birmingham (UK) in 1953 that phenothiazines were globally accepted as a viable clinical option for the treatment of psychological conditions (Elkes et al., 1954).

Phenothiazines all have the same three-ring structure containing one sulphur and a nitrogen atom at positions C-9 and C-10 of the tricyclic ring, respectively (Figure 1.13). The length of the linking alkyl connector, the terminal amine, as well as substituents at the C-2 position, determines the activity of the derivative (Jaszczyzyn et al., 2012). Phenothiazines

Figure 1.13: Chemical structure of the core unit of phenothiazines.



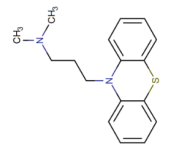
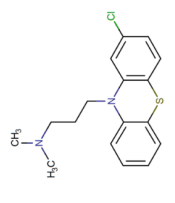
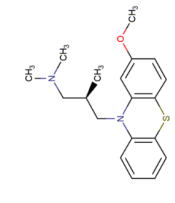
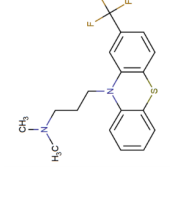
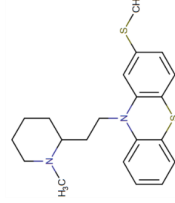
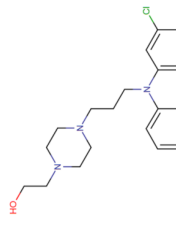
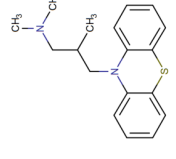
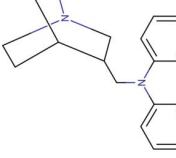
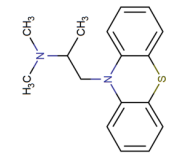
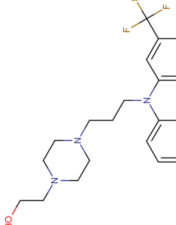
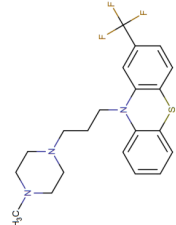
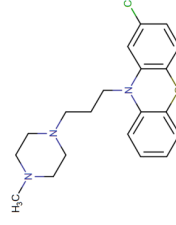
Drawn using ChemDraw.

are subdivided into three groups (piperazines, piperadines or aliphatic) dependent on the substituent at the nitrogen atom (Figure 1.14) (Archer et al., 1963).

1.7.4 Antibacterial activity of phenothiazines

Many of the phenothiazines have a broad range of antibacterial activities (both bacteriostatic and bactericidal) against *Mycobacteria*, some Gram-positive and Gram-negative bacteria (Bailey et al., 2008; Yamasaki, Fujioka, et al., 2016; Bettencourt et al., 2000; Kaatz et al., 2003; Nehme et al., 2018; Amaral, Kristiansen, et al., 2000). The *in vitro* activity of phenothiazines has been confirmed in an animal model. Of 60 Swiss albino mice challenged with the median lethal dose of *S. Typhimurium*, treatment with trifluoperazine at 15 and 30 $\mu\text{g}/20\text{ g}$ mouse (a sub MIC) reduced mortality by 84% and 87%, respectively (Mazumder et al., 2001). Fluphenazine and various other phenothiazine derivatives showed similar protective effects in *S. Typhimurium* and *E. coli* infection (Dastidar, Chaudhury, et al., 1995; Komatsu et al., 1997).

Figure 1.14: Chemical structures of the phenothiazines that possess antimicrobial activities.

Aliphatic				Piperidine
 Promazine	 Chlorpromazine	 Levopromazine	 Trifluopromazine	 Thioridazine
Piperazine				
 Perphenazine	 Trimeprazine	 Mequitazine	 Promethazine	
 Fluphenazine	 Trifluoperazine	 Prochlorperazine		

Drawn using ChemDraw Professional 16.0.

1.7.5 Proposed mechanisms of the antibacterial activity of phenothiazines

1.7.6 Effects on Bacterial Cellular Replication

The phenothiazines fluphenazine, thioridazine, perphenazine and chlorpromazine have been shown to bind to DNA either by intercalation with, or stacking on, the DNA helix (Ben-Hur et al., 1980; De Mol, Posthuma, et al., 1983; De Mol and Busker, 1984; Viola et al., 2003). Upon photo-ionisation there is a transfer of electrons between the DNA and the phenothiazine cations; this process is linked to single stranded DNA breaks (Viola et al., 2003). Upon intercalation with the DNA helix, the phenothiazine inhibits coiling and uncoiling of the helix as well as all DNA-based processes (De Mol, Posthuma, et al., 1983), most notably cellular replication (Eisenberg et al., 2008; Sharma, Kaur, et al., 2006). The degree to which phenothiazines can intercalate with DNA is dependent on the guanosine-cytosine content of the DNA helix (De Mol, Posthuma, et al., 1983).

1.7.7 Membrane Damaging Effects

The antibacterial activity of phenothiazines has been suggested to result from their ability to damage the bacterial membrane of Gram-positive and Gram-negative bacteria (Dastidar, Kristiansen, et al., 2013). At sub-MIC concentrations, phenothiazines increase OM permeability and fluidity, and depolarise the plasma membrane of *S. aureus* (Kaatz et al., 2003; Zilberstein, Liveanu, et al., 1990; Kristiansen, 1979). At low concentrations this membrane damage causes changes in cell structure and affects the functionality of many inner and outer membrane-bound proteins (Labedan, 1988; Plenge-Tellechea et al., 2018). This effect of phenothiazines on the outer and inner membrane may be due to the cationic charge and amphiphilic nature of the compounds. In human erythrocytes and model cell membranes the amphiphilic properties of chlorpromazine have been shown to allow the hydrophobic tricyclic structure to partition into the inner portion of the lipid bilayer and interact with

the lipid tails, while the hydrophilic propylamine tail of chlorpromazine is able to interact with the polar headgroups (Jiang et al., 2017; Plenge-Tellechea et al., 2018). When present in the lipid bilayer, chlorpromazine can assist in lipid translocation and has been shown to cause dissolution of the lipid bilayer at high concentrations (>5 mM) (Jiang et al., 2017). Although limited in-depth studies have been performed in bacterial cells, and despite differences in the bacterial cell membrane of eukaryotes and prokaryotes, it has been hypothesised that phenothiazines may affect the bacterial membrane in a similar manner to that described for mammalian cells (Kristiansen, 1979).

1.7.8 Effects on Energy Generation

Phenothiazines have been widely reported to affect the flux of ions across the bacterial membrane. An increase in calcium influx and potassium efflux has been noted at sub-MIC concentrations of chlorpromazine and thioridazine in a variety of bacterial and fungal species including *S. aureus* and *Saccharomyces cerevisiae* (Zilberstein, Liveanu, et al., 1990; Kristiansen, 1979; Eilam, 1983; Eilam, 1984; Kristiansen, Mortensen, et al., 1982). The addition of high concentrations of each cation partially reverses this effect, with higher concentrations of phenothiazine being required to elicit the same response. The effect of phenothiazines on ion flux has been shown to be dependent on the presence of metabolic energy with the removal of glucose causing reversion of the cell to a pre-exposure phenotype (Eilam, 1983). This suggests that the phenothiazine does not affect ion flux simply through increased membrane permeability. The hypothesis that phenothiazines require energy for uptake into the cell was not supported as chlorpromazine was able to cross the bacterial membrane in the absence of glucose (Eilam, 1984). This effect of phenothiazines on ion flux has been suggested to occur by one, or both, of two mechanisms. The first is a result of inhibition of calcium-dependent processes and the second is a result of disruption of cation-dependent ATPases (Eilam, 1983; Eilam, 1984; Zilberstein, Liveanu, et al., 1990).

The changes in ion flux induced by phenothiazines results in disruption of the bacterial membrane potential and PMF (Kaatz et al., 2003; Zilberstein, Liveanu, et al., 1990). Any change in the flux of ions across the membrane can alter the membrane potential and result in hyperpolarisation or depolarisation of the membrane (Krulwich et al., 2011; Lodish et al., 2000). Though a change in a single component of the PMF is usually buffered by a counteracting increase in the other, a change in either the membrane potential or pH gradient can cause a disturbance in the maintenance of the PMF, which can have detrimental impacts in terms of metabolism and energy-dependent cellular process (Farha et al., 2013). Such processes include ATP synthesis, cell division (Strahl et al., 2010), efflux of toxic substances (Paulsen et al., 1996), flagellar motility (Manson et al., 1977) and nutrient uptake (Tanaka et al., 2018).

Phenothiazines have been shown to inhibit many ATPases found in eukaryotic and microbial cells though changes in their conformation, including: F_1F_0 -ATPase, Na^+/K^+ -ATPase, Ca^{2+}/Mg^{2+} -ATPase and Ca^{2+} -ATPase (Bhattacharyya et al., 1999; Bullough et al., 1985; Dabbeni-Sala et al., 1990). Detailed experiments of the interaction of phenothiazines with ATPases have been primarily conducted using those from mitochondrion or erythrocytes. However, ATPases from bacterial sources possess very similar structural and functional features and may be expected to respond to phenothiazines in a similar manner. Given that ATP synthases play the primary role in energy generation and maintenance of the PMF, inhibition of these proteins by phenothiazines may lead to detrimental cellular effects.

1.7.9 Use of phenothiazines as antibiotic adjuvants

While the antimicrobial activities of phenothiazines generally occur at concentrations greater than those clinically achievable, the potential of phenothiazines to be used as antibiotic adjuvants was noted as early as 1969 (Manion et al., 1969). Manion

et al., 1969 observed that isoniazid resistance in *Mycobacterium* can be delayed or prevented when combined with sub-inhibitory concentrations of phenothiazine. The mechanism was not reported. More recently, it has been shown that phenothiazines are able to inhibit the formation of biofilms (Baugh et al., 2012), act as plasmid curing agents (Mándi et al., 1975; Spengler et al., 2003), potentiate the activity of antibiotics and increase the intracellular accumulation of efflux pump substrates (Bailey et al., 2008; Kaatz et al., 2003; Amaral, Kristiansen, et al., 2000; Yamasaki, Fujioka, et al., 2016).

1.7.10 Chlorpromazine as an Efflux Inhibitor

Chlorpromazine and other phenothiazines potentiate the activity of, and increase the intracellular concentration of antibiotics against a wide range of bacterial species (Kaatz et al., 2003; Bailey et al., 2008; Coutinho et al., 2009; Kristiansen, Hendricks, et al., 2007; Viveiros et al., 2005). This potentiation has been rationalised by the ability of phenothiazines to inhibit efflux pumps. However, very little is known about the mechanism by which this occurs. Because the vast majority of research regarding phenothiazines as efflux inhibitors has centered on chlorpromazine and has been undertaken in the context of the AcrAB-TolC complex of *Salmonella* and *E. coli*, here only the efflux inhibitory activity of chlorpromazine against AcrAB-TolC will be discussed.

Chlorpromazine has been suggested to inhibit the AcrAB-TolC efflux pump as evidenced by (i) potentiation of the activity of a wide range of AcrB substrates against *E. coli* and *S. Typhimurium* and (ii) an increase in the intracellular accumulation of AcrB substrates including ciprofloxacin, norfloxacin, ethidium bromide and Hoescht H33342 against the same organisms (Kaatz et al., 2003; Bailey et al., 2008; Yamasaki, Fujioka, et al., 2016). These activities occur at sub-MICs of chlorpromazine.

Interestingly, hypersusceptibility of *S. Typhimurium* to chlorpromazine results when efflux pump genes (*acrB*, *acrD*, *acrF* and *tolC*) or regulatory genes (*marA* and *ramA*) are

deleted; deletion of *acrB* and *tolC* result in the greatest decrease in MIC in relation to wild type *S. Typhimurium* (Bailey et al., 2008; Yamasaki, Fujioka, et al., 2016). In addition, the overexpression of *acrAB* decreases the susceptibility of a Δ *acrB* *S. Typhimurium* strain to chlorpromazine (Yamasaki, Fujioka, et al., 2016). Another important finding is that chlorpromazine exerted no efflux inhibitory effects when used against an *acrB*-deficient strain (Yamasaki, Fujioka, et al., 2016). Together, this data indicates chlorpromazine may elicit its activity through direct interactions with AcrAB-TolC or its regulatory system.

Effect of Chlorpromazine on AcrAB-TolC Gene Expression

Bailey et al., 2008 showed that 200 μ g/ml of chlorpromazine increased the expression of *ramA*, whilst simultaneously causing a reduction in the expression of *acrB*. This reduction in expression correlated with an increase in the susceptibility of *S. Typhimurium* for a variety of AcrAB-TolC substrates (Lawler et al., 2013). Furthermore, chlorpromazine and other phenothiazines increased the expression of *ramA* to levels greater than those observed in response to inactivation of *acrB* (Lawler et al., 2013). Although inactivation of the transcriptional activator *ramA* conferred increased susceptibility to chlorpromazine, their data indicated that chlorpromazine did not directly induce the expression of *ramA* (Bailey et al., 2008). Instead, it was proposed that chlorpromazine either binds directly to AcrB inactivating it, or reduces the expression of this protein via interactions with regulatory proteins, or via an unknown mechanism. As a response, the bacterium compensates for the lack of AcrB via a positive feedback mechanism on *ramA*. This may occur from increased intracellular accumulation of metabolites that may bind to the transcriptional repressor RamR increasing *ramA* transcription (Lawler et al., 2013).

1.7.11 The efflux inhibitory activity of other phenothiazines

Apart from chlorpromazine, little work has been done regarding the mode of action of phenothiazines as efflux inhibitors. However, recently Wassmann et al. 2018 selected

for *S. aureus* mutants resistant to thioridazine. These mutants contained mutations in *cls*, important for the synthesis of membrane cardiolipin. Given that thioridazine interacts with negatively charged phospholipids, the authors proposed that thioridazine may bind to cardiolipin allowing it to pass into, and accumulate within, the cytoplasmic membrane. This disturbance of the membrane in turn damages the electrochemical gradient giving rise to the inhibition of a variety of energy-dependent processes. Interestingly, growth kinetic experiments revealed that while deletion of *cls* resulted in resistance to thioridazine, the strain had a growth kinetic profile similar to the wild type when thioridazine was used in combination with dicloxacillin. Therefore, while cardiolipin was suggested to be important for the bactericidal activity of thioridazine it was not essential when considering the ability of thioridazine to potentiate the activity of antibiotics (Wassmann, et al., 2018).

1.7.12 Non-selectivity of chlorpromazine as an efflux inhibitor

As discussed, chlorpromazine has multiple modes of action including effects on the bacterial membrane, cellular replication and energy generation, as well as several effects on mammalian cells. Therefore, while this compound may directly interact with the AcrAB-TolC protein complex, it is unlikely that its efflux inhibitory effects are selective. Indeed, the non-specific effect of chlorpromazine may contribute to its ability to inhibit efflux. In addition, these non-specific effects may contribute to the mechanism underlying its high cytotoxicity.

1.7.13 Clinical usefulness of phenothiazines

The clinical use of phenothiazines as antibiotic adjuvants is limited by their cytotoxicity; chlorpromazine, fluphenazine, thioridazine, trifluoperazine and triflupromazine are toxic to hepatoma tissue culture cells, with EC₅₀ values of 45 to 125 μ M (Faria et al., 2015). The piperidinic class are the most toxic. This cytotoxicity means the average achievable human serum levels (30-100 ng/ml, 0.15-2.5 ng/ml and 0.5-3.0 ng/ml for

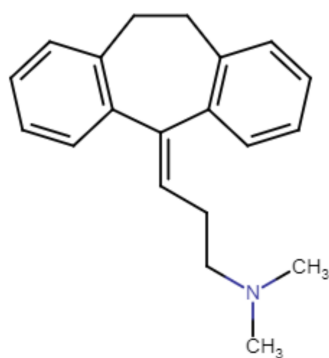
chlorpromazine, thioridazine and trifluoperazine, respectively) are $\sim 1,000$ fold lower than the concentration at which antibacterial activity is detected. However, there is a large inter-individual variation in the pharmacokinetics. An issue with the pharmacological data for phenothiazines is that most is derived from steady state dosing as opposed to a C_{\max} for a single dose; which may be more appropriate for the use of these drugs as an antibiotic adjuvant. In all cases, the metabolites are often more psychoactive and persistent but little is known about their antibacterial effects.

1.7.14 Efflux inhibitory activity of amitriptyline

Like chlorpromazine, amitriptyline is a tricyclic antidepressant capable of inhibiting efflux by the AcrAB-TolC pump (Figure 1.15). In relation to chlorpromazine, even less is known about the mode of action underlying the efflux inhibitory activity of amitriptyline. However, like chlorpromazine, amitriptyline (against *S. Typhimurium*) possesses its own antimicrobial activity, synergises with antibiotics and increases the accumulation of the AcrB substrate ethidium bromide (Bailey et al., 2008). In addition, hypersusceptibility to amitriptyline occurs when *ramA* is deleted in *S. Typhimurium* and exposure to amitriptyline results in the induction of *ramA* (Lawler et al., 2013). Given this, it is proposed that amitriptyline possesses a mode of action similar to that exhibited by chlorpromazine and inhibits efflux by *S. Typhimurium* through interactions with the AcrB pump protein.

In further support of this hypothesis, it has been noted that the efflux inhibitor Pa β N was able to potentiate the antimicrobial activity of amitriptyline against clinical *E. coli* isolates (Laudy et al., 2017). Given that the activity of Pa β N has been, in part, rationalised by interactions with AcrB, the authors concluded that amitriptyline is likely a substrate of AcrAB-TolC able to pass through the AcrB pump of *E. coli*.

Figure 1.15: Structure of amitriptyline



Drawn using Chemdrawn 18.0.

Chapter Two

Materials and Methods

2.1 Bacterial strains, growth and identification

Salmonella enterica serovar Typhimurium SL1344 (Wray et al., 1978) and *Escherichia coli* K-12 MG1655 (Blattner et al., 1997) were used as the wild type strains throughout. *E. coli* MG1655 was one of the model organisms of choice as AcrAB-TolC is most frequently studied, and as a consequence most well understood, in this organism. In addition, at the time of writing a crystal structure for AcrB and the AcrAB-TolC tripartite complex had only been solved for *E. coli*. *S. Typhimurium* contains an AcrAB-TolC pump with a very high degree of similarity with that of *E. coli* and has also been used widely in the context of AcrAB-TolC, particularly when considering the activity of efflux pump inhibitors. In the Piddock Laboratory *S. Typhimurium* is used as the model organism when considering the activity of and inhibition of AcrAB-TolC.

All bacterial strains were routinely grown under static incubation at 37°C on Lennox lysogeny agar (Sigma, UK, L2897), supplemented with antibiotics where appropriate. Overnight liquid cultures were grown in lysogeny broth (LB) (Sigma, USA, L3022), Iso-sensitest broth (Oxoid, UK, CM0473) or 3-(N-morpholino)propanesulfonic acid (MOPs) minimal medium at 37°C under shaking incubation (180 rpm) in an Inova 44

shaking incubator (New Brunswick, UK). MOPs minimal medium was prepared by adding 100 ml of 10 X MOPs buffer (Teknova, USA, M2106) to 10 ml of 0.132 M dipotassium phosphate (Teknova, USA, M2102) and 10 ml of 20% glucose (Teknova, USA, G0520). For *S. Typhimurium* SL1344, MOPs minimal medium was supplemented with 25 μ M of histidine (Sigma, UK, HG100) to allow for growth. For *E. coli* MG1655 MOPs minimal medium was supplemented with 1 μ g/ml of thiamine (Sigma, UK, T4625). All bacterial strains used throughout this study are listed in Table 2.1. All strains and working stocks were stored at -80°C and -20°C, respectively on ProtectTM cryopreservation beads (Technical Service Consultants, UK, Tn/80-GN).

Table 2.1 Bacterial strains used throughout this project.

Bacterial species	Genotype	Resistance phenotype	Laboratory strain	Source
<i>S. Typhimurium</i> SL1344	Wild type		L354	(Wray et al., 1978)
	<i>ramR::aph</i>	Kan ^R	L1322	(Ricci, Busby, et al., 2012)
	RamR L158P		L1870	This study
	RecN R78H, BarA R9A*fs10, GyrA S83F		L1876	This study
	GyrA S83F		L1912	This study
	BamEW73STOP		L1873	This study
	BamEV26Gfs*50		L1874	This study
	AcrB D408A		L1804	(Wang-Kan et al., 2017)
	Wild type with pMW82	Amp ^R	L1407	(Lawler et al., 2013)
	Wild type with pMW82- <i>pramA</i>	Amp ^R	L1232	(Lawler et al., 2013)
	Wild type with pMW82- <i>pacrAB</i>	Amp ^R	L1852	(Ricci, Attah, et al., 2017)
	RamR L158P with pMW82	Amp ^R	L1933	This study
	RamR L158P with pMW82- <i>pramA</i>	Amp ^R	L1948	This study
	RamR L158P with pMW82- <i>pacrAB</i>	Amp ^R	L1929	This study
	<i>ramR::aph</i> with pMW82	Amp ^R	L1934	This study
	<i>ramR::aph</i> with pMW82- <i>pramA</i>	Amp ^R	L1409	This study
	<i>ramR::aph</i> with pMW82- <i>pacrAB</i>	Amp ^R	L1705	This study
<i>E. coli</i> MG1655	Wild type		I364	(Blattner et al., 1997)
	<i>marR::aph</i>	Kan ^R	I1205	This study
	MarR K141Sfs*150		I1145	This study
	MarR A105Rfs*114		I1147	This study
	AcrB D408A		I1124	(Wang-Kan et al., 2017)
	AcrB D408A PitB A38V		I1204	This study

Wild type with pMW82	Amp ^R	I1149	Marshall, unpublished
Wild type with pMW82- <i>pmarA</i>	Amp ^R	I886	Marshall, unpublished
Wild type with pMW82- <i>pacrAB</i>	Amp ^R	I1206	Marshall, unpublished
MarR K141Sfs*150 with pMW82	Amp ^R	I1219	This study
MarR K141Sfs*150 with pMW82- <i>pmarA</i>	Amp ^R	I1212	This study
MarR K141Sfs*150 with pMW82- <i>pacrAB</i>	Amp ^R	I1209	This study
MarR A105Rfs*114 with pMW82	Amp ^R	I1220	This study
MarR A105Rfs*114 with pMW82- <i>pmarA</i>	Amp ^R	I1213	This study
MarR A105Rfs*114 with pMW82- <i>pacrAB</i>	Amp ^R	I1210	This study
<i>marR::aph</i> with pMW82	Amp ^R	I1221	This study
<i>marR::aph</i> with pMW82- <i>pmarA</i>	Amp ^R	I1214	This study
<i>marR::aph</i> with pMW82- <i>pacrAB</i>	Amp ^R	I1211	This study
Wild type with pSIM18	Hgr ^R		(Chan et al., 2007)
<i>marR::aph</i>	Kan ^R	I1116	(Baba et al., 2006)
<i>bamE::aph</i>	Kan ^R	I1304	(Baba et al., 2006)
<i>barA::aph</i>	Kan ^R	I1304	(Baba et al., 2006)
<i>recN::aph</i>	Kan ^R	I1305	(Baba et al., 2006)
<i>E. coli</i> DE3 BL21 pTrc RamR-His	Amp ^R	L1936	This study
pTrc RamR L158P-His	Amp ^R	L1938	This study
pTrc MarR-His	Amp ^R	I1222	This study
pTrc MarR K141Sfs*150-His	Amp ^R	I1223	This study
pTrc MarR A105Rfs*114-His	Amp ^R	I1223	This study
<i>P. aeruginosa</i> K1454 NalC S127P		G134	(Srikumar et al., 2000)
<i>A. baumannii</i> AB211 AdeS A94V		C94	(Hornsey et al., 2011)

Kanamycin, Kan. Ampicillin, Amp. Hygromycin, Hgy.

All strains were routinely purity checked by API-20E tests (Biomérieux, France, 20100) and Gram-staining. The API-20E utilises a series of biochemical tests that allow for the identification of *Enterobacteriales* species. A single colony was resuspended in 5 ml of sterile distilled water. This suspension was dispensed into the wells of the API-20E test strip and the strip was incubated, under static incubation, overnight at 37°C. The results were recorded and interpreted as per the manufacturers instructions (<http://biomanufacturing.org/uploads/files/587872707301898351-api20einstructions.pdf>).

2.2 Molecular biology techniques

2.2.1 Polymerase chain reaction (PCR)

PCRs were performed using a SensoQuest thermocycler (Geneflow, UK). For colony PCR, a single colony was resuspended in 50 µl of nuclease free water and the suspension boiled for 5 minutes, followed by centrifugation in a table top refrigerated centrifuge (Eppendorf, UK) (room temperature, 3,600 xg, 30 secs). The following reaction mixture was used: 45 µL of 1 X MyTaqTM Red master mix (Bioline, UK, BIO-25043), 1 µl of each primer (25µM) and 5 µl of lysed template DNA. Each primer was produced by Invitrogen (Invitrogen, UK) and the primers are listed in Table 2.2. The melting temperature of each primer was calculated using the NEB TM calculator (<https://tmcalculator.neb.com/#!/main>).

The generic cycling parameters used for each PCR, unless otherwise stated, are shown in Table 2.3. The resulting PCR amplicon was purified using the QIAquick[®] PCR Purification Kit (QIAGEN, Germany, 28104) and the amplicon was eluted in 30 µl of nuclease free water to both minimise the concentration of salt when needed (to ensure successful electroporation) and maximise the DNA yield (for successful DNA sequencing). The purified PCR amplicon was separated by gel electrophoresis for approximately 1 hour at 100 V on a 1% agarose gel. The gel was prepared by dissolving agarose (Fischer Scientific, UK, BP1356) in 1 X Tris-borate-EDTA (TBE) (Merck, UK, 11666703001) buffer

Table 2.2 Primers used throughout this project.

Primer number	Primer	Sequence	Annealing temperature (°C)	Purpose of the primer
2012	<i>gyrA</i> fwd	ATACAGTAGAGGGATAGCGG	58	Amplification of the <i>S. Typhimurium gyrA</i> gene. Primers bind up and downstream of the <i>gyrA</i> gene
2013	<i>gyrA</i> rev	CCGTACCGTCATAGTTATCC	58	
1262	<i>ramR</i> fwd	GCGGGATCCTTGACATTCCAC CGTTGCGAC	68	Amplification of the <i>S. Typhimurium ramR</i> gene. Primers bind up and downstream of the <i>ramR</i> gene
1263	<i>ramR</i> rev	GCGGGATCCAGGCCAGCAGT GTTCGGTAA	68	
1528	<i>marR</i> fwd	ACCTGACGGCGGACGAAGTGGC	68	Amplification of the <i>E. coli marR</i> gene. Primers bind up and downstream of the <i>marR</i> gene
1529	<i>marR</i> rev	GTTCCGCAACGCCCTGGCGG	58	
2326	<i>bamE</i> fwd	TCTCGTTCCGGGCTATCAT	65	Amplification the first 300bp of the <i>S. Typhimurium barA</i> gene
2327	<i>bamE</i> rev	GGACGCTGATAAGTTGGCCG	65	
2328	<i>barA</i> fwd	CTGGCCCGCCTGTTGGGAGG	63	Amplification of the <i>S. Typhimurium barA</i> gene. Primers bind up and downstream of the <i>barA</i> gene.
2329	<i>barA</i> rev	GCATTACGCCGCCAGCGCGC	63	
2330	<i>recN</i> fwd	TGTTGGCGCAACTGACCATC	58	Amplification of the first 460bp of the <i>S. Typhimurium recN</i> gene.

2331	<i>recN</i> rev	GCGGCTTCGTTGGCATAGCT	58	
2384	<i>marR::aph</i> fwd	TAAAGCAAAGCTTTAGCTAACG GCAGCAACACC	58	Amplification of <i>marR::aph</i> from <i>E. coli</i> BW25113 <i>marR::aph</i> . Primers bind 200bp up and downstream of the <i>marR</i> gene.
2385	<i>marR::aph</i> rev	TGCTTACCTACGATTCCAGGTTG TCCTCGATC	58	
2386	pTrc- <i>ramR</i> fwd	GCTCGTCCGAAAGAGTGAAGACA AAAAACAAGCATTAAGGCGG CAACCCAGGCGATAGCG	58	Amplification of the <i>S. Typhimurium ramR</i> gene for TA cloning. Contains a cleavable His tag linker.
2387	pTrc - <i>ramR</i> rev	TCAATGATGATGATGATGGC TACCGCGGGAACAAGAGCAGCTT GCTCCTCGCGAGTCAGCG	58	
2388	pTrc- <i>marR</i> (1) fwd	AAAAGTACCAGCGATCTGTCAA TGAAATTATTCATTGGGTCGCTT AATCCATATGGTTAATCAGAAGA	53	Amplification of the <i>E. coli marR</i> gene for TA cloning. Contains a cleavage His tag linker. Used to amplify from MG1655 MarR wildtype and A105Rfs*114
2389	pTrc- <i>marR</i> (1) rev	TCAATGATGATGATGATGGC TACCGCGGGAACAAGAGCAGCCG GCAGGACTTTCTTAAGCA	53	Amplification of the <i>E. coli marR</i> gene for TA cloning. Contains a cleavage His tag linker. Used to amplify from MG1655 MarR wild type, K141Sfs*150 and A105Rfs*114

2390	pTrc- <i>marR</i> (2) rev	TCAATGATGATGATGATGGC TACCGCGGGAACAAGAGCAGCCGG CAGGACTTTTAAAGCAAATAC	53	Amplification of the <i>E. coli marR</i> gene for TA cloning. Contains a cleavage His tag linker. Used to amplify from MG1655 MarR K141Sfs*150
2391	pTrc check fwd	GAGAAAAAGCGAAGCGGCAC	58	Amplification of a portion of pTrc containing the inserted <i>ramR</i> or <i>marR</i> gene. Used to check that TA cloning was successful.
2392	pTrc check rev	TGAAAAATCTTCTCTCATCCGCC	58	
1233	<i>PramA</i> fwd	GGGTCTAGACTCTATCAAACTCGTC AGCG	65	Amplification of the <i>S. Typhimurium ramA</i> promoter
1240	<i>PramA</i> rev	GGCTCTAGAGTTGACATTCAACCGTT GCGA	65	
234	ST <i>acrB</i> fwd	GGATCACACCTTATTGCCAG		Amplification of the <i>S. Typhimurium acrB</i> gene Primers bind up and downstream of the <i>acrB</i> gene.
235	ST <i>acrB</i> rev	CGGCCTTATCAACAGTGAGC		
332	EC <i>acrB</i> fwd	CTGATCACCCAGTGACGGCAT		Amplification of the <i>E. coli acrB</i> gene Primers bind up and downstream of the <i>acrB</i> gene.
333	EC <i>acrB</i> rev	CGTATGAGATCCTGAGTTGG		

2627	EC <i>pitB</i> fwd	CTTGATATATCCACAGGCG	57	Amplification of the <i>E. coli pitB</i> gene. Primers bind up and downstream of the <i>acrB</i> gene
2628	EC <i>pitB</i> rev	GACAATGGCATAGGCAACG	57	
2600	ST <i>acrB</i> 408D fwd	CATCGGCTTGCTGGTGGATGA	72	Amplification of the AcrB 408D allele
2601	ST <i>acrB</i> 408A fwd	CATCGGCTTGCTGGTGGATAC	72	Amplification of the AcrB 408A allele
2602	ST <i>acrB</i> 408A/D rev	GATCGGGCCAGTCTTTCAACG	72	Amplification of the AcrB 408A/D allele
1057	ST <i>acrB</i> RT-PCR fwd	GTCCTCAAGTAGCTTCCT	57	Used for amplification of <i>acrB</i> by RT-PCR
1058	ST <i>acrB</i> RT-PCR rev	GTAATCCGAAATATCCTCCTG	57	
932	ST <i>rrsH</i> RT-PCR fwd	TACCTGGTCTTGACAT	54	Used for amplification of <i>rrsH</i> , as a measure of 16s, by RT-PCR
933	ST <i>rrsH</i> RT-PCR rev	GACTTAACCCCAACATTTC	54	

with 0.05 µg/ml of Midori Green Advance (Nippon Genetics, Japan, MG04). The stained nucleic acids were visualised under a blue light transilluminator using the G:BOX gel documentation system (Syngene, UK). A 1 Kb Hyperladder (Bioline, UK, H1-618110A) and a negative contamination control containing no template DNA was electrophoresed in a well alongside each PCR amplimer.

Table 2.3 Generic PCR cycling conditions when using the MyTaqTM Red master mix

Cycle	Temperature	Time	Number of cycles
Initial denaturation	95°C	5 minutes	1
Denaturation	95°C	30 seconds	30
Primer annealing	*°C	30 seconds	30
Extension	72°C	1 minute per kb of amplimer	30
Final extension	72°C	3 minutes	1

* The annealing temperature used for each primer pair is shown in Table 2.2.

2.2.2 DNA sequencing of PCR amplimers

The DNA concentration of the purified PCR product was quantified using a Nanodrop spectrophotometer (Thermo Scientific, UK). For sequencing the following reaction was set up: 0.32 pg/ml of the forward primer with 5-10 ng of DNA was made to a final volume of 10 µl with nuclease free water. A second reaction was made with the reverse primer. The reactions were sequenced by the Functional Genomics Laboratory (The University of Birmingham, UK), where each sample was labelled and sequenced with a BigDye[®] Cycle Terminator Sequencing kit (Applied Biosciences, USA, 4337455) and a ABI 3730 Capillary sequencer (Applied Biosystems, USA). The sequences were visualised as chromatograms in Chromas (Version 2.6) and subsequently exported in FASTA format and aligned to the respective reference sequence using the Multiple Sequence Alignment tool from Clustal Omega (EMBL-EBI) (<https://www.ebi.ac.uk/Tools/msa/clustalo/>).

2.2.3 Isolation of plasmids

The plasmids used in this study are detailed in Table 2.4. Cultures of plasmid-containing strains were grown overnight at 37°C, or 30°C if the plasmid contained a temperature sensitive origin of replication, under shaking incubation (180 rpm) in an Inova 44 shaking incubator. The culture was centrifuged (3,600 xg RPM, 2 minutes) in a Hereaus Megafuge 40R and the pellet was prepared for plasmid isolation with the GeneJET Plasmid Miniprep Kit (Thermo Scientific, UK, K0502). Each plasmid was eluted in 30 µl of nuclease free water and stored at -20°C until use.

Table 2.4 Plasmids used in this study.

Plasmid	Description	Antibiotic resistance markers	References
pMW82	Medium copy promoter trap vector containing a promoterless <i>gfp</i> gene. Used for gene reporting.	Amp ^R	(Bumann et al., 2007)
pTrc-His	Used for high-level gene expression, under the control of an inducible <i>trc</i> promoter, in <i>E. coli</i> . Contains a N-terminal polyhistidine tag.	Amp ^R	(Gupta et al., 1997)
pSIM18	A temperature sensitive, low copy number vector containing the lambda recombinase system.	Hgr ^R	(Chan et al., 2007)
pUC19	A high copy number vector with an empty backbone. Used as a cloning vector.	Amp ^R	(Norrandar et al., 1983)

Kanamycin, Kan; ampicillin, Amp; hygromycin, Hgr.

2.2.4 Preparation of electrocompetant cells

A starting culture was prepared by inoculating 100 ml of culture with 2 ml of overnight culture followed by incubation at 37°C, under shaking incubation (180 rpm) in a Innova 44 incubator until an OD₆₀₀ of 0.6-0.8 was reached. Once reached, the culture was divided into

two 50 ml falcon tubes (Greiner Bio-One, Germany, 227261), centrifuged in a Herasus 40R megacentrifuge (4°C, 3,600 xg, 10 minutes) and the supernatant discarded. The pellet was transferred to ice and resuspended in 10 ml of ice cold 15% glycerol (Fisher Reagents, USA, BP229-1). After three washes in 15% glycerol, each pellet was resuspended in 1ml of 15 % glycerol and transferred to two 1.5 ml microcentrifuge tubes (Greiner Bio-One, Germany, 616201). Finally, each tube was centrifuged (4°C, 3,600 xg, 2 minutes) and the pellets resuspended in 200 µl of 15% glycerol. Each aliquot was stored at -80°C until further use.

2.2.5 Electroporation

Once thawed on ice, 50 µl of eletrocompetant cells were transferred to an ice cold electroporation cuvette (Geneflow, UK, E6-0060). For electroporation, 2 µl of plasmid was added to the cuvette, pipetted up and down and the mixture incubated on ice for five minutes to allow interaction of the plasmid with the cells. A positive control with pUC19 and a negative control with nuclease free water was also set up. A gene Pulser II electroporator (Bio Rad, USA) was used and a current (2.5 kV) applied to the cuvette for five seconds. The electroporated cells were immediately transferred to 1 ml of LB broth (warmed to 37°C) and the cells were left to recover for 1.5 hours at 37°C under shaking incubation (180 rpm) in a Innova 44 shaking incubator, or for 2-3 hours at 30°C if the plasmid had a temperature sensitive origin of replication. After recovery, 100 µl of the bacterial suspension was plated onto LB agar, containing the appropriate antibiotic, and incubated overnight at 37°C. An additional 100 µl was plated onto LB agar containing no antibiotic to determine the viability of the bacterial cells. The remaining bacterial suspension was left overnight on the bench at room temperature, and in the instance of no initial transformants, was centrifuged and 100 µl plated onto LB agar with antibiotics and incubated overnight at 37°C.

2.3 Susceptibility of strains to AcrB substrates in the presence and absence of efflux inhibitors

2.3.1 Determination of the minimal inhibitory activity (MIC) of antimicrobials on agar

The MIC of efflux inhibitors, dyes and a range of antibiotics was determined using the agar doubling dilution method described by the British Society for Antimicrobial Chemotherapy (BSAC) (Andrews, 2001). The European committee of antimicrobial susceptibility testing (EUCAST) strain *E. coli* ATCC 25922 was used as the quality control strain.

Fresh antimicrobial stocks were prepared on the day of use. Compound powder was weighed in a volumetric flask, on an analytical balance (Denver Instrument, USA, TP214), and dissolved in the appropriate solvent; taking into consideration its potency. All compounds used in susceptibility assays are described in Table 2.5. The antimicrobial stock solutions were double diluted to the appropriate concentrations in sterile plastic universal containers (Greiner, UK, 201170). 20 ml of cooled, molten Iso-Sensitest agar (Oxoid, UK, CM0471) was added aseptically using a peristaltic pump dispenser (Jencons Scientific Ltd, UK) to each universal and the resulting agar suspension was poured into labelled sterile petri dishes (Greiner, UK, 632181). Two plates containing Iso-Sensitest agar alone and an additional plate containing xylose lysine deoxycholate (XLD) agar (Oxoid, UK, CM0569) were also prepared as a start, a finish and a purity plate respectively. Each plate was dried, upside down with the lids removed, for ~20 minutes in a 60°C oven. The density of each overnight culture, prepared in Iso-sensitest broth (Oxoid, UK, CM0473) was diluted 1:100 to a McFarland density of 0.5 giving an inoculum concentration of 1×10^4 CFU/ml of bacteria. Each organism was applied to the wells of a PTFE MIC template

Table 2.5 Antibiotics used throughout this study

Compound	Abbreviation	Compound class	Potency/ purity (%)	Solvent	Supplier	Catalogue number
Amitriptyline	AMI	Tricyclic antidepressant	98	Water	Sigma, UK	A8404
Ampicillin	AMP	β -lactam	97	1.0 M sodium biocarbonate	Sigma, UK	A9393
Chloramphenicol	CHL	Chloramphenicol	98	70% methanol	Sigma, UK	C0378
Chlorpromazine	CPZ	Phenothiazine	98	Water	Sigma, UK	C8138
Ciprofloxacin	CIP	Fluroquinolone	98	Water with acetic acid	Sigma, UK	C17850
Ethidium bromide	ETBR	Dye	95	Water	Sigma, UK	E7637
Hoechst H3342	H33342	Dye	98	DMSO	Sigma, UK	H3570
Hygromycin B	HGR	Aminocyclitol glycoside	98	Water	Sigma, UK	H2734
Kanamycin	KAN	Aminoglycoside	65	Water	Sigma, UK	K1876
Minocycline	MIN	Tetracycline	89-95	Water	Sigma, UK	M9511
Nalidixic acid	NAL	Quinolone	98	Water with acetic acid	Sigma, UK	N8878
Norfloxacin	NOR	Quinolone	98	Water with acetic acid	Sigma, UK	N9890
Phe-arg-beta naphthylamide	Pa β N	Efflux inhibitor	98	Water	Cambridge Bioscience, UK	HY-101444A
Spectinomycin	SPC	Aminocyclitol glycoside	98	70% ethanol	Sigma, UK	S9007
Tetracycline	TET	Tetracycline	95	70 % methanol	Sigma, UK	T3383

and using a 32 pin multipoint inoculator (AQS manufacturing, UK) the plates were inoculated with 1 μ l of culture per spot. The start and finish Iso-Sensitest agar plates were the first and last plates to be inoculated. The plates were incubated overnight at 37°C. The MIC was defined as the lowest compound/drug concentration at which visible growth was inhibited. Strains inhibited by 2 doubling dilutions \geq the wild type parental strain were defined as ‘resistant’ and those where the MIC value was 2 doubling dilutions \leq the breakpoint concentration were defined as ‘susceptible’. The assay was validated by comparing the values for *E. coli* ATCC 25922 against the EUCAST MIC breakpoints (https://www.eucast.org/clinical_breakpoints/) and the internal database collated by the Piddock group.

2.3.2 Chequerboard assay to determine potentiation of antibiotic activity

To determine whether chlorpromazine, amitriptyline and Pa β N are able to potentiate the activity of AcrB substrates, the MIC of chloramphenicol, ciprofloxacin, nalidixic acid, tetracycline and ethidium bromide were determined in combination with doubling dilution concentrations of chlorpromazine and amitriptyline.

Antibiotic, chlorpromazine, amitriptyline and Pa β N stocks were prepared as described in Section 2.3.1, to a concentration four times higher than the desired final concentration. An overnight culture ($\sim 1 \times 10^{10}$ in Iso-Sensitest broth) was diluted 1:1000 giving an inoculum concentration of $\sim 1 \times 10^7$ CFU/ml. First, 50 μ l of Iso-sensitest broth was dispensed, using a multi-channel pipette, into the wells of columns 2-12 of a 96-well round-bottomed microtitre plate (FisherBrand, UK). Next, 50 μ l of antibiotic was added to the wells of columns 1 and 2. Two-fold serial dilutions with a multi-channel pipette were then carried out from column 2-11, removing and dispensing 50 μ l. The 50 μ l withdrawn from column 11 was discarded. Next, 50 μ l of chlorpromazine, amitriptyline or Pa β N were added to the first row. Two-fold serial dilutions, with a multi-channel were then carried out from row 1-7 across

the plate, removing, carefully dispensing and mixing 50 μ l. The 50 μ l withdrawn from row 7 was discarded. Finally, 50 μ l of diluted bacterial culture was added to each well and the plate was incubated overnight at 37°C. This plate layout allowed row 8 and column 12 to be used to determine the individual MIC of the antibiotic and the inhibitor, respectively. As a compound free growth control, no compound was added to the final well of column 12 and row 8. The MIC of each compound alone and in combination was used to determine the fractional inhibitory concentration (FIC) using the following calculation; where I is the efflux inhibitor and A is the antibiotic. The value of this calculation allowed the combination to be categorised as either synergistic (≤ 0.5), antagonistic (≥ 4) or neutral (0.5 to 4).

$$\text{FIC index} = \left(\text{FIC}_I \frac{\text{MIC of I in combination}}{\text{MIC of I alone}} \right) + \left(\text{FIC}_A \frac{\text{MIC of A in combination}}{\text{MIC of A alone}} \right)$$

2.3.3 Disk diffusion assay

The ability of chlorpromazine and amitriptyline to potentiate AcrB substrates was also determined using a disk diffusion assay. Isosensitest agar plates containing amitriptyline (55 μ g/ml or 110 μ g/ml) or chlorpromazine (25 μ g/ml or 50 μ g/ml) or Pa β N (50 μ g/ml) were prepared to 25 ml in 90 mm petri dishes. Before use the surface of the agar was dried thoroughly, upside down with the lids off, for 10 minutes at 60°C. Several morphologically similar colonies of the desired strain on LB agar were suspended in a saline solution to a McFarland density of 0.5. The plates were inoculated by swabbing the suspension over the entire surface of the agar. Antimicrobial disks containing chloramphenicol (30 μ g), tetracycline (30 μ g), nalidixic acid (30 μ g) or ciprofloxacin (5 μ g) were applied to the surface of the agar and the plates incubated at 37°C for 16 hours aerobically. Antibiotic-free disks were used as negative controls. The disks were purchased from Oxoid, UK (CT0013B, CT0054B, CT0031B, CT0425B and CT0998B, respectively). The size of the zone of inhibition was measured using a ProtoCOL 3 Automated Colony and Zone Sizing System (Don Whitley

Scientific, UK). Three independent biological replicates, each with three technical replicates were done. For each biological replicate, the mean of the technical replicates was calculated and compared to that of the other biological replicates.

2.3.4 Well diffusion assay

A well diffusion assay was also used to determine the ability of chlorpromazine and amitriptyline to potentiate the activity of ethidium bromide and norfloxacin. Isosensitest agar plates containing amitriptyline (55 µg/ml or 110 µg/ml), chlorpromazine (25 µg/ml or 50 µg/ml), were prepared to 25 ml in 90 mm petri dishes. Before use the surface of the agar was dried thoroughly, upside down with the lids off, for 10 minutes at 60°C. Several morphologically similar colonies of the desired strain on LB agar were suspended in a saline solution to a McFarland density of 0.5. The plates were inoculated by swabbing the suspension over the entire surface of the agar. A hole of 8 mm in diameter was punched using a sterile metal borer and 50 µl of ethidium bromide or norfloxacin was added to the wells at final concentrations of 750 µg/ml and 5 µg/ml, respectively. Sterile distilled water was used as a negative control. The agar plates were incubated at 37°C for 16 hours. The size of the zone of inhibition was measured using a ProtoCOL 3 Automated Colony and Zone Sizing System (Don Whitley Scientific, UK). Three independent biological replicates, each with three technical replicates were done. For each biological replicate, the mean of the technical replicates was calculated and compared to that of the other biological replicates.

2.4 Characterisation of the efflux inhibitory profiles of inhibitors

2.4.1 Hoechst 33342 accumulation assay

Hoechst 33342 (H33342) is a dye that fluoresces upon interaction with DNA; the accumulation of H33342 can be determined by measuring this fluorescence over time. The

accumulation of H33342 can be used to infer the level of efflux; efflux inhibition results in a lower level of efflux and thus H33342 accumulation. This assay was performed as previously described (Coldham et al., 2010) with a few modifications as indicated below.

Pre-warmed LB broth (10 ml) was inoculated with a 4% inoculum (250 μ l) of overnight culture in LB broth and grown at 37°C with aeration until the culture reached mid-logarithmic growth (OD_{600} 0.5). The culture was then centrifuged in a Herasus 40R megacentrifuge (3,500Xg, room temperature, 10 minutes) and the pellet resuspended in an equal volume of sterile Dulbecco's phosphate buffered saline (DPBS) (Sigma, USA, D8537) to an OD_{600} of 0.1. For each strain, aliquots of 180 μ l were added to three wells of a black plastic flat bottomed 96 well plate (Corning, USA, 3991), 176 μ l (to allow for the volume of efflux inhibitor) was added to three additional wells. To the wells containing 176 μ l of culture, 4 μ l of the desired efflux inhibitor was added at a concentration four times higher than the desired final concentration of inhibitor in the well. Sterile PBS (Sigma, UK, D8537) and boiled cells were used as a blank and as a control for no efflux activity, respectively. In addition, a control including 176 μ l with 4 μ l of resuspension buffer was used as a control for experiments with an efflux inhibitor.

The fluorescence of each well was measured every minute, for three minutes, after which 20 μ l of H33342 (25 μ M) (Sigma Aldrich, UK, B2261) was injected giving a final concentration of 2.5 μ M. The fluorescence was then measured (gain adjusted to 2315), for 100 minutes, with readings every minute using a BMG FLUOstar Optima microplate reader (excitation and emission wavelengths were 350 nm and 460 nm, respectively). Three independent biological replicates, each with three technical replicates were undertaken. For each biological replicate, the mean of the technical replicates was calculated from the steady state values and compared to that of the other biological replicates.

2.4.2 Ethidium bromide accumulation assay

Like Hoechst H33342, ethidium bromide is also a dye that fluoresces upon intercalation with DNA. This method measures the decrease in the fluorescence of pre-loaded ethidium bromide after the addition of glucose to stimulate efflux (Paixão et al., 2009).

Cultures were grown overnight, subcultured and pelleted as described in Section 2.4.1. The pellets were washed in 10 ml of re-suspension buffer (0.1 M, pH 7.0 potassium phosphate buffer (PPB) (Sigma, UK, P0662) with 1 mM MgCl₂ (Sigma, M8266) and centrifuged in a Herasus 40R megacentrifuge (3,600 xg, room temperature, 10 minutes). The pellets were re-suspended in resuspension buffer to an OD₆₀₀ of 0.2 with 50 µg/ml of ethidium bromide (Sigma, USA, E8367) and 100 mM of carbonyl cyanide m-chlorophenyl hydrazine (CCCP) (Alfa Aesar, UK, L06932). After incubation at room temperature for one hour, the suspension was centrifuged (2,500 xg, room temperature, 10 minutes) to remove extracellular ethidium bromide and CCCP. Each pellet was re-suspended in 3 ml of resuspension buffer. For each strain, aliquots of 195 µl were added to three wells of a black, plastic, flat bottomed 96 well plate (Corning, USA, 3991), 191 µl (to allow for the volume of efflux inhibitor) was added to three additional wells. To the wells containing 191 µl of culture, 4 µl of efflux inhibitor (at 50 X the final concentration) was added. Resuspension buffer and boiled cells were used as a blank and as a control for no efflux activity. In addition, a control including 191 µl with 4 µl of resuspension buffer was used as a control for experiments with an efflux inhibitor.

The fluorescence of each well was measured every minute, for three minutes, after which 5 µl of a 100 mM glucose solution (Sigma Aldrich, UK, G8270) was injected giving a final concentration of 25 mM. The fluorescence was then measured (gain adjusted to 1460), for 60 minutes, with readings every minute using a FLUOstar Optima microplate reader (excitation and emission wavelengths were 545 nm and 600 nm, respectively). For each

biological replicate, the mean of the technical replicates was calculated from the endpoint steady state value and compared to that of the other biological replicates. As steady state values were used in the analysis of this assay, here the end point accumulation of ethidium bromide was determined rather than assessing the rate of efflux of this compound.

2.4.3 Norfloxacin accumulation assay

This method was performed according to the method described by Mortimer et al., 1993, with a few modifications. Pre-warmed Iso-Sensitest broth (10 ml) was inoculated with a 4% inoculum of overnight culture (250 μ l) and grown at 37°C with aeration until cells reach an OD₆₀₀ of 0.7-0.8. The culture was then centrifuged in a Herasus 40R megacentrifuge (3,600 xg, 20 minutes, 4°C) and the pellet washed once and re-suspended in an equal volume of sterile ice cold 50 mM PPB (pH 7.0). The resulting suspension was centrifuged again and re-suspended in 10 ml of ice cold PPB to an OD₆₀₀ of 0.2. The suspension was then left to equilibrate, with a magnetic flea, for 10 minutes in a water bath at 37°C.

Aliquots of 1 ml of bacterial suspension were added to ice cold 1.5 ml microcentrifuge tubes and each sample was treated with 10 μ g/ml of norfloxacin for five minutes on ice. The samples were centrifuged (4,000 xg, five minutes, 4°C) in a refrigerated microcentrifuge (Eppendorf, UK) and the pellet resuspended in 1 ml of 0.1 M glycine (pH 3.0) (Sigma, UK, G8898). For the samples to be treated with efflux inhibitor, 10 μ l of chlorpromazine, Pa β N or amitriptyline were added, each at 10 times their final desired concentration. The samples were incubated for two hours at room temperature, centrifuged in a Herasus 40R megacentrifuge (3,600 xg, five minutes) and the fluorescence (excitation and emission wavelengths 281 nm and 440 nm, respectively) of a 1:10 dilution of the supernatant into 0.1 M glycine was determined using a Jencon 660 spectrophotometer. Three independent biological replicates, each with three technical replicates were undertaken. For each biological replicate, the mean of the technical

replicates was calculated and compared to that of the other biological replicates.

2.5 Determination of damage to the outer membrane

2.5.1 ATP luciferin-luciferase membrane permeability assay

Measuring the leakage of ATP, a large cellular constituent, into the extracellular environment can be used as a method to determine damage to the bacterial OM (O'Neill et al., 2004). This relies on the use of the luciferin-luciferase reaction. The firefly luciferase catalyses the ATP-dependent oxidation of D-luciferin to oxyluciferin resulting in the production of light. The amount of light produced is directly proportional to the amount of ATP in the sample.

An appropriate volume of pre-warmed LB broth was inoculated with a 4% inoculum of overnight culture and grown at 37°C with aeration until an optical density of OD₆₀₀ 0.3 was reached. The efflux inhibitors chlorpromazine, amitriptyline and PaβN were prepared to a concentration 10 times higher than the desired concentration. Aliquots of 9 ml of culture were dispensed into sterile plastic universals and 1 ml of an efflux inhibitor stock was added. For the control with no inhibitor 1 ml of water was added. Each sample was incubated for one hour at 37°C with aeration. After incubation, each sample was centrifuged in a Herasus 40R megacentrifuge (3,600 xg, room temperature, 15 minutes) and the supernatant stored at 4°C until use.

The concentration of ATP in the supernatant was determined using the Molecular Probes ATP determination kit (Invitrogen, UK, A22066). This kit utilises a bioluminescence assay which relies on light produced from the luciferin-luciferase reaction to quantify the concentration of ATP. The D-luciferin stock was prepared by diluting 50 µl of 20 X reaction buffer (500 mM tricine pH 7.8, 2 mM EDTA, 2 mM sodium azide and 100mM MgSO₄) in 950 µl of sterile nuclease free water. This 1 ml of 1 X reaction buffer was added to one vial

of D-luciferin, the resulting 10 mM stock was stored, protected from light, at -20°C. A 100 mM stock of dithithreitol (DTT) was prepared by adding 1.62 ml of sterile nuclease free water to the provided 25 mg of DTT. Aliquots of 160 µl DTT were stored at -20°C until use. To make the standard reaction solution 8.9 ml of sterile nuclease free water was added to a sterile plastic universal. To this, 500 µl of 20 X reaction buffer, 100 µl of 100 mM DTT, 500 µl of 10 mM D-luciferin and 2.5 µl of 5 mg/ml of firefly luciferase was added. The reaction solution was stored, protected from light on ice, until use.

To make the standard curve, from which the concentration of ATP can be quantified, the provided 5 mM ATP solution was diluted in nuclease free water to 10 times the following concentrations: 1, 2, 5, 10, 20, 30, 40, 50, 60, 70, 80, 90, 100, 200, 300, 400, 500, 600, 700, 800, 900 and 1,000 nM. Fresh ATP standards were made and run with each assay.

To each well of a flat, clear bottomed black 96 well plate (Corning, UK, CLS3603-48EA), 90 µl of the standard solution and 10 µl of the ATP standard or culture supernatant was added. A single technical replicate of the ATP standard and two technical replicates of each sample were run on each plate. Blanks containing 90 µl of standard solution and 10 µl of water were also used to correct for background luminescence. The luminescence was measured using a FLUOstar Optima microplate reader (optic module:lum plus). The luminescence readings of the ATP standards were plotted and the equation of the line displayed in the form $y=mx+b$; where m is the slope and b the y-intercept. The amount of ATP in each sample was then calculated from the equation of the line. Three independent biological replicates, each with two technical replicates were undertaken. For each biological replicate, the mean of the technical replicates was calculated and compared to that of the other biological replicates.

2.5.2 DisC3(5) membrane depolarisation assay

Damage to the OM often increases membrane permeability allowing positively charged ions to cross from the extracellular to the intracellular environment. This results in depolarisation; a reversion of the electrical charge inside the cell from negative to positive and the outside of the cell from positive to negative. Changes in the membrane potential can be detected by the voltage dependant fluorescent dye 3,3'Dipropylthiadicarbocyanine iodide (DisC3(5)).

An appropriate volume of pre-warmed LB broth was inoculated with a 4% inoculum of overnight culture and grown at 37°C with aeration until an optical density of OD₆₀₀ 0.3 was reached. The cultures were harvested by centrifugation in a Herasus 40R megacentrifuge (3,600 xg, room temperature, 15 minutes), washed and re-suspended in 5 mM of a sodium HEPES buffer (Sigma, UK, H7006) supplemented with 20 mM of glucose (Sigma, UK, G8270) and 0.5 mg/ml of BSA (pH 7.4) (Sigma, UK, A3803) to reduce the absorption of DisC3(5) to polystyrene surfaces. A 100 µM stock of DisC3(5) (Sigma, UK, 43608) was prepared in dimethyl sulfoxide (DMSO) (Sigma, UK, D4540) and stored protected from light on ice until use. Stocks of efflux inhibitor were prepared to concentrations 10 times greater than the final desired concentration.

To the wells of a black, flat, clear bottomed 96-well plate (Corning, UK, CLS3603-48EA) 135 µl of each bacterial suspension was added. Two technical replicates of each sample were run on each plate. Blanks containing sodium HEPES buffer only or boiled cells were used as blank and maximal fluorescence controls, respectively. The fluorescence was measured throughout the assay using a FLUOstar Optima at varying excitation and emission wavelengths. The background fluorescence was measured for 3 minutes (excitation and emission of 610 nm and 660 nm, respectively). After obtaining the baseline, 1.35 µl of 100 µM DisC3(5) was added to each well giving a final concentration of 1 µM DisC3(5) and 1%

DMSO (suitability for maintaining solubility and fluorescence of the dye). The fluorescence was measured for 10 minutes at one minute intervals (excitation and emission of 600 nm and 670 nm, respectively). Next, 15 μ l of the test compound was added to the cell suspension and the fluorescence was measured for 30 minutes at one minute intervals (excitation and emission of 600 nm and 670 nm, respectively). Three independent biological replicates, each with two technical replicates were undertaken. For each biological replicate, the mean of the technical replicates was calculated and compared to that of the other biological replicates.

2.6 Selection of antimicrobial or putative efflux inhibitor-resistant mutants and identification of mutations conferring resistance

2.6.1 Mutant selection experiments

Mutants resistant to efflux inhibitors were selected on agar. Agar plates supplemented with the desired efflux inhibitor were made by incorporating the inhibitor into molten LB agar. The concentrations used for each inhibitor and the number of parallel cultures are shown in Table 2.6. Once set, the plates were dried in a 60°C oven for 20 minutes.

An appropriate volume of overnight culture was centrifuged in a Herasus 40R megacentrifuge (3, 600 xg, room temperature, 15 minutes) and concentrated in LB broth by a factor of 100 (e.g. 400 ml to 4 ml) giving an inoculum concentration of approximately 1×10^9 CFU/ml. The agar plates were inoculated with 50 μ l of bacterial culture using the Whitley Automated Spiral plater (Don Whitley Scientific, UK) and incubated aerobically at 37°C for up to seven days, or until the appearance of colonies which were counted. To calculate the CFU/ml in the overnight culture, the culture was diluted 1:1000, followed by three serial 1:10 dilutions in LB broth. Each solution (50 μ l) was spread onto individual LB agar plates and incubated overnight at 37°C. Colonies were counted and replicate plated onto compound-free LB agar, LB agar containing the selecting compound at the selecting concentration and XLD agar (for species identification). The antibiotic susceptibility of

each colony (or up to 90 if more than 90 colonies were selected) was determined by agar MIC. One representative clone from each MIC profile was prepared for whole genome sequencing (WGS).

The viable count was calculated by:

$$\text{Viable count (CFU/ml)} = \frac{\text{No of colonies x dilution factor}}{\text{Volume plated}}$$

The mutation frequency was calculated by:

$$\text{Mutation frequency (CFU/ml)} = \frac{\text{No of colonies x viable count}}{\text{volume plated x concentration factor}}$$

The mutation rate was calculated using the MSS maximum likelihood method: where Pr is the proportion of cell with random mutants, m is the number of mutations per culture, r is the observed number of mutants, μ is the mutation rate and Nt is viable count.

$$Pr = \frac{m}{r} \sum_{i=0}^{r-1} \frac{Pi}{(r-i+1)}$$

$$u = \frac{m}{2Nt}$$

2.6.2 Isolation of DNA for whole genome sequencing

Cultures of putative mutants and parental strains to be sequenced were grown overnight at 37°C with aeration. The culture was centrifuged in a Herasus 40R

Table 2.6 Conditions used to select for efflux inhibitor resistance

Organism	Selecting drug	Selecting concentration ($\mu\text{g/ml}$)	Number of parallel cultures
<i>S. Typhimurium</i> SL1344	Chlorpromazine	150	1
	Chlorpromazine + ciprofloxacin	50 0.03	1
	Pa β N	1,024	1
	Pa β N + ciprofloxacin	50 0.03	1
	Ciprofloxacin	0.03	30
<i>E. coli</i> MG1655	Chlorpromazine	160	20
		170	20

megacentrifuge (14,000 rpm, room temperature, 2 minutes) and the pellet prepared for DNA isolation with the Norgen genomic isolation kit (Norgen, Biotek Corp, Canada, 24750). The DNA was eluted in 30 μl of nuclease free water and stored at -20°C until use. The DNA concentration was quantified using the QubitTM DNA assay kit (Invitrogen, UK, Q32851), according to manufacturers instructions. The kit uses a fluorescent dye that binds DNA allowing for quantification of DNA using a fluorometer. An appropriate volume of Qubit working solution was prepared by diluting the Qubit dsDNA reagent 1:200 into Qubit dsDNA buffer. To separate Qubit tubes, 190 μl of working solution and 10 μl of each standard was added. For each DNA sample, 1 μl of DNA was mixed with working solution to a final volume of 200 μl . Each standard and sample reaction was incubated at room temperature for 2 minutes and the fluorescence measured using a Qubit 3 Fluorometer (Invitrogen, UK).

2.6.3 Whole genome sequencing and data analysis

Each efflux inhibitor-resistant mutant was sent to the Beijing Genomics Institute (BGI) (Hong, Kong) for paired-end sequencing using an Illumina HiSeq 4,000 platform. The sequencing assembly and analysis was performed using the Galaxy online platform. First, each fastq file was run through FASTQ Groomer to ‘groom’ each file into a Sanger-confirming

fastq file. The ‘groomed’ file was then processed using Trimmomatic to remove the first 20 bp of each read. The quality of each trimmed sequence was determined using FASTQC and if the quality of the reads was low an additional 10 bp from each read was trimmed.

Each sequence was assembled using FastQC interlacer (to create a single fastq file from the individual paired-end reads), velveth (to convert each read to a k-mer) and velvetg (to assemble the overlapping k-mers into contigs). Each assembled sequence was mapped against a reference genome and variant calling was performed using SNIPPY. SNIPPY returned a BAM file and provided a list of SNPS and INDELS (insertions and deletions) and their location on the chromosome. The reference genomes were ASM21085v2 and ASM584v2 for *S. Typhimurium* SL1344 and *E. coli* MG1655, respectively. Each genome was downloaded from EnsembleBacteria. To confirm any SNPs and INDELS identified, the genome browser Artemis (Sanger Institute, UK) was used to visualise the BAM file for each mutant with reference to the fastq file of the annotated reference genome.

2.6.4 Confirmation of mutations identified by WGS

Cell lysates were prepared from each efflux inhibitor-resistant mutant and a PCR performed according the method detailed in Section 2.2.1 with primers that anneal up and downstream of the mutation site (Table 2.2). The resulting PCR amplicons were prepared for DNA sequencing as described in Section 2.2.2.

2.7 Homology modelling of SL1344 AcrB and SL1344 RamR and MG1655 MarR mutant proteins

Homology models of SL1344 AcrB, SL1344 RamR L158P, MG1655 MarR A105Rfs*114 and MG1655 MarR K141Sfs*150 were built using Modeller 9.21. The code to model each protein was written following a tutorial outlined on the SaliLab Modeller webpage (<https://salilab.org/modeller/tutorial/basic.html>). First, it was necessary to

convert the amino acid sequences of each protein into a PIR format that can be read by Modeller. This was saved as an alignment (.ali) file.

Modeller 9.21 contains a basic Python interpreter and each file was run through the Modeller command line as a standard Python script. To search for related protein sequences the `build_profile.py` python script was written. This script created an alignment object that was converted to a more compact profile to allow for a more efficient database search. The generated profile contained the protein data bank (PDB) sequences with the greatest percentage identify to the target sequence. To choose the most appropriate template sequence to which the target sequence was aligned the `compare.py` script was written. Each PDB file used in this script was downloaded from the PDB website and saved in the same folder directory as the `compare.py` script. Next, the `align.py` script was written to align the target sequence with the structure of the most identical PDB structure. Once run, this script produced an alignment file for the target and template sequence in both PIR (.ali) and a PAP (.pap) format. The PAP format allows for easy visualisation while the PIR format was used in the subsequent model build. The model was then built by running the `model.py` script. This script calculated the model based on the template of the most identical PDB structure and the alignment file produced from the `align.py` script. Each model built was saved in the same directory as a PDB file and a log file with each successful model was produced. Each model was then evaluated by way of a DOPE energy calculation using the `evaluate.py` script. A high DOPE score indicates a number of unfavourable interactions and a lower degree of similarity of the target structure to the template structure. Finally, the models were visualised using PyMOL version 2.4.

2.8 Characterisation of *ramR* and *marR* mutants

2.8.1 Growth kinetics

Following overnight growth, each culture was diluted 1:100 into LB Broth. To the wells of a round bottomed 96-well plate (Corning, UK, CLS3367-50EA), 100 μ l of each culture was added in triplicate. The optical density at OD₆₀₀ was measured using a FLUOstar Optima for 16 hours at 37°C with readings every 10 minutes. Three independent biological replicates, each with three technical replicates were undertaken.

2.8.2 Fluorescence reporting assays measuring the expression of *ramA*, *marA* and *acrAB*

Green fluorescent protein (GFP) reporter fusion constructs on a pMW82 vector with the promoter regions of *ramA*, *marA* and *acrAB* fused with *gfp* were used (Lawler et al., 2013). The plasmid constructs were isolated and transformed into the appropriate strain by electroporation as according to Sections 2.2.3 and 2.2.5.

Overnight cultures were grown in MOPS minimal media supplemented with 50 μ g/ml of ampicillin. After incubation overnight, 10 ml of pre-warmed MOPS minimal media, containing 50 μ g/ml of ampicillin was inoculated with a 4% inoculum of overnight culture grown in MOPS minimal media and grown at 37°C, with aeration, until an optical density of OD₆₀₀ 0.9 was reached. For each strain, 100 μ l of culture was added to six wells of a black, clear, bottomed, 96 well plate (Corning, UK, CLS3603-48EA). To three of these wells, chlorpromazine was added to a final concentration of 25 μ g/ml. An empty vector control containing no *gfp* fusion was used as a control for basal fluorescence. The FLUOstar Optima simultaneously measured the fluorescence (excitation and emission wavelengths of 494 nm and 520 nm, respectively) and absorbance (600 nm) at 37°C for 16 hours, with readings every three minutes.

2.9 Construction of *E. coli* MG1655 *marR::aph*

The *marR::aph* cassette was PCR amplified from a previously constructed *E. coli* BW25113 *marR::aph* mutant. Then conditions for colony PCR, described in Section 2.2.1, were used with an annealing temperature of 58°C. Following PCR, the reaction was Dpn1 digested to remove methylated template DNA. The digestion was performed by mixing the 50 µl PCR product with 5 µl of CutSmart™ buffer (New England Biolabs, USA, B72045) and 5 µl of Dpn1 enzyme (NEB, USA, R0176S). The digestion reaction was incubated for 30 minutes at 37°C and the enzyme subsequently inactivated by incubation for 10 minutes at 80°C. After digestion, 10 µl of the PCR product was run by gel electrophoresis on a 1% agarose gel detailed in Section 2.2.1.

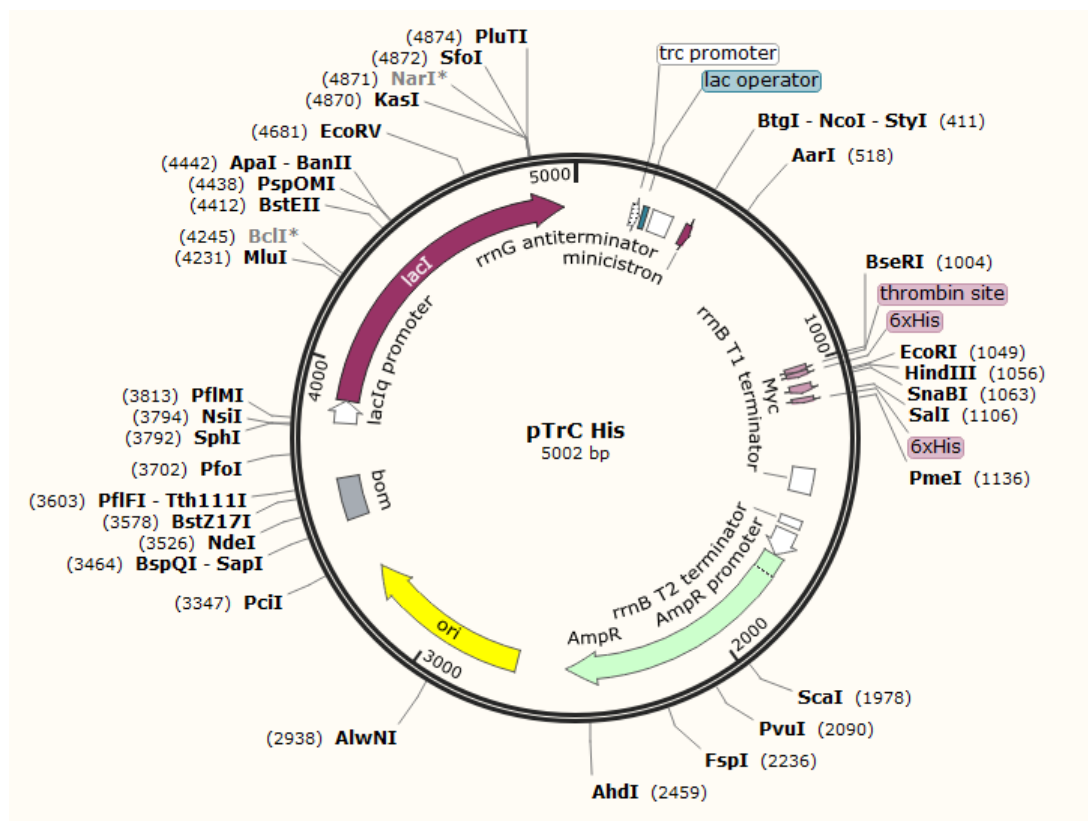
An *E. coli* MG1655 strain containing pSIM18 (a λ-red helper plasmid) was grown overnight at 30°C, with aeration, in LB broth supplemented with 150 µg/ml of hygromycin B. To 100 ml of prewarmed LB, containing 150 µg/ml of hygromycin, 1 ml of overnight culture was added. The culture was incubated at 30°C with aeration until an OD₆₀₀ of 0.3 was reached. The culture was then decanted into two 50 ml falcon tubes and the cells were heat shocked in a 42°C water bath for 15 minutes. The cells were then immediately placed on ice for 10 minutes. Once cooled, the cultures were centrifuged in a Herasus 40R megacentrifuge (3,600 xg, 4°C, 10 minutes) and the pellet resuspended in 50 ml of ice cold 15% glycerol. This step was repeated twice more. After the second centrifugation, the pellet was re-suspended in 1.5 ml of ice cold 15% glycerol and transferred to a 2 ml microcentrifuge tube. Finally, the culture was centrifuged (4,000 xg, 4°C, 2 minutes) in a table top refrigerated centrifuge (Eppendorf, UK) and re-suspended in 100 µl of 15% glycerol. Finally, the competent cells were electroporated with 5 µl of the *marR::aph* PCR product as described in section 2.2.5 and plated onto LB agar containing 50 µg/ml of kanamycin (to confirm successful recombination), LB agar containing 150 µg/ml of hygromycin B (to

confirm loss of pSIM18) and LB agar alone (to confirm viable growth).

To confirm successful recombination a cell lysate was prepared from the candidate colonies and a PCR performed as detailed in Section 2.2.1 with primers that anneal up and downstream of the inactivation site (Table 2.2). In addition, the PCR amplimers were prepared for DNA sequencing as described in Section 2.2.2.

2.10 Construction of mutant and wild type RamR and MarR on pTrc-His

Mutant and wild type *ramR* and *marR* were introduced into a pTrc vector (Figure 2.1) using a pTrcHis2 TOPO[©] TA expression kit (Invitrogen, UK, K4400-01). The pTrcHis2 expression kit utilises a TA cloning strategy to introduce *ramR* and *marR* into the pTrcHis vector. Due to the presence of the *trc* gene the pTrc vectors are used for high-level gene expression for protein production in *E. coli*. pTrcHis also contains a *lacO* sequence and in the absence of IPTG the Lac repressor, encoded by *lacI*, binds *lacO*, preventing its expression and the subsequent expression of *trc*. Upon the addition of IPTG the *lacI* promoter is repressed and the expression of *trc* is induced. In addition, pTrcHis contains an N-terminal polyhistidine (6 x His) tag that renders it as a suitable vector for downstream purification of the recombinant proteins via nickel-immobilised affinity chromatography.

Figure 2.1: pTrcHis vector map.

This vector includes a *trc* promoter and a 6X-His tag making it ideal for the high level expression of genes in *E. coli*. Vector map made in SnapGene.

The pTrcHis vector was provided linearized with 3' thymidine overhangs and a bound topoisomerase. When used with a Taq polymerase a single adenosine is added to the PCR product at the 3' end allowing the product to ligate with the vector.

2.10.1 Design of primers for TA cloning

The nucleotide sequence of the gene of interest was isolated from *Escherichia coli*. The start codon of the gene of interest was removed as the pTrcHis vector contains a start codon located upstream of the TA cloning insertion site (<https://www.thermofisher.com/order/catalog/product/V36020?uk&en#/V36020?uk&en>). Each forward primer was designed with ~60bp homology to the target gene. Each reverse primer was designed with ~25-30bp homology to the target gene. In addition, the His-tag located on the pTrc vector is not cleavable and the presence of these bulky amino acids can cause downstream problems in assays utilising the purified protein. Therefore, to each reverse primer a thrombin cleavage site was introduced followed by an additional C-terminal 6 x His tag to allow for removal of these amino acids if necessary. The native stop codon of the gene of interest was also included to each reverse primer. In addition, for MG1655 MarR K141Sfs*150 the mutation site is located at the 3' end of the gene. Therefore, the mutation site conferring the K141Sfs*150 deletion was incorporated into the reverse primer.

2.10.2 Producing PCR products for TA cloning

Each respective target gene was amplified using lysates from SL1344 wild type, SL1344 RamR L158P, MG1655 wild type, MG1655 MarR A105Rfs*114 and MG1655 MarR K141Sfs*150. Using the cloning primers listed in Table 2.2, the following PCR reaction was set up with the reagents provided in the pTrcHis2 TOPO[®] TA expression kit: 100 ng of DNA was added to 5 µl of 10 X PCR buffer (100 mM Tris-HCl (pH 7.4), 1 mM EDTA, 2 mM DTT, 0.1% Triton X-100, 100 µg/ml BSA and phenol red), 50 mM dNTPs (12.5 mM

of each dATP, cATP, dATP and dATP at pH 8.0), 1 μ l of each primer (25 μ M), 1 μ l of Taq polymerase and nuclease free water to a final volume of 50 μ l. The cycling conditions, gel visualisation and PCR purifications were performed as described in Section 2.2.1. The purified PCR amplicon was used immediately or stored at -20°C until further use.

2.10.3 TA cloning reaction and transformation

To introduce the amplified DNA templates into pTrcHis the following cloning reaction was set up: to a 0.5 ml microcentrifuge tube (Greiner, UK, 667201), 4 μ l of PCR product and 1 μ l of pTrcHis2 TOPO cloning vector was added. The reaction was incubated at room temperature for five minutes.

For the transformation, 2 μ l of the TOPO cloning reaction was added to a thawed vial of the One Shot[®] cells provided with the pTrcHis2 TOPO[©] TA expression kit and mixed gently (with no pipetting). The reaction was incubated on ice for 30 minutes and the cells subsequently heat shocked at 42°C in a water bath without shaking. The cells were then immediately transferred to ice and 250 μ l of the provided SOC medium at room temperature was added to the vial. The tube was then incubated horizontally for 30 minutes at 37°C with agitation. Finally, 50 μ l of cells were plated onto pre-warmed LB agar plates containing 50 μ g/ml of ampicillin and 0.5% glucose. An additional 50 μ l of cells was plated onto LB agar as a viability control. Each plate was incubated overnight at 37°C.

Transformants were re-streaked onto LB agar plates containing 50 μ g/ml of ampicillin and incubated overnight at 37°C. To confirm successful cloning a plasmid prep, PCR, gel visualisation, PCR purification and DNA sequencing was performed with the check primers described in Table 2.2 using the conditions detailed in Sections 2.2.3, 2.2.1 and 2.2.2. Once successful cloning was confirmed, the pTrcHis vector containing the insert was purified according to Section 2.2.3. *E. coli* BL21 DE3 was made competent and electroporation with the purified vector was performed as per Sections 2.2.4 and 2.2.5.

2.11 Purification of mutant and wild type RamR

2.11.1 Pilot expression

Given that each expression construct and each recombinant protein has different elements that effect its optimal expression, a pilot expression was performed to determine the optimal conditions for maximal protein expression.

An overnight culture of 5 ml of LB broth containing 50 µg/ml of ampicillin was inoculated with a single recombinant colony and grown overnight at 37°C with aeration. The following day 10 ml of pre-warmed LB broth was inoculated with a 4% inoculum of overnight culture and grown at 37 °C with aeration until an optical density of OD₆₀₀ 0.6 was reached. Once reached, a 1 ml aliquot of cells was put into a microcentrifuge tube and centrifuged (3,600 xg, room temperature, 30 seconds) in a table top centrifuge (Eppendorf, UK). The supernatant was removed and the pellet frozen at -20°C. This sample was designated as time point zero. To the remaining culture, 1 µl of a 1 M stock of IPTG (Sigma, UK, I6758) was added, giving a final concentration of 1 mM IPTG. Growth was continued at 37°C with aeration. Every hour, for five hours after induction 1 ml of culture was removed, placed into a microcentrifuge tube and centrifuged (3,600 xg, room temperature, 30 seconds) in a table top centrifuge (Eppendorf, UK). The supernatant was removed and the pellet stored at -20°C until separation by sodium dodecyl sulfate (SDS)-PAGE.

2.11.2 SDS-PAGE

Each cell pellet was re-suspended in 100 µl of 1 X SDS-PAGE sample buffer. A five times concentration of SDS-PAGE buffer was made as follows: 5% SDS (Merck, UK, L3771) with 50% glycerol (Sigma, UK, G5516), 0.05% bromophenol blue (Sigma, UK, B-8026), 0.25 M DTT (Sigma, UK, D9760) and 0.225 M Tris HCl (pH 6.8) (Merck, UK, 10812846001). Each sample was boiled for five minutes and centrifuged (3,600 xg, room temperature, 30

seconds) in a table top centrifuge (Eppendorf, UK). To the wells of a NuPAGE, 4-12%, Bis-Tris, 10 well, mini gel (Invitrogen, UK, NP0321PK2), 5 μ l of sample was added. The proteins were electrophoresed against 2 μ l of an Magic Mark XP western standard (20-220kDa) ladder (Invitrogen, UK, LC5602). The samples were run until the dye front reached the bottom of the gel (\sim 20 minutes) at 200 V in 1 X NuPAGE MOPS SDS running buffer (Invitrogen, UK, NP001). Once electrophoresed, the gel was placed into a 120 mm x 120mm square petri dish (King Scientific, UK, PDTVSQ120MM).

2.11.3 Staining of SDS PAGE

The electrophoresed gel produced after SDS-PAGE (Section 2.11.2) was washed three times, for five minutes each, with 100 ml of deionised water to remove SDS and buffer salts which interfere with the binding of the stain to the protein. The gel was then stained with enough Simply Blue™ SafeStain (Invitrogen, UK, LC6065) to cover the gel (20 ml). The gel was stained for 1 hour at room temperature with gentle shaking. After staining the gel was washed twice with 100 ml of deionised water for 1 hour each. The gel was visualised by eye.

2.11.4 Full scale expression

An overnight culture of 5 ml of LB broth containing 50 μ g/ml of ampicillin was inoculated with single recombinant colony and grown overnight at 37°C with aeration. The following day, 250 ml of pre-warmed LB broth was inoculated with a 4% inoculum of overnight culture and grown at 37°C with aeration until an optical density of OD₆₀₀ 0.6 was reached. Once reached, 25 μ l of a 1 M stock of IPTG was added giving a final concentration of 1 mM IPTG. Growth was continued at 37°C with aeration until the optimal time point was reached. The cells were then aliquoted into 50 ml falcon tubes and centrifuged in Herasus 40R megacentrifuge (3,600 Xg, 10 minutes, 4°C). The cell pellet was either used immediately in purification or stored at -80°C until further use.

2.11.5 Purification by Ni-NTA chromatography

Purification of SL1344 RamR wild type and RamR L158P recombinant 6xHis-tagged proteins was performed using the QIAexpress[®] Ni-NTA Fast Start system (QIAGEN, UK, 30600). The QIAexpress system utilises a nickel nitrilotriacetic acid (NI-NTA) ion-affinity chromatography matrix to which recombinant proteins can be isolated through binding of a 6xHis tag to the Ni-NTA matrix. Here, the recombinant proteins are soluble and were purified according to the manufacturer's instructions under native conditions in order to preserve the secondary and tertiary protein structure. All buffers used throughout purification were provided as part of the QIAexpress[®] Ni-NTA Fast Start system, unless otherwise specified.

Once thawed on ice, the cell pellet produced from the full-scale expression was resuspended in 10 ml of native lysis buffer supplemented with the provided lysozyme and Benzonase[®]. The lysate suspension was incubated on ice for 30 minutes with occasional mixing. After incubation the lysate was centrifuged in a Herasus 40R megacentrifuge (3,600 X g, 30 minutes, 4°C) and the supernatant containing the soluble protein retained. To 5 µl of the supernatant sample, 5 µl of 2 x SDS-PAGE (2% SDS with 20% glycerol, 0.02% bromophenol blue, 0.1 M DTT and 0.09 M Tris HCl (pH 6.8)) was added and the sample stored at -20°C until further use.

The Fast Start Resin was re-suspended by inverting the column several times, the seal was broken, the cap removed and the storage buffer was left to flow out of the column. Once the buffer was removed, the lysate supernatant was applied to the column. The flow through was collected and 5 µl of 2 x SDS-PAGE buffer was added to 5 µl of flow through. The sample was stored at -20°C until further use. Next, the column was washed twice with 4 ml of the provided native wash buffer and the flow through of each wash was collected. To 5 µl of each wash flow through 5 µl of 2 x SDS-PAGE buffer was added and the samples stored at -20°C until further use. The recombinant protein was then eluted in two 1 ml aliquots

of native elution buffer and the flow through of each collected. To 5 μ l of each elution flow through 5 μ l of 2 x SDS-PAGE buffer was added and the samples stored at -20°C until further use. Finally, the samples were separated by SDS-PAGE and the gel stained as described in Sections 2.11.2 and 2.11.3.

2.11.6 Protein concentration quantification

The protein concentration was quantified using a QubitTM assay kit (Invitrogen, UK, Q33221) according to the manufacturer's instructions. The kit uses a fluorescent dye that stains protein allowing for quantification of protein concentration using a fluorometer. An appropriate volume of Qubit working solution was prepared by diluting the Qubit protein reagent 1:200 into the Qubit protein buffer. To separate Qubit tubes, 190 μ l of working solution and 10 μ l of each standard was added. For each protein sample, 1 μ l was mixed with working solution to a final volume of 200 μ l. Each standard and sample reaction was incubated at room temperature for 30 minutes and the fluorescence measured using a Qubit 3 Fluorometer (Invitrogen, UK).

2.11.7 Western blot

To determine the presence of a purified recombinant protein a western blot was performed using anti-His tag antibodies. To the purified protein, 5 μ l of 2 X SDS-PAGE buffer was added and the samples separated by SDS-PAGE as described in Section 2.11.2. After separation the lip of the gel was removed, the gel was placed into a 120 mm x 120 mm square petri dish and washed once with 150 ml of distilled water.

The protein was transferred from the SDS-PAGE gel to a polyvinylidene fluoride (PVDF) membrane using the iBlotTM 2 Dry Blotting System (Invitrogen, UK, IB21001) for 7 minutes at 20 V. The buffers used for blocking and antibody binding were prepared using the solutions included in the iBindTM horseradish peroxidase (HRP) western system

(Invitrogen, UK, SLF100). For the iBind solution, 500 μ l of the provided 100 x additive was added to 10 ml of 1 x iBind buffer and 40 ml of sterile distilled water. For the primary antibody, 2 μ l of Anti-6x-His monoclonal mouse antibody (Invitrogen, UK, MA1-21315-HRP) was added to 2 ml of the prepared iBind solution. For the secondary antibody, 1 μ l of anti-mouse IgG HRP linked antibody (Cell Signalling Technology, USA, 70765) was added to 2 ml of the prepared iBind solution.

The western blot, including blocking, washing and antibody incubations was performed using the iBind Flex western device (Invitrogen, UK, SLF200). First, the blotted membrane was immersed in 10 ml of iBind buffer. The iFlex card (Invitrogen, UK, SLF2010) was placed onto the iFlex western device and saturated with iBind buffer (10 ml). Next, two aliquots of 1 ml of iBind buffer were pipetted next to each other onto the iFlex card. The membrane was then placed protein side down on top of the pooled iBind buffer, with the lowest molecular weight region closest to the bottom of the western device. A roller was used to remove any air bubbles that would interfere with the contact between the membrane and the iFlex card. The lid of the iFlex was shut and the solutions were added sequentially to wells 1-4 as follows: 2 ml of primary antibody, 2 ml of iBind solution, 2 ml of secondary antibody and 6 ml of iBind solution. The membrane was then incubated anywhere from 3 hours to overnight.

After incubation, the membrane was placed in a 120 mm x 120 mm square petri dish containing 50 ml of distilled water. The membrane was developed using a Westar Supernova chemiluminescent substrate kit (Cyanagen, Italy, XLS30100). The developed membrane was visualised using an Amersham 680 Imager (Cytiva, UK).

2.12 Determination of protein DNA binding

The promoter of *ramA* (*pramA*) of *S. Typhimurium* SL1344 was amplified according to the method detailed in Section 2.2.1 using primers that bind upstream of the *ramA* gene

producing a 171bp product containing the predicted promoter site. The PCR amplicon was run on a 1% agarose gel and the product was gel excised using a QIAquick[®] Gel Extraction Kit (QIAGEN, Germany, 28706) and eluted in 30 µl of nuclease free water. The separation of the amplicons by gel electrophoresis and the subsequent gel extraction was repeated a further four times to remove any accompanying DNA impurities.

To determine any interaction between the wild type and mutant RamR protein with *pramA*, an electrophoretic mobility shift assay (EMSA) was performed using a fluorescence based EMSA kit (Molecular Probes, UK, E33075). For the protein and DNA reactions, 1 µl of DNA (at the following concentrations 25 nmol, 10 nmol and 5 nmol) was mixed, in a 0.5 ml microcentrifuge tube, with 1 µl of purified *pramA*. Additional protein only and DNA only controls were prepared by mixing 1 µl of protein (at the same concentrations) or DNA with 1 µl of nuclease free water. To each sample, 2 µl of nuclease free water with 2 µl of 5 X binding buffer (750 mM KCl, 0.5 mM DTT, 0.5 mM EDTA and 50 mM Tris (pH 7.4)) was added. Each reaction was incubated for 20 minutes at room temperature.

The samples were separated by a non-denaturing PAGE. 2 µl of 6 X EMSA gel-loading solution was added to each sample and mixed gently. Each sample was then added to individual wells of a premade NuPAGE, 17 well, 4-12%, Bis-Tris (1.0 mm) mini gel (Invitrogen, UK, NP0329BOX) and run at 200 V for ~ 1.5 hours at 4°C. 1 X TBE was used as the running buffer. Before the addition of the samples, the gel was pre-run at 200 V for 20 minutes at 4°C. After separation by non-denaturing PAGE, the gel was placed into a 120 mm x 120 mm square petri dish. To the petri dish, 5 µl of SYBR Green EMSA gel in 50 ml of 1 X TBE buffer was added. The gel was incubated for 20 minutes, protected from light, with agitation. After incubation, the gel was washed three times with 150 ml of distilled water. The stained nucleic acids were visualised under a blue light transilluminator using the G:BOX gel documentation system (Syngene, UK). An EMSA in which DNA-protein binding is observed results in the shift of the free DNA band to higher up the gel matrix as

a result of an increase in molecular mass upon protein binding.

2.13 Transcriptomic analysis

2.13.1 RNA sequencing

The RNA samples were previously prepared by Dr Alison Baylay (PhD student, Piddock group) as follows: *S. Typhimurium* SL1344 was grown to an OD₆₀₀ of 0.6 in MOPS minimal media, supplemented with 2.6 mM of L-histidine. The cells were then exposed to chlorpromazine (50 µg/ml) or PaβN (100 µg/ml) for two hours. The RNA was extracted using a SV total isolation system (Promega, USA) and the concentration of RNA and DNA quantified using Qubit fluorimetric quantification. DNase treatment with the Turbo DNA-free kit (Thermo Fisher Scientific, UK) was performed, if required. The samples were paired-end sequenced using an Illumina HiSeq 4,000 system by BGI, Hong Kong. The RNA sequences were deposited in ArrayExpress on 12/06/2020 (accession no. E-MTAB-8190).

2.13.2 Bioinformatic analysis

Analysis of the RNA-sequencing data was performed in collaboration with Dr Alasdair Ivens from The University of Edinburgh, UK. To start, a FASTQC analysis was undertaken to determine the quality of the RNA-sequencing reads. The poly-A tails were removed using Cutadapt (Version 1.9) and the trimmed sequences were mapped against the reference sequence FQ312003.1 (downloaded from Bacteria Ensemble) using Bowtie2. The data was normalized to that with the lowest number of mapped reads, also known as counts. The mapped reads per gene was converted to Log₂ values and quantile normalized. Finally, the *limma* package from Bioconductor was used to compare the gene transcriptions of two data sets using the normalized data and determine the significance of each of these comparisons.

Here, the differentially transcribed genes were sorted dependent on their significance.

A P value of ≤ 0.005 was considered to be significant. The significant genes were then sorted into groups using the Clusters of Orthologous Groups (COG) database. The COG annotations were downloaded from the MicroScope and Microbial Genome Annotation and Analysis Platform.

2.14 RT-PCR to determine *acrB* expression post exposure to chlorpromazine

Three biological replicate overnight cultures of *S. Typhimurium* SL1344 were grown in MOPS minimal medium at 37°C. Following overnight growth, four starter cultures from each biological replicate were set up in MOPS minimal medium and incubated at 37°C with shaking until an OD₆₀₀ of 0.6-0.8 was reached. Chlorpromazine was then added to the cultures at the following concentrations; 0, 50, 100 and 200 µg/ml and incubation was continued at 37°C with shaking for an additional 30 minutes. RNA preparations were made and quantified as previously described (Bailey et al., 2008). cDNA was synthesized from 2 µg of total RNA using the SuperScript III cDNA synthesis kit (Invitrogen, UK, 18080051). Quantitative RT-PCRs were set up in a Bio-Rad PCR tray (Bio-Rad, UK, HSL9601) using 1 µl of neat cDNA for the test gene (*acrB*) and 1 µl of a 1:1000 dilution of cDNA for 16s in a 25 µl reaction containing 12.5 µl of iQ SYBR Green Supermix (Bio-Rad, UK, 1708880), 1 µl of primers (500 nM) and 9.5 µl of sterile water. Quantitative RT-PCR was carried out in a CFX96 real-time machine (Bio-Rad, UK) using the protocol described in Table 2.7. Data were analysed using CFX Manager (Bio-Rad, UK) and expression ratios were calculated using the $\delta\delta C_t$ method and normalized to the expression of 16s (Pfaffl, 2001).

Table 2.7 RT-PCR cycling conditions for the amplification of *acrB*

Cycle	Temperature (°C)	Time	Number of cycles
Initial denaturation	95	5 minutes	1
Denaturation	95	30 seconds	40
Primer annealing	57.3	30 seconds	40
Extension	72	30 seconds	40
Final extension	72	3 minutes	1

2.15 Allele specific quantitative PCR

Allelic specific PCR was used to identify the presence or absence of the 1223G allele conferring the D408A substitution within *S. Typhimurium* SL1344. This method allows the detection of single SNPs by the use of two allele-specific primers that only amplify their complementary allele; one specific for the wild type allele (408D) and one specific for the mutant allele (408A). Although this method is typically performed with primers differing in their terminal 3' nucleotide, due to the energy binding cost of the mutant allele primer being insufficient to prevent binding to the wild type sequence, an additional mismatch was incorporated at the penultimate nucleotide in order to destabilise the base pairing between the primers and the corresponding non-target template.

Table 2.8 Quantitative PCR cycling conditions for amplifying the D408A allele

Cycle	Temperature (°C)	Time	Number of cycles
Initial denaturation	95	5 minutes	1
Denaturation	95	30 seconds	30
Primer annealing	50-95	7.5 minutes with increments of 0.5 every 5 seconds	30
Extension	72	90 seconds	30
Final extension	72	3 minutes	1

Each mutant candidate was screened for both the wild type and the mutant allele using a real time qPCR. Each mutant was cultured on lysogeny broth. Bacteria from each colony were transferred into 50 µl of molecular grade water in a 96-well PCR plate (Bio-Rad, UK, HSL9601) and the cells were lysed by heating at 99°C for 10 minutes. The PCR reaction mixture was made to a final volume of 20 µl containing 1 µl of lysate, 1 µl of the forward and reverse primer (Table 2.2) and 17 µl of iQ SYBR Green mastermix (Bio-Rad, UK, 1708880). For each sample, two primer combinations were used to amplify the sequence conferring the wild type 408D allele (primers 2600 and 2602) and the mutant 408A allele (primers 2601 and 2602). The qPCR was performed on a BioRad C1000 Themocycler using the cycling

conditions detailed in Table 2.8.

2.16 Statistical analysis

With the exception of the mutant selection experiments where a variable number of replicates were performed (Table 2.6). Each experiment was repeated at least three times. The number of each biological and technical replicates performed is displayed in the figure legend of each graph where appropriate. For each biological replicate, the mean of the technical replicates was calculated and compared to that of the other biological replicates. Each biological replicate is shown on graphs accompanied by the mean and standard deviation, except where curves are required e.g. membrane depolarization and growth kinetics, where the mean of all the biological replicates was plotted. To determine statistical significance, unless otherwise specified an unpaired Student's T-test with Welch's correction or a one-way Analysis of Variance (ANOVA) was performed using GraphPad Prism (Version 7.0). The statistical test used is described alongside each dataset in each results chapter.

An unpaired Student's T test was used for normally distributed data, with equal variance, where the mean of two independent groups was compared. As a result this statistical test was used for analysis of the following experiments:

- Disk diffusion assays where differences between strains was not compared
- Well diffusion assays where differences between strains was not compared
- Ethidium bromide accumulation assays
- Norfloxacin accumulation assays
- Hoescht H33342 accumulation assays
- GFP reporting assays

- Comparison of gene expression data
- Growth Kinetics

The Welch's correction allows for comparison between data which is assumed to have unequal variances. A one way ANOVA was used to compare the means of two or more independent groups with equal variance. For each T-test that is performed there is a risk of incurring a Type I error (a false positive). Therefore, instead of multiple t-tests an ANOVA is used. As a result this statistical test was used for the analysis of the following experiments:

- Disk diffusion assays where multiple strains across a variety of antibiotic concentrations were compared
- Membrane permeability assays where multiple strains across a variety of compound concentrations were compared
- Membrane potential assays where multiple strains across a variety of antibiotic concentrations were compared

A P value of ≤ 0.05 was considered to be significant for all tests, unless otherwise specified.

Chapter Three

Are antipsychotics efflux inhibitors?

Considering their role in innate and evolved resistance, efflux pumps are targets for the discovery and development of antimicrobial adjuvants (Marquez, 2005); their inhibition prevents the extrusion of antibiotics to restore their antibacterial activity (Green et al., 2020; Lamut et al., 2019; Opperman and Nguyen, 2015; Sjuts et al., 2016; Vargiu, Ruggerone, et al., 2014).

One strategy to identify potential efflux inhibitors is to screen and repurpose drugs already in clinical use for indications other than infectious diseases (Lomovskaya and Bostian, 2006). Considering their pharmacokinetics and toxicology are well described, their use may be invaluable in terms of bypassing the time and costs associated with drug development. Amongst the drugs considered for repurposing, there is evidence that the first generation antipsychotic medications chlorpromazine and amitriptyline behave as efflux inhibitors (Bailey et al., 2008). Whilst these activities occur at concentrations greater than those clinically achievable and/or desirable, chlorpromazine and amitriptyline potentiate antibiotic activity at sub-antibacterial inhibitory concentrations (Bailey et al., 2008; Coutinho et al., 2009; Kristiansen, Hendricks, et al., 2007; Ying et al., 2007), increase the accumulation of AcrB substrates (Bailey et al., 2008; Kaatz et al., 2003; Kristiansen, Hendricks, et al., 2007; Martins et al., 2011) and induce the expression of *ramA* in *S. Typhimurium* (Lawler et al.,

2013); a response that has been previously associated with a lack of efflux. Despite some evidence to suggest chlorpromazine and amitriptyline may interact with AcrB (Bailey et al., 2008; Yamasaki, Fujioka, et al., 2016; Laudy et al., 2017), the mechanism by which these compounds elicit their efflux inhibitory activity is largely unknown. Understanding the mechanism of efflux inhibition is essential for facilitating the design of more active and less cytotoxic efflux inhibitors.

3.1 Hypothesis

- The efflux inhibitory activity of chlorpromazine and amitriptyline against *S. Typhimurium* and *E. coli* is a result of direct interactions with the AcrB pump protein of the AcrAB-TolC complex.

3.2 Aims and objectives

- To confirm the ability of chlorpromazine and amitriptyline to potentiate the antibiotic activity of AcrB substrates against Gram-negative strains overexpressing efflux pumps.
- To assess the impact of chlorpromazine and amitriptyline on the efflux of the AcrB substrates Hoechst H33342, ethidium bromide and norfloxacin from *S. Typhimurium* SL1344 and *E. coli* MG1655.
- To rationalise the efflux inhibitory activity of chlorpromazine and amitriptyline using molecular docking and dynamics simulations of these compounds with AcrB. Performed in collaboration with The University of Cagliari, Italy.
- To determine whether the efflux inhibitory phenotype observed in the presence of chlorpromazine result from non-efflux effects on the OM.

3.3 Synergy/potentialiation of antibiotic activity by chlorpromazine and amitriptyline

3.3.1 The use of strains overexpressing efflux pumps in synergy assays

Unpublished research undertaken by the Piddock team has shown that limited antibiotic potentiation occurs when the AcrB substrates ciprofloxacin, tetracycline, chloramphenicol and ethidium bromide are combined with compounds from a 1.5k chemical compound library against wild type strains of *Salmonella* Typhimurium SL1344, *Escherichia coli* MG1655, *Pseudomonas aeruginosa* PAO1 and *Acinetobacter baumannii* AB211. Therefore, to maximise the sensitivity of these assays, strains overexpressing multidrug efflux pumps were used in all synergy/potentialiation assays. In order for the results obtained for this thesis to be directly comparable to results obtained by others, the same over-expressing strains as used previously were used for all synergy assays. These were as follows: *E. coli* BW25113 *marR::aph* and *S. Typhimurium* SL1344 *ramR::aph* which overexpress the *acrAB-tolC* efflux pump, *P. aeruginosa* K1454 which is a strain of PAO1 containing a mutation within *nalC* that overexpresses the efflux pump *mexAB-oprM* and *A. baumannii* AB211 which contains a mutation within *ades* and overexpresses *adeABC*. Justification for the use of overexpressing strains lies in the evidence that overexpression of efflux genes confers clinically relevant levels of resistance (Baucheron, Tyler, et al., 2004; Giraud, Cloeckert, Kerboeuf, et al., 2000; Magnet et al., 2001; Mazzariol et al., 2000; Piddock et al., 2000). When an efflux pump is inhibited in an over-expressing strain a larger increase in antibiotic susceptibility is observed compared to a wild type strain. As such, overexpressing strains are frequently used to determine the extent of antibiotic potentiation (Coelho et al., 2015; Ferrer-Espada et al., 2019; Lomovskaya, Warren, et al., 2001; Rgen et al., 2011).

3.3.2 Chequerboard assays to determine potentiation of the activity of AcrB substrates by chlorpromazine and amitriptyline

Both chlorpromazine and amitriptyline have some intrinsic antibacterial activity (Table 3.1). Chequerboard assays were performed in combination with a range of substrates of the AcrAB-TolC efflux pump; chloramphenicol, nalidixic acid, tetracycline, ciprofloxacin, norfloxacin and ethidium bromide against *E. coli* BW25113 *marR::aph*, *S. Typhimurium* SL1344 *ramR::aph*, *P. aeruginosa* K1454 and *A. baumannii* AB211. The use of several Gram-negative species, including *A. baumannii* and *P. aeruginosa* which do not possess AcrAB-TolC, provides information on whether chlorpromazine and amitriptyline are specific for AcrAB-TolC alone, or also target homologous efflux pumps. A range of substrates were used to determine whether chlorpromazine and amitriptyline selectively potentiate the activity of a single antibiotic/class or are broad spectrum.

Table 3.1 MIC of chlorpromazine and amitriptyline against a variety of Gram-negative organisms.

Strain	MIC ($\mu\text{g/ml}$)	
	Chlorpromazine	Amitriptyline
<i>S. Typhimurium</i> SL1344	256	512
<i>S. Typhimurium</i> SL1344 <i>ramR::aph</i>	1,024	888
<i>E. coli</i> MG1655	256	512
<i>E. coli</i> MG1655 <i>marR::aph</i>	256	444
<i>A. baumannii</i> AB211	128	222
<i>P. aeruginosa</i> K1454	2,048	1,775

The combinations of each antibiotic with 1/4, 1/8 and 1/16 the MIC concentration of amitriptyline, chlorpromazine and Pa β N are displayed in Table 3.2, Table 3.3 and Table 3.4. Changes in MIC by two doubling dilutions were considered to be ‘significant’ and are highlighted. In addition, FIC indices, based on the Lowe additivity formula, were calculated to determine the significance of antibiotic-drug combinations. An FIC value of ≤ 0.5 indicates synergy, < 4.0 indicates no effects and ≥ 4.0 indicates antagonism (Hall, Middleton, et al., 1983). The FIC values for each combination are displayed in Appendix Table 3.1, Appendix

Table 3.2 and Appendix Table 3.3. It is important to note that for each antibiotic-inhibitor combination where the FIC value indicated synergy ($\text{FIC} \leq 0.5$) a ‘significant’ \geq two doubling dilution increase in susceptibility was also observed.

In combination with antibiotics, amitriptyline increased the susceptibility of *S. Typhimurium* overexpressing AcrAB-TolC to chloramphenicol, nalidixic acid and tetracycline, but not to ciprofloxacin or ethidium bromide (Table 3.2 and Appendices Table 3.1). Amitriptyline also increased the susceptibility of *A. baumannii* to chloramphenicol and *P. aeruginosa* to nalidixic acid. Chlorpromazine increased the susceptibility of *S. Typhimurium* to chloramphenicol, ciprofloxacin, tetracycline, and nalidixic acid, but not to ethidium bromide (Table 3.3 and Appendices Table 3.2). Chlorpromazine also increased the susceptibility of *P. aeruginosa* to chloramphenicol, nalidixic acid, tetracycline and ethidium bromide, but not to ciprofloxacin. Chlorpromazine did not increase the susceptibility of *A. baumannii* to any of the tested substrates. Neither amitriptyline or chlorpromazine potentiated the activity of norfloxacin against any strain, or, of any of the tested substrates against *E. coli* overexpressing AcrAB-TolC. In chequerboard assays, the positive control Pa β N was the most potent efflux inhibitor; the only compounds with which synergy was not observed was ciprofloxacin and norfloxacin, against *E. coli* and *A. baumannii*, and tetracycline and ethidium bromide against *E. coli* (Table 3.4 and Appendices Table 3.3).

Table 3.2 MIC of compounds alone, and with amitriptyline, against *S. Typhimurium* SL1344 *ramR::aph*, *E. coli* BW25113 *marR::aph*, *A.baumannii* AB211 and *P.aeruginosa* K1454.

Antibiotics	Amitriptyline (AMI) concentration	MIC ($\mu\text{g/ml}$)			
		SL1344 <i>ramR::aph</i>	BW25113 <i>marR::aph</i>	AB211	K1454
Chloramphenicol	No AMI	16	4	256	256
	1/16 MIC AMI	8	4	256	128
	1/8 MIC AMI	4	4	128	128
	1/4 MIC AMI	2	2	64	128
Ciprofloxacin	No AMI	0.06	0.004	512	0.25
	1/16 MIC AMI	0.03	0.03	512	0.25
	1/8 MIC AMI	0.03	0.008	512	0.25
	1/4 MIC AMI	0.004	0.004	512	0.125
Nalidixic acid	No AMI	8	4	1,024	1,024
	1/16 MIC AMI	8	4	1,204	512
	1/8 MIC AMI	4	4	1,024	256
	1/4 MIC AMI	2	2	1,024	256
Tetracycline	No AMI	8	2	256	64
	1/16 MIC AMI	4	2	256	64
	1/8 MIC AMI	2	2	256	64
	1/4 MIC AMI	1	1	256	32
Norfloxacin	No AMI	0.25	0.03	512	1
	1/16 MIC AMI	0.12	0.06	512	1
	1/8 MIC AMI	0.25	0.03	512	1
	1/4 MIC AMI	0.25	0.03	512	1
Ethidium bromide	No AMI	512	128	256	2,048
	1/16 MIC AMI	512	64	256	2,048
	1/8 MIC AMI	512	128	256	2,048
	1/4 MIC AMI	256	64	128	1,024

Bold font indicates ≥ 2 fold decrease in MIC value in comparison to the antibiotic alone. The MIC of AMI was 888 $\mu\text{g/ml}$, 444 $\mu\text{g/ml}$, 222 $\mu\text{g/ml}$ and 1,775 $\mu\text{g/ml}$ against SL1344 *ramR::aph*, BW25113 *marR::aph*, AB211 and K1454, respectively. The mode of three biological replicates is shown.

Table 3.3 MIC of compounds alone and with CPZ against *S. Typhimurium* SL1344 *ramR::aph*, *E. coli* BW25113 *marR::aph*, *A. baumannii* AB211 and *P. aeruginosa* K1454.

Antibiotics	Chlorpromazine (CPZ) concentration	MIC ($\mu\text{g/ml}$)			
		SL1344 <i>ramR::aph</i>	BW25113 <i>marR::aph</i>	AB211	K1454
Chloramphenicol	No CPZ	8	4	64	128
	1/16 MIC CPZ	4	2	64	64
	1/8 MIC CPZ	2	2	64	32
	1/4 MIC CPZ	1	2	32	32
Ciprofloxacin	No CPZ	0.03	0.008	128	0.25
	1/16 MIC CPZ	0.03	0.008	128	0.25
	1/8 MIC CPZ	0.015	0.008	128	0.25
	1/4 MIC CPZ	0.008	0.004	128	0.25
Nalidixic acid	No CPZ	8	4	512	512
	1/16 MIC CPZ	4	2	512	128
	1/8 MIC CPZ	4	2	512	128
	1/4 MIC CPZ	0.5	2	512	64
Tetracycline	No CPZ	4	2	512	32
	1/16 MIC CPZ	4	1	512	16
	1/8 MIC CPZ	2	1	256	8
	1/4 MIC CPZ	1	1	256	8
Norfloxacin	No CPZ	0.25	0.03	256	1
	1/16 MIC CPZ	0.5	0.03	256	1
	1/8 MIC CPZ	0.5	0.03	256	0.5
	1/4 MIC CPZ	0.5	0.03	128	0.5
Ethidium bromide	No CPZ	1,024	128	128	4,096
	1/16 MIC CPZ	512	128	64	1,024
	1/8 MIC CPZ	512	64	64	1,024
	1/4 MIC CPZ	512	64	64	256

Bold font indicates ≥ 2 fold decrease in MIC in comparison to the antibiotic alone. The MIC of CPZ was 1,024 $\mu\text{g/ml}$, 256 $\mu\text{g/ml}$, 128 $\mu\text{g/ml}$ and 2,048 $\mu\text{g/ml}$ against SL1344 *ramR::aph*, BW25113 *marR::aph*, AB211 and K1454, respectively. The mode of three biological replicates is shown.

Table 3.4 MIC of compounds alone, and with Pa β N, against *S. Typhimurium* SL1344 *ramR::aph*, *E. coli* BW25113 *marR::aph*, *A. baumannii* AB211 and *P. aeruginosa* K1454.

Antibiotics	Pa β N concentration	MIC (μ g/ml)			
		SL1344	BW25113	AB211	K1454
		<i>ramR::aph</i>	<i>marR::aph</i>		
Chloramphenicol	No Pa β N	4	4	128	256
	1/16 MIC Pa β N	0.5	N/D	16	8
	1/8 MIC Pa β N	0.5	0.5	16	1
	1/4 MIC Pa β N	0.25	0.5	8	1
Ciprofloxacin	No Pa β N	0.06	0.015	256	0.25
	1/16 MIC Pa β N	0.015	N/D	256	0.12
	1/8 MIC Pa β N	0.015	0.008	256	0.06
	1/4 MIC Pa β N	0.004	0.008	128	0.06
Nalidixic acid	No Pa β N	16	4	1,024	1,024
	1/16 MIC Pa β N	0.5	N/D	256	4
	1/8 MIC Pa β N	0.5	0.5	256	2
	1/4 MIC Pa β N	0.25	0.5	128	2
Tetracycline	No Pa β N	2	2	512	64
	1/16 MIC Pa β N	1	N/D	512	32
	1/8 MIC Pa β N	0.5	1	256	16
	1/4 MIC Pa β N	0.25	1	128	4
Norfloxacin	No Pa β N	0.25	0.06	256	1
	1/16 MIC Pa β N	0.25	0.06	256	0.5
	1/8 MIC Pa β N	0.06	0.06	256	0.25
	1/4 MIC Pa β N	0.015	0.03	64	0.03
Ethidium bromide	No Pa β N	512	256	256	2,048
	1/16 MIC Pa β N	256	N/D	128	256
	1/8 MIC Pa β N	128	128	64	256
	1/4 MIC Pa β N	64	128	64	256

Bold font indicates ≥ 2 fold decrease in MIC compared to antibiotic alone. The Pa β N MIC was 1,024 μ g/ml, 256 μ g/ml, 1,024 μ g/ml and 1,024 μ g/ml against SL1344 *ramR::aph*, BW25113 *marR::aph*, AB211 and K1454. N/D; not determined. The mode of three biological replicates is shown.

3.3.3 Disk diffusion assays to determine whether chlorpromazine and amitriptyline potentiated the activity of AcrB substrates

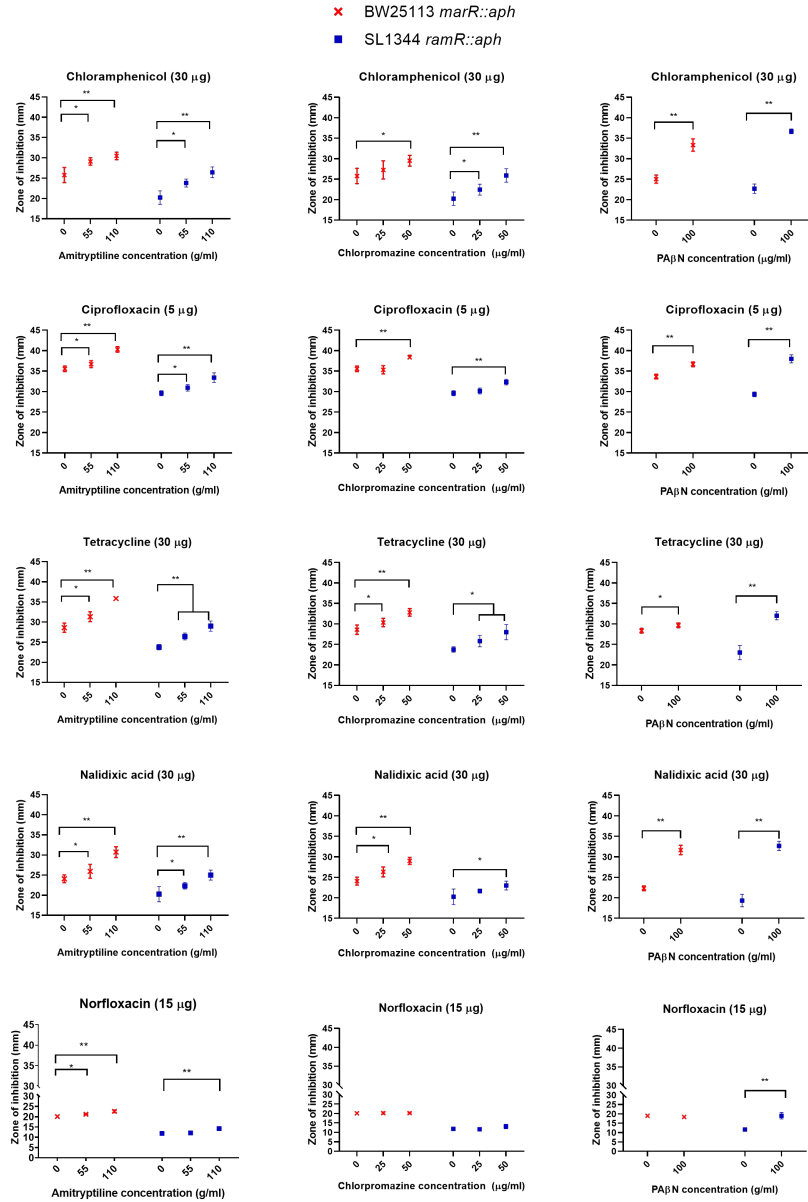
Interestingly, when tested in a chequerboard assay, neither chlorpromazine nor amitriptyline potentiated the activity of norfloxacin against any strain, or, of any of the tested substrates against *E. coli* overexpressing AcrAB-TolC. Chequerboard assays rely on the use of doubling dilutions and therefore it was hypothesized that these assays are not sensitive enough to determine the synergistic activity of compounds with activity at higher concentrations. Therefore, a disk diffusion assay in which Isosensitest agar plates were supplemented with varying concentrations of chlorpromazine and amitriptyline was used to assess the effect of these compounds on the antibiotic susceptibility of *E. coli* and *S. Typhimurium* that overexpressed AcrAB-TolC. The known efflux inhibitor Pa β N was used as a positive control.

These disk diffusion assays confirmed that chlorpromazine and amitriptyline potentiate the activity of AcrB substrates. For both *E. coli* and *S. Typhimurium*, the zones of inhibition for chloramphenicol, tetracycline, ciprofloxacin and nalidixic acid were significantly larger in the presence of chlorpromazine, amitriptyline and Pa β N than in their absence (Figure 3.1). An exception is that the activity of norfloxacin (15 μ g) was not significantly potentiated by chlorpromazine against both *S. Typhimurium* and *E. coli* or by Pa β N against *S. Typhimurium*. No zone was observed utilizing ethidium bromide on a disk. This was a result of poor diffusion of ethidium bromide through the agar.

3.3.4 Well diffusion assays to determine potentiation of the activity of norfloxacin and ethidium bromide by chlorpromazine and amitriptyline

The lack of synergy with norfloxacin was hypothesized to be a consequence of the high potency of this antibiotic at the concentration available on the disk (15 μ g). Norfloxacin,

Figure 3.1: Comparisons of the zone of inhibition obtained for disks containing chloramphenicol, ciprofloxacin, amitriptyline, tetracycline and nalidixic acid, when used in combination with chlorpromazine, amitriptyline and the positive control PAβN.



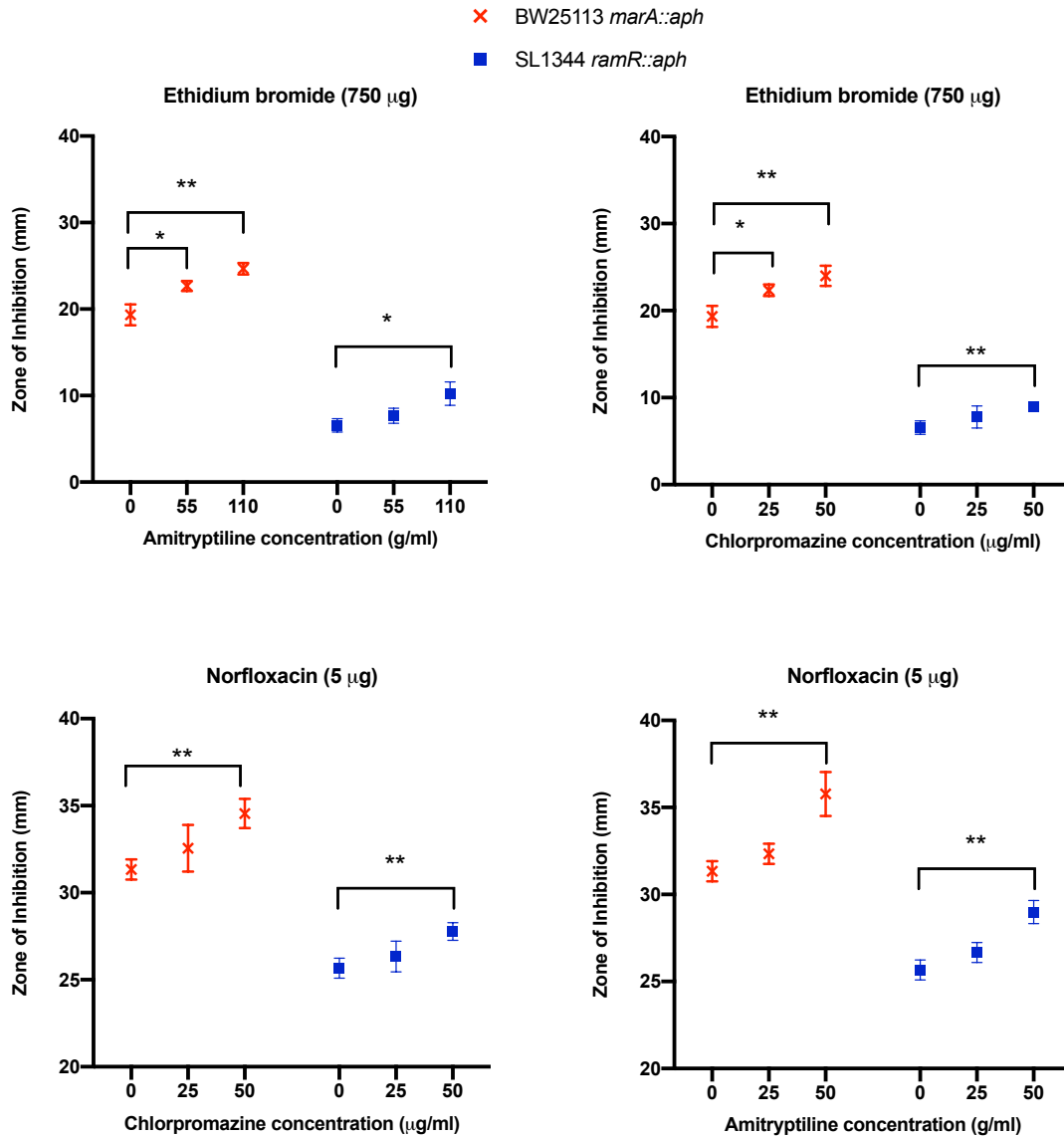
The graph shows the mean and standard deviation of three biological replicates. Each biological replicate was calculated from the mean of three technical replicates. Data were analysed by a Student's *t* test with Welch's correction. Single and double asterisks denote a significant difference of $P < 0.05$ and $P < 0.001$, respectively in comparison to the untreated control.

like ciprofloxacin, is a quinolone with very high potency. The lack of an observable zone in disk diffusion assays with ethidium bromide was thought to be due to the high concentration at which it elicits its antimicrobial activity; incorporating high concentrations of ethidium bromide on a paper disk likely prevents the ability of this compound to migrate through the agar. Therefore, well diffusion assays were undertaken in which ethidium bromide and norfloxacin were incorporated into holes within Isosensitest agar plates supplemented with increasing concentrations of chlorpromazine and amitriptyline. This assay was hypothesized to allow ethidium bromide to more effectively and more evenly migrate through the agar. The concentration of norfloxacin used was reduced from 15 μg in the disk diffusion assay to 5 μg in the well. Against both *E. coli* BW25113 *marR::aph* and *S. Typhimurium* SL1344 *ramR::aph*, chlorpromazine and amitriptyline were able to potentiate the activity of norfloxacin and ethidium bromide; the zone of inhibition for both substrates was significantly larger in the presence of amitriptyline and chlorpromazine than in their absence (Figure 3.2).

3.4 The impact of chlorpromazine and amitriptyline on the accumulation of AcrB substrates

The efflux inhibitory activity of chlorpromazine and amitriptyline against *S. Typhimurium* SL1344 and *E. coli* MG1655 was measured by determining their ability to increase the intracellular accumulation of AcrB substrates; Pa β N was used as a positive control. Unfortunately, due to limited fluorescence, efflux and accumulation assays could not be performed with all substrates used in the synergy assays. Therefore, well described substrates of AcrB were used for the accumulation (H33342 and norfloxacin) and efflux assays (ethidium bromide); ethidium bromide, H33342 and norfloxacin are fluorescent either intrinsically (norfloxacin) or upon intercalation with DNA (H33342 and ethidium bromide) (Blair and Piddock, 2016; Elkins et al., 2002).

Figure 3.2: Comparisons of the zone of inhibition obtained for well diffusion assay with ethidium bromide and norfloxacin when used in combination with chlorpromazine and amitriptyline.



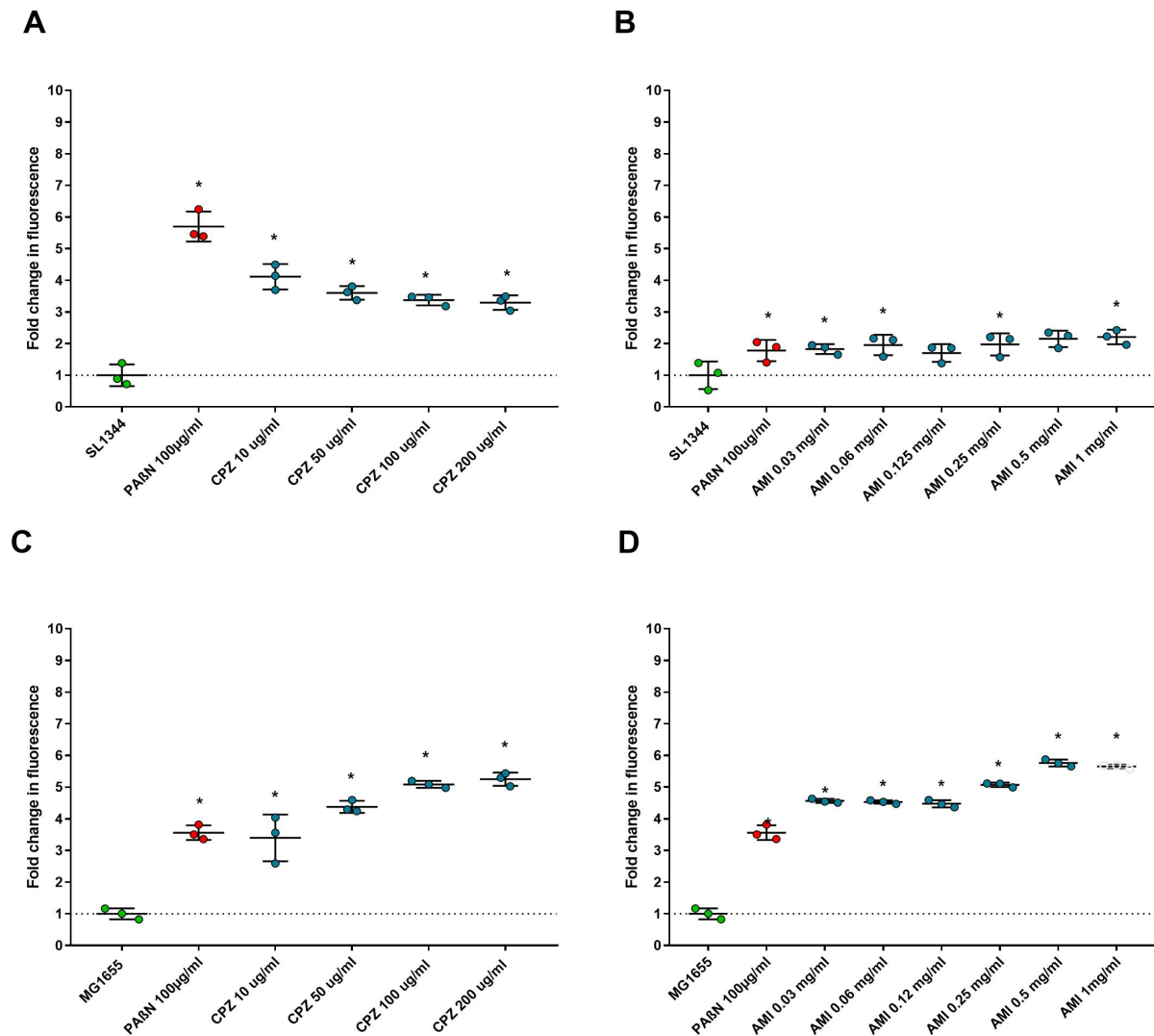
The graph shows the mean and standard deviation of three biological replicates. Each biological replicate was calculated from the mean of three technical replicates. Data were analysed by a Student's *t* test with Welch's correction. Single and double asterisks denote a significant difference of $P < 0.05$ and $P < 0.001$, respectively in comparison to the untreated control.

3.4.1 Chlorpromazine and amitriptyline increase the accumulation of ethidium bromide

Bacteria were preloaded with ethidium bromide and treated with the proton (H^+) ionophore carbonyl cyanide m-chlorophenyl hydrazine (CCCP); which prevents the efflux of ethidium bromide by inhibiting the PMF. Upon energisation with glucose, the activity of the efflux pump is restored and the efflux of ethidium bromide can be measured over time (Paixão et al., 2009). Efflux inhibition results in a decrease in the efflux of ethidium bromide and thus higher intracellular concentrations.

Compared with untreated controls, both chlorpromazine and amitriptyline significantly increased the accumulation of ethidium bromide by *E. coli* (chlorpromazine $P=0.0054-0.0001$ and amitriptyline $P=<0.0001$) and *S. Typhimurium* (chlorpromazine $P=0.0004-0.0006$ and amitriptyline $P=0.0133-0.377$) (Figure 3.3). However, the impact of these compounds was strain specific. Both chlorpromazine and amitriptyline increased the accumulation of ethidium bromide by *E. coli* in a concentration-dependent manner, the highest concentration of chlorpromazine (200 $\mu\text{g/ml}$) and amitriptyline (1 mg/ml) increased ethidium bromide accumulation by 5.25 fold and 5.65 fold compared to the untreated control. At all concentrations of chlorpromazine and amitriptyline, the decrease in ethidium bromide efflux by *E. coli* was greater than that observed by Pa β N (3.55 fold). Chlorpromazine also increased the accumulation of ethidium bromide by *S. Typhimurium* in a dose-dependent manner. However, the greatest increase in ethidium bromide accumulation (4.11 fold) was observed at the lowest concentration of chlorpromazine (10 $\mu\text{g/ml}$). This increase was higher than that observed with Pa β N (5.40 fold). All concentrations of amitriptyline increased the accumulation of ethidium bromide by *S. Typhimurium* to a similar extent (1.61-2.20 fold), suggesting that this compound saturated the pump/pumps at relatively low concentrations. This increase in ethidium bromide

Figure 3.3: Accumulation of ethidium bromide in the presence of chlorpromazine or amitriptyline.



Accumulation of ethidium bromide in the presence of chlorpromazine (A) and amitriptyline (B) in *S. Typhimurium* SL1344. Accumulation of ethidium bromide in the presence of chlorpromazine (C) and amitriptyline (D) in *E. coli* MG1655. The graph shows the mean and standard deviation of three biological replicates. Each biological replicate was calculated from the mean of three technical replicates. Data were analysed by a Student's t test with Welch's correction. Single asterisks denote a significant difference of $P < 0.05$ in comparison to the untreated control. Chlorpromazine; CPZ. Amitriptyline; AMI.

accumulation by amitriptyline was comparable to that by Pa β N (1.78 fold). It is important to note that previous studies have shown that the ability of chlorpromazine to decrease the efflux of ethidium bromide was ablated in strains lacking AcrB, suggesting that its efflux inhibitory activity is specific for this pump (Bailey et al., 2008).

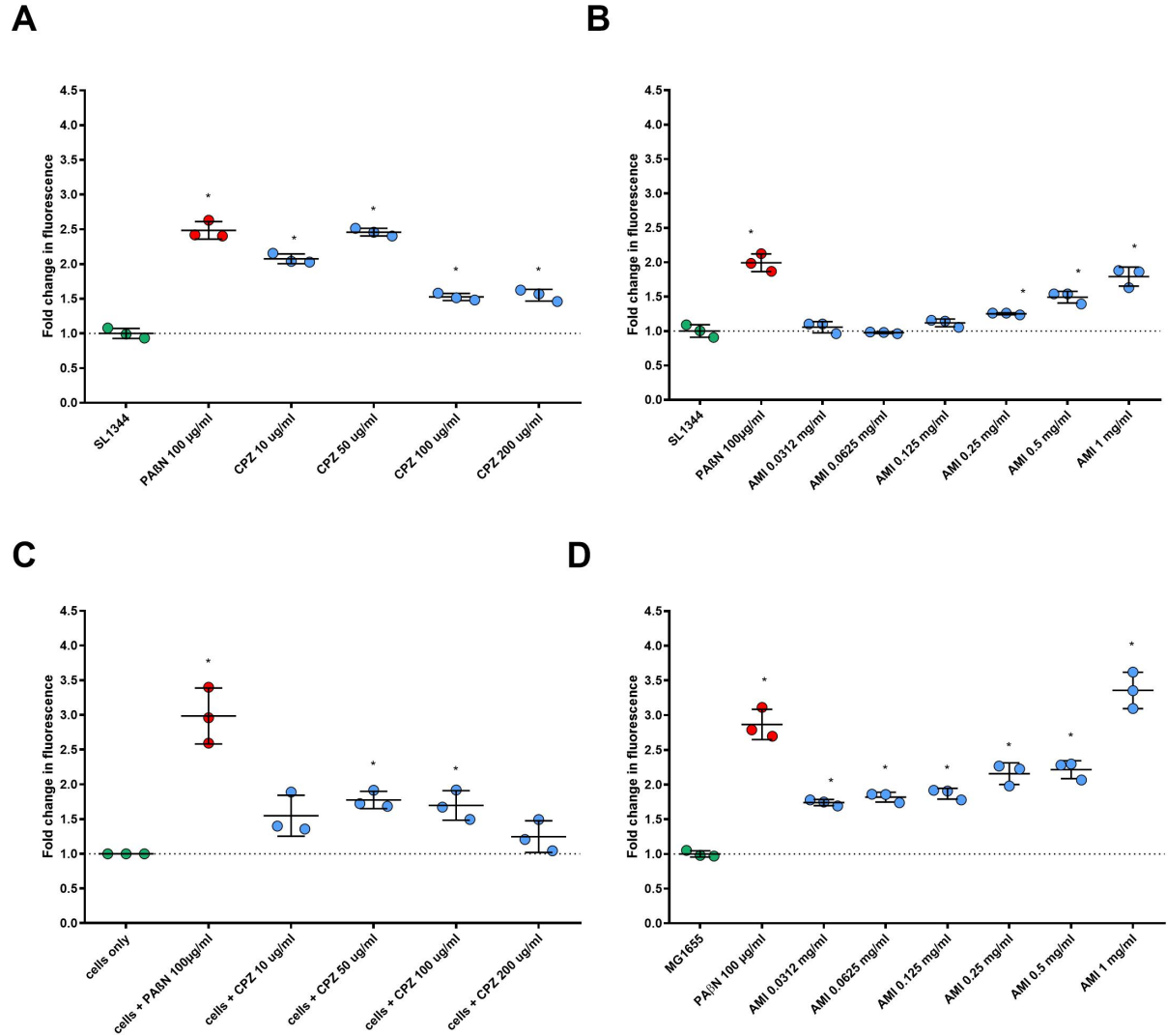
3.4.2 Chlorpromazine and amitriptyline increase the accumulation of Hoechst H33342

Accumulation assays can be used to infer the level of efflux; efflux inhibition results in a lower level of efflux and thus substrate accumulation. Chlorpromazine and amitriptyline significantly increased the accumulation of H33342 from wild type *E. coli* MG1655 (chlorpromazine $P=0.0328-0.0004$ and amitriptyline $P=\leq 0.0001$) and *S. Typhimurium* SL1344 (chlorpromazine $P=<0.0001-0.0010$ and amitriptyline $P=0.0012-0.0024$) (Figure 3.4). Amitriptyline increased the accumulation of H33342 from *E. coli* and *S. Typhimurium* in a dose-dependent manner, in which the largest fold increase in accumulation was observed in the presence of 1 mg/ml of amitriptyline; 3.35 fold and 1.79 fold increases by *E. coli* and *S. Typhimurium*, respectively. The greatest increase in the accumulation of H33342 relative to the unexposed control by chlorpromazine occurred when *E. coli* (1.77 fold) and *S. Typhimurium* (2.45 fold) were exposed to 50 μ g/ml. At increasing chlorpromazine concentrations H33342 accumulation decreased. The increase in H33342 accumulation by chlorpromazine and amitriptyline was comparable to that observed by Pa β N for *E. coli* (2.86 fold) and *S. Typhimurium* (1.96 fold).

3.4.3 Chlorpromazine and amitriptyline inhibit the efflux of norfloxacin only in strains overexpressing AcrAB-TolC

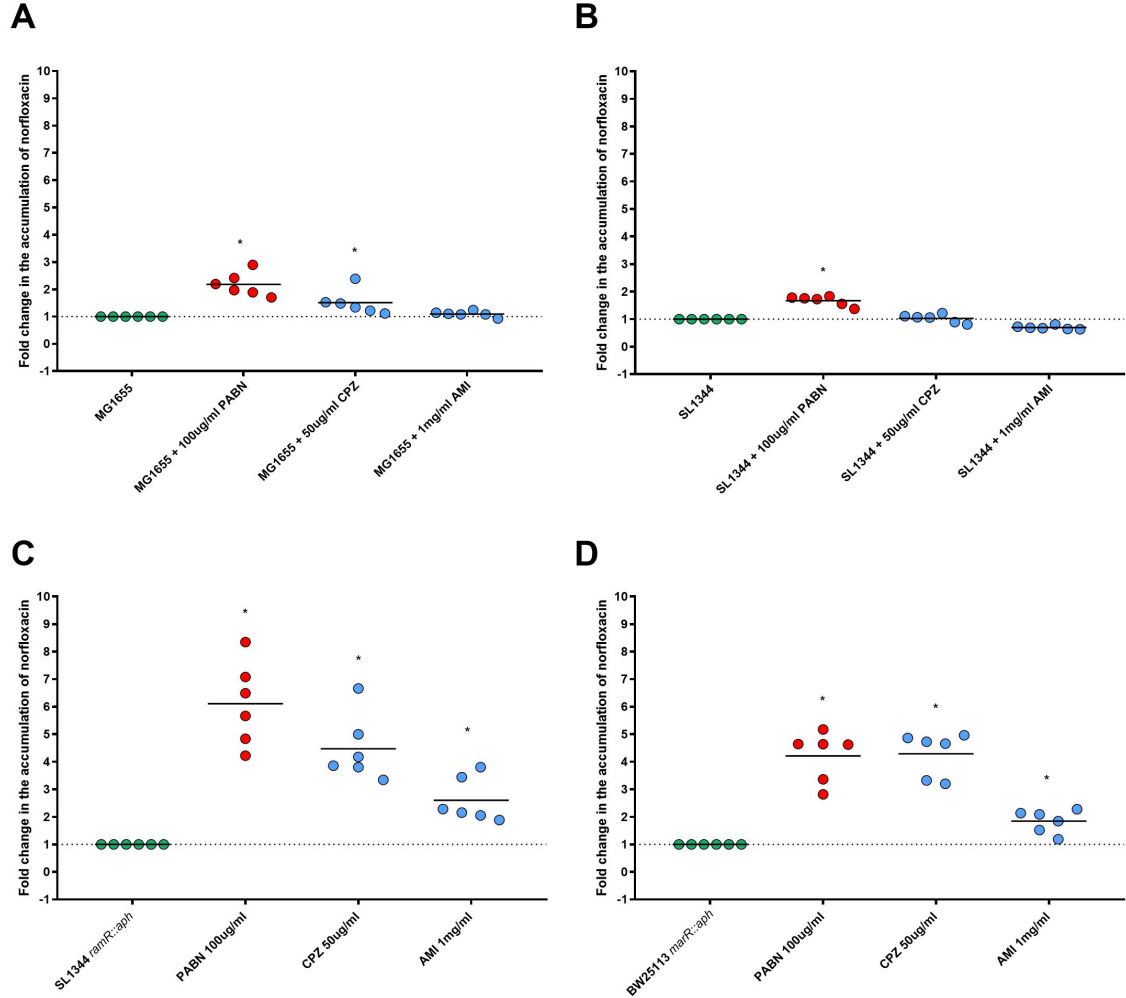
Chlorpromazine and amitriptyline did not inhibit the efflux of norfloxacin from wild type *E. coli* and *S. Typhimurium* (Figure 3.5). Therefore, this experiment was repeated with strains overexpressing AcrAB-TolC. The use of overexpressing strains provides a more

Figure 3.4: Accumulation of Hoechst H33342 in the presence of chlorpromazine or amitriptyline.



Accumulation of Hoechst H33342 in the presence of chlorpromazine (A) and amitriptyline (B) in *S. Typhimurium* SL1344. Accumulation of Hoechst H33342 in the presence of chlorpromazine (C) amitriptyline (D) in *E. coli* MG1655. The graph shows the mean and standard deviation of three biological replicates. Each biological replicate was calculated from the mean of three technical replicates. Data were analysed by a Student's t test with Welch's correction. Single asterisks denote a significant difference of $P < 0.05$ in comparison to the untreated control. Chlorpromazine; CPZ. Amitriptyline; AMI.

Figure 3.5: Accumulation of norfloxacin in the presence of chlorpromazine or amitriptyline.



(A) Fold change in the accumulation of norfloxacin in the presence of chlorpromazine and amitriptyline in *E. coli* MG1655, (B) *S. Typhimurium* SL1344, (C) *E. coli* BW25113 *marR::aph* and (D) *S. Typhimurium* SL1344 *ramR::aph*. The graph shows the mean and standard deviation of six biological replicates. Each biological replicate was calculated from the mean of two technical replicates. Data were analysed by a Student's t test with Welch's correction. Single asterisks denote a significant difference of $P < 0.05$ in comparison to the untreated control. Chlorpromazine; CPZ. Amitriptyline; AMI.

sensitive method to determine the extent of efflux inhibition. Chlorpromazine (50 µg/ml) increased the accumulation of norfloxacin from *E. coli* and *S. Typhimurium* by 4.28 ($P=0.0002$) and 4.50 fold ($P=0.0009$), respectively (Figure 3.5). Amitriptyline (1 mg/ml) increased the accumulation of norfloxacin from *E. coli* BW25113 *marR::aph* and *S. Typhimurium* SL1344 *ramR::aph* by 1.83 ($P=0.0042$) and 2.50 fold ($P=0.0047$), respectively. The inhibition of norfloxacin efflux was comparable to, or less, than efflux inhibition by PaβN against *E. coli* (4.20) and *S. Typhimurium* (6.07 fold).

3.5 *In silico* experiments to elicit the interaction, if any, of chlorpromazine and amitriptyline with AcrB

In order to rationalise the efflux inhibitory activity of chlorpromazine and amitriptyline, their propensity to bind AcrB from *E. coli* (AcrB_{EC}) and *S. Typhimurium* (AcrB_{ST}) was determined by molecular docking, molecular dynamics and subsequent free energy calculations. These *in silico* experiments were performed by collaborators from The University of Cagliari, Italy (Chiara Fais, Attilio Vargiu, Guiliano Mallocci and Paolo Ruggerone).

3.5.1 Chlorpromazine and amitriptyline bind to a well-characterised substrate/inhibitor binding region of AcrB

The blind ensemble docking revealed a high overlap in the binding poses of chlorpromazine and amitriptyline to AcrB_{EC} and AcrB_{ST} (Appendix Figure A3.1). Of note, the binding poses for both compounds were located largely within the distal binding pocket (DP) at a phenylalanine-rich region known as the hydrophobic trap (HT). In addition, blind docking of ethidium bromide and norfloxacin revealed an overlap in the binding sites of these AcrB substrates with that of chlorpromazine and amitriptyline (Appendix Figure A3.1).

3.5.2 Molecular dynamics simulations confirm the binding of chlorpromazine and amitriptyline to the hydrophobic trap

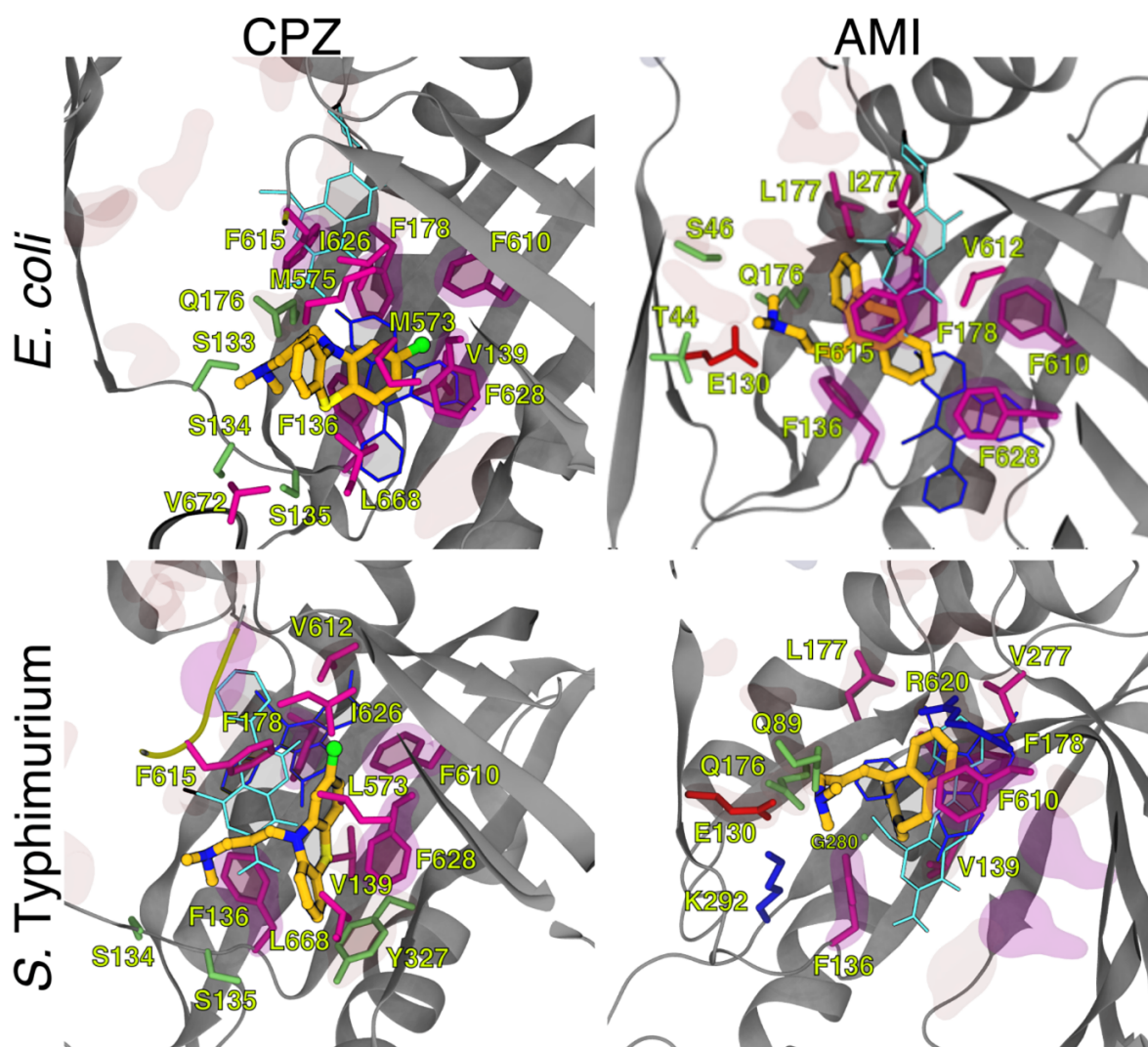
The molecular dynamics trajectories confirmed the binding of chlorpromazine, amitriptyline, norfloxacin and ethidium bromide within the DP (Figure 3.6). The number of direct contacts made by chlorpromazine and amitriptyline with the hydrophobic residues lining this region were as follows: chlorpromazine made 10 contacts with both AcrB_{EC} and AcrB_{ST}, amitriptyline made 8 contacts with AcrB_{EC} and 6 with AcrB_{ST}. Importantly, chlorpromazine occupied a larger fraction of the DP than amitriptyline and had a larger steric clash with the known efflux inhibitor MBX3132 to AcrB_{EC}. In contrast, amitriptyline bound slightly upward of the DP and made contacts with the hydrophilic residues E130 and Q176 (Figure 3.6 and Appendix Table 3.5).

The scoring energies calculated from the docking and dynamics simulations for chlorpromazine and amitriptyline were similar for both AcrB_{EC} and AcrB_{ST} (Appendix Table A3.4 and A3.6). In addition, the dynamics scoring energies were also similar for chlorpromazine, amitriptyline, norfloxacin and ethidium bromide against AcrB_{EC} and AcrB_{ST} (Appendix Table 3.6)

Importantly, molecular dynamics revealed that while chlorpromazine, amitriptyline, ethidium bromide and norfloxacin all bound stably to the DP, chlorpromazine and amitriptyline featured a much greater steric clash with the binding of ethidium bromide to both AcrB_{EC} and AcrB_{ST} compared to norfloxacin (Figure 3.6). The binding poses of norfloxacin were found to lie slightly away from those of chlorpromazine and amitriptyline; above chlorpromazine in AcrB_{EC} and AcrB_{ST}, above amitriptyline in AcrB_{EC} and below amitriptyline in AcrB_{ST}.

Finally, the molecular dynamics simulations show that chlorpromazine, but not

Figure 3.6: Representative conformations obtained from molecular dynamics simulations showing the most stable binding poses of chlorpromazine and amitriptyline within the DP of AcrB_{EC} and AcrB_{ST}



The protein is shown as grey ribbons. Chlorpromazine (CPZ) and Amitriptyline (AMI) are coloured according to element (C, S, N and Cl as dark yellow, light yellow, blue and green, respectively). The side chains of the DP are labelled and the residues of the hydrophobic trap displayed in magenta. The most stable conformations of ethidium bromide are shown as sticks in cyan and blue, respectively. Image provided by Attilio Vargiu. University of Cagliari, Italy.

amitriptyline, bound to a recently characterized region of AcrB, the CH3 entry gate (Zwama et al., 2018) (Appendix Figure 3.2). Binding at this position clashed with several binding poses of both ethidium bromide and norfloxacin (Appendix Figure 3.2).

3.6 Is the observed synergistic phenotype due to membrane damage by chlorpromazine?

3.6.1 ATP leakage from Gram-negative bacteria following exposure to chlorpromazine

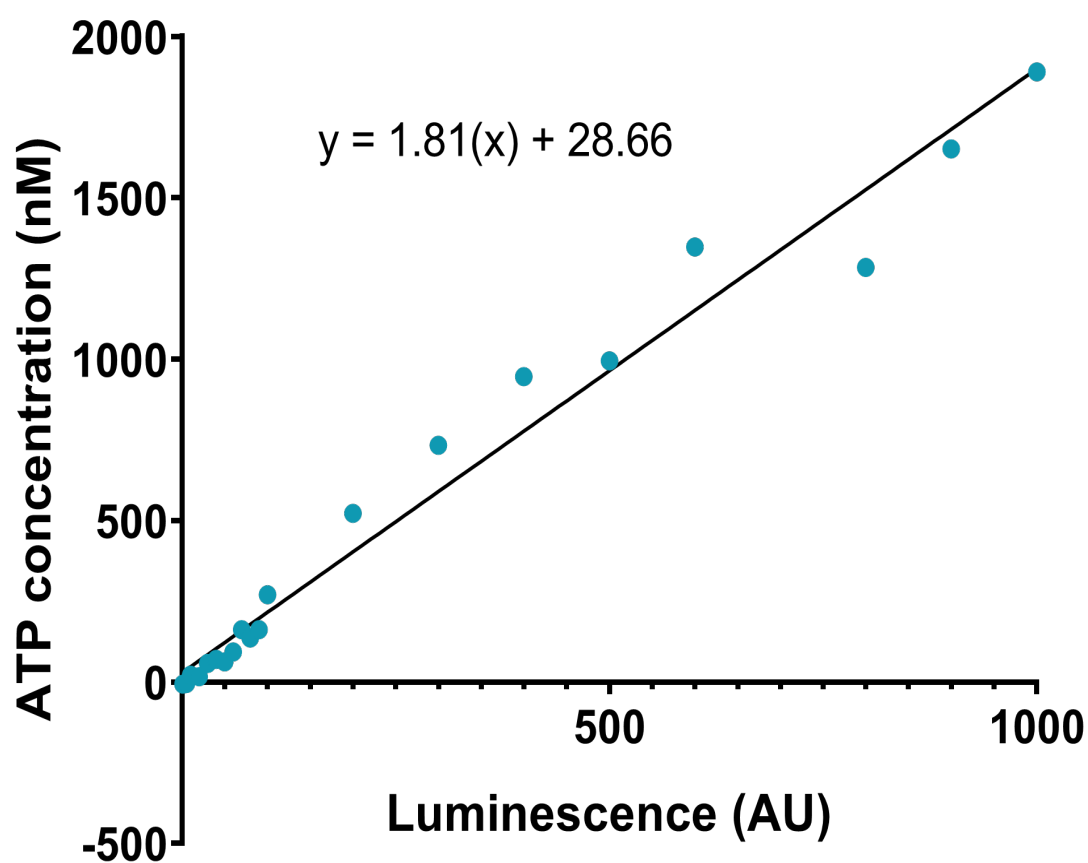
Chlorpromazine has its own intrinsic antimicrobial activity, independent of its ability to inhibit efflux. To date, the mechanism of this antimicrobial activity has been linked to the ability of this compound to intercalate DNA and inhibit replication (Ben-Hur et al., 1980; De Mol, Posthuma, et al., 1983; De Mol and Busker, 1984), inhibit calmodulins (Martins et al., 2011), inhibit the ability of the bacterial cell to generate energy and alter cellular morphology (Amaral and Lorian, 1991; Amaral, Kristiansen, et al., 2000; Kristiansen and Blom, 1981). The impact of chlorpromazine, if any, on the OM of Gram-negative bacteria has been crudely studied and instead assumptions have been made from experiments performed in eukaryotic cells (Jiang et al., 2017; Labedan, 1988; Plenge-Tellechea et al., 2018). Many compounds identified by synergy assays as ‘hits’ in efflux inhibitor screens mimic the effects of efflux inhibitors by potentiating antibiotic activity via non-specific damage to the OM. In addition, efflux inhibitors can also possess both specific efflux inhibitory effects alongside the ability to damage the bacterial membrane. While in principal this does not limit their use as an efflux inhibitor, it is a strong indicator that these compounds would also damage eukaryotic cells and exhibit cytotoxicity. Therefore, it is important to elicit the mode of efflux inhibition of chlorpromazine and determine whether its efflux inhibitory phenotype is a result of specific interactions with efflux proteins, and/or their regulatory proteins, or due to damage to the bacterial membrane.

A primary indicator regarding damage to the bacterial cell membrane is the leakage of large cellular constituents (e.g. ATP) into the extracellular environment (O'Neill et al., 2004). To determine if, and the extent to which, chlorpromazine damages the OM of *S. Typhimurium* SL1344 and *E. coli* MG1655, both strains were exposed to increasing concentrations of chlorpromazine for one hour. Following this, the firefly luciferase was used to quantify the amount of ATP in the extracellular medium. Luciferase catalyses the oxidation of D-luciferin to oxyluciferin resulting in the production of light that can be measured. This reaction is ATP-dependent and thus the amount of oxyluciferin (and light) produced is directly proportional to the amount of ATP present in the sample. In short, membrane damage leads to greater ATP leakage and thus higher luminescence.

In order to quantify the amount of ATP in the sample, a standard curve must be generated in which ATP-containing samples are substituted for standard solutions containing varying known concentrations of ATP (Figure 3.7). This was done for each experiment as fluorescence backgrounds of the working solutions increase over time. The amount of ATP in the experimental samples was quantified by substituting the measured value of luminescence (x) into the linear regression equation ($y = mx + b$), where m is the slope of the line and b is the y-intercept.

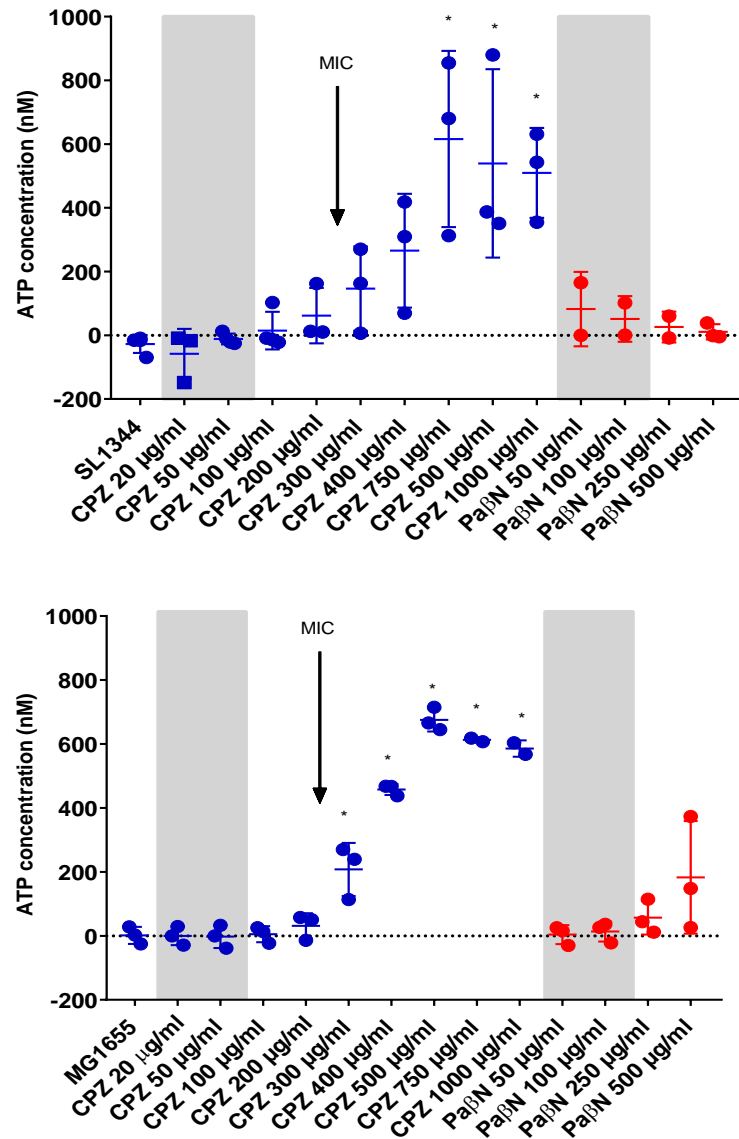
Analysis of the concentration of ATP in the extracellular medium upon exposure to chlorpromazine for one hour revealed OM damage (Figure 3.8). However, this was dependent on the chlorpromazine concentration. Exposure of the bacteria to efflux inhibitory concentrations ($\leq 100 \mu\text{g/ml}$) resulted in low ($< 100 \text{ nM}$) concentrations of ATP present in the extracellular medium of *S. Typhimurium* and *E. coli*. This data suggested no membrane damaging effects at the concentrations that potentiate AcrB substrate activity. At chlorpromazine concentrations $> 100 \mu\text{g/ml}$, the amount of ATP in the extracellular medium increased proportional to the concentration of chlorpromazine. Interestingly, when compared against the same efflux inhibitory concentrations of Pa β N, an efflux inhibitor

Figure 3.7: An example of a standard curve showing luminescence in relation to the concentration of ATP for one biological replicate.



A linear regression curve was fitted and the linear regression equation displayed on the graph.

Figure 3.8: ATP leakage from *E. coli* MG1655 and *S. Typhimurium* SL1344 upon exposure to increasing concentrations of chlorpromazine.



(A) *S. Typhimurium* SL1344, (B) *E. coli* MG1655. The concentrations of chlorpromazine and PaβN at which efflux inhibition was observed is highlighted in grey. The MIC of chlorpromazine is displayed. The graph shows the mean and standard deviation of three biological replicates. Each biological replicate was calculated from the mean of three technical replicates. Asterisks indicate a statistically significant difference ($P < 0.05$), calculated using a one-way ANOVA, in relation to the unexposed control. CPZ; Chlorpromazine, PaβN; Phe-arg beta naphthylamide.

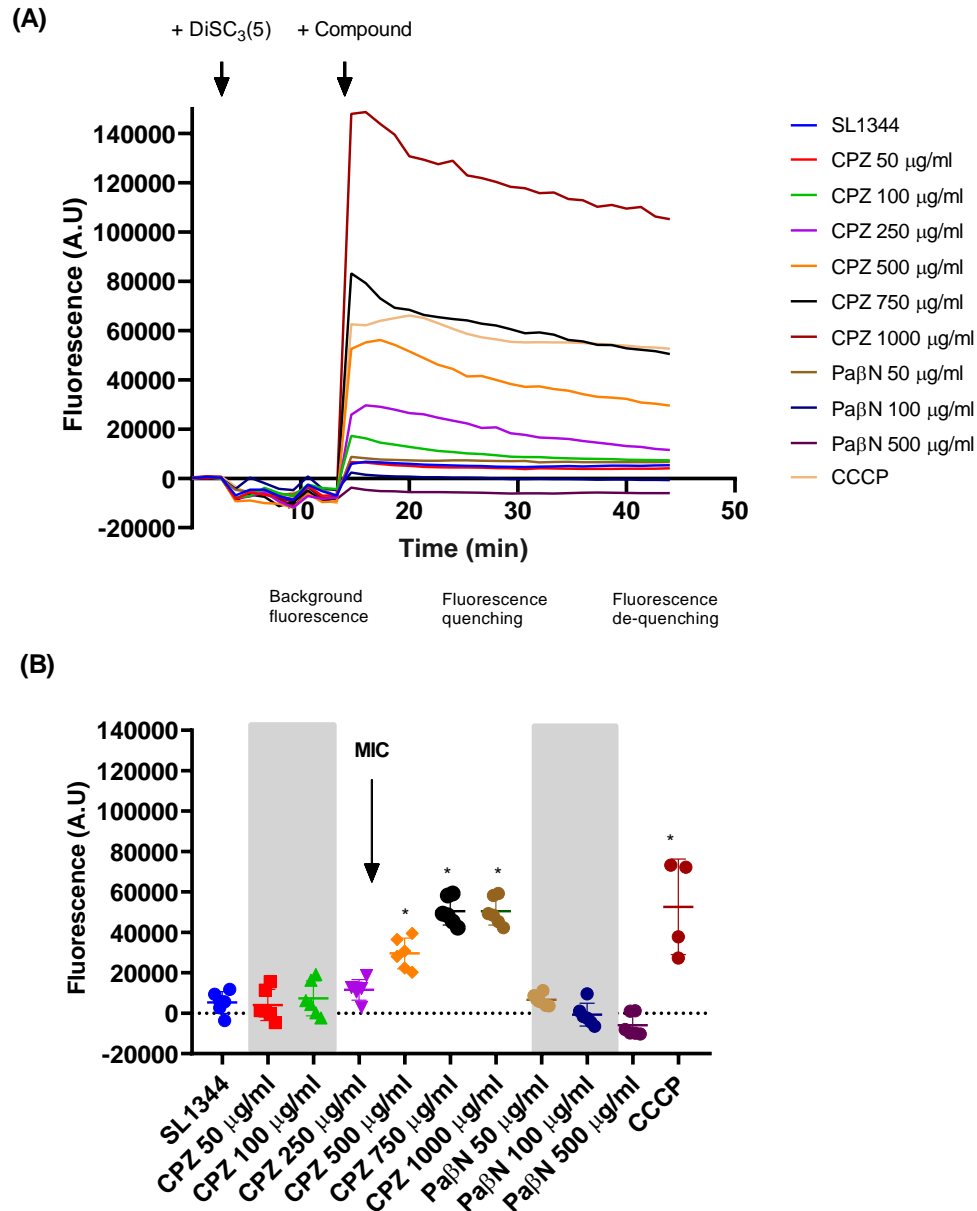
able to permeabilise the membrane, chlorpromazine permeabilised the membrane more than PaβN against *S. Typhimurium* and *E. coli*.

3.6.2 Ability of chlorpromazine and amitriptyline to depolarise the inner membrane

The membrane potential is a difference in the electrical charge between the inside and the outside of the cell, with most bacterial cells have a resting membrane potential of 40 mV to -70 mV with respect to the outside of the cell. Damage to the OM often increases membrane permeability allowing positively charged ions to cross from the extracellular to the intracellular environment. This results in depolarisation, where there is a reversion in the electrical charge inside the cell from negative to positive and the outside of the cell from positive to negative. Changes in the membrane potential can be detected by the voltage dependant distribution of fluorescent dyes.

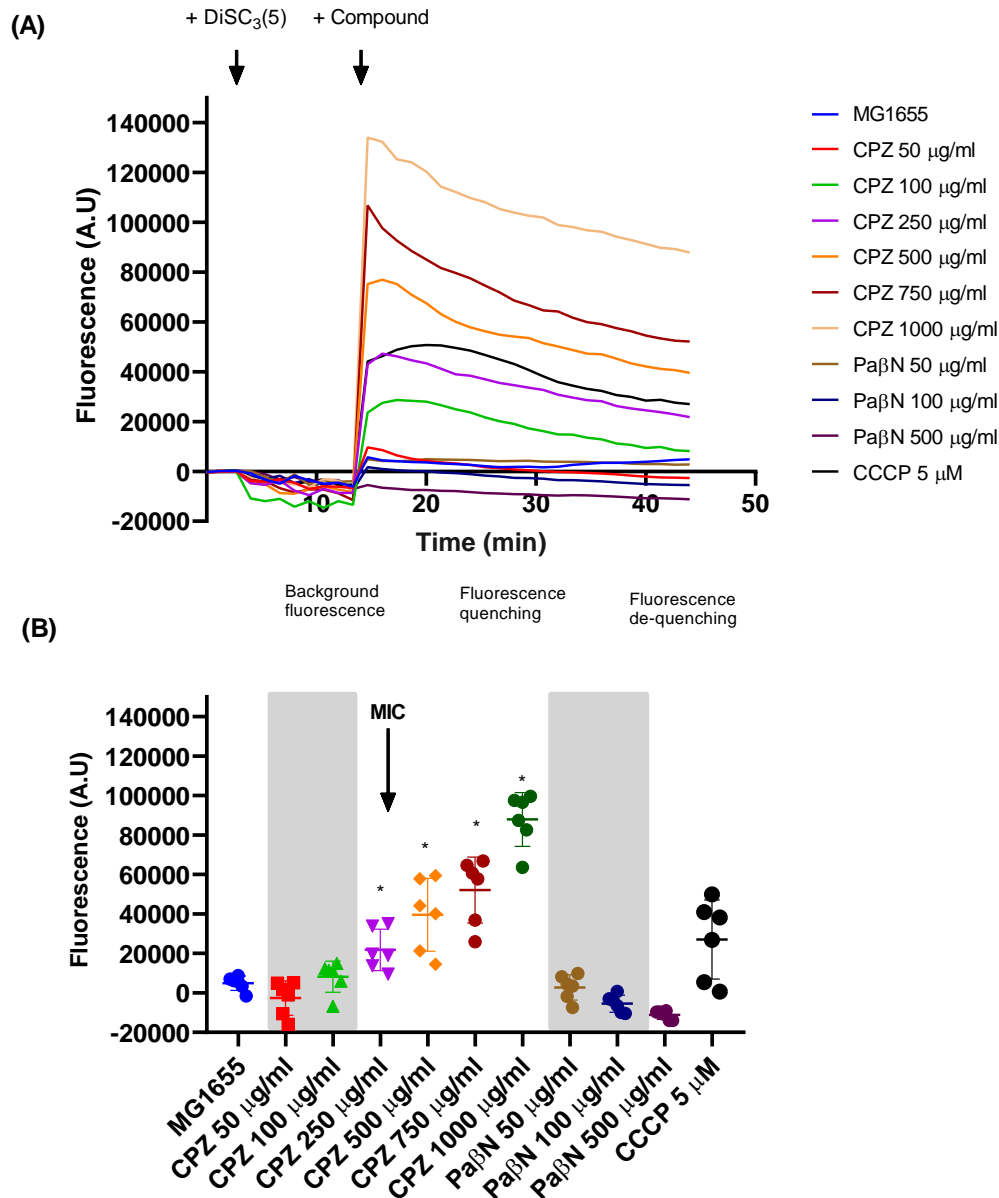
The cationic membrane-permeable fluorescent dye DiSC₃(5) was used to determine membrane depolarisation in the presence and absence of chlorpromazine. In polarised cells DiSC₃(5) accumulates until the Nernst equilibrium is achieved. Accumulation of this dye quenches the inherent fluorescence of the bacterial cells. Upon depolarisation, the dye moves from the intracellular to the extracellular environment resulting in dequenching and thus an increase in fluorescence that can be measured over time. Chlorpromazine depolarised the IM of *S. Typhimurium* SL1344 and *E. coli* MG1655 in a concentration dependent manner (Figure 3.9 and Figure 3.10). The concentrations of chlorpromazine which elicited statistically significant IM depolarisation of *E. coli* ($\leq 100 \mu\text{g/ml}$) ($P=<0.0001$) and *S. Typhimurium* ($\geq 250 \mu\text{g/ml}$) ($P=<0.0001-0.0002$) were the same as those that increased the OM permeability of both strains (Figure 3.9 and Figure 3.10).

Figure 3.9: Effect of chlorpromazine on the membrane potential sensitive fluorescent dye DiSC₃5 in *S. Typhimurium* SL1344.



(A) Changes in the fluorescence of DiSC₃5 in the cell suspension. The time points of DiSC₃5 and compound addition are highlighted by arrows. The graph shows the mean of four biological replicates. (B) The maximum fluorescence values upon the addition of chlorpromazine/CCCP/ PaβN. Efflux inhibitory concentrations of chlorpromazine and PaβN are displayed in grey. The graph shows the mean and standard deviation of four biological replicates. Each biological replicate was calculated from the mean of two technical replicates. Asterisks indicate a statistically significant difference ($P < 0.05$), calculated using a one-way ANOVA, in relation to the unexposed control. CPZ; Chlorpromazine.

Figure 3.10: Effect of chlorpromazine on the membrane potential sensitive fluorescent dye DiSC₃5 in *E. coli*.



(A) Changes in the fluorescence of DiSC₃5 in the cell suspension. The time points of DiSC₃5 and compound addition are highlighted by arrows. The graph shows the mean of four biological replicates. (B) The maximum fluorescence values upon the addition of chlorpromazine/CCCP/ PaβN. Efflux inhibitory concentrations of chlorpromazine and PaβN are displayed in grey. The graph shows the mean and standard deviation of four biological replicates. Each biological replicate was calculated from the mean of two technical replicates. Asterisks indicate a statistically significant difference ($P < 0.05$), calculated using a one-way ANOVA, in relation to the unexposed control. CPZ; Chlorpromazine.

However, although statistically insignificant, small increases in membrane depolarisation were observed at chlorpromazine concentrations at which efflux inhibition is observed; 50 $\mu\text{g}/\text{ml}$ against *E. coli* and 50 $\mu\text{g}/\text{ml}$ and 100 $\mu\text{g}/\text{ml}$ against *S. Typhimurium*.

CCCP, a known protonophore, was used as a positive control. The amount of depolarisation in *S. Typhimurium* observed by CCCP was similar to that exhibited by chlorpromazine. However, at the highest chlorpromazine concentration (500 $\mu\text{g}/\text{ml}$), the IM of *E. coli* MG1655 was depolarised to a greater extent than that by CCCP. Interestingly, Pa β N did not depolarise the membrane of *E. coli* or *S. Typhimurium*, even at the highest concentration (500 $\mu\text{g}/\text{ml}$).

3.7 Discussion

Chlorpromazine and amitriptyline have been identified as potential efflux inhibitors (Bailey et al., 2008; Bettencourt et al., 2000; Coutinho et al., 2009; Kaatz et al., 2003; Kristiansen, Hendricks, et al., 2007; Lawler et al., 2013; Martins et al., 2011; Ying et al., 2007). However, their mode of efflux inhibition is poorly understood and the nature of their interaction with multidrug efflux proteins is unknown.

Synergy assays including chequerboard, disk diffusion and well diffusion assays were performed to determine the ability of chlorpromazine and amitriptyline to potentiate the activity of antibiotics. The antibiotics chosen (chloramphenicol, tetracycline, nalidixic acid, ciprofloxacin, norfloxacin and ethidium bromide) are all substrates of the AcrAB-TolC efflux pump. Although it is preferable for antibiotic adjuvants to not possess antibacterial activity, both chlorpromazine and amitriptyline have some intrinsic antibacterial activity. However, this occurred at concentrations higher than those clinically achievable or desirable.

The impact of a compound on antibiotic potency in combination, in comparison to individual antibiotic activity can be determined by measuring the FIC index value. The

value of this calculation allows the given combination to be divided into three categories; synergistic (≤ 0.5), antagonistic (≥ 4) and neutral ($0.5 - 4$). However, there are problems with FIC calculations. (i) Various definitions have been described in the literature leading to confusion regarding interpretation (Te Dorsthorst et al., 2002). (ii) The calculation can be unreliable as on occasion dose-response curves cannot be generated, this is a problem with the chequerboard set up - the compounds are diluted serially by two-fold which can result in large differences in concentrations from well to well. This can be overcome by repeating with smaller differences in concentrations. (III) It is not clear which MIC values should be read and utilised in an FIC calculation and so depending on the chosen MIC values the FIC index can vary. For these reasons, the chequerboard results were displayed as MIC values and the FIC values are presented as support of these with calculations for all antibiotic-inhibitor combinations.

Chequerboard assays showed that synergy was observed between amitriptyline and chlorpromazine and certain AcrAB-TolC substrates against *S. Typhimurium*. However, neither chlorpromazine or amitriptyline potentiated the activity of norfloxacin against any strain, or of any of the tested substrates against *E. coli* (a two-fold increase in antibiotic potency was used as a cut off to indicate synergy). Given that chequerboard assays rely on the use of doubling dilutions, for drugs such as amitriptyline and chlorpromazine with antibacterial activity at high concentrations, the effective concentrations may fall between two dilutions and small differences in susceptibility may not be observed. Therefore, disk and well diffusion assays in which differences in susceptibility are more readily detected were used. The results of the disk and well diffusion assays showed that chlorpromazine and amitriptyline potentiated the activity of all tested antibiotics (chloramphenicol, ciprofloxacin, tetracycline, nalidixic acid, norfloxacin and ethidium bromide) against *S. Typhimurium* and *E. coli*.

In addition, in chequerboard assays, chlorpromazine potentiated the activity of

certain substrates (chloramphenicol, nalidixic acid, tetracycline and ethidium bromide) against *P. aeruginosa* and amitriptyline potentiated the activity of chloramphenicol against *A. baumannii* and nalidixic acid against *P. aeruginosa*. The ability of both compounds to potentiate antibiotic activity against strains that do not possess AcrAB-TolC, but have pumps that share homology with this pump (MexAB-OprM of *P. aeruginosa* and AdeABC of *A. baumannii*), suggests chlorpromazine and amitriptyline have a broader spectrum of activity.

Subsequently, accumulation assays were performed to determine the ability of chlorpromazine and amitriptyline to inhibit the efflux of the AcrB substrates ethidium bromide, H33342 and norfloxacin. Both chlorpromazine and amitriptyline inhibited the efflux of all substrates. However, the extent of this inhibition was concentration and strain-dependent. Interestingly, chlorpromazine and amitriptyline inhibited efflux of ethidium bromide and H33342 to a greater extent in *E. coli* compared to *S. Typhimurium* (an exception is that chlorpromazine inhibited the efflux of H33342 to a similar extent in both strains). This difference in efflux inhibition suggests differences in the way that chlorpromazine interacts with *E. coli* and *S. Typhimurium*.

Reasons underlying the difference in the activity of chlorpromazine and amitriptyline against *E. coli* and *S. Typhimurium* can be inferred by looking at the structure of AcrB. A crystal structure of AcrB_{ST} is not available. Therefore, the structure of AcrB_{EC} and AcrB_{ST} were compared using a homology model of AcrB_{ST} based on the crystal structure of AcrB from *E. coli* (PDB – 1iwg) (Appendix Figure 1) (Murakami, Nakashima, Yamashita, and Yamaguchi, 2002). AcrB from *E. coli* (AcrB_{EC}) and *S. Typhimurium* (AcrB_{ST}) share 94.97% sequence homology and are very similar in structure with a root mean square deviation (RMSD) of 2.4 Å. However, very small differences in sequence alignments can produce marked structural changes. Therefore, although AcrB_{EC} and AcrB_{ST} appear to be very similar there may be differences in protein structure that

result in chlorpromazine being able to saturate AcrB at lower concentrations in *S. Typhimurium* compared with *E. coli*. However, until a crystal structure of AcrB_{ST} is available, homology models only provide a prediction of protein structure. As such, only assumptions about differences between the interaction of ligands with AcrB_{EC} and AcrB_{ST} can be made.

It is important to note that similarities were observed in the docking and dynamics scoring energies of amitriptyline and chlorpromazine with AcrB_{EC} and AcrB_{ST}. This is at contrast with the hypothesis that these compounds interact differently with AcrB from these strains. However, the reliability of these calculations is limited by two main factors. (i) These docking and dynamics simulations were performed with a AcrB_{ST} homology model which may not be a true representation of the ‘real world’ structure of AcrB in this organism. (ii) Energy scoring calculations based on docking and dynamics are very crude methods of determine the strength of protein-ligand interactions.

Previous studies have provided insights regarding the interaction of RND transporters and their substrates and inhibitors and have identified key structural determinants that allow for discrimination between the two (Eicher, Cha, et al., 2012; Jewel et al., 2020; Liu and Chen, 2017; Ramaswamy et al., 2017; Vargiu, Collu, et al., 2011; Vargiu and Nikaido, 2012). Here, to investigate whether the observed efflux inhibitory activity of chlorpromazine and amitriptyline could be rationalised by the propensity to bind to AcrB_{EC} and AcrB_{ST}, molecular docking, molecular dynamics and free energy calculations were performed by collaborators from The University of Cagliari, Italy. Molecular docking is used to predict the position and orientation of a ligand when it is bound to a protein; hundreds of possible binding orientations are generated and a scoring function is applied to find the lowest energy conformations in which the ligand would be predicted to bind. Molecular dynamics studies simulate the dynamic behaviour of molecular system by mapping the movements of atoms and molecules. The simulations can

then be analysed and the binding free energies calculated to find the most favourable conformation which is usually the conformation that requires the lowest energy requirement.

The blind ensemble docking calculations and subsequent molecular dynamics simulations revealed that both chlorpromazine and amitriptyline are able to bind to the DP of AcrB_{EC} and AcrB_{ST} at the HT; a known inhibitor and substrate binding site (Nakashima, Sakurai, Yamasaki, Hayashi, et al., 2013; Sjuts et al., 2016; Kinana et al., 2016; Vargiu, Collu, et al., 2011; Vargiu, Ruggerone, et al., 2014). Binding of chlorpromazine and amitriptyline at this region overlapped with the binding sites of the AcrB substrates ethidium bromide and norfloxacin. The ΔG values were similar for chlorpromazine, amitriptyline, norfloxacin and ethidium bromide against both AcrB_{EC} and AcrB_{ST}. Thereby indicating there are no large differences in the binding affinity of these compounds to AcrB of these strains. However, binding free energy calculations are not the most reliable method for calculating the extent of/tightness of binding.

The ability of chlorpromazine and amitriptyline to bind to the DP and clash with the binding of ethidium bromide and norfloxacin led to the hypothesis that these compounds elicit their efflux inhibitory properties by interfering with the ability of AcrB to efflux substrates. The exact mechanism of this action is unknown but three hypotheses can be made. The first, is that binding of these inhibitors hinders, or prevents, the conformational changes that are essential for substrate extrusion. The second, is that chlorpromazine and amitriptyline are competitive inhibitors that bind to AcrB, thereby blocking substrate binding and extrusion. The third, is that chlorpromazine and amitriptyline are themselves substrates of the pump and as such they compete with AcrB substrates for binding sites and as a result are extruded instead of, or before, other substrates. Note that any hypothesis does not necessarily preclude the other. To explore the first and second hypothesis further ligand-binding studies and X-ray crystallography of

chlorpromazine and amitriptyline with AcrB are desirable. To explore the third hypothesis and determine whether chlorpromazine and amitriptyline outcompete binding by norfloxacin and ethidium bromide and are preferentially extruded, efflux/accumulation experiments utilising chlorpromazine and amitriptyline as the substrates are required. Unfortunately, the degree to which chlorpromazine intrinsically fluoresces was insufficient to allow these experiments to be performed with the available equipment.

An important observation was that the efflux and accumulation assays showed that, consistently, chlorpromazine appears to possess more potent efflux inhibitory activities than amitriptyline. The increased efflux inhibitory activity of chlorpromazine can be explained by analysis of the locations to which this inhibitor bound AcrB. Chlorpromazine was able to occupy a larger fraction of the DP than amitriptyline and made a larger number of contacts (10) with the residues lining the hydrophobic trap than amitriptyline (6-8). In contrast, amitriptyline bound slightly upward to the DP making contacts with hydrophilic residues. This tighter interaction of chlorpromazine with the HT may be a result of the presence of an additional chlorine atom that can form C-Cl... π interactions with the aromatic rings of the hydrophobic residues that line this region (Matter et al., 2009). Interestingly, chlorpromazine made the same number of contacts with AcrB_{ST} and AcrB_{EC}, whereas amitriptyline made a reduced number of contacts with AcrB_{ST} (6) in comparison to that made with AcrB_{EC} (8). This observation may provide a rationale to the drastically increased efflux inhibitory activity of amitriptyline against *E. coli* in comparison to that observed against *S. Typhimurium*.

In addition, the molecular dynamics simulations showed that chlorpromazine, but not amitriptyline, was able to bind to a recently characterized region of AcrB, the CH3 entry gate (Zwama et al., 2018). Both norfloxacin and ethidium bromide bound this location and thus the increased potency of chlorpromazine may be attributed to this compound being able to interfere with binding of these substrates not only at the DP but also at the CH3 entry gate. Substrates that bind at this region of AcrB are usually planar, aromatic and cationic. While

amitriptyline and chlorpromazine are cationic and aromatic, neither are planar. However, chlorpromazine possesses a phenothiazine ring that confers a flatter conformation than that observed by amitriptyline.

Another observation from the efflux and accumulation assays was that chlorpromazine and amitriptyline inhibited the efflux of norfloxacin only in *E. coli* and *S. Typhimurium* strains that overexpressed AcrAB-TolC. This suggests that the efflux inhibitory activity of these compounds is less potent in the presence of norfloxacin. This can be explained by the molecular dynamics simulations which show that chlorpromazine and amitriptyline have a greater steric clash with ethidium bromide compared to norfloxacin.

It is important to note that there are disadvantages that accompany *in silico* molecular docking and dynamics simulations. Although the most popular computational method to predict ligand interactions, the main disadvantage of molecular docking is the limitations surrounding accounting for protein flexibility. Most docking methods use rigid protein conformations and as such there is restricted sampling of the possible conformations for which the ligand is able to bind to the protein (Guedes et al., 2018; Pinzi et al., 2019). The field of molecular docking is constantly evolving and new methods are being utilised that increase the protein flexibility (Pinzi et al., 2019). However, the cost and time associated with these models increases proportional with the flexibility of the protein (Santos et al., 2019). This lack of flexibility means the scoring functions applied to estimate binding affinity are very approximate in nature and often do not align with *in vivo* experimental models (Santos et al., 2019; Salmaso et al., 2018).

It is due to these reasons that molecular docking is, more often than not, combined with molecular dynamics simulations which assumes all factors within the simulation are flexible (Santos et al., 2019; Salmaso et al., 2018). However, molecular dynamics is also limited by the number of possible binding conformations that are generated. Currently,

this is because most computers are only capable of simulations millionths or even billionths of a second in length (Durrant et al., 2011; Salmaso et al., 2018). Meaning this process has to be repeated hundreds, if not thousands, of times to generate as many orientations as possible. While *in silico* molecular docking and dynamics simulations provide key information regarding ligand-protein interactions, it is essential to confirm these observations in ‘real world’ models. Therefore, before making assumptions about their interactions it would be advantageous to look at the binding of chlorpromazine and amitriptyline with AcrB using methods including nuclear magnetic resonance (NMR) imaging, X-ray crystallography and ligand binding studies utilising a combination of SPR, isothermal calimetry (ITC) and microscale thermophoresis (MST)

Antibiotic potentiation can result from a number of mechanisms outside of specific efflux inhibition (Aldridge et al., 1986; Ammeter et al., 2019; Courtney et al., 2017; Vaara, 1992); in many cases, antibiotic synergy results from non-specific damage to the bacterial membrane (Ferrer-Espada et al., 2019; Vaara, 1992; Muheim et al., 2017; Corbett, Wise, et al., 2017). Here, specific refers to efflux inhibition as a direct result of interaction with efflux proteins and efflux regulatory proteins. Non-specific refers to efflux inhibition resulting from interference with the energy source required for the activity of AcrAB-TolC. Although membrane damage does not necessarily preclude the use of potentiators as efflux inhibitors, it is a strong indicator that an adjuvant may possess a similar mode of action against eukaryotic cells and exhibit significant cytotoxicity. The cytotoxicity that accompanies most currently identified efflux inhibitors severely limits their clinical use (Aron et al., 2018; Lamers et al., 2013; Lomovskaya, Warren, et al., 2001; Lomovskaya and Bostian, 2006; Nguyen et al., 2015). Therefore, it is important to thoroughly investigate the mode of action of efflux inhibitors to determine whether their activity results from non-specific membrane effects or from specific interactions with efflux proteins.

The luciferin-luciferase reaction was used as an indirect measure of ATP

concentration. Membrane permeabilisation allows the leakage of large macromolecules (including ATP) into the extracellular environment. Therefore, the luciferin-luciferase reaction is often used to determine the extent to which an antibacterial compound can damage the OM by measuring the intracellular or extracellular concentration of ATP post-exposure to an antibiotic agent (de Rautlin de la Roy et al., 1991; Heller et al., 2019; Yasir et al., 2019). Some studies have attempted to use this assay to determine the impact of a compound on cellular metabolism based on the assumption that slight impairments to the bacterial membrane will inhibit components of the respiratory chain, leading to a downstream reduction in ATP production (Hilpert et al., 2010; Spindler et al., 2011). However, this is not a reliable method of determining the impact of a compound on the generation of energy and interpretation as such can be misleading.

Chlorpromazine damaged both the inner and the outer membrane of *E. coli* and *S. Typhimurium*. This was likely due to its cationic and amphiphilic nature (Jiang et al., 2017; Plenge-Tellechea et al., 2018). The damage to the OM of both strains occurred at chlorpromazine concentrations considerably higher ($>200\text{ }\mu\text{g/ml}$) than the concentrations for which efflux inhibition was observed ($\sim 50\mu\text{g/ml}$). Based on these data, efflux inhibition by chlorpromazine appeared to be independent of its non-specific effect on the OM. However, even increases in membrane permeability small enough to allow the diffusion of ions with permeability coefficients of $\sim 10\text{-}14\text{ cm/s}$ (e.g. Na^+ and K^+) (Yang et al., 2015), without causing irreversible membrane damage, can have large impacts on global cellular processes (Benarroch et al., 2020; Krulwich et al., 2011; Murínová et al., 2014; Roe et al., 1998; Olson, 1993). This is difficult to assess by investigating the impact of chlorpromazine on the OM only. Therefore, it was also important to determine the impact of this compound on the bacterial IM. In addition, omics technologies including transcriptomics, proteomics and metabolomics can be useful for understanding the physiological changes induced by non-lethal membrane damage.

The PMF is one of the ways by which cellular energy is created and is dependent on both the electrical potential and pH gradients (Krulwich et al., 2011; Lodish et al., 2000). Increased membrane permeability alters the flux of ions across the membrane, altering the electrical potential resulting in hyperpolarization or depolarization of the membrane and a reduction in the amount of energy produced from the PMF. Considering that many efflux pumps, including AcrAB-TolC, are proton/substrate antiporters driven by the PMF (Blair, Webber, et al., 2015), non-specific efflux inhibition occurs due to interference with the ability of the bacterial cell to generate or maintain an energized cell membrane. For example, the mode of action of the efflux inhibitor CCCP relies solely on its ability to uncouple the PMF (Viveiros et al., 2005). Here, efflux inhibitory concentrations of chlorpromazine (50 $\mu\text{g/ml}$) resulted in membrane depolarization. Although the same concentration of chlorpromazine resulted in insignificant increases in membrane permeability in comparison to the unexposed control, depolarization can result from very small increases in OM permeability. This allowed the following hypothesis to be made: at low concentrations, chlorpromazine may elicit its efflux inhibitory activity, in part, by inducing very small increases in membrane permeability that are insufficient to cause irreversible membrane damage but are able to change the flux of ions in such a way that alters the pH/electrical potential, thereby interfering with the PMF resulting in the observed efflux inhibition. The impact of chlorpromazine on the pH and electrical potential can be measured by utilization of radiolabeled membrane permeants as a pH probe and the membrane permeant tetraphenylphosphonium cation as an electrode (Kaatz et al., 2003; Zilberstein, Agmon, et al., 1984; Moreno et al., 2015).

For any compound (e.g. chlorpromazine) that interferes with the membrane potential it is difficult, in a whole-cell environment, to decipher whether the observed efflux inhibitory phenotype is due to specific or non-specific efflux inhibition. For chlorpromazine, both mechanisms are likely to contribute to its overall efflux inhibitory activity. The efflux-specific inhibitory activity of chlorpromazine could be determined in a cell free experiment with

protein alone. Previously, purified AcrAB-TolC has been reconstituted into proteoliposomes supplemented with a pH gradient to allow activity of the AcrB pump (Zgurskaya et al., 1999). Within a proteoliposome, the ability of chlorpromazine to inhibit efflux, independent of non-specific effects on the cell membrane, can be determined. Any interference of chlorpromazine with the pH gradient can be controlled for within the liposome environment. In addition to proteoliposomes, the specific efflux inhibition of chlorpromazine can be rationalised by ligand-binding studies and X-ray crystallography of chlorpromazine with purified AcrB protein or AcrB regulatory proteins.

3.8 Key finding

- The first-generation antipsychotics chlorpromazine and amitriptyline potentiated the activity of AcrB substrates against four exemplars of Gram-negative species.
- Chlorpromazine and amitriptyline increased the intracellular accumulation of the AcrB substrates H33342, ethidium bromide and norfloxacin in *S. Typhimurium* SL1344 and *E. coli* K12 strains.
- The efflux inhibitory activity of chlorpromazine and amitriptyline was due to competitive inhibition. Both compounds interact with the efflux protein AcrB, clashing with the binding of ethidium bromide and norfloxacin.
- Chlorpromazine damaged both the outer and the inner membrane, these off-target effects may contribute to this compounds mode of efflux inhibition.

Chapter Four

Resistance to efflux inhibitors can evolve and description of mutants selected in the laboratory

4.1 Background

Most screening programmes used to identify efflux inhibitors rely on identifying synergy between the test compound and an antibiotic. However, for many compounds mode of action studies are not done. As a result, little is known about the mode of action of most compounds described as efflux pump inhibitors.

Evidence that chlorpromazine is an efflux inhibitor has existed since 2005 (Viveiros et al., 2005). However, its mode of action is not well understood. Here, *in silico* molecular dynamics simulations presented in Chapter Three propose that the efflux inhibitory activity of chlorpromazine is through direct interactions of this compound with AcrB. However, the evidence that chlorpromazine elicits its efflux inhibitory activity via AcrB does not preclude a mechanism of efflux inhibition independent from direct interactions with the AcrB pump (e.g. via membrane permeabilisation). Therefore, it is important to determine the molecular interactions underlying the mode of efflux inhibition of chlorpromazine.

Traditionally, drug-resistant mutant selection experiments are used to identify the

mechanism of resistance to a given antibiotic. This can, in some cases, be useful to identify a molecular target. However, these experiments are dependent on a compound possessing antibacterial activity. The absence of, or limited, antibacterial activity of putative efflux inhibitors combined with the structural complexity of tripartite efflux pumps means that it is difficult to perform mutant selection experiments. Therefore, mutant selection experiments utilising efflux inhibitors are often performed in the presence of an antibiotic substrate (Nguyen et al., 2015). Unfortunately, these experiments are very difficult to design and the presence of selective pressure from the antibiotic can result in target site mutations within genes that confer antibiotic, but not inhibitor, resistance.

4.2 Hypothesis

- Resistance to efflux inhibitors will result from exposure of *S. Typhimurium* SL1344 and *E. coli* MG1655 to chlorpromazine and/or Pa β N.

4.3 Aims and Objectives

- To design experiments with the efflux inhibitors chlorpromazine and Pa β N, in the presence and absence of ciprofloxacin that give rise to mutants with decreases in susceptibility to the inhibitor alone.
- To characterise the selected mutants to reveal the molecular targets responsible for resistance of *S. Typhimurium* SL1344 and *E. coli* MG1655 to chlorpromazine or Pa β N.

4.4 Post exposure of *Salmonella* to chlorpromazine with ciprofloxacin gives rise to fluoroquinolone-resistant colonies only

A combination approach was first used in mutant selection experiments in which chlorpromazine at an efflux inhibitory concentration (50 μ g/ml) was combined with ciprofloxacin (0.03 μ g/ml), an AcrB substrate. Exposure to this combination produced 255

Table 4.1 Frequency and rate of mutation upon exposure to *S. Typhimurium* and *E. coli* MG1655 to efflux inhibitors in the presence and absence of ciprofloxacin.

Organism	Selecting drug	Selecting concentration (µg/ml)	Viable count	Number of parallel cultures	Total number of colonies	<i>m</i> value	Mutation frequency (CFU/ml)	Mutation rate (CFU/ml)
<i>S. Typhimurium</i> SL1344	Chlorpromazine	150	1.23×10^{10}	1	310	69.9	5.04×10^{-9}	5.66×10^{-9}
	Chlorpromazine + Ciprofloxacin	$50 + 0.05$	1.18×10^9	1	255	57	4.32×10^{-8}	4.83×10^{-8}
	PaβN	1,024	1.92×10^9	1	5	2.9	1.52×10^{-10}	1.51×10^{-9}
	PaβN + Ciprofloxacin	$50 + 0.03$	1.92×10^9	1	1	1.05	5.47×10^{-10}	1.04×10^{-10}
<i>E. coli</i> MG1655	Ciprofloxacin	0.03	3.94×10^9	30	197	22.85	2.74×10^{-8}	2.89×10^{-9}
		160	2.02×10^9	20	556	0.19	2.75×10^{-9}	1.36×10^{-9}
	Chlorpromazine	170	2.02×10^9	20	4	2.7	1.98×10^{-11}	9.40×10^{-11}

colonies on the initial selecting medium (Table. 4.1). The mutation frequency and mutation rate were 4.32×10^{-8} CFU/ml and 4.83×10^{-8} CFU/ml, respectively. This was similar to the mutation frequency and mutation rate of *S. Typhimurium* SL1344 resistance to ciprofloxacin alone (2.74×10^{-8} CFU/ml and 2.89×10^{-9}) (Table. 4.1).

The selected *S. Typhimurium* mutants were not resistant to chlorpromazine (Table 4.2); each mutant showed reduced susceptibility to only ciprofloxacin and nalidixic acid. WGS revealed this change in susceptibility was a result of a substitution (S83P) within GyrA (Table 4.3). Mapping of the mutant sequence against wild type *S. Typhimurium* SL1344 on Artemis 18.0.2 revealed the presence of this SNP at position 2373816 of the chromosome (Figure 4.1). In addition, to confirm the identified SNP was not a sequencing error, the mutation was confirmed by PCR and subsequent DNA sequencing of the amplicon (Figure 4.1).

Table 4.2 Susceptibility of *S. Typhimurium* mutants selected with chlorpromazine in combination with ciprofloxacin.

Strain (MIC phenotype group)	Selecting concentration	MIC (μ g/ml)						
		CPZ	Pa β N	CIP	CHL	TET	NAL	ETBR
SL1344 wild type		256	512	0.03	8	2	8	1,024
1	50 + 0.03	256	512	1	8	2	<128	1,024

CPZ; chlorpromazine; Pa β N, phenylalanine-arginine beta-naphthylamide; CIP, ciprofloxacin; CHL, chloramphenicol; TET, tetracycline; NAL, nalidixic acid; ETBR, ethidium bromide. The wild type parental strains are shown in blue. A decrease in susceptibility is shown in red. The mode of three biological replicates is shown.

Table 4.3 Mutations identified in the *S. Typhimurium* SL1344 mutant selected upon exposure to chlorpromazine (50 μ g/ml) and ciprofloxacin (0.03 μ g/ml).

Gene product	Nucleotide change (position)	Amino acid change (position)	Effect
GyrA	C \rightarrow T (248/2637)	Serine \rightarrow Phenylalanine (83/878)	Substitution

4.5 Exposure to inhibitor alone selects for colonies of *S. Typhimurium* SL1344 and *E. coli* MG1655 that are able withstand chlorpromazine

Due to the difficulty selecting mutants with decreased susceptibility to chlorpromazine when this efflux inhibitor was combined with ciprofloxacin, mutant selection experiments were carried out with chlorpromazine as the sole selective pressure. Until recently, it was thought that the selection of antibiotic-resistant bacteria only occurs in the ‘mutant-selective window’. i.e. the range of antibiotic concentrations between the MIC of the susceptible population and the resistant population. Therefore, mutants are typically selected using drug concentrations one and two times the MIC for the parental strain. However, in this study, at these concentrations of chlorpromazine, no resistant mutants were obtained. Andersson et al., 2014, revealed that very low concentrations of a compound can select for resistant mutants in both laboratory and natural environments. Therefore, sub-MIC concentrations of chlorpromazine were used to select for chlorpromazine-resistant *E. coli* MG1655 (160 µg/ml and 170 µg/ml) and *S. Typhimurium* SL1344 mutants (160 µg/ml). The mutation rates and frequency for each strain and chlorpromazine concentration are shown in Table 4.1.

The antibiotic susceptibility of each mutant (or 10 if ≥ 10 mutants were selected) was determined using a panel of antibiotics that represent a variety of classes. Each mutant was grouped dependent on its phenotype as shown in Table 4.4. Each mutant was 1-2 doubling dilutions less susceptible to chlorpromazine than the parental strain. Usually, a single doubling dilution difference in MIC is not considered to be significant as this can lie within the error of the method. However, given that this change in MIC was repeatedly observed, these mutants were considered to be less susceptible to chlorpromazine. In addition, the *S. Typhimurium* mutants were MDR with decreased susceptibility to all tested antibiotics, PaβN and ethidium bromide. Both the *E. coli* mutant phenotype groups

Resistance to efflux inhibitors can evolve and description of mutants selected in the laboratory

were resistant to PaβN, ciprofloxacin, nalidixic acid and tetracycline. In addition, the mutants of phenotype group 1 were resistant to ethidium bromide (Table 4.4).

Table 4.4 Susceptibility of chlorpromazine-resistant *S. Typhimurium* SL1344 and *E. coli* MG1655 mutants.

Strain (MIC phenotype group)	Selecting concentration (μg/ml)	MIC (μg/ml)						
		CPZ	PaβN	CIP	CHL	TET	NAL	ETBR
SL1344 wild type		256	512	0.03	4	2	8	1,024
1	160	512	2,048	0.12	16	4	32	2,048
MG1655 wild type		256	1,024	0.06	16	8	16	1,024
1	170	512	2,048	0.12	64	32	64	2,048
2	160	1,024	2,048	0.12	64	16	32	1,024

CPZ; chlorpromazine; PaβN, phenylalanine-arginine beta-naphthylamide; CIP, ciprofloxacin; CHL, chloramphenicol; TET, tetracycline; NAL, nalidixic acid; ETBR, ethidium bromide. The parental strains are shown in blue. A decrease in susceptibility is shown in red. The mode of three biological replicates is shown.

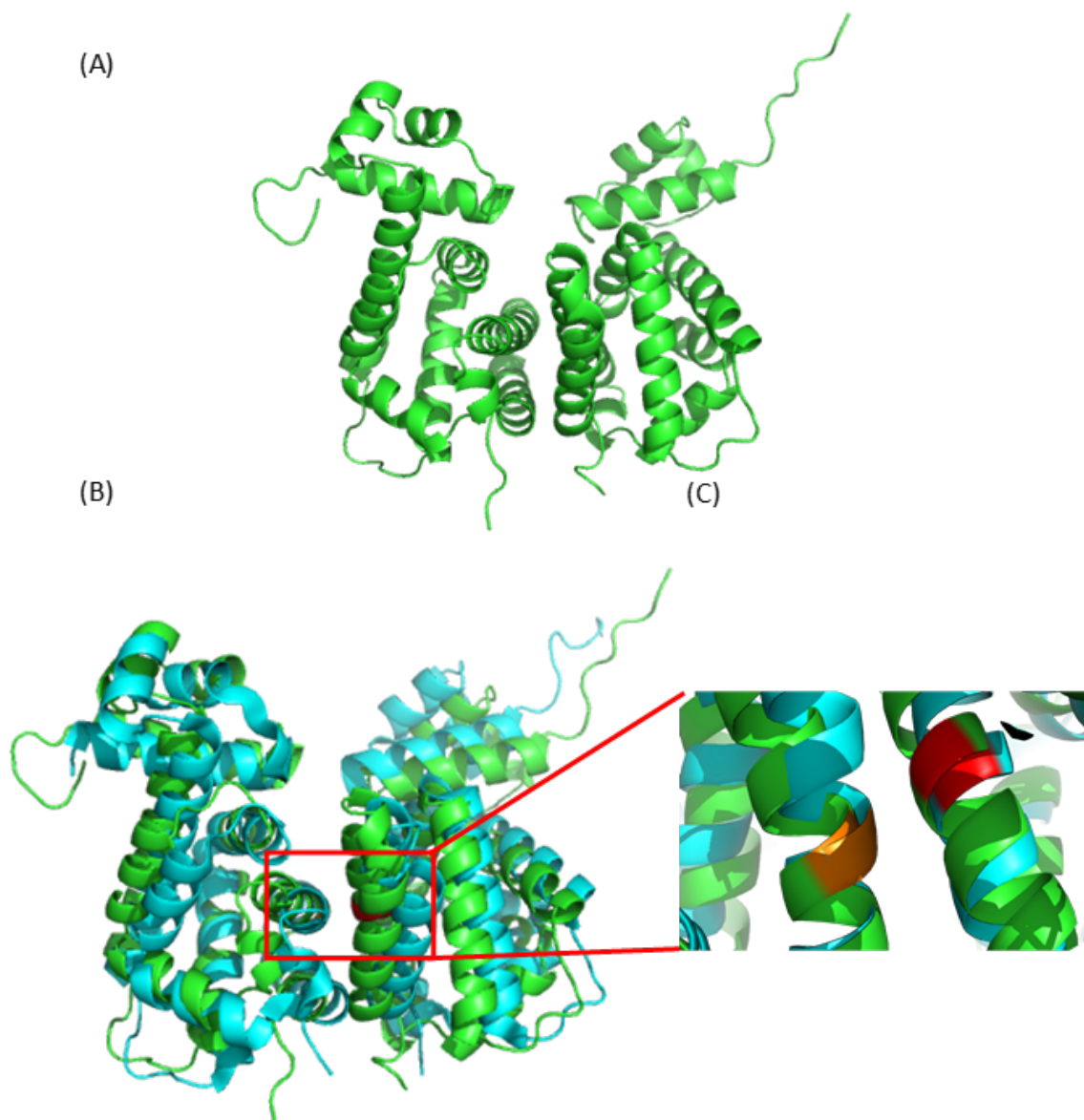
4.5.1 Resistance to chlorpromazine is conferred by mutations within genes that regulate expression of *acrAB* and *tolC*

WGS of one representative mutant from each MIC phenotype group revealed the presence of mutations within coding regions of the genome of each mutant (Table 4.5). In *S. Typhimurium* SL1344 a SNP resulting in the substitution of a leucine for a proline (L158P) within the dimerisation domain of the transcriptional repressor RamR was observed. This mutant is referred to as RamR L158P throughout. Mapping of SL1344 RamR L158P against the wild type sequence revealed the presence of the T→C SNP on the forward strand at position 637742 of the chromosome (Figure 4.2). This mutation was confirmed by PCR and DNA sequencing of the amplicons (Figure 4.2). Using Modeller 9.24, a homology model of RamR L158P was made using the crystal structure of SL1344 RamR wild type as a reference template (PDB- 3vvx) (Figure 4.3). The homology model was aligned against the wild type (PDB-3vvx) structure in PyMOL and the mutation site on chain A and B are highlighted.

Table 4.5 Mutations and subsequent substitutions conferring chlorpromazine resistance identified by whole genome sequencing of a representative mutant from each MIC phenotype group.

Strain (MIC phenotype group)	Gene product	Nucleotide change (position)	Amino acid change (position)	Effect	Nomenclature
<i>S. Typhimurium</i> SL1344 (1)	RamR	T→C (473/582)	Leucine → Proline (158/144)	Substitution	RamR L158P
<i>E. coli</i> MG1655 (1)	MarR	AAGA→AA (420/435)	Lysine → Serine (141/144)	Frameshift	MarR K141Sfs*150
<i>E. coli</i> MG1655 (2)	MarR	GCG→GG (322/435)	Alanine → Arginine (105/144)	Frameshift (premature stop codon)	MarR A105Rfs*114

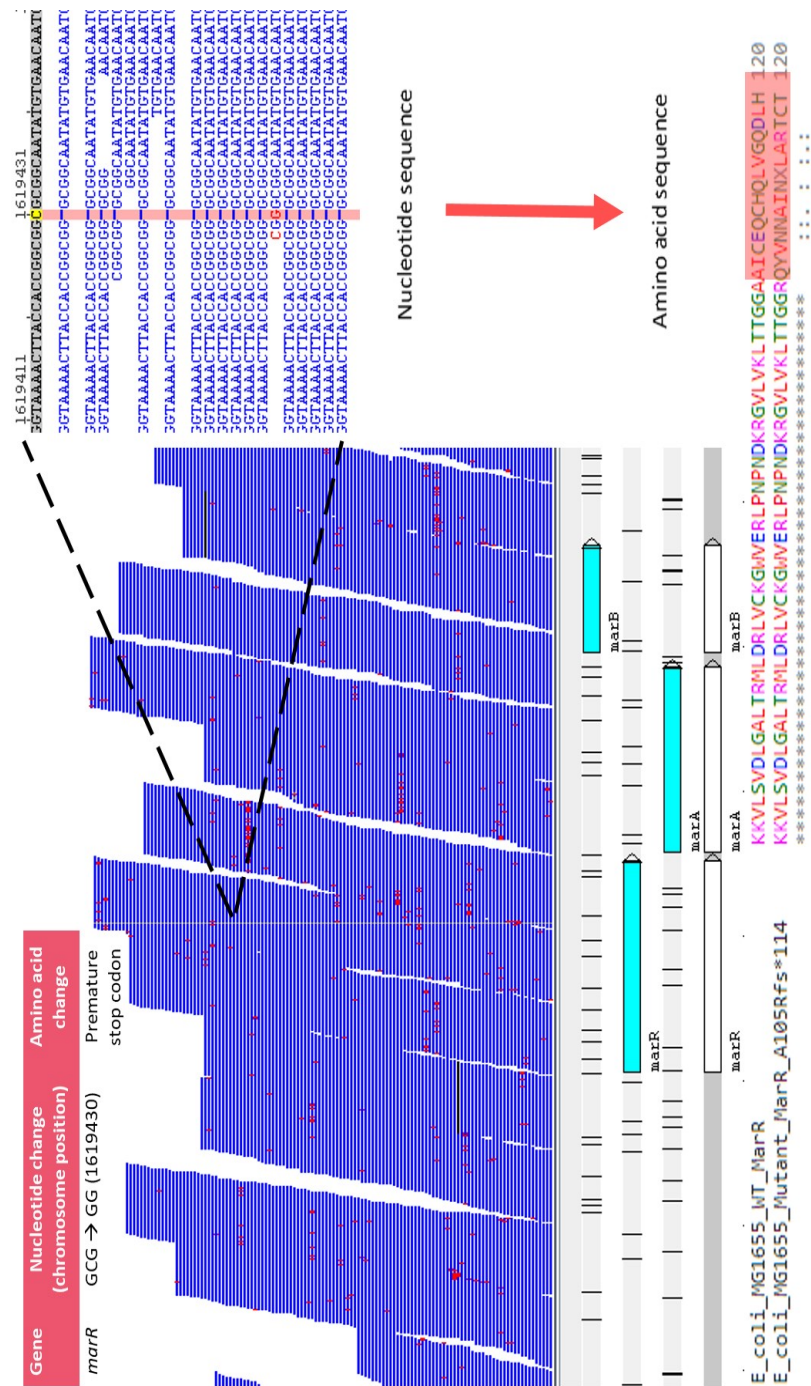
Figure 4.3: Homology model of SL1344 RamR L158P.



(A) Homology model of RamR L158P built with Modeller 9.21 using the crystal structure of RamR wild type (PDB-3vvx) as the template structure. The ribbon structure was visualised in PyMOL. (B) PyMOL alignment of the homology model of RamR L158P (green) against the crystal structure of RamR wild type (PDB - 3vvx) (cyan). The mutation sites are displayed in red (Chain A) and orange (Chain B) on both RamR L158P and RamR wild type. (C) Close-up view of the mutation sites of RamR on Chain A and Chain B. Colours as shown in (B).

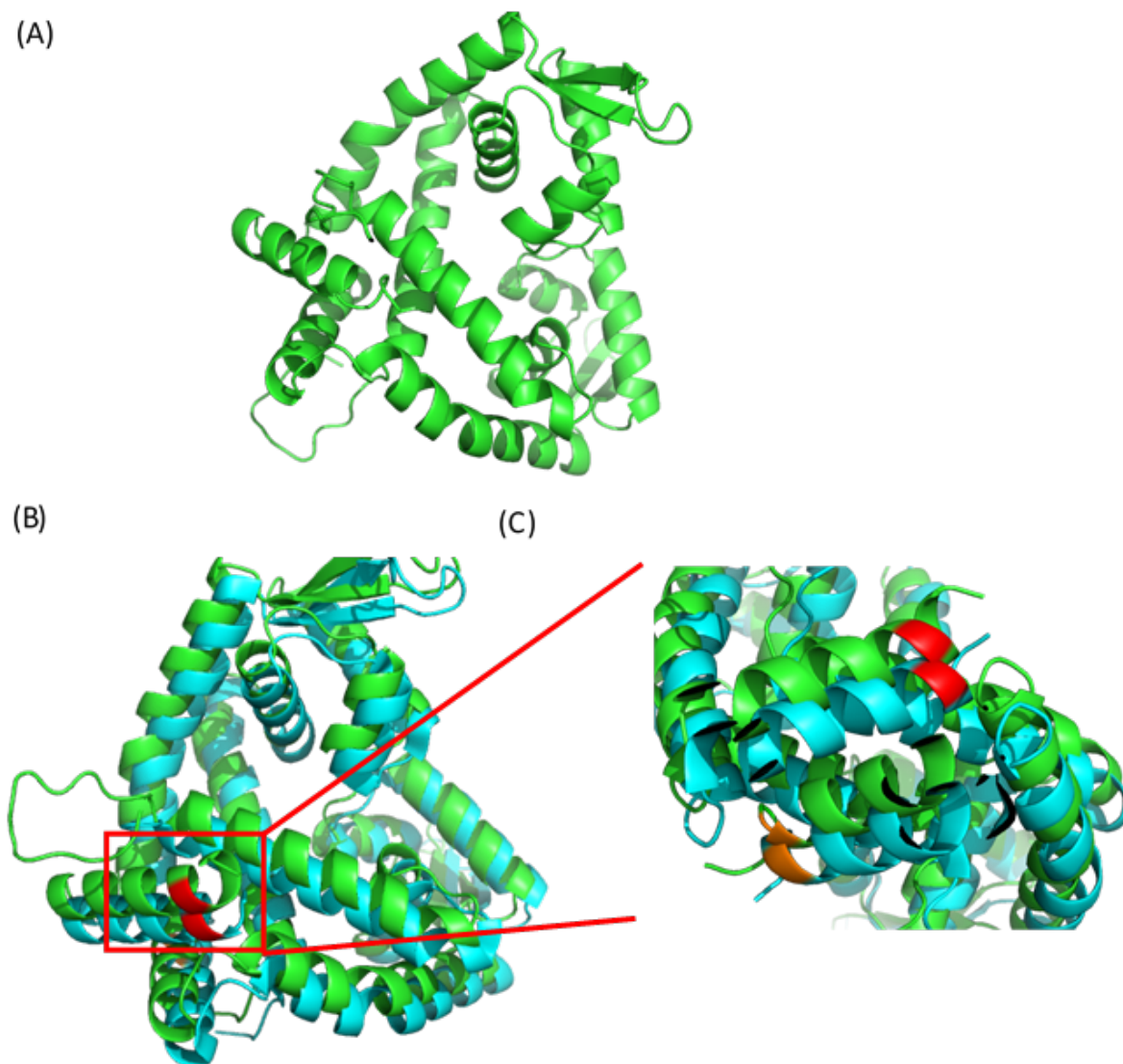
In *E. coli*, nucleotide deletions in *marR* were observed. The first mutant possessed a deletion of two bases at nucleotide positions 420-421/435 conferring a frameshift from amino acid position 141 within the C-terminal domain of MarR. This frameshift increased the protein length from 144 to 150 amino acids and is hereafter referred to as MarR K141Sfs*150. The second mutant contained a deletion at nucleotide position 311/435 conferring a frameshift from amino acid position 105 and resulted in the introduction of a premature stop codon at amino acid position 114. This mutation is hereafter referred to as MarR A105Rfs*114. Mapping of the MG1655 MarR K141Sfs*149 and MarR A105Rfs*114 mutants against the wild type MG1655 sequence revealed the presence of nucleotide deletions on the forward strand at chromosome position 1619537 (Figure 4.4) and 1619430 (Figure 4.5), respectively. Both mutations were confirmed by PCR and DNA sequencing of the amplimers (Figure 4.2, 4.4 and 4.5). Using Modeller 9.24, homology models of MarR K141Sfs*150 (Figure 4.6) and MarR A105Rfs*114 (Figure 4.7) were made using the crystal structure of MarR wild type as a reference template (PDB-3voe). The homology models were aligned against the wild type (PDB-3voe) structure in PyMOL and the deletion sites on chain A and B are highlighted.

Figure 4.5: Artemis 18.0.2 analysis of the mutant *E. coli* MG1655 sequence and subsequent translation of the sequenced DNA to confirm the presence of the MarR A105Rfs*114 frameshift



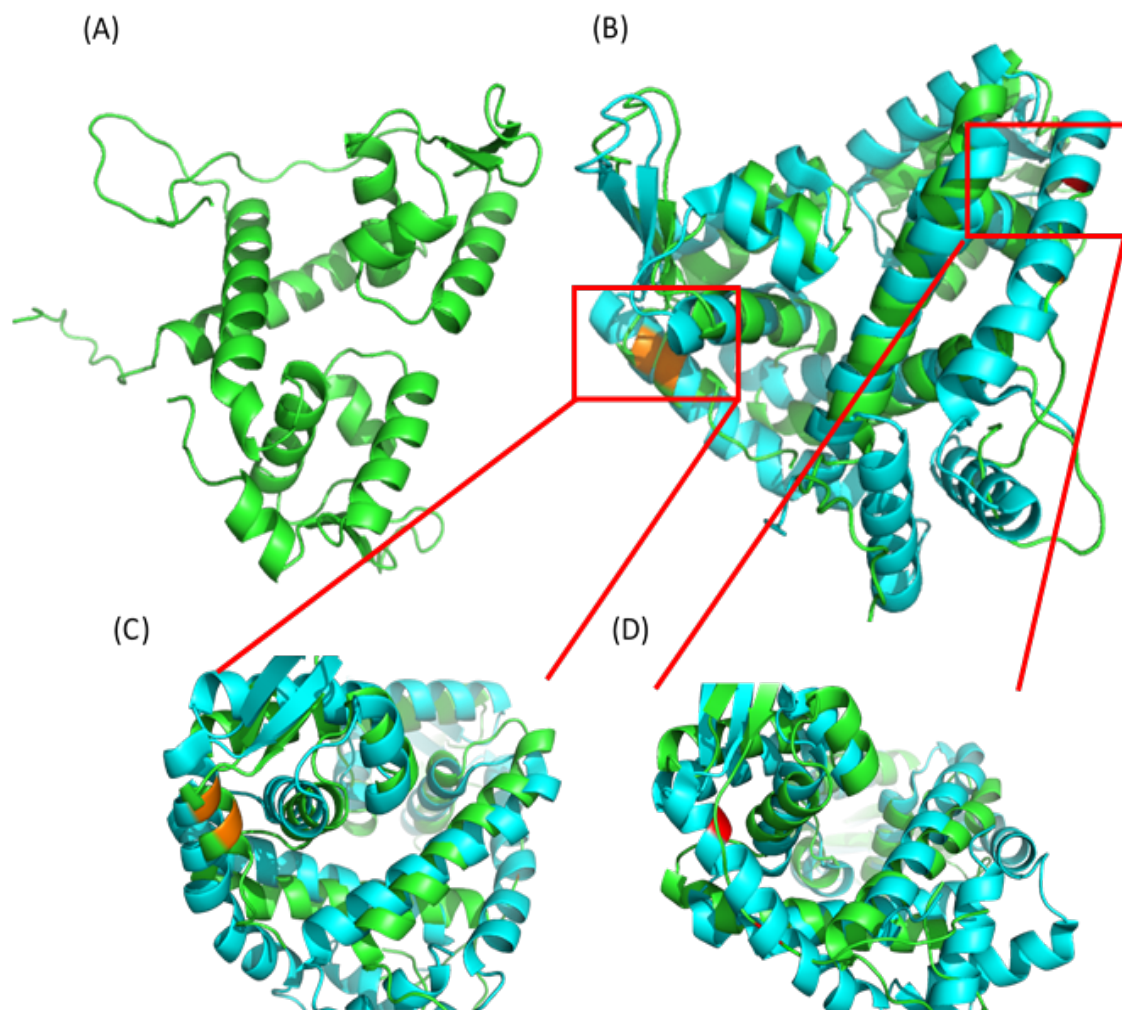
E. coli MG1655 containing MarR A105Rfs*114 was aligned against the whole genome of wild type *E. coli* MG1655. The deletion site is highlighted as a red line.

Figure 4.6: Homology model of MG1655 MarR K141Sfs*150.



(A) Homology model of MarR K141Sfs*150 built with Modeller 9.21 using the crystal structure of MarR wild type (PDB-3vov) as the template structure. The ribbon structure was visualised in PyMOL. (B) PyMOL alignment of the homology model of MarR K141Sfs*150 (green) against the crystal structure of MarR wild type (PDB - 3vov) (cyan). The mutation sites are displayed in red (Chain A) and orange (Chain B) on both MarR K141Sfs*150 and MarR wild type. (C) Close-up view of the mutation sites of MarR on Chain A and Chain B. Colours as shown in (B).

Figure 4.7: Homology model of MG1655 MarR A105Rfs*114.



(A) Homology model of MarR A105Rfs*114 built with Modeller 9.21 using the crystal structure of MarR wild type (PDB-3voe) as the template structure. The ribbon structure was visualised in PyMOL. (B) PyMOL alignment of the homology model of MarR A105Rfs*114 (green) against the crystal structure of MarR wild type (PDB - 3voe) (cyan). The mutation sites are displayed in red (Chain A) and orange (Chain B) on both MarR A105Rfs*114 and MarR wild type. (C) Close-up view of the mutation sites of MarR on Chain B. (D) Close up view of the mutation sites of MarR on Chain A.

4.6 Mutants resistant to the efflux inhibitor Pa β N can be selected

To determine whether *S. Typhimurium* SL1344 mutants resistant to Pa β N can be selected, mutant selection experiments were carried out in which Pa β N (at efflux inhibitory concentrations - 50 μ g/ml) was combined with ciprofloxacin (0.03 μ g/ml). The mutation frequency (5.47×10^{-10} CFU/ml) and rate (1.04×10^{-10} CFU/ml) was very low producing a single mutant colony. Further mutant selection experiments were performed in which *S. Typhimurium* SL1344 was exposed to 2X the MIC (1,024 μ /ml) of Pa β N alone. Under these conditions, five colonies were produced. The mutation frequency and rate were 1.52×10^{-10} CFU/ml and 1.51×10^{-9} CFU/ml, respectively.

The MIC of a panel of antibiotics against each mutant was determined. Each mutant was grouped dependent on its MIC phenotype (Table 4.6). Consistent with the *S. Typhimurium* mutants selected with chlorpromazine in combination with ciprofloxacin, the *S. Typhimurium* mutant selected with Pa β N and ciprofloxacin was only less susceptible to ciprofloxacin and nalidixic acid. WGS (Table 4.7) revealed this fluoroquinolone resistance was conferred by a S83P substitution within GyrA. Additional mutations in these fluoroquinolone-resistant mutants were observed in the genes encoding RecN and BarA. A SNP resulted in a substitution (R78H) within RecN. Deletion of a single base at nucleotide position 24/2757 of *barA* resulted in a frameshift and the introduction of a premature stop codon at amino acid position 10/918 of BarA. Referred to as BarA R9Afs*10 throughout.

The mutant sequence was mapped against the SL1344 wild type sequence using Artemis 18.0.2. GyrA S83F was found on the forward strand at position 2373816 of the chromosome (Figure 4.8). BarA R9Afs*10 was found on the forward strand at position 3128004 of the chromosome (Figure 4.9). RecN R78H was found on the forward strand at position 2384684 of the chromosome (Figure 4.10). The presence of each mutation was confirmed by PCR and subsequent DNA sequencing of the amplicons (Figure 4.8, 4.9 and

4.10).

Table 4.6 Susceptibility of *S. Typhimurium* mutants selected with PaβN in the presence and absence of ciprofloxacin.

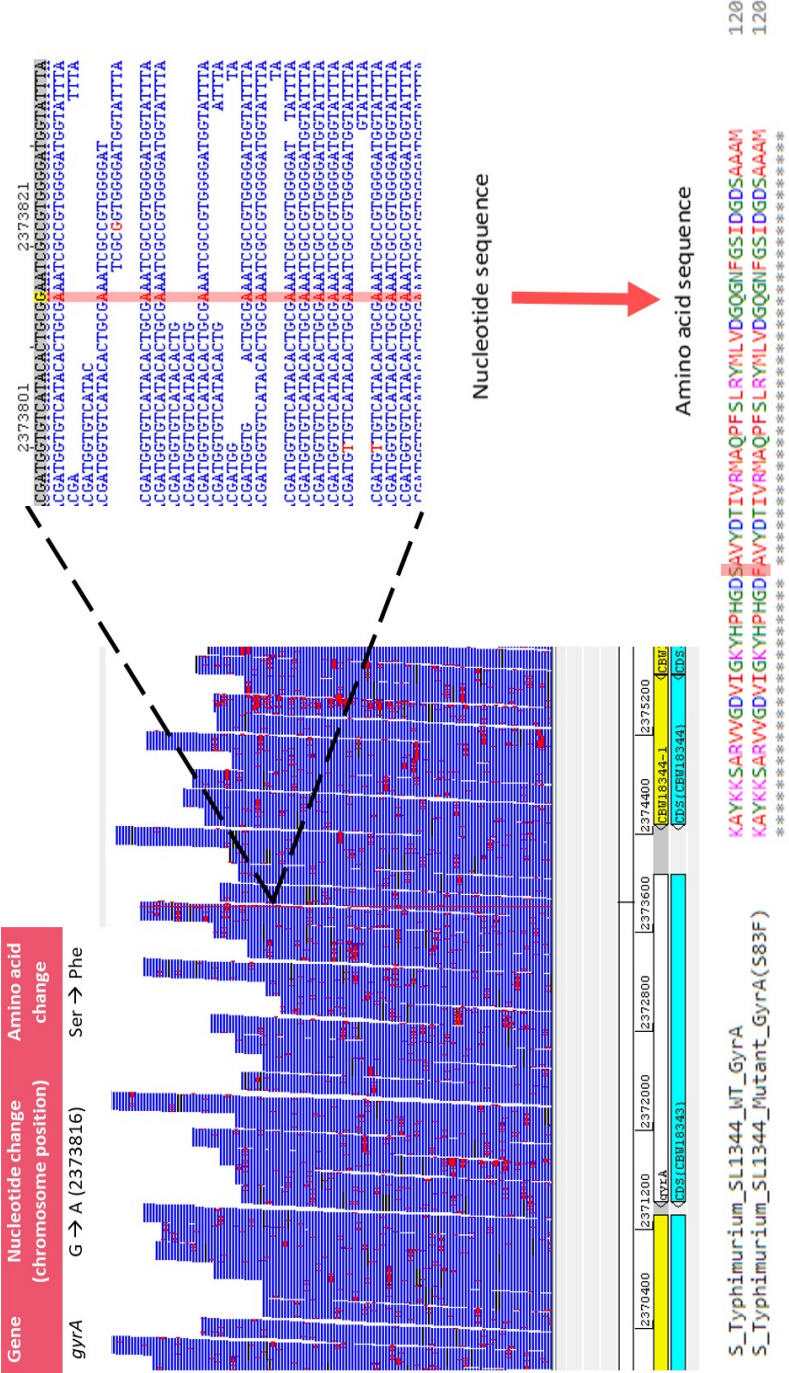
Strain (MIC phenotype group)	Selecting concentrations (μg/ml)	MIC (μg/ml)						
		PaβN	CPZ	CIP	CHL	TET	NAL	ETBR
SL1344 wild type		512	256	0.03	8	2	8	1,024
(1)	50 + 0.03	512	256	1	8	2	128	1,024
(1)	1,024	1,024	256	0.03	4	2	8	1,024
(2)	1,024	1,024	256	0.06	4	2	8	1,024

CPZ; chlorpromazine; PaβN, phenylalanine-arginine beta-naphthylamide; CIP, ciprofloxacin; CHL, chloramphenicol; TET, tetracycline; NAL, nalidixic acid; ETBR, ethidium bromide. The wild type parental strains are shown in blue. A decrease in susceptibility is shown in red. An increase in susceptibility is shown in orange. The mode of three biological replicates is shown.

Table 4.7 Mutations and substitutions identified in the *S. Typhimurium* SL1344 mutant selected upon exposure to Pa β N and ciprofloxacin.

Strain (MIC phenotype group)	Gene product	Nucleotide change (position)	Amino acid change (position)	Effect	Nomenclature
<i>S. Typhimurium</i> SL1344 (1)	GyrA	C→T (248/2637)	Serine → Phenylalanine (83/878)	Substitution	GyrA S83F
	RecN	G→A (233/1662)	Arginine → Histidine (78/553)	Substitution	RecN R78H
	BarA	CAC→CC (24/2757)	Arginine → Alanine (9/918)	Frameshift (premature stop codon)	BarA R9Afs*10

Figure 4.8: Artemis 18.0.2 analysis of the resistant mutant *S. Typhimurium* SL1344 sequence and subsequent translation of the sequenced DNA to confirm the presence of the GyrA (S83F) substitution



S. Typhimurium SL1344 containing GyrA (S83F) was aligned against the whole genome of wild type *S. Typhimurium*. The mutation site is highlighted as a red line. *gyrA* is transcribed on the reverse strand and the S83F substitution is conferred by a C → T mutation at nucleotide position 248/2637. When reading a BAM file Artemis displays the forward strand only. Therefore, the SNP is shown as the reverse complement (A → G)

The SL1344 mutants selected with Pa β N showed two MIC phenotypes. The mutants in both phenotype groups were \geq two-doubling dilutions less susceptible to Pa β N than wild type SL1344. In addition, a one-doubling dilution increase in susceptibility to chloramphenicol and a one-doubling dilution decrease in susceptibility to ciprofloxacin was observed for mutants in phenotype group 1. The whole genome of one representative mutant from each MIC phenotype group was sequenced. Analysis revealed mutations in coding regions of the genome of each mutant. Both mutants contained a single mutation in *bamE* (also known as *smpe*), encoding the protein BamE. The first mutant possessed a SNP resulting in the substitution of a tryptophan for a premature stop codon at amino acid position 73/112 (W73STOP). The second mutant possessed a deletion of a single base at nucleotide position 77/339 resulting in a frameshift that produced a premature stop codon at amino acid position 50/112. This mutant is hereafter called BamE V26Gfs*50.

Mapping of the SL1344 BamE W73STOP and BamE V26Gfs*50 mutant sequences against the wild type SL1344 sequence using Artemis 18.0.2 revealed the presence of these mutations on the forward strand at position 2836479 (Figure 4.11) and position 2836337 (Figure 4.12) of the chromosome, respectively. The presence of both mutations was confirmed by PCR and DNA sequencing of the amplicons (Figures 4.11 and 4.12).

4.6.1 Susceptibility of single *barA*, *recN* and *bamE* *E. coli* Keio Collection knockouts

To confirm whether the genes in which mutations were observed have any effect on the activity of Pa β N, the MIC of Δ *barA*, Δ *recN* and Δ *bamE* *E. coli* BW25113 sourced from the Keio Collection was determined and compared to the MIC of the *E. coli* BW25113 wild type strain. Due to time limitations surrounding the construction of knockouts in *Salmonella*, the readily available Keio collection *E. coli* strains were used as a crude first screen to determine whether the absence of these genes alter Pa β N susceptibility. When compared to the MIC

Table 4.8 Mutations identified in the *S. Typhimurium* SL1344 mutants selected upon exposure to PaβN.

Strain (MIC phenotype group)	Gene product	Nucleotide change (position)	Amino acid change (position)	Effect	Nomenclature
SL1344 (1)	BamE	G→A (218/339)	Tryptophan → STOP (73/112)	Substitution (Premature stop codon)	BamE W73STOP
SL1344 (2)	BamE	GTG→GG (77/339)	Valine → Glycine (26/112)	Frameshift (Premature stop codon)	BamE V26Gfs*50

of Pa β N against wild type *E. coli* BW25113 (256 μ g/ml), Δ *bamE* BW25113 was one-fold more susceptible to the action of Pa β N (MIC - 128 μ g/ml). The MIC of Pa β N against Δ *barA* and Δ *recN* BW25113 were the same as for *E. coli* BW25113 (256 μ g/ml).

4.7 Discussion

As hypothesised in Chapter three, the efflux inhibitory activity of chlorpromazine is suggested to result from a direct interaction with AcrB. Alternatively, the efflux activity of chlorpromazine and amitriptyline may be due to additional interactions with other targets such as those involved in the regulation of, or activity of, efflux pumps. This activity may be non-specific (e.g. membrane damage) and/or dependent on interactions with targets that have not been previously described as being involved with the activity of efflux pumps. Therefore, it is important to elucidate the molecular targets of a given compound before making assumptions about its biological interactions.

Analysis of mutants selected in exposure experiments are one of the simplest means by which the mode of action of a compound can be identified. However, the structural complexity of tripartite efflux pumps means it is difficult to determine the mode of action of efflux pump inhibitors (Nguyen et al., 2015). Another major challenge limiting mode of action studies is that efflux pump inhibitors often have limited antibacterial activity. This means it is difficult to design mutant selection experiments in which an inhibitor provides the sole selective pressure. Instead, to elucidate the molecular targets of an efflux pump inhibitor, mutant selection experiments are typically performed in which an inhibitor-antibiotic combination is used to provide the selective pressure. Unfortunately, this strategy often results in the selection of target site mutations conferring resistance to the antibiotic alone (Lomovskaya and Bostian, 2006; Nguyen et al., 2015).

The mutation rates for each mutant selection experiment were calculated using the MSS-maximum likelihood method. This method was chosen as it allows a mutation rate

to be calculated at all values of m (Foster, 2006; Rosche et al., 2000). However, direct comparison of the mutation rate for each selecting condition is limited as the number of parallel cultures is varied. This increase in the number of parallel cultures from one to 20/30 was a result of a change in methodology for the later mutant selection experiments in order to increase the robustness and accuracy of the MSS-maximum likelihood calculation. Nonetheless, the following observations were made. The rate of resistance emergence in the presence of chlorpromazine combined with ciprofloxacin was also similar to the rate of ciprofloxacin resistance. Unsurprising, given that resistance resulting from exposure to chlorpromazine in combination with ciprofloxacin was conferred by a single *gyrA* mutation. Only a single mutant resulted from exposure of *S. Typhimurium* to Pa β N in combination with ciprofloxacin. This difficulty selecting for mutants was accompanied by a lower mutation rate compared to the rates observed for resistance to Pa β N and ciprofloxacin when either were used as the sole selecting agent. This increase in mutation rate reflects the multiple mutations that emerged upon exposure to this combination; second step mutations occur at a much lower rate (Rosche et al., 2000; Pope et al., 2008). The mutation rates when chlorpromazine and Pa β N were used as the sole selecting agent against *S. Typhimurium* were similar to the rates observed for ciprofloxacin resistance. Interestingly, an increase in the selective pressure by just 10 μ g/ml of chlorpromazine drastically reduced the mutation rate of *E. coli* resistance to chlorpromazine from 1.36×10^{-9} CFU/ml at 160 μ g/ml of chlorpromazine to 9.40×10^{-11} CFU/ml at 170 μ g/ml. Resistance of *E. coli* to chlorpromazine was conferred by mutations within *marR*. Mutations within *marR* typically confer low level resistance unless accompanied by an additional target site mutation (Alzrigat et al., 2017). Mutants conferring a low level of resistance are less likely to be selected for at higher selecting concentrations as they do not provide a large fitness benefit.

To facilitate the identification of the primary mode of action of chlorpromazine and Pa β N, mutant selection experiments were done with *S. Typhimurium* mutants exposed to

a combination of chlorpromazine or Pa β N and ciprofloxacin. When *S. Typhimurium* was exposed to chlorpromazine in combination with ciprofloxacin, mutants were selected for that only had decreased susceptibility to ciprofloxacin and nalidixic acid. As described by others, the absence of chlorpromazine resistance is likely a result of low selective pressure exerted by the efflux inhibitor.

The observed fluoroquinolone resistance resulted from a substitution (S83F) within GyrA, a topoisomerase enzyme that is essential for preventing the bacterial chromosome from under/over winding and tangling during DNA replication. GyrA is one of the primary molecular targets for the antibiotic action of quinolones in Gram-negative bacteria (Champoux, 2001; Gellert et al., 1976; Corbett and Berger, 2004) and quinolone resistance typically results from chromosomal mutations within *gyrA* (Eaves et al., 2004; Heisig, 1996; Herrera, 1993; Nakamura et al., 1989; Ouabdesselam et al., 1995; Randall et al., 2005; Vila et al., 1996; Yamagishi et al., 1986). In particular, substitutions at codon 83 are common in *Salmonella* isolates resistant to quinolones (Barnard et al., 2001; Hansen et al., 2003; Heisig, 1996; Lindstedt et al., 2004; Ling et al., 2003; Ouabdesselam et al., 1995; Piddock, 2002; Randall et al., 2005; Su, Chiu, et al., 2004).

Consistent with the chlorpromazine and ciprofloxacin combination experiments, *S. Typhimurium* mutants selected after exposure to Pa β N in combination with ciprofloxacin were only resistant to ciprofloxacin and nalidixic acid. This was also conferred by a substitution (S83F) within GyrA. In the mutants studied, this substitution was accompanied by an additional substitution (R78H) within RecN and a frameshift at codon position 9 of BarA. Interestingly, the susceptibility of *S. Typhimurium* SL1344 BarA R9Afs*10, RecN R78H, GyrA S83F was the same as *S. Typhimurium* GyrA S83F indicating that the presence of mutations within *barA* and *recN* did not further decrease antibiotic susceptibility relative to *S. Typhimurium* SL1344 GyrA S83F. In addition, *barA* and *recN* mutations did not confer cross resistance to Pa β N indicating that the proteins

encoded by these genes are unlikely to be directly involved in the mode of action of this compound. Instead, it is likely that the mutations in *barA* and *recN* are coincident bystander or compensatory mutations.

Mutations in genes can incur a fitness cost in the absence of selective pressure; single point mutations in *gyrA* have been associated with neutral, beneficial and costly fitness effects dependent on the bacterial species (Rozen et al., 2007; Andersson et al., 2010; Lindgren et al., 2005; Marcusson et al., 2009; Machuca et al., 2014; Baker et al., 2013). The reported fitness costs of *gyrA* mutations in *Salmonella* are varied. While Giraud, Cloeckert, Baucheron, et al., 2003 and Webber, Ricci, et al., 2013 have shown that S83F substitutions result in impaired growth of *S. Typhimurium* compared to the wild type, Knopp et al., 2018 show fitness costs are only associated with *gyrA* mutations when combined with secondary mutations. In terms of its degree of selective pressure, Pa β N potentiates the activity of ciprofloxacin to a greater extent than chlorpromazine in synergy assays (Chapter 3) and therefore will provide a greater selective pressure than chlorpromazine when combined with ciprofloxacin at the same concentration. Therefore, the presence of Pa β N, even at low concentrations, will induce a stress response and may compound any fitness defects that result from the presence of a *gyrA* mutation. As a result, the observed mutations in *barA* and *recN* may ameliorate any cumulative fitness costs incurred in the presence of the additional selective pressure exerted by Pa β N. However, before assumptions can be made regarding the presence of compensatory mutations, the biological role of the mutated genes must be considered.

BarA is part of the BarA/SirA two-component system of *Salmonella* (Teplitski et al., 2003; Lou et al., 2019; Altier et al., 2000). Upon activation by metabolic end products, BarA phosphorylates SirA preventing it from binding target DNA (Zere et al., 2015; Pernestig et al., 2001; Chavez et al., 2010; Teplitski et al., 2003). The main target genes of SirA are those belonging to the Csr regulatory system; a system heavily involved in the bacterial

response to stress (Lou et al., 2019; Potts, Guo, et al., 2019; Zere et al., 2015).

CsrA is a regulatory RNA binding protein that, dependent on the target, behaves as a posttranscriptional repressor or activator (Suzuki et al., 2002). In general, CsrA activates genes involved in exponential growth and represses those involved in growth during stationary phase and genes involved in oxidative, osmotic and acid stress resistance (Potts, Guo, et al., 2019; Vakulskas et al., 2015; Romeo et al., 2013; Edwards, Patterson-Fortin, et al., 2011). In *Salmonella*, CsrA is regulated by CsrB and CsrC, which bind CsrA and antagonise its activity (Vakulskas et al., 2015; Potts, Guo, et al., 2019; Altier et al., 2000; Fortune et al., 2006; Potts, Vakulskas, et al., 2017; El Mouali et al., 2018).

Typically, under conditions of stress, when growth is not a priority, CsrB is upregulated. Consequently, more CsrA is sequestered and there is a decrease in the expression of genes that are essential for growth and an increase in those involved in stress resistance and virulence (El Mouali et al., 2018; Teplitski et al., 2003; Altier et al., 2000). BarA, through its interaction with CsrA, is involved in the bacterial stress response; mutations within *barA* are known to reduce the expression of *csrB* releasing CsrA to interact with its RNA targets (Suzuki et al., 2002). Given that CsrA typically represses genes involved in the stress response it is unknown why exposure to Pa β N (an inducer of the stress response through damage to the outer membrane) (Lomovskaya, Warren, et al., 2001; Lomovskaya and Bostian, 2006) would result in the selection of mutations that would largely suppress the stress response. However, the impact of the stress response is complicated. Typically, exposure of susceptible strains to antibiotics results in an induction of a stress response. However, in antibiotic-resistant strains, a reorganisation of the metabolic network can occur to circumvent the metabolic fitness costs of antibiotic resistance mutations; this reorganisation is partly mediated by a reduction in the stress response (Händel et al., 2013).

Although CsrA predominately represses stress response genes, some, including *acrA*, *acrB*, *ompF*, *ompC* and *fhuABCD* are activated by CsrA (Ricci, Attah, et al., 2017; Potts, Guo, et al., 2019; Potts, Vakulskas, et al., 2017). This nature of CsrA as both an activator and repressor of the stress response means the response of CsrA to environmental stress is complex and the impact of mutations within this regulatory network is most likely multifaceted. It is also important to note that the mutations observed could be coincident bystander mutations and are not representative of the link between the Csr and BarA systems. Further phenotypic studies are required to elucidate the role that *barA* mutations play, if any, in the mechanism of resistance to Pa β N and ciprofloxacin. However, based on what is known about the biology of BarA, the following hypotheses can be proposed. (i) Alterations to the stress response, through a mutation in BarA, may confer Pa β N tolerance allowing bacteria to withstand the additional selective pressure exerted when Pa β N is combined with ciprofloxacin. (ii) The additional selective pressure exerted by Pa β N may compound any fitness defects incurred by the presence of a *gyrA* mutation. A mutation in *barA* may compensate for this fitness cost through the upregulation of genes that promote bacterial growth, efflux and alterations in membrane permeability and the downregulation of genes that are non-essential for bacterial growth.

RecN is also a stress response protein involved in the repair of double stranded DNA (dsDNA) breaks (Uranga et al., 2017). The repair of dsDNA breaks is initiated by the RecBCD enzyme complex which unwinds the DNA and makes a new 3' end producing single stranded DNA (ssDNA). RecBCN then loads RecA onto the ssDNA (Keyamura et al., 2013; Kowalczykowski, 2000; Dillingham et al., 2008). In *Bacillus subtilis* RecN is then recruited to the dsDNA break and its ATPase activity is stimulated; the ATPase activity of RecN is suggested to promote RecA-mediated DNA strand exchange to repair the break (Sanchez, Kidane, et al., 2006; Uranga et al., 2017). Due to difficulties purifying RecN, little is known about the RecA-RecN interaction in *E. coli* and *Salmonella* (Uranga et al., 2017; Reyes

et al., 2010; Warr et al., 2019). However, in these organisms, the repair of dsDNA breaks is severely attenuated in the absence or mutation of *recN* (Meddows et al., 2005; Sargentini et al., 1986; Youssef et al., 2014; Picksley et al., 1984; Uranga et al., 2017).

Like *barA*, it is unknown why a mutation within *recN* was selected for upon exposure to Pa β N in combination with ciprofloxacin. Given the role that RecN plays in the bacterial response to stress, mutations within *recN* may also be selected to reduce the metabolic output (e.g. through a decrease in the expression of virulence genes) allowing for compensation for any fitness costs incurred by a *gyrA* mutation under the additional selective pressure of Pa β N. Interestingly, in *E. coli*, lack of a functional RecABCD system reduced the emergence of *gyrA* mediated ciprofloxacin resistance (Urios et al., 1991; Qin et al., 2015). Therefore, *recN* mutations, which reduce the functionality of RecN are likely to be second-step mutations. In addition, during antimicrobial-induced DNA stress genomic instability may be observed (Do Thi et al., 2011; Cirz et al., 2005; Gutierrez et al., 2013; Baharoglu, Krin, et al., 2013; Shapiro, 2015). It is suggested that under conditions of stress a homogenous bacterial population is less desirable and an increase in genetic variability is advantageous to increase the probability of proliferating a mutation that confers a fitness advantage under conditions of stress (Shapiro, 2015). A mutation in *recN* resulting in a decrease in the effectiveness of the RecA DNA repair protein is hypothesised to increase the appearance of mutations resulting in a more heterogeneous population. Hypermutability is a highly advantageous phenotype for ameliorating the fitness costs associated with antibiotic resistance as it leads to a greater probability of incurring compensatory mutations (Björkman and Andersson, 2000; Perron et al., 2010; Hughes et al., 2017).

The data presented here supports previous evidence that it is difficult to select mutants in the presence of an antibiotic with decreased susceptibility to an efflux inhibitor. However, although not potent, Pa β N and chlorpromazine possess a degree of antibacterial activity which allowed mutant selection experiments in the presence of the inhibitor alone to be

performed.

The appearance of chlorpromazine-resistance was rare; at the MIC of chlorpromazine no chlorpromazine-resistant *S. Typhimurium* and *E. coli* mutants were selected. Here, *S. Typhimurium* and *E. coli* mutants resistant to chlorpromazine were selected at sub-MIC. Given that experiments at the MIC of a drug predominantly select for mutations that ablate a compounds antibacterial activity, the mutations within *ramR* and *marR* selected at sub-MICs, at which efflux inhibitory activity is observed (100-200 µg/ml), may be more relevant in terms of the mode of action of chlorpromazine as an efflux inhibitor.

Mutations conferring efflux inhibitor-resistance may abolish ligand binding (Tenover, 2006; Munita et al., 2016; Blair, Webber, et al., 2015). However, the hypothesis that these mutations occur conferring substitutions in the ligand binding site of chlorpromazine was not supported. Instead, WGS revealed that chlorpromazine resistance was conferred by mutations within *ramR* and *marR* of *S. Typhimurium* and *E. coli*, respectively. In their resting state RamR and MarR bind to the promoter regions of the transcriptional activators *ramA* and *marA*, respectively, thereby preventing their expression (Baucheron, Coste, et al., 2012; Ricci, Busby, et al., 2012; Alekshun, Levy, et al., 2001; Alekshun, Kim, et al., 2002). Upon ligand binding, the conformation of RamR and MarR is altered such that the proteins are unable to bind DNA. Subsequently *ramA* and *marA* are expressed and overproduction of RamA and MarA occurs with accompanying overexpression of *acrAB-tolC* (Baucheron, Coste, et al., 2012; Martin, Jair, et al., 1996; Alekshun and Levy, 1997; Alekshun, Levy, et al., 2001; Abouzeed et al., 2008; Cohen, Hachler, et al., 1993). Given that ligand binding is essential for derepression of the AcrAB-TolC regulatory system, it seems unlikely that these mutations prevent the antibacterial or efflux inhibitory activity of chlorpromazine simply by preventing its binding to MarR and RamR. Instead, based on data from this study showing that chlorpromazine binds AcrB, it is proposed that chlorpromazine is a substrate of AcrB and that alteration of RamR and MarR confers resistance to chlorpromazine by

overexpressing *ramA* and *marA*, respectively. This consequently increases efflux of this compound by AcrAB-TolC and hence resistance.

Mutations within *ramR* and *marR* have been widely reported in the literature as conferring antibiotic resistance to both clinical and laboratory strains of *Salmonella* and *E. coli*, respectively (Notka et al., 2002; Alekshun, Levy, et al., 2001; Alekshun, Kim, et al., 2002; Seoane et al., 1995; Linde et al., 2000; Watanabe et al., 2012). These mutations often result in an inability of the repressor to bind DNA, typically as a result of mutations directly in the DNA binding domains or from mutations that result in global conformational changes in protein secondary structure.

Here, the mutations within *marR* that confer resistance to chlorpromazine result in frameshifts from amino acid positions 105 and 141. Neither mutations have been previously described. Position 105 is found within the linker region of MarR connecting the N-/C-terminal domain to the rest of the protein. The linker region is highly flexible and is essential in order to accommodate the structural shifts that occur when the DNA binding domains of each MarR monomer interact with DNA (Alekshun, Levy, et al., 2001). It is known that upon ligand binding, the conformation of MarR is altered and its flexibility constrained allowing MarR to dissociate from the DNA (Duval et al., 2013; Alekshun, Levy, et al., 2001). Therefore, it is hypothesised that mutation within the sequence encoding the linker domain may mimic ligand binding by reducing the flexibility of MarR thereby preventing DNA binding. Importantly, a frameshift at position 105 results in a premature stop codon at residue 113/145. While the sequence coding for the DNA binding domain is translated, it is hypothesised that in this mutant the conformation of the truncated protein is largely altered compared to the wild type protein. These conformational changes prevent DNA binding at the *marA* promoter region and result in expression of *marA*. In support of this hypothesis, an *E. coli* MDR clinical isolate containing a deletion of the last 18 amino acids at the C-terminal of MarR was found to be significantly altered in its ability to form a dimer

and bind DNA (Notka et al., 2002).

The α -helices of the C-terminus of MarR is essential for protein function and mutations that result in altered protein structure and DNA binding in this region have been frequently described (Alekshun and Levy, 1997; Alekshun, Levy, et al., 2001; Seoane et al., 1995; Linde et al., 2000; Watanabe et al., 2012). Considering the importance of the C-terminus for maintaining the conformation of the MarR dimer, the frameshift at amino acid position 141 within the C-terminal of MarR, may also alter the protein conformation, likely by preventing dimerisation of the individual monomers. Like MarR A105Rfs*114, MarR K141Sfs*150 is hypothesised to alter the conformation of MarR such that it is unable to bind to the promoter region of *marA* thus resulting in consequent overexpression of *marA* and increased efflux activity by AcrAB-TolC.

Resistance of *S. Typhimurium* to chlorpromazine was conferred by the substitution L158P within RamR. Residue L158 lies within the dimerisation domain of RamR. Although the L158P substitution has not been previously described, the substitutions Y59H, M84I and E160D have been previously revealed to incur protein instability when compared to the wild type protein (Liu and Chen, 2017). Interestingly, while mutations Y59H and M84I show a greater affinity to form a RamR dimer, E160P has a reduced dimerisation affinity and is predicted to be largely altered in structure. This is a consequence of residue location, E160P is located within α -helix 8b which is involved in the dimerisation of RamR through hydrogen bonding and hydrophobic interactions (Yamasaki, Nikaido, et al., 2013a). In addition, it has been suggested that substitutions in the dimerisation domain increase the distance between the HTH of the DNA binding domain, thereby reducing the affinity of the interaction with DNA (Liu and Chen, 2017). This is especially important when considering proline substitutions; proline is known to disrupt α -helical structures (Li, Goto, et al., 1996). Considering this, and the impact of the E160P substitution, L158P (which lies at the dimerisation interface) is hypothesised to possess an

altered conformation relative to the wild type as a result of disruptions in its α helical structures thereby reducing the ability to form RamR dimers. In addition, L158P lies three amino acids outside of the residue (Phe155) that is essential for all ligand interactions (Yamasaki, Nikaido, et al., 2013a). Therefore, a substitution near this site may induce conformational changes that mimic ligand binding and result in reduced DNA binding affinity and consequent expression of *ramA*. Taken together, the RamR L158P protein is predicted to have a reduced affinity for DNA as a result of altered protein conformation.

Given the structures of MarR and RamR and the residues in which the frameshifts and substitutions are located, here it is hypothesised that resistance towards chlorpromazine is conferred by overexpression of the transcriptional activators MarA and RamA resulting from conformational changes in MarR and RamR that prevent/reduce the binding of these proteins with the promoter regions of *marA* and *ramA*, respectively.

S. Typhimurium mutants resistant to Pa β N were successfully selected and two phenotypes were observed. The resistance phenotypes were conferred by two independent mutations within *bamE*; the substitution W73STOP resulting in a truncated protein and the frameshift V26Gfs*50. BamE, also known as SmpA, is a lipoprotein involved in biogenesis of the OM of *Salmonella* as part of the BAM complex (Fardini et al., 2009; Lewis et al., 2008). Composed of the OMP BamA and four lipoproteins (BamBCDE), the BAM complex is responsible for recognising, assembling and inserting β -barrel proteins into the OM of Gram-negative bacteria (Rossiter et al., 2011; Fardini et al., 2009). Although not involved directly in the assembly of the OMPs, BamE is suggested to be required for stabilising the protein-protein interactions of the BAM complex (Rossiter et al., 2011; Fardini et al., 2009; Sklar et al., 2007; Silhavy and Malinverni, 2011). BamE is essential for the virulence of *Salmonella*; deletion of *bamE* results in a significant attenuation of oral and parenteral infections in a mouse model (Lewis et al., 2008). In addition, deletion of *bamE* causes severe permeability defects and a reduction in the number of OMPs (Fardini

et al., 2009).

Pa β N is known to cause extensive membrane damage (Lomovskaya and Bostian, 2006; Lomovskaya, Warren, et al., 2001). This membrane damage accounts for the antimicrobial activity of this compound and may contribute to its ability to potentiate the activity of an antibiotic; reducing their intracellular concentration though increases in membrane permeability. Through directed evolution experiments the OM damaging activity of Pa β N against *E. coli* has been rationalised by the identification of a target site (LpxM) in the LPS layer of the OM (Schuster, Bohnert, et al., 2019). Based on the biological role of BamE and the impact of deletion of this protein, BamE can be proposed as a potential direct target of Pa β N against *S. Typhimurium*; Pa β N may destabilise the BAM complex through interaction with BamE resulting in an increase in membrane permeability. Mutation of this protein may prevent the binding or activity of Pa β N and thus ameliorate its membrane damaging activity. However, as discussed mutation/deletion of *bamE* also results in increases in membrane permeability (Fardini et al., 2009). There is evidence to suggest this is true here; *S. Typhimurium bamE* mutants were increased in their susceptibility to chloramphenicol, a drug that is sensitive to alterations in membrane permeability.

4.8 Key findings

- Exposure of *S. Typhimurium* SL1344 to a combination of chlorpromazine/Pa β N and ciprofloxacin selected fluoroquinolone-resistant mutants only.
- Fluoroquinolone resistance was conferred by a substitution (S83F) within GyrA.
- The GyrA S83F substitution, conferring fluoroquinolone resistance to a *S. Typhimurium* mutant selected upon exposure to Pa β N and ciprofloxacin, was accompanied by an additional frameshift and substitution within BarA and RecN, respectively.

- Despite their low antibacterial activity, exposure of *S. Typhimurium* SL1344 and *E. coli* MG1655 to chlorpromazine and *S. Typhimurium* SL1344 to Pa β N resulted in the selection of resistant mutants.
- Chlorpromazine resistance was conferred by mutations within the transcriptional repressors *ramR* and *marR* of *S. Typhimurium* SL1344 and *E. coli* MG1655, respectively.
- Pa β N resistance was conferred by mutations within *bamE* of *S. Typhimurium*.

Chapter Five

Phenotypic characterisation of chlorpromazine-selected *E. coli* MG1655 *marR* and *S. Typhimurium ramR* mutants

5.1 Background

Resistance of *S. Typhimurium* SL1344 and *E. coli* MG1655 to chlorpromazine was conferred by mutations within genes encoding RamR and MarR, respectively. RamR and MarR are transcriptional repressors of RamA and MarA; both transcriptional activators of the AcrAB-TolC efflux pump. Ligand binding or mutation of RamR and MarR ablates the binding of RamR and MarR to the promoters of *ramA* and *marA* resulting in de-repression of *ramA* and *marA*. A concomitant increase in the expression of *acrAB-tolC* confers resistance to AcrB substrates as a result of increased efflux activity.

5.2 Hypothesis

- The selected chlorpromazine-resistant *S. Typhimurium* and *E. coli* mutants are increased in their expression of *ramA* and *marA*, respectively.
- Resistance of *S. Typhimurium* and *E. coli* to chlorpromazine is conferred by increased

expression of *acrAB* and a resulting increase in efflux activity.

- The mechanism underlying resistance of *S. Typhimurium* SL1344 RamR L158P to chlorpromazine is a result of an inability of the mutant protein to bind the promoter of *ramA*.

5.3 Aims

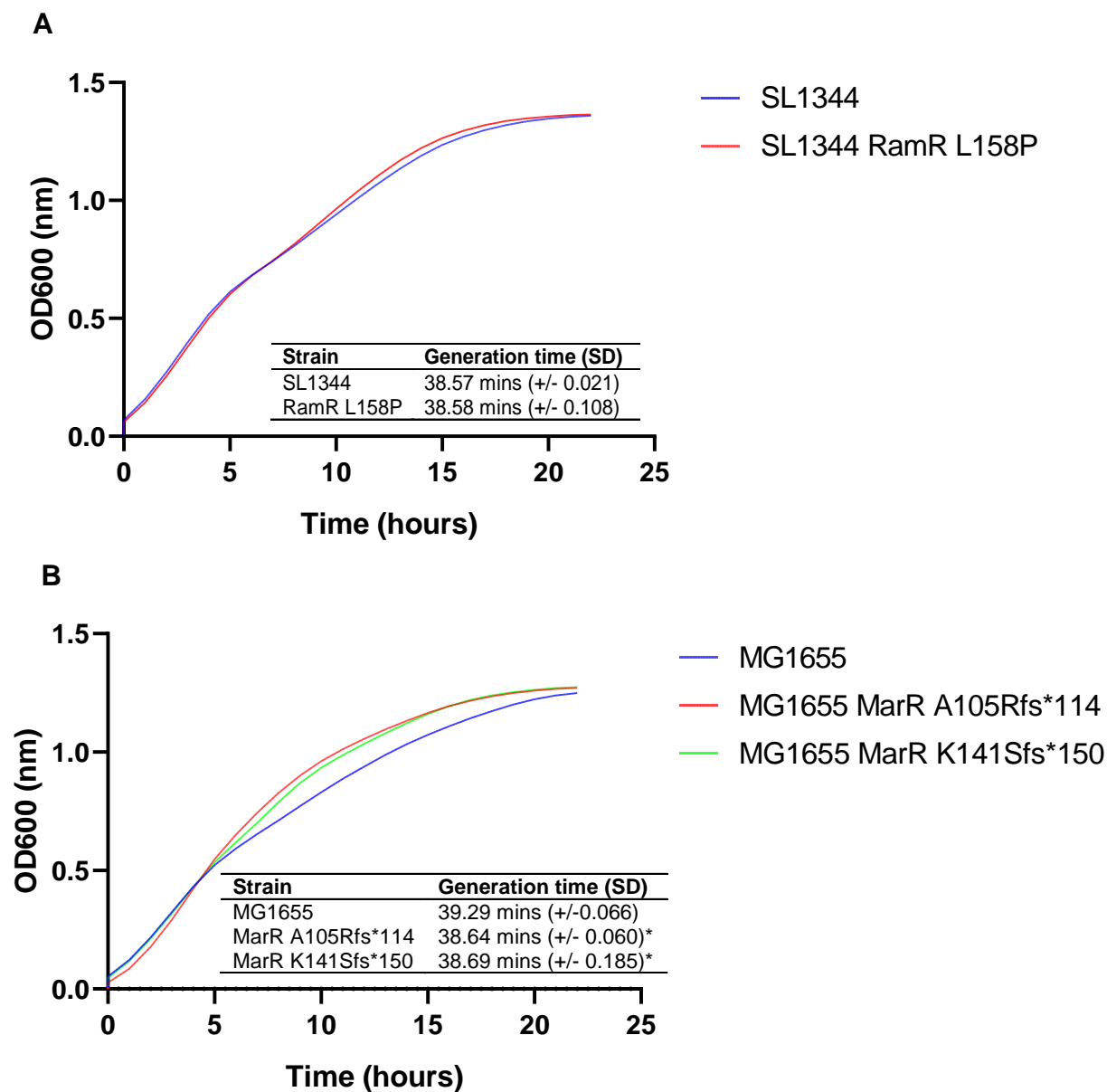
- To undertake a phenotypic characterisation of *S. Typhimurium* SL1344 RamR L158P *E. coli* MG1655 MarR A105Rfs*114 and MG1655 MarR K141Sfs*150.
- Determine the impact of SL1344 RamR L158P, MG1655 MarR A105Rfs*114 and MG1655 MarR K141Sfs*150 on: the susceptibility of *S. Typhimurium* SL1344 and *E. coli* MG1655 to AcrB substrates, the expression of *ramA*, *marA* and *acrAB* and the accumulation and efflux of AcrB substrates.
- Purification of the RamR mutant and wild type protein.
- Electrophoretic mobility shift (EMSA) assay to determine the binding of the mutant and wild type RamR protein to the promoter region of *ramA*.

5.4 Phenotype of *S. Typhimurium* SL1344 and *E. coli* MG1655 and their respective chlorpromazine resistant mutants

5.5 Growth kinetics

The growth of wild type *S. Typhimurium* SL1344, wild type *E. coli* MG1655 and their respective chlorpromazine-resistant mutants was determined by measuring the optical density at OD₆₀₀ over 24 hours (Figure 5.1). The growth curve of the SL1344 RamR L158P mutant was similar to wild type SL1344 with no significant difference in the generation time. In contrast, the MG1655 MarR A105Rfs*114 and MarR K141Sfs*150 mutants grew faster

Figure 5.1: Growth curves and generation times of (A) *S. Typhimurium* SL1344, (B) *E. coli* MG1655 and their respective chlorpromazine-resistant mutants.



The Growth curves and generation times are shown as the mean of three biological replicates. Data was analysed by a Students T test compared to the wild type strains. Single asterisks denote a significant difference of $P < 0.05$.

(by around 0.5 minutes) compared to the wild type MG1655 as shown by significant differences in the generation times between the mutants and the wild type ($P = 0.0003$ and $P = 0.0006$, respectively).

5.6 Antimicrobial susceptibility

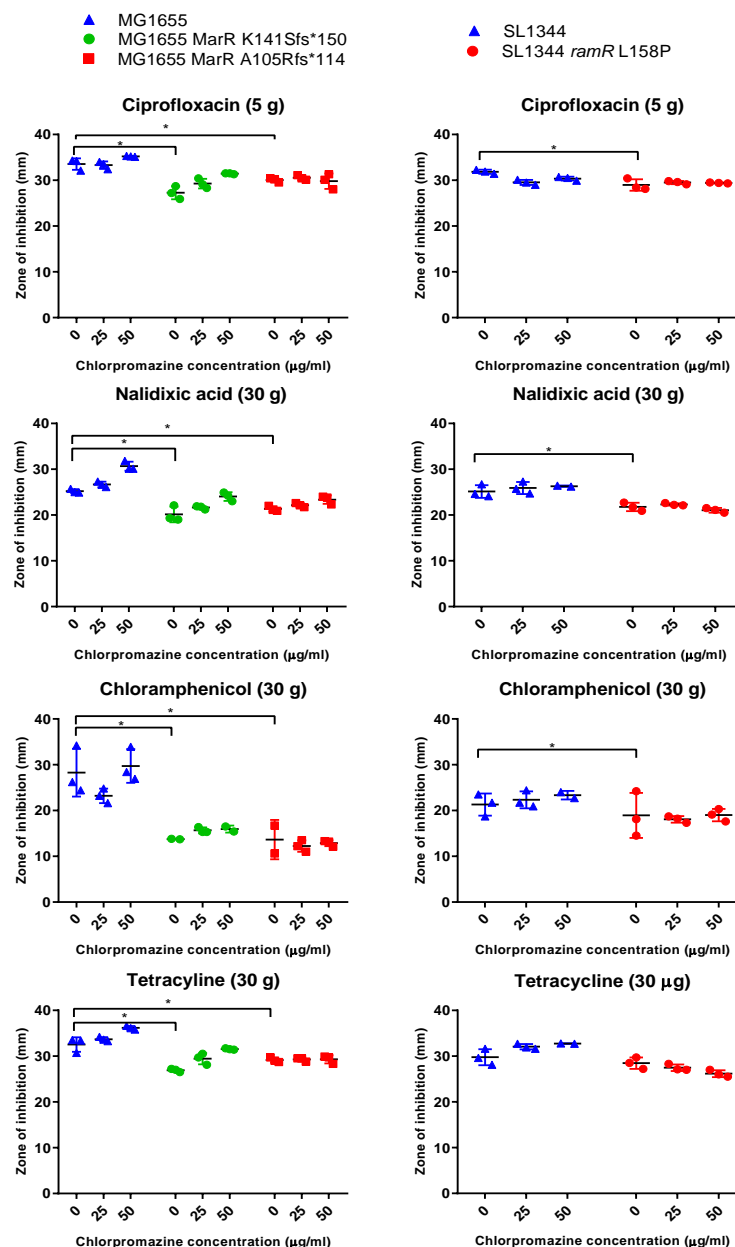
Disk diffusion assays confirmed that SL1344 RamR L158P, MG1655 MarR A105Rfs*114 and MG1655 MarR K141Sfs*150 were less susceptible to four AcrB substrates (nalidixic acid, chloramphenicol, ciprofloxacin and tetracycline) than their respective wild type strains (Figure 5.2). In addition, chlorpromazine potentiated the activity of nalidixic acid, chloramphenicol, tetracycline and ciprofloxacin against wild type *E. coli* MG1655 and nalidixic acid, chloramphenicol and tetracycline against wild type *S. Typhimurium* SL1344. Chlorpromazine potentiated the activity of all tested antibiotics against *E. coli* MG1655 MarR K141Sfs*150 and of nalidixic acid and ciprofloxacin against MG1655 MarR K105Rfs*114. In contrast, the presence of the substitution L158P in RamR of *S. Typhimurium* ablated the ability of chlorpromazine to potentiate antibiotic activity. In fact, chlorpromazine further increased the susceptibility of *S. Typhimurium* RamR L158P to tetracycline and nalidixic acid.

5.7 Construction of *E. coli* MG1655 *marR::aph*

Throughout this chapter, SL1344 RamR L158P, MG1655 MarR A105Rfs*114 and MG1655 MarR K141Sfs*150 were compared to strains in which *ramR* or *marR* were inactivated (*E. coli* MG1655 *marR::aph* and *S. Typhimurium* SL1344 *ramR::aph*).

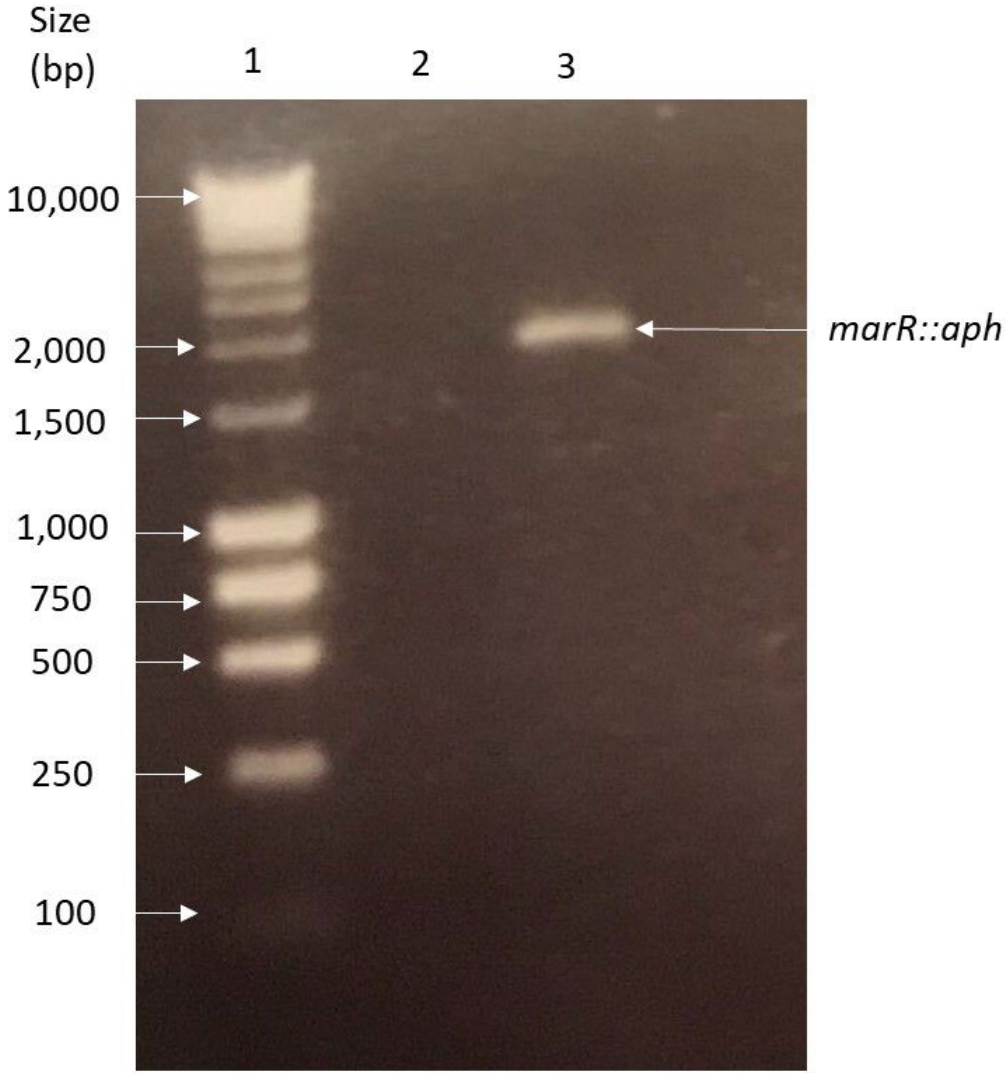
In order to construct *E. coli* MG1655 *marR::aph*, *marR::aph* was amplified from *E. coli* BW25113 *marR::aph* (Figure 5.3) and electroporated into wild type *E. coli* MG1655 carrying pSLTS. Three mutant candidates were selected on LB agar containing kanamycin at 50 µg/ml. These three colonies were incubated overnight at 37°C to ‘cure’ pSLTS and

Figure 5.2: Comparison of the zones of inhibition obtained against *S. Typhimurium* SL1344, *E. coli* MG1655 and their respective chlorpromazine-resistant mutants using antibiotic-containing disks.



The graph shows the mean and standard deviation of three biological replicates. Each biological replicate was calculated from the mean of three technical replicates. Data were analysed by a Two-way ANOVA. Single asterisks denote a significant difference of $P < 0.05$ in comparison to the untreated control.

Figure 5.3: PCR amplification of *marR::aph* from *E. coli marR::aph* BW25113.



Lane	Sample	Primer pair	Size (bp)
1	Nippon genetics 1kb ladder plus		
2	Contamination control	2384 + 2385	
3	<i>marR::aph</i> from <i>E. coli</i> BW25113	2384 + 2385	1,736

each was restreaked onto LB agar containing kanamycin (50 µg/ml) and LB agar containing ampicillin (50 µg/ml). No growth on LB ampicillin confirmed the loss of pSLTS.

To confirm the successful construction of *E. coli* MG1655 *marR::aph*, *marR* was amplified from all three candidates and wild type *E. coli* MG1655 using check primers that bind up and downstream of the gene of interest (Figure 5.4). Amplimers of 1,736 bp and 793 bp were produced for one candidate and for the wild type *marR*, respectively confirming insertion of the kanamycin resistance marker. DNA sequencing of the purified candidate amplimer confirmed the introduction of the kanamycin cassette.

5.8 Effect of mutations within *ramR* and *marR* on the expression of *acrAB* and its regulatory genes

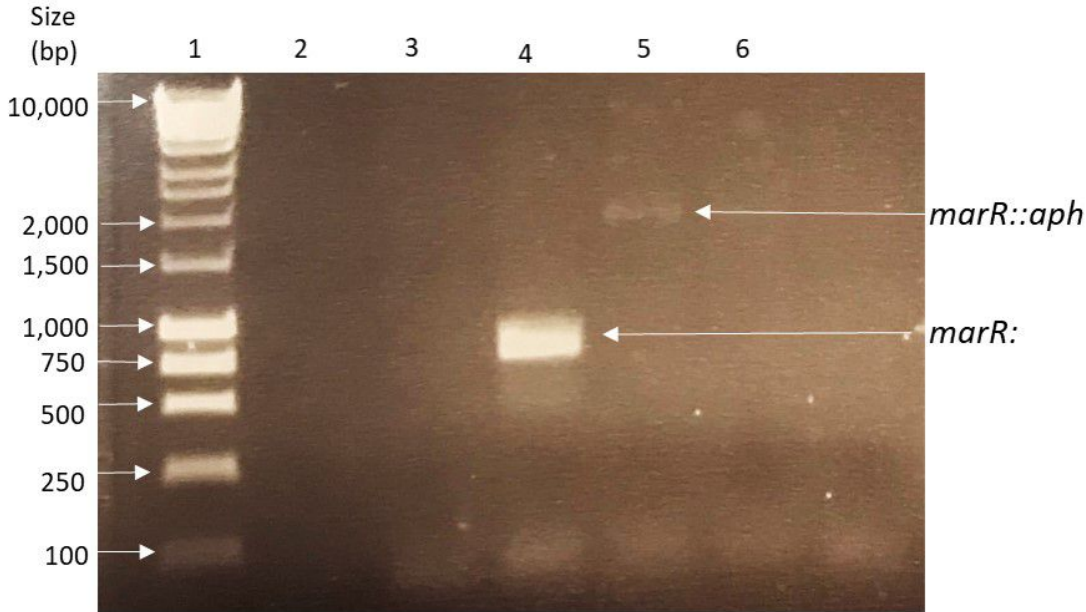
It was hypothesised that mutations within the genes encoding RamR and MarR would result in overexpression of *ramA* and *marA*, respectively. Each accompanied by overexpression of *acrAB* and increased efflux of AcrB substrates from *E. coli* MG1655 and *S. Typhimurium* SL1344.

To determine whether the chlorpromazine-resistant mutants SL1344 RamR L158P, MG1655 MarR A105Rfs*114 and MG1655 MarR K141Sfs*150 cause overexpression of efflux pump and efflux regulatory genes, promoter-GFP constructs containing the promoter regions of *ramA*, *marA* or *acrAB* were used to determine the activity of the *ramA*, *marA* and *acrAB* promoters in the wild type and mutants strains.

5.8.1 Transformation of promoter-GFP constructs into the *S. Typhimurium* and *E. coli* mutants.

The pMW82-*pramA* and pMW82-*pacrAB* plasmids were isolated from wild type *S. Typhimurium* SL1344 and electroporated into SL1344 RamR L158P and SL1344 *ramR::aph*. Colonies of each electroporation on LB agar containing 50 µg/ml of ampicillin and no growth

Figure 5.4: PCR amplification of *marR* from *E. coli* MG1655 and the three *marR::aph* mutant candidates



Lane	Sample	Primer pair	Size (bp)
1	Nippon genetics 1kb ladder plus		
2	Contamination control	1528 + 1529	
3	Contamination control	2384 + 2385	
4	<i>marR</i> from <i>E. coli</i> MG1655 wild type	1528 + 1529	793
5	<i>marR::aph</i> from candidate 1	2384 + 2385	1,736
6	<i>marR::aph</i> from candidate 2	2384 + 2385	1,736
7	<i>marR::aph</i> from candidate 3	2384 + 2385	1,736

of a negative control with no plasmid confirmed the successful transformation of pMW82-*pramA* and pMW82-*pacrAB* into SL1344 RamR L158P and SL1344 *ramR::aph*.

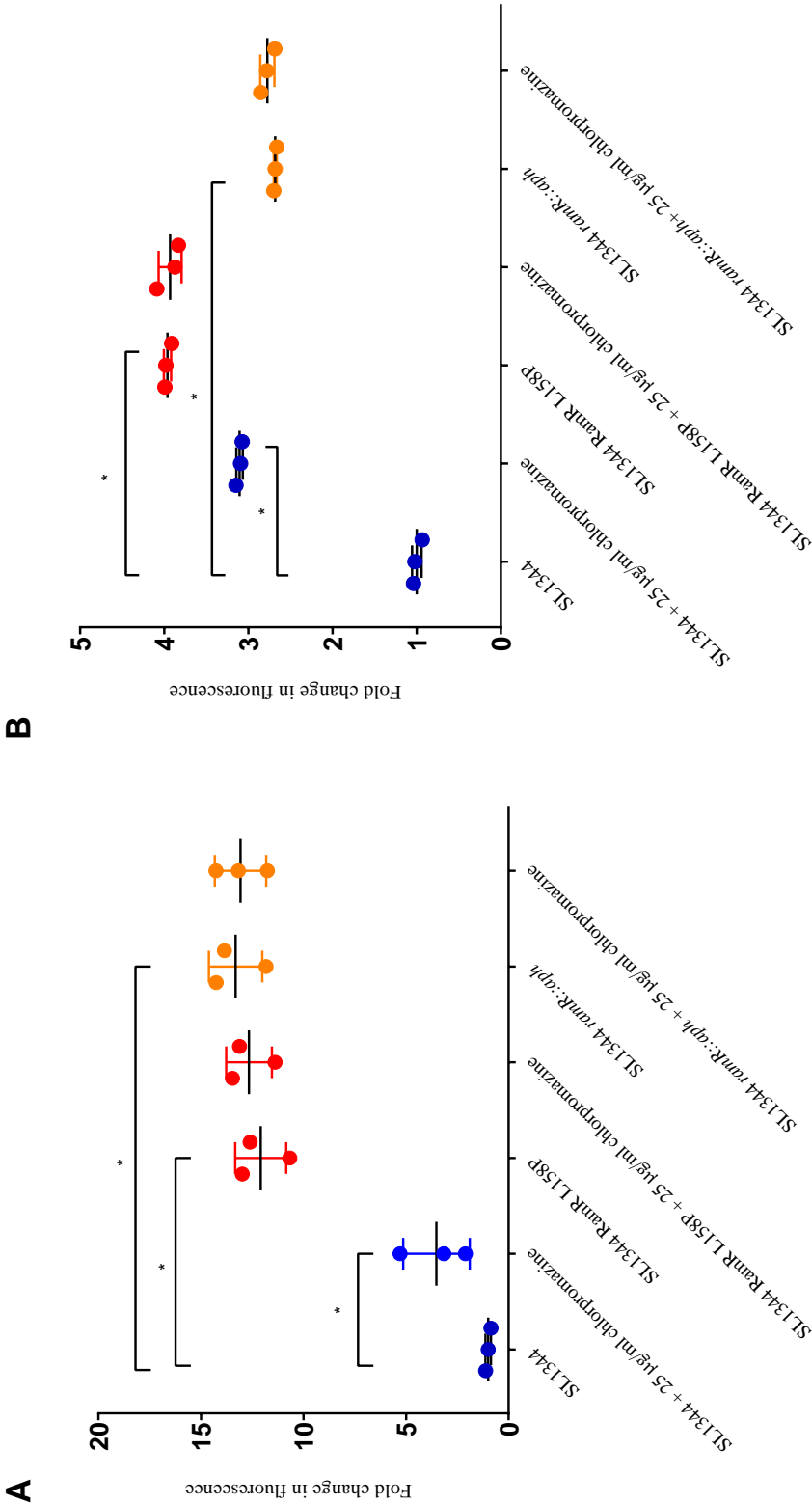
pMW82-*pmarA* and pMW82-*pacrAB* plasmids were isolated from wild type *E. coli* and electroporated into MG1655 MarR A105Rfs*114, MG1655 MarR K141Sfs*150 and MG1655 *marR::aph*. Colonies of each electroporation on LB agar containing 50 µg/ml of ampicillin and no growth of a negative control with no plasmid confirmed successful transformation of pMW82-*pmarA* and pMW82-*pacrAB* into MG1655 MarR A105Rfs*114, MG1655 MarR K141Sfs*150 and MG1655 *marR::aph*.

5.8.2 The substitution L158P in RamR of *S. Typhimurium* increased the basal expression of *ramA* and *acrAB*

Previous evidence has shown that exposure to chlorpromazine results in the induction of *ramA* and *acrAB* in *S. Typhimurium* (Lawler et al., 2013). In comparison to that in wild type SL1344, in the absence of chlorpromazine, the expression of *ramA* was significantly higher in SL1344 *ramR::aph* ($P = <0.0001$) and SL1344 RamR L158P ($P = 0.0001$); with observed fold increases of 13.31 and 11.89, respectively. Chlorpromazine increased the expression of *ramA* in wild type *S. Typhimurium* SL1344 by 3.52 fold (Figure 5.5). In contrast, the addition of chlorpromazine to SL1344 *ramR::aph* and SL1344 RamR L158P did not further increase *ramA* expression.

In comparison to wild type SL1344, the expression of *acrAB* was significantly higher in SL1344 *ramR::aph* ($P = <0.0001$) and SL1344 RamR L158P ($P = <0.0001$). Surprisingly, the increase in *acrAB* expression in SL1344 RamR L158P, relative to wild type SL1344 was higher (3.96 fold) than that observed in SL1344 *ramR::aph* (2.68 fold). Chlorpromazine increased the expression of *acrAB* from wild type *S. Typhimurium* SL1344 by 3.10 fold ($P = <0.0001$) (Figure 5.5). Like *ramA* expression, the addition of chlorpromazine to SL1344 *ramR::aph* and SL1344 RamR L158P did not further increase the expression of *acrAB*.

Figure 5.5: Effect of the RamR L158P substitution on (A) *ramA* and (B) *acrAB* expression compared to wild type *S.* Typhimurium SL1344 and SL1344 *ramR::aph* in the presence and absence of 25 µg/ml of chlorpromazine.



The graph shows the mean and standard deviation of three biological replicates. Each biological replicate was calculated from the mean of three technical replicates. Data were analysed by a T-test with Welch's correction. Single asterisks denote a significant difference of $P < 0.05$ in comparison to the untreated control

5.8.3 Deletions within MarR of *E. coli* MG1655 increase the basal expression of *marA* and *acrAB*

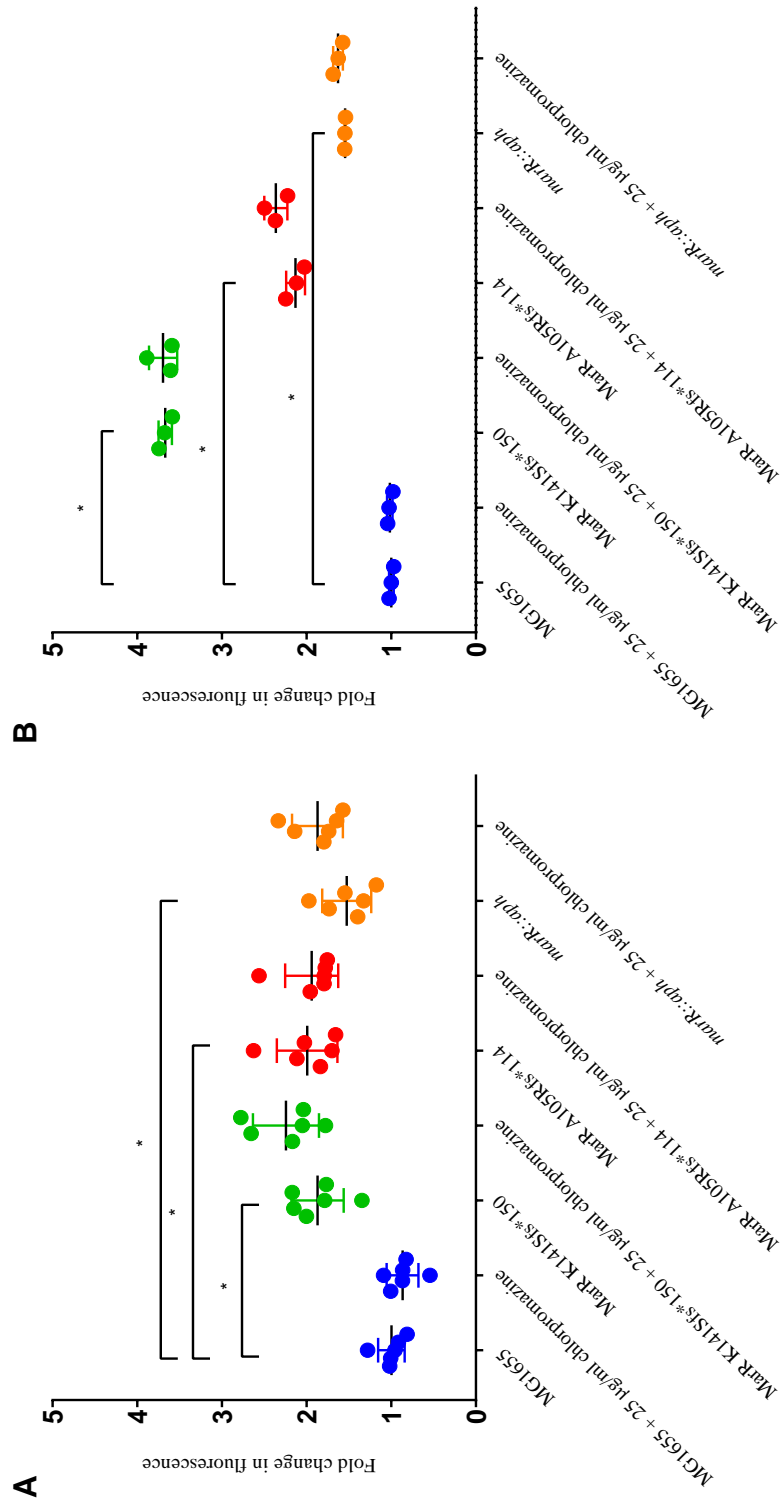
In comparison to wild type MG1655, in the absence of chlorpromazine, the expression of *marA* was significantly higher in MG1655 MarR A105Rfs*114 ($P = <0.0001$), MG1655 MarR K141Sfs*150 ($P = 0.0001$) and MG1655 *marR::aph* ($P = 0.0028$) (Figure 5.6); with observed fold increases of 1.98, 1.87 and 1.52, respectively.

In comparison to wild type MG1655, the expression of *acrAB* was significantly higher ($P = <0.0001$) in MG1655 MarR A105Rfs*114, MG1655 MarR K141Sfs*150 and MG1655 *marR::aph* with fold increases of 2.13, 3.67 and 1.55 (Figure 5.6). Like *S. Typhimurium*, the chlorpromazine-resistant mutants had a greater increase in the expression of *acrAB* than did MG1655 *marR::aph*, relative to wild type MG1655. Interestingly, although the expression of *acrAB* was increased in MG1655 MarR A105Rfs*114 and MG1655 *marR::aph* by a fold change similar to the increase in *marA* expression, MG1655 MarR K141Sfs*150 showed a greater increase in the expression of *acrAB* (3.67 fold) compared to the increase in *marA* (1.87 fold). Chlorpromazine (25 µg/ml) did not induce *marA* or *acrAB* in any background (Figure 5.6)

5.8.4 Exposure of *S. Typhimurium* to chlorpromazine increases the expression of *acrB*

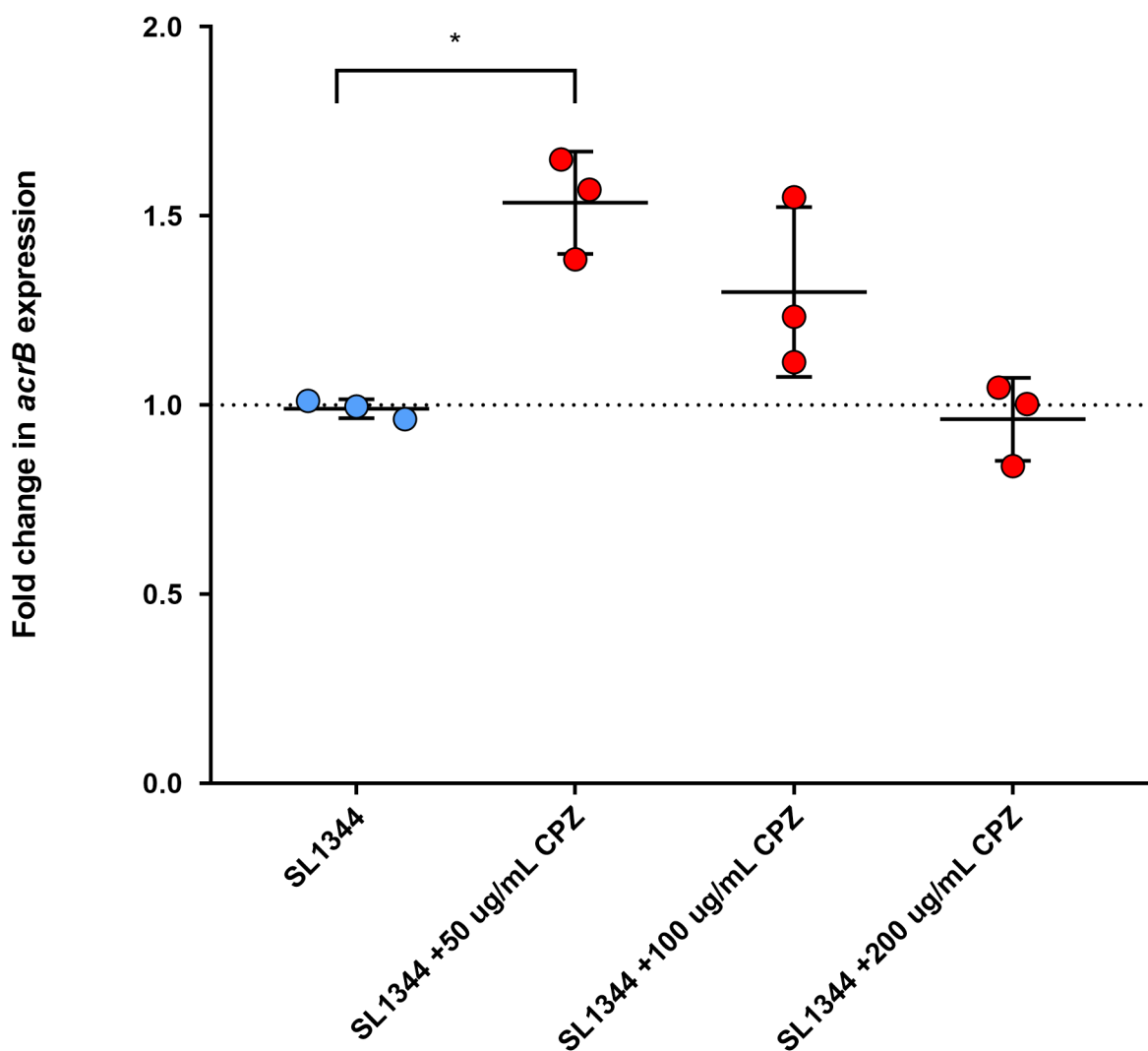
Previously, Bailey et al., 2008 reported that upon exposure to 200 µg/ml of chlorpromazine the expression of *acrB* was repressed by 40% in relation to the unexposed wild type, despite an increase in the expression of the transcriptional activator *ramA*. In contrast, here, reporting assays with *S. Typhimurium* SL1344 post exposure to 50 µg/ml of chlorpromazine revealed an increase in the expression of *acrB*. To confirm this, reverse transcription PCRs (RT-PCRs) were performed with *acrB* of SL1344 post exposure to

Figure 5.6: Effect of deletions within MarR on (A) *marA* and (B) *acrAB* expression compared to wild type *E. coli* MG1655 and MG1655 *marR::aph* in the presence and absence of 25 µg/ml of chlorpromazine.



The lower fluorescence values of the *E. coli* GFP-reporter constructs resulted in greater variability. The graph shows the mean and standard deviation of six biological replicates. Each biological replicate was calculated from the mean of three technical replicates. Data were analysed by a T-test with Welch's correction. Single asterisks denote a significant difference of $P < 0.05$ in comparison to the untreated control

Figure 5.7: Fold change in normalised *acrB* expression in SL1344 +/- chlorpromazine at 50, 100 and 200 µg/mL.



The graph shows the mean and standard deviation of three biological replicates. Each biological replicate was calculated from the mean of three technical replicates. Data were analysed by a Student's *t* test with Welch's correction. Asterisks denote a significant difference of $P < 0.05$ in comparison to the untreated control.

increasing concentrations of chlorpromazine (Figure 5.7). These RT-PCRs revealed that, in support of previous data, the expression of *acrB* was reduced in the presence of 200 µg/ml of chlorpromazine. However, this reduction did not reach statistical significance. At 50 µg/ml and 100 µg/ml (concentrations at which efflux inhibition is observed) an increase in the expression of *acrB* by 1.54-fold (54 %) and 1.30-fold (30 %) was observed, confirming the GFP reporting assays that suggested chlorpromazine increases the expression of *acrB* at efflux inhibitory concentrations.

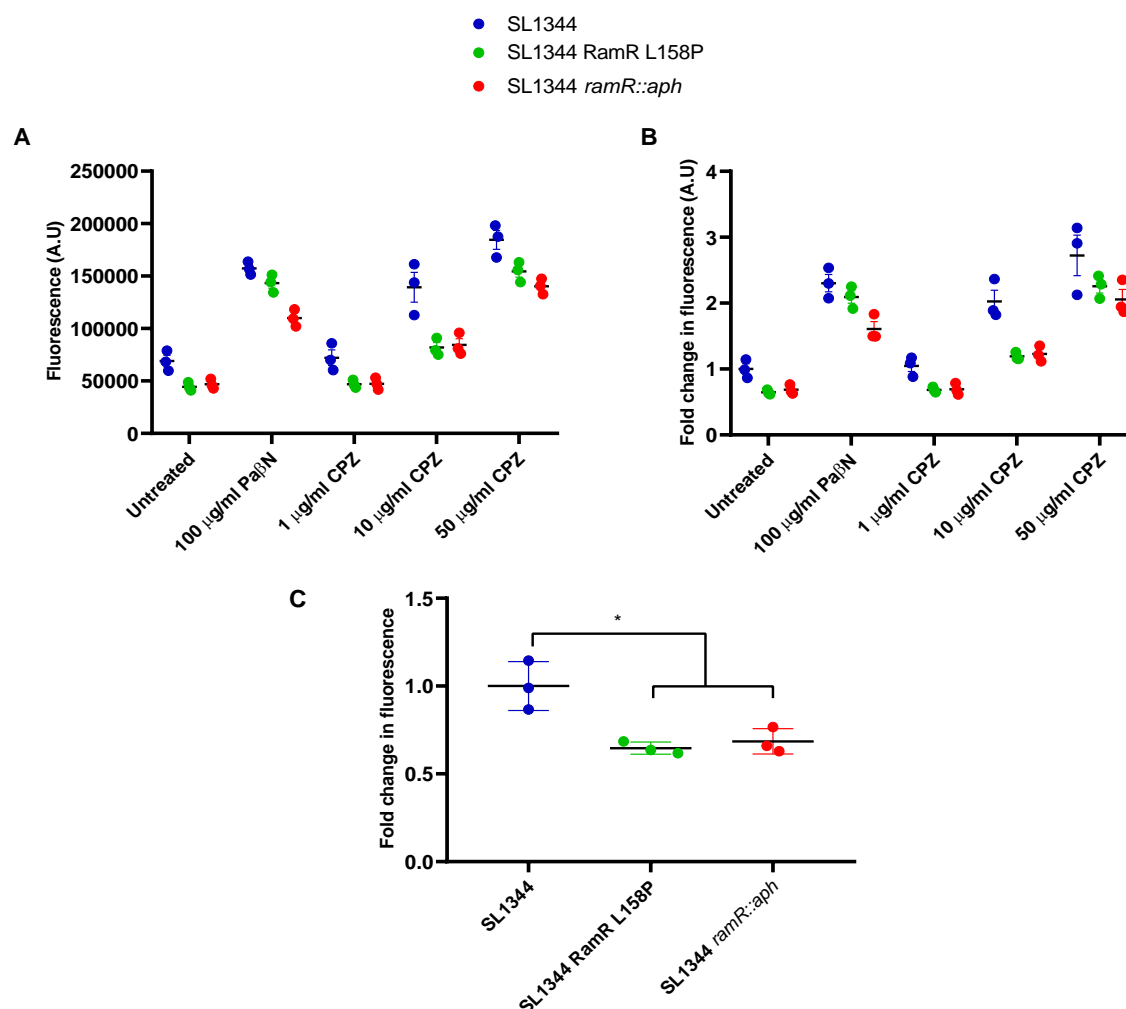
5.9 Impact of mutations within *ramR* and *marR* on the intracellular accumulation of AcrB substrates

The increase in the expression of *ramA*, *marA* and *acrAB* resulting from mutations within *ramR* and *marR* was hypothesised to confer an increase in the efflux of AcrB substrates by SL1344 and MG1655 compared to the wild type parental strains. Here, H33342 accumulation and ethidium bromide efflux assays were used to infer the level of efflux in wild type and mutant SL1344 and MG1655 in the presence and absence of chlorpromazine and PaβN. It should be noted that a higher level of efflux results in less substrate accumulation.

5.9.1 A substitution within RamR results in a decrease in the intracellular accumulation of Hoechst H33342

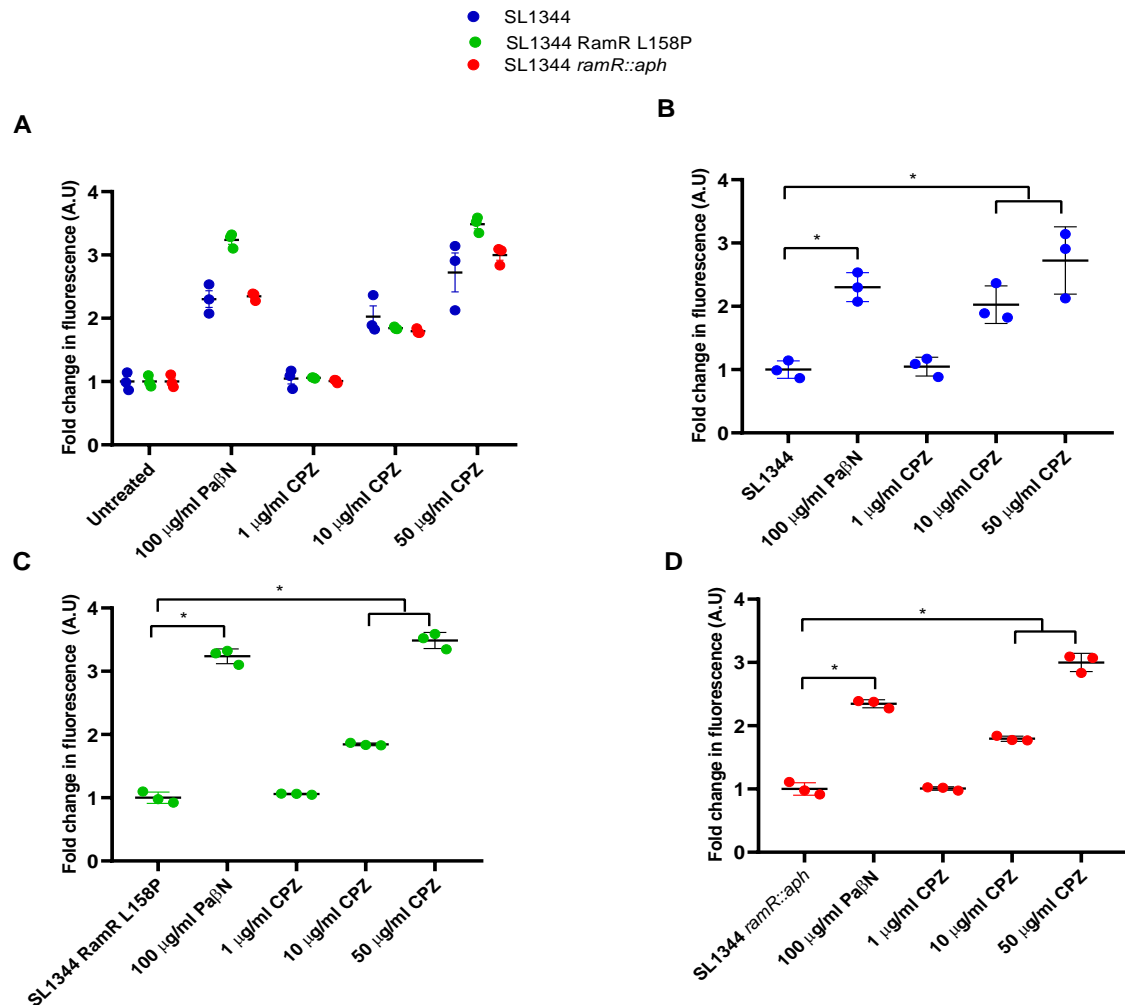
SL1344 RamR L158P ($P = 0.0130$) and SL1344 *ramR::aph* ($P = 0.0254$) accumulated significantly less H33342 compared to wild type SL1344 (Figure 5.8 and 5.9). Chlorpromazine (10 and 50 µg/ml) and PaβN increased the accumulation of H33342 from both wild type SL1344 and the mutant strains. These data suggest the activity of chlorpromazine is not ablated against the SL1344 RamR mutants (Figure 5.8 and 5.9). In terms of fold change, relative to the basal efflux of each respective strain in the absence of inhibitor, chlorpromazine at 10 µg/ml increased the accumulation of H33342 from SL1344, SL1344 RamR L158P and

Figure 5.8: Accumulation of Hoechst H33342 within *S. Typhimurium* SL1344 RamR WT, RamR L158P and *ramR::aph* in the presence and absence of chlorpromazine, relative to unexposed wild type SL1344.



The graph shows the mean and standard deviation of three biological replicates. Each biological replicate was calculated from the mean of three technical replicates. Accumulation of Hoescht H33342 shown as raw fluorescence values (A) and fold change (B). Comparison of the basal accumulation of Hoechst in fold change with respect to wild type SL1344 (C). Data were analysed by a Student's t test with Welch's correction. Single asterisks denote a significant difference of $P < 0.05$ in comparison to the untreated control. Chlorpromazine; CPZ. Phe-arg beta naphthylamide; PaβN.

Figure 5.9: Accumulation of Hoechst H33342 within *S. Typhimurium* SL1344 RamR WT, RamR L158P and *ramR::aph* in the presence and absence of chlorpromazine, relative to the unexposed wild type of each respective strain.



The graph shows the mean and standard deviation of three biological replicates. Each biological replicate was calculated from the mean of three technical replicates. Comparison of Hoechst H33342 accumulation shown as a fold change relative to each respective untreated strain (A). Accumulation of Hoescht in the presence of chlorpromazine in SL1344 wild type (B), SL1344 RamR L158P (C) and SL1344 *ramR::aph* (D) shown as fold change with respect to wild type SL1344. Data were analysed by a Student's t test with Welch's correction. Single asterisks denote a significant difference of $P < 0.05$ in comparison to the untreated control. Chlorpromazine; CPZ. Phe-arg beta naphthylamide; Pa β N.

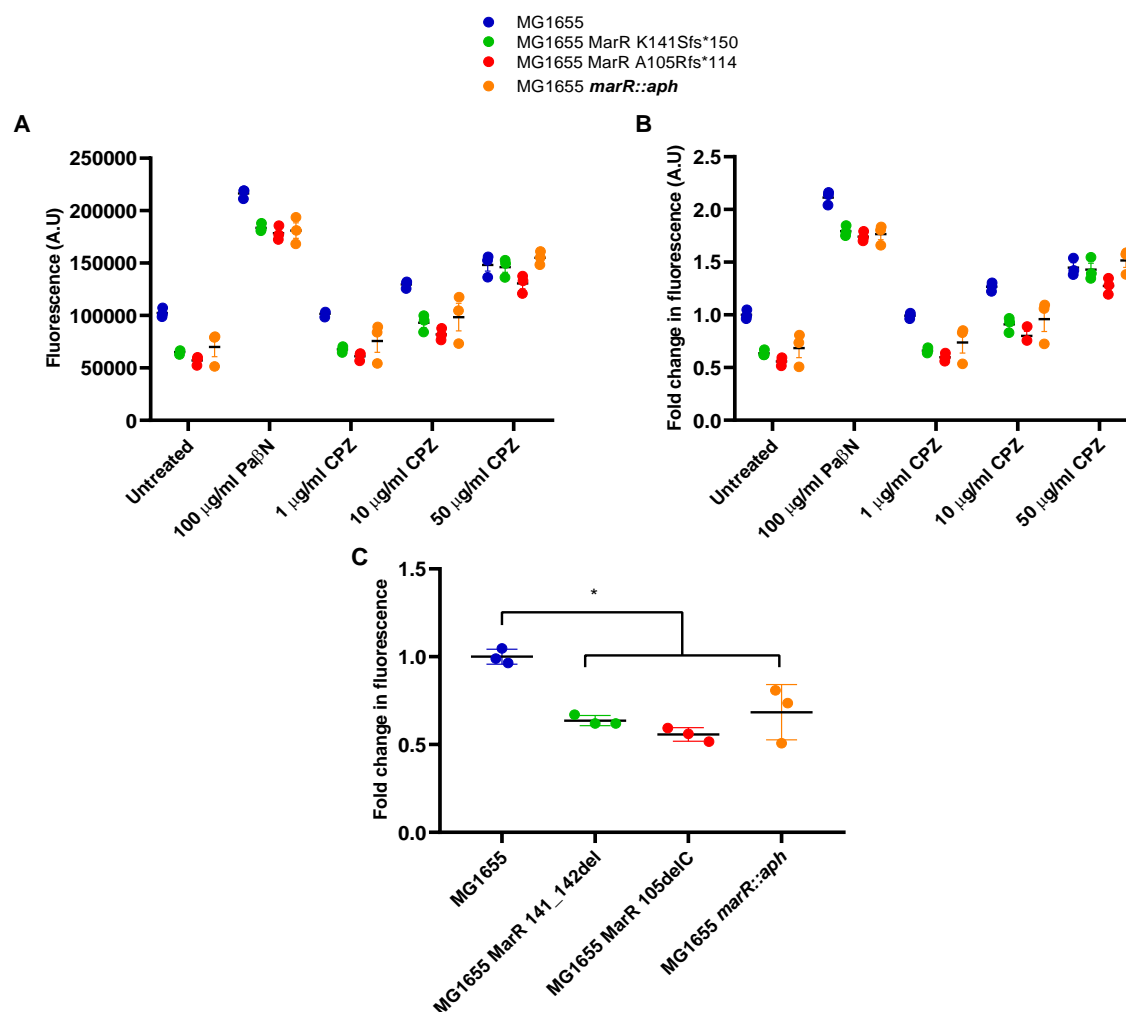
SL1344 *ramR::aph* to a similar extent (~ 2 fold). However, chlorpromazine, at 50 $\mu\text{g/ml}$, increased the accumulation by SL1344 RamR L158P to a greater extent (3.48 fold) than wild type SL1344 (2.72 fold) and SL1344 *ramR::aph* (2.99 fold) (Figure 5.9). This discrepancy in efflux inhibition between strains was also noted with Pa β N. However, this increased efflux inhibitory activity of chlorpromazine (at 50 $\mu\text{g/ml}$) and Pa β N against SL1344 RamR L158P was not observed when comparing the raw fluorescence values (Figure 5.8). This discrepancy is due to SL1344 RamR L158P having a lower basal value of accumulation of H33342, due to increased efflux, than wild type SL1344 producing a higher fold change difference. Nonetheless, the accumulation of H33342 by SL1344 *ramR::aph* was increased by chlorpromazine and Pa β N to a lower extent than SL1344 RamR L158P despite their similar uninduced basal values (Figure 5.8).

5.9.2 Deletions within MarR result in a decrease in the intracellular accumulation of Hoechst H33342

Like *S. Typhimurium*, it was hypothesised that the increase in the expression of *marA* and *acrAB* resulting from deletions within MarR would confer an increase in the efflux capability of the mutant strains MG1655 MarR A105Rfs*114 and MG1655 MarR K141Sfs*150 compared to wild type MG1655.

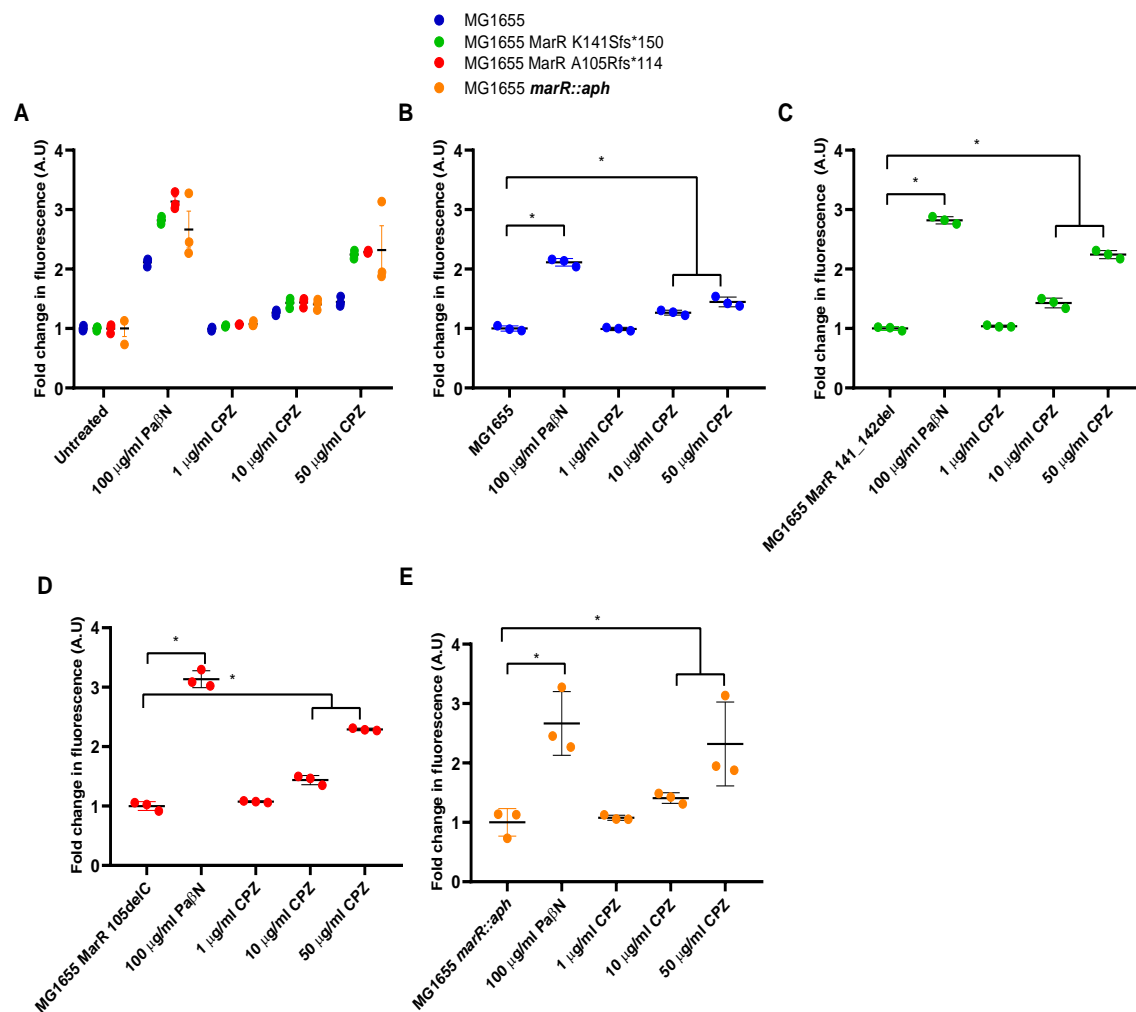
MG1655 MarR A105Rfs*114 ($P = 0.0002$), MG1655 MarR K141Sfs*150 ($P = 0.0003$) and MG1655 *marR::aph* ($P = 0.0284$) accumulated significantly less H33342 compared to wild type MG1655 (Figure 5.10). Like *S. Typhimurium*, chlorpromazine (10 and 50 $\mu\text{g/ml}$) and Pa β N inhibited the efflux of H33342 from both the wild type and the mutant strains (Figure 5.10 and 5.11). In terms of fold change, relative to the level of basal efflux in the absence of inhibitor for each respective strain, the degree to which efflux was inhibited by 10 $\mu\text{g/ml}$ of chlorpromazine was similar for wild type MG1655 and the MarR mutants (Figure 5.11). However, the efflux of H33342 was inhibited to a greater extent at 50 $\mu\text{g/ml}$ of

Figure 5.10: Accumulation of Hoechst H33342 within *E. coli* MG1655 MarR and the mutants MarR K141Sfs*150, MarR A105Rfs*114 and *marR::aph* in the presence and absence of chlorpromazine, relative to unexposed wild type MG1655.



The graph shows the mean and standard deviation of three biological replicates. Each biological replicate was calculated from the mean of three technical replicates. Accumulation of Hoescht H33342 in the presence and absence of chlorpromazine shown as raw fluorescence values (A) and fold change (B). Comparison of the basal accumulation of Hoechst in fold change with respect to wild type MG1655 (C). Data were analysed by a Student's t test with Welch's correction. Single asterisks denote a significant difference of $P < 0.05$ in comparison to the untreated control. Chlorpromazine; CPZ. Phe-arg beta naphthylamide; PaβN.

Figure 5.11: Accumulation of Hoechst H33342 within *E. coli* MG1655 MarR and the mutants MarR K141Sfs*150, MarR A105Rfs*114 and *marR::aph* in the presence and absence of chlorpromazine, relative to the unexposed wild type of each respective strain.



The graph shows the mean and standard deviation of three biological replicates. Each biological replicate was calculated from the mean of three technical replicates. Comparison of Hoechst H33342 accumulation shown as a fold change relative to each respective untreated strain (A). Accumulation of Hoescht in the presence of chlorpromazine in *E. coli* MG1655 wild type (B), MG1655 MarR K141Sfs*150 (C), MG1655 MarR A105Rfs*114 (D) and *marR::aph* (E) shown as fold change with respect to wild type MG1655. Data were analysed by a Student's t test with Welch's correction. Single asterisks denote a significant difference of $P < 0.05$ in comparison to the untreated control. Chlorpromazine; CPZ. Phe-arg beta naphthylamide; PaβN.

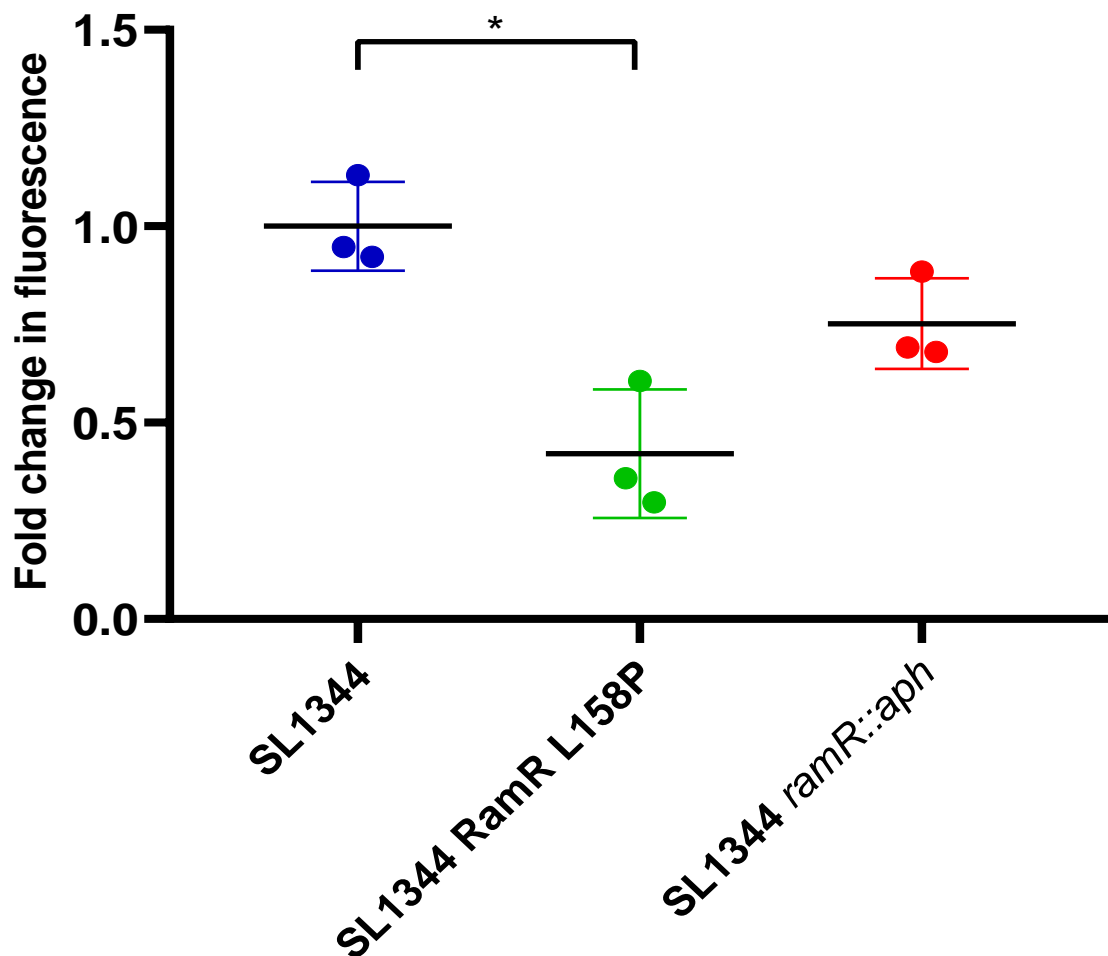
chlorpromazine and 100 µg/ml of PaβN against MG1655 MarR A105Rfs*114 (2.29 and 3.13 fold, respectively) and MarR K141Sfs*150 (2.23 and 2.81 fold, respectively) compared to the amount of efflux inhibition observed at the same concentrations of chlorpromazine and PaβN against wild type MG1655 (1.44 and 2.11 fold, respectively) (Figure 5.10). Although chlorpromazine and PaβN appear to inhibit the efflux of H33342 from the MarR mutants to a greater extent than wild type MG1655, the accumulation of H33342 in the mutants in terms of raw values does not exceed that for wild type MG1655 (Figure 5.10). At 50 µg/ml of chlorpromazine a plateau was reached where the level of H33342 accumulation was similar for each strain indicating there is a maximal level of efflux inhibition for chlorpromazine against MG1655.

5.9.3 Mutations within *ramR* but not *marR* result in a decrease in the intracellular accumulation of ethidium bromide from *S. Typhimurium* and *E. coli*

In addition to H33342, SL1344 RamR L158P ($P = 0.0420$) accumulated significantly less ethidium bromide compared to wild type SL1344 (Figure 5.12). Unlike H33342, the reduction in the accumulation of ethidium bromide was greater for SL1344 RamR L158P compared to SL1344 *ramR::aph*.

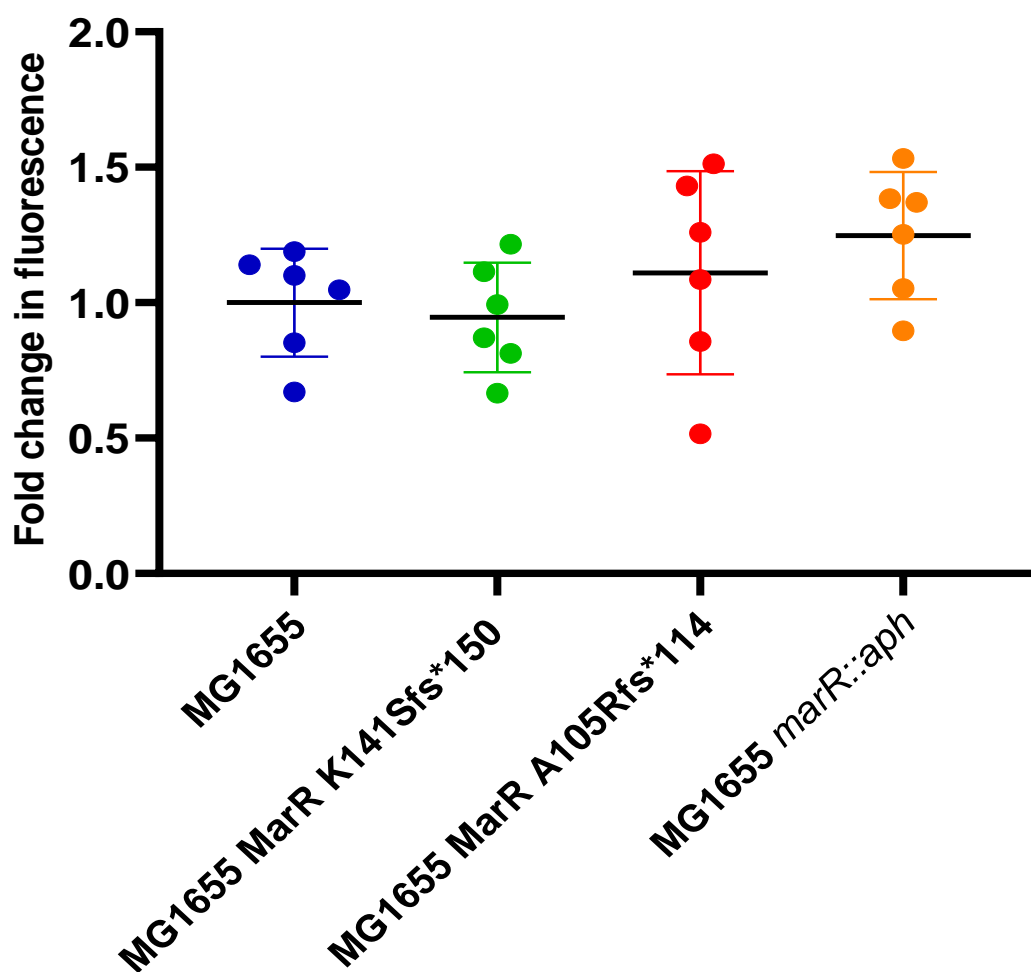
In contrast, the accumulation of ethidium bromide was not significantly altered in MarR K141Sfs*150, MarR A105Rfs*114 and *marR::aph*, compared to wild type MG1655 (Figure 5.13). There was a slight increase in ethidium bromide accumulation in MarR A105Rfs*114 and *marR::aph* and a decrease in MarR K141Sfs*150 compared to wild type MG1655. However, this was not statistically significant and the reliability of this cannot be assessed due to large variability in the data from the ethidium bromide efflux assay in *E. coli*.

Figure 5.12: Accumulation of ethidium bromide within *S. Typhimurium* SL1344 RamR WT, RamR L158P and *ramR::aph* in the presence and absence of chlorpromazine.



The graph shows the mean and standard deviation of three biological replicates. Each biological replicate was calculated from the mean of three technical replicates. Comparison of the basal accumulation of ethidium bromide in fold change with respect to wild type SL1344 Data were analysed by a Student's t test with Welch's correction. Single asterisks denote a significant difference of $P < 0.05$ in comparison to the untreated control.

Figure 5.13: Accumulation of ethidium bromide within *E. coli* MG1655 MarR and the mutants MarR K141Sfs*150, MarR A105Rfs*114 and *marR::aph* in the presence and absence of chlorpromazine



The graph shows the mean and standard deviation of three biological replicates. Each biological replicate was calculated from the mean of three technical replicates. Comparison of the basal accumulation of ethidium bromide in fold change with respect to wild type MG1655. Data were analysed by a Student's t test with Welch's correction. Single asterisks denote a significant difference of $P < 0.05$ in comparison to the untreated control.

5.10 Do mutations within *ramR* and *marR* impact on the ability of chlorpromazine to damage the outer and inner membrane of *S. Typhimurium* SL1344 and *E. coli* MG1655?

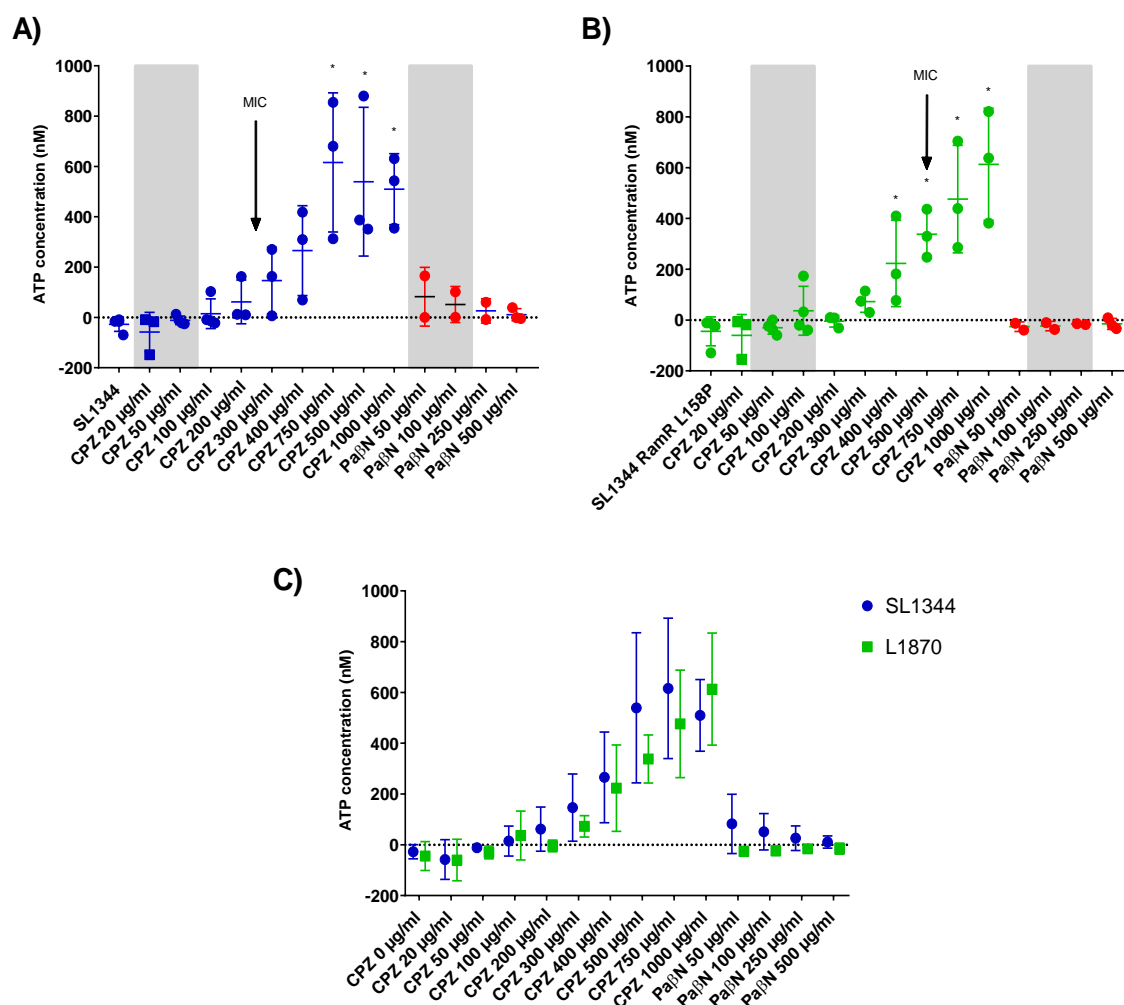
To determine whether mutation of *ramR* and *marR* impacted on the ability of chlorpromazine to elicit its antibacterial activity through membrane damage, the ability of chlorpromazine to permeabilise the OM and depolarise the IM was determined.

5.10.1 The presence of mutations within *ramR* and *marR* impair the ability of chlorpromazine to permeabilise the outer membrane of *S. Typhimurium* SL1344 and *E. coli* MG1655

Like wild type *S. Typhimurium* SL1344 and *E. coli* MG1655, analysis of the concentration of ATP in the extracellular medium, upon exposure to chlorpromazine for one hour revealed OM damage to each of the chlorpromazine-resistant *marR* and *ramR* mutants (Figure 5.14 and 5.15). Consistent with the wild type strains, this was dependent on the concentration of chlorpromazine. Exposure of the bacteria to efflux inhibitory concentrations ($\leq 100 \mu\text{g/ml}$) resulted in low ($< 100 \text{ nM}$) concentrations of ATP present in the extracellular medium of the *S. Typhimurium* and *E. coli* mutants. At increasing concentrations of chlorpromazine the amount of ATP in the extracellular medium increased.

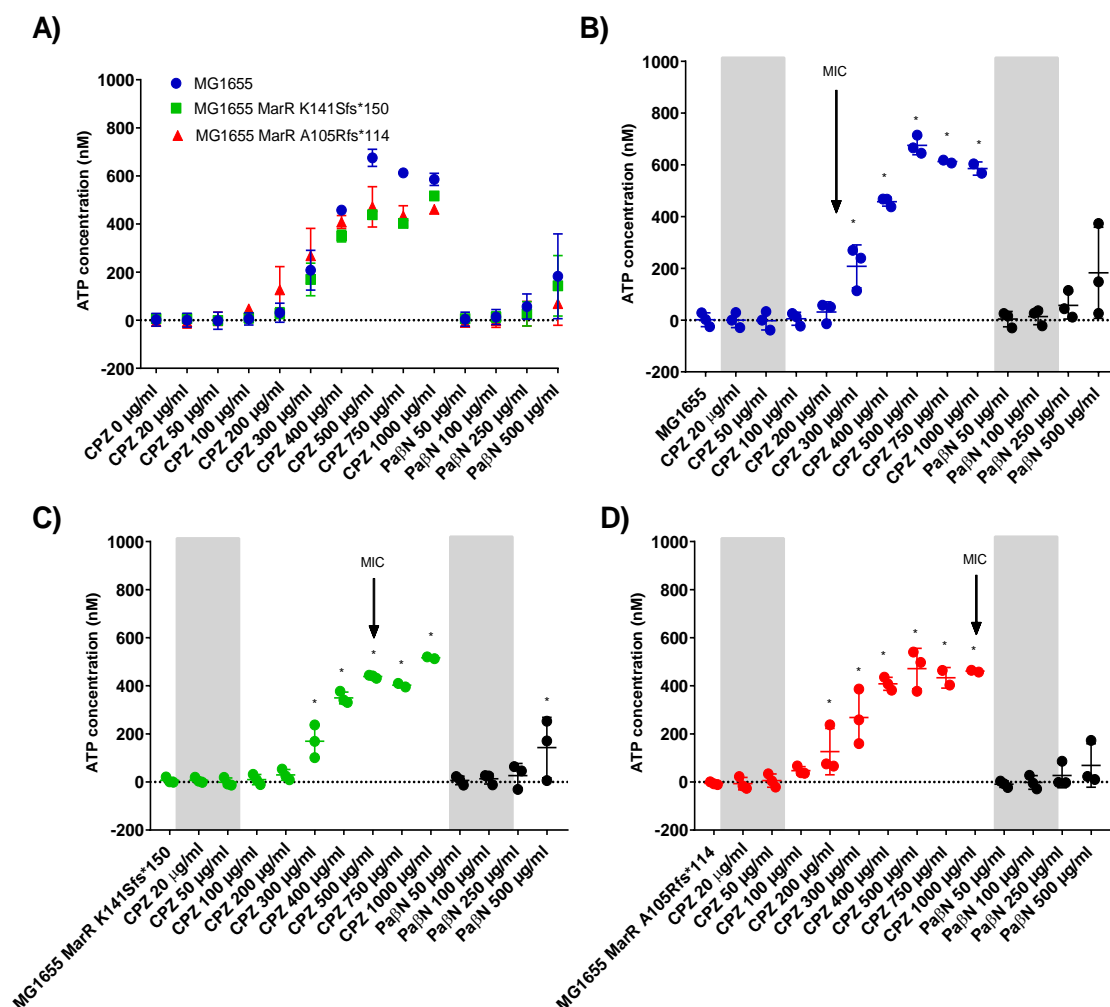
For SL1344 RamR L158P, MG1655 MarR K141Sfs*150 and MG1655 MarR A105Rfs*114 the concentration of ATP in the extracellular medium was lower, at a given concentration, when compared to the respective wild type strains (Figure 5.14 and 5.15). This is likely representative of the higher MIC values of the *ramR* and *marR* mutant strains compared to wild type SL1344 and MG1655.

Figure 5.14: ATP leakage from *S. Typhimurium* SL1344 wild type and RamR L158P upon exposure to increasing concentrations of chlorpromazine.



The graph shows the mean and standard deviation of three biological replicates. Each biological replicate was calculated from the mean of three technical replicates. (A) *S. Typhimurium* SL1344 wild type and (B) SL1344 RamR L158P. (C) Comparison of *S. Typhimurium* SL1344 wild type and SL1344 RamR L158P. The concentrations of chlorpromazine at which efflux inhibition was observed is highlighted in grey. The MIC of chlorpromazine is displayed. Asterisks indicate a statistically significant difference ($P < 0.05$), calculated using a one-way ANOVA, in relation to the unexposed control. CPZ; Chlorpromazine, PaβN; Phe-arg beta naphthylamide

Figure 5.15: ATP leakage from *E. coli* MG1655, MarR K141Sfs*150 and MarR A105Rfs*114 upon exposure to increasing concentrations of chlorpromazine.

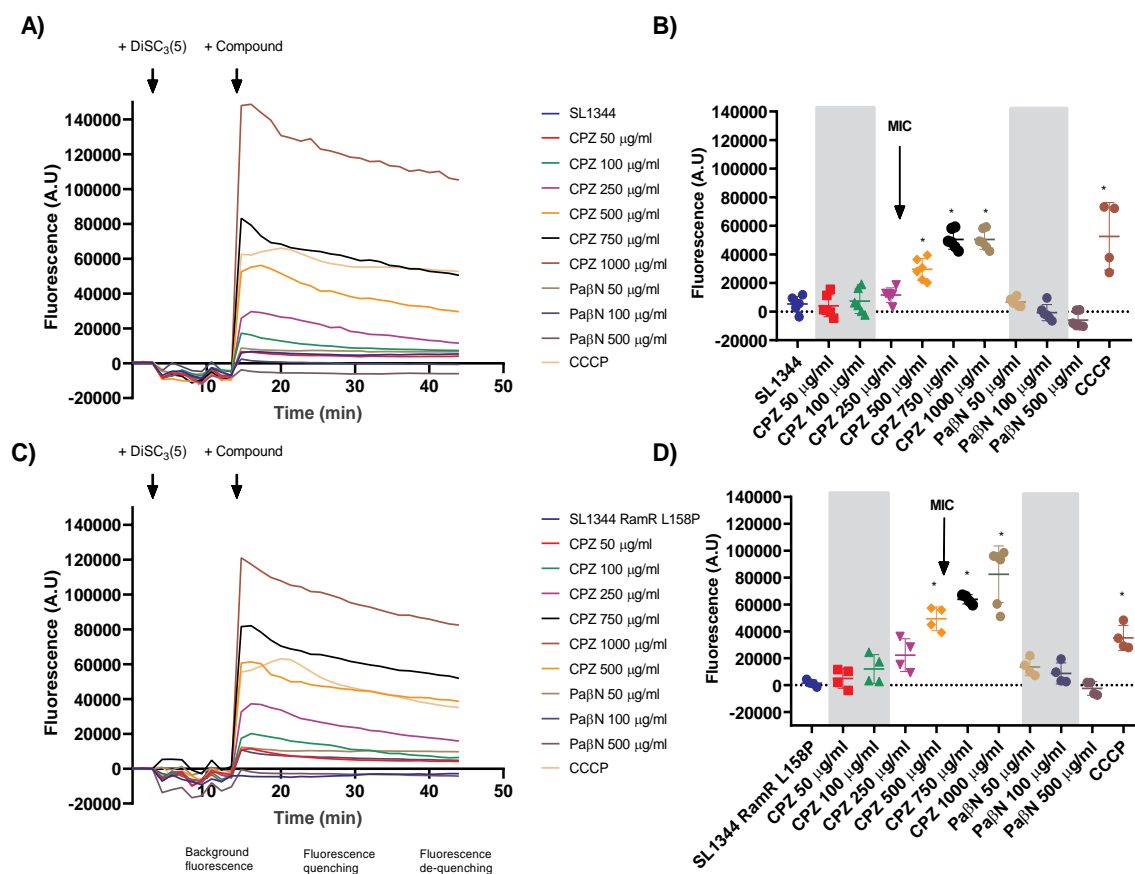


The graph shows the mean and standard deviation of three biological replicates. Each biological replicate was calculated from the mean of three technical replicates. (A) *E. coli* MG1655 wild type, (B) MG1655 MarR K141Sfs*150 and (C) MG1655 MarR A105Rfs*114. (D) Comparison of *E. coli* MG1655 wild type and the *E. coli* mutants. The concentrations of chlorpromazine at which efflux inhibition was observed is highlighted in grey. The MIC of chlorpromazine is displayed. Asterisks indicate a statistically significant difference ($P < 0.05$), calculated using a one-way ANOVA, in relation to the unexposed control. CPZ; Chlorpromazine, PaβN; Phe-arg beta naphthylamide.

5.10.2 The presence of mutations within *ramR* and *marR* impair the ability of chlorpromazine to depolarise the inner membrane of *S. Typhimurium* SL1344 and *E. coli* MG1655

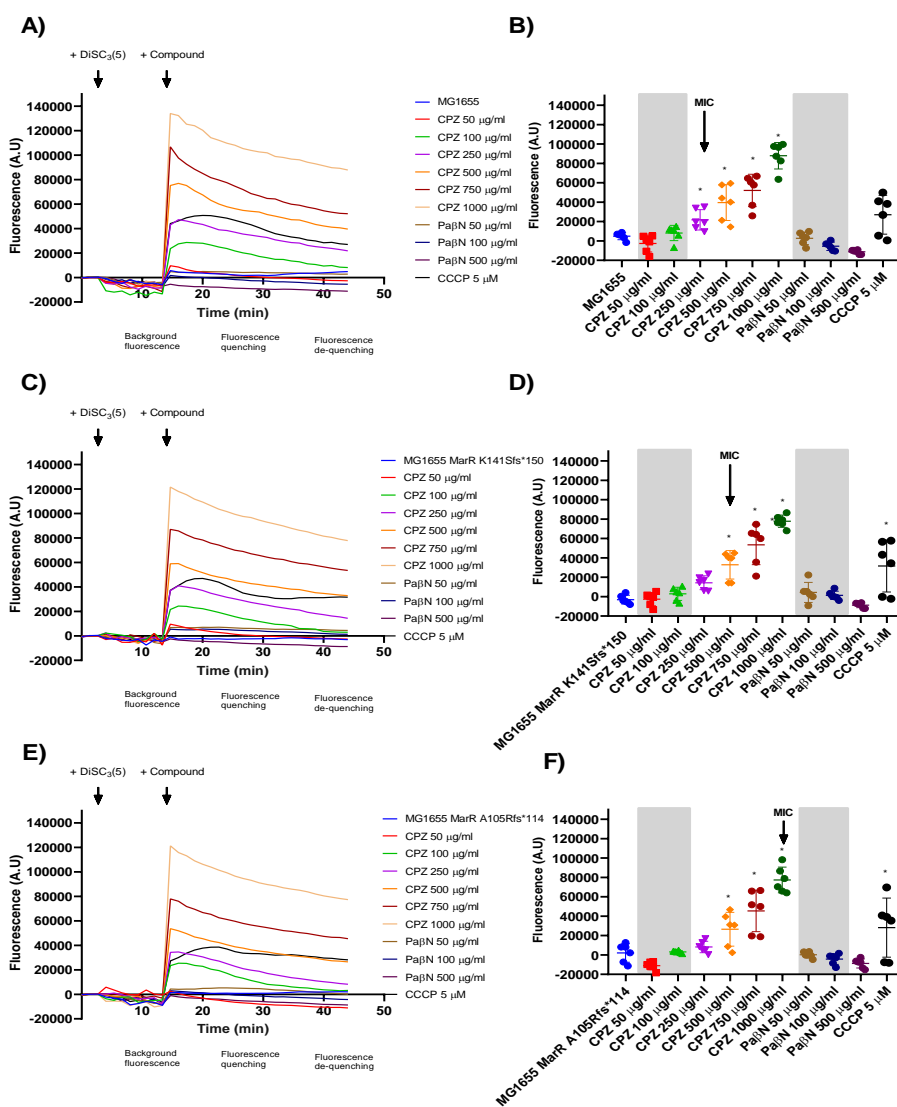
Chlorpromazine depolarised the IM of wild type *S. Typhimurium* SL1344 and *E. coli* MG1655 and their respective *ramR* and *marR* mutants in a concentration dependent manner (Figure 5.16 and 5.17). Consistent with their impact on membrane permeability, the presence of *marR* mutations decreased the ability of chlorpromazine to depolarise the membrane (non-statistically significant) relative to wild type MG1655 (Figure 5.18). Like membrane permeability, this was likely representative of the higher MIC of MG1655 MarR K141Sfs*150 and MG1655 MarR A105Rfs*114 compared to wild type MG1655. In contrast, chlorpromazine depolarised the membrane of SL1344 RamR L158P to a greater extent (non-statistically significant) compared to wild type SL1344 at all concentrations up to 1000 µg/ml (Figure 5.18).

Figure 5.16: Effect of chlorpromazine on the membrane potential sensitive fluorescent dye DiSC₃5 in *S. Typhimurium* SL1344 wild type and RamR L158P.



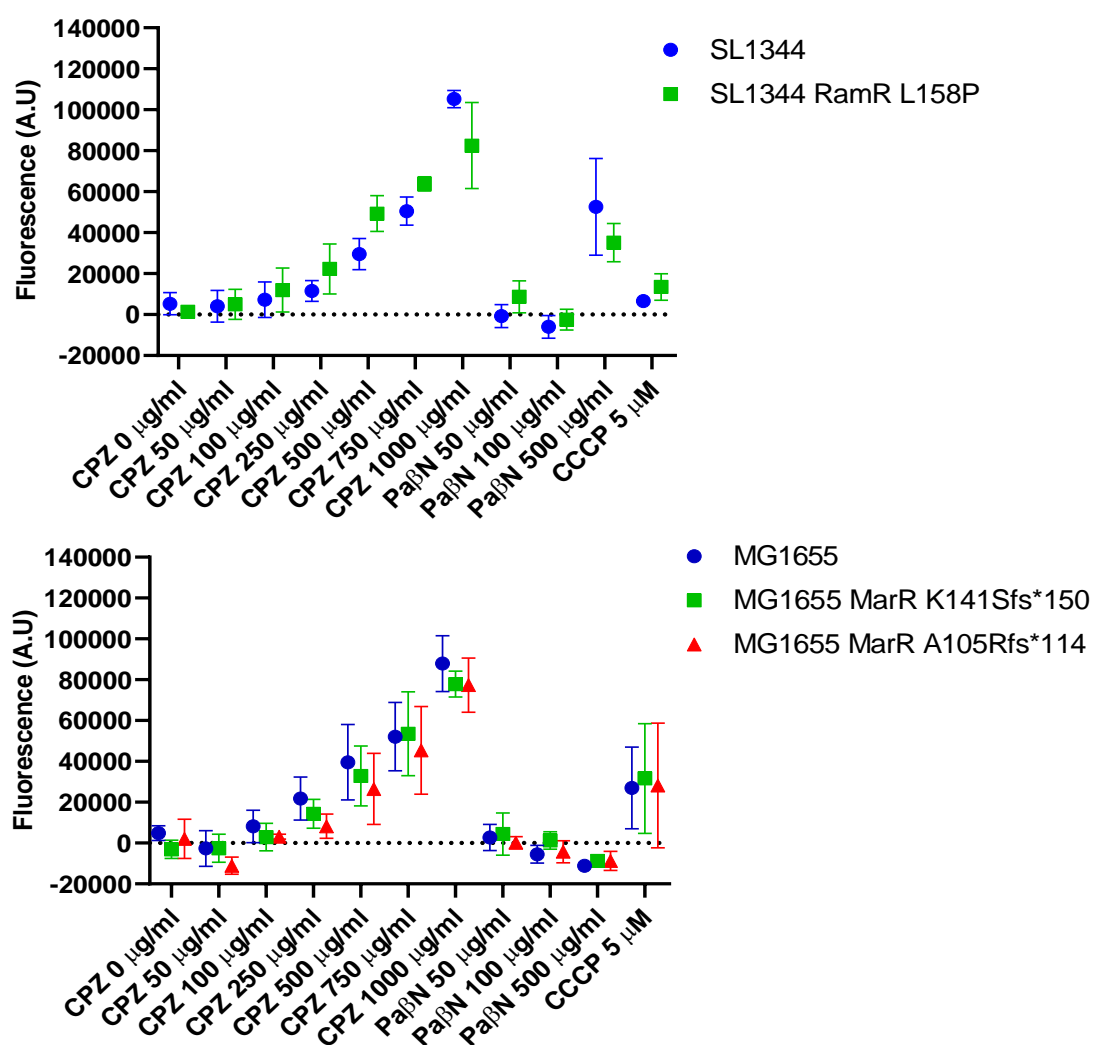
Changes in the fluorescence of DiSC₃5 in the cell suspension of SL1344 wild type (A) and RamR L158P (B). The time points of DiSC₃5 and compound addition are highlighted by arrows. The maximum fluorescence values upon the addition of chlorpromazine/CCCP/ PaβN to SL1344 wild type (C) and RamR L158P (D). Efflux inhibitory concentrations of chlorpromazine and PaβN are displayed in grey. (A and C) The mean of four biological replicates each with two technical replicates is shown. (B and D) The graphs show the mean and standard deviation of four biological replicates. Each biological replicate was calculated from the mean of two technical replicates. Asterisks indicate a statistically significant difference ($P < 0.05$), calculated using a one-way ANOVA, in relation to the unexposed control. CPZ; Chlorpromazine. PaβN; Phe-arg beta naphthylamide.

Figure 5.17: Effect of chlorpromazine on the membrane potential sensitive fluorescent dye DiSC₃₅ in *E. coli* MG1655, MarR K141Sfs*150 and MarR A105Rfs*114



The spread of four biological replicates is shown. Changes in the fluorescence of DiSC₃₅ in the cell suspension of MG1655 wild type (A) MarR K141Sfs*150 (C) and MarR A105Rfs*114 (D). The time points of DiSC₃₅ and compound addition are highlighted by arrows. The maximum fluorescence values upon the addition of chlorpromazine/CCCP/ PaβN to MG1655 wild type (B) MarR K141Sfs*150 (D) and MarR A105Rfs*114 (F). Efflux inhibitory concentrations of chlorpromazine and PaβN are displayed in grey. (A, C and E) The mean of four biological replicates each with two technical replicates is shown. (B, D, F) The graphs show the mean and standard deviation of four biological replicates. Each biological replicate was calculated from the mean of two technical replicates. Asterisks indicate a statistically significant difference ($P < 0.05$), calculated using a one-way ANOVA, in relation to the unexposed control. CPZ; Chlorpromazine. PaβN; Phe-arg beta naphthylamide.

Figure 5.18: Effect of chlorpromazine on the membrane potential sensitive fluorescent dye DiSC₃₅ in *S. Typhimurium* SL1344 and *E. coli* MG1655 and their respective chlorpromazine resistant mutants.



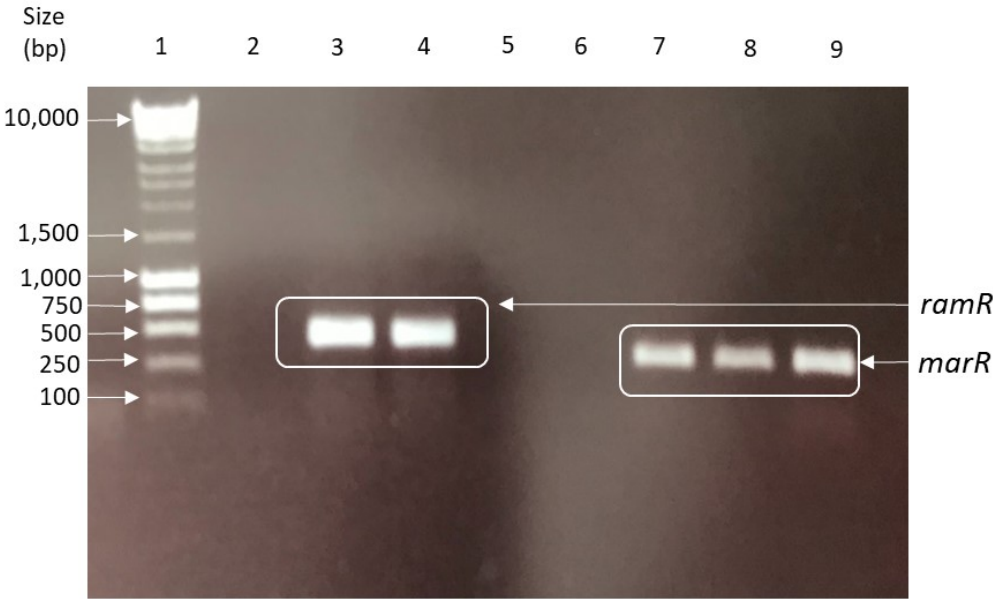
The graphs show the mean and standard deviation of four biological replicates. Each biological replicate was calculated from the mean of two technical replicates. Asterisks indicate a statistically significant difference ($P < 0.05$), calculated using a one-way ANOVA, in relation to the unexposed control. CPZ; Chlorpromazine. PaβN; Phe-arg beta naphthylamide.

5.11 Construction of vectors for overexpression of RamR and MarR

For optimal protein purification it is essential to artificially increase the amount of protein produced by the bacteria. The pTrc vectors are used for high-level protein expression due to the presence of the *trc* gene. This vector also contains an N-terminal polyhistidine (6 x His) tag that renders it as a suitable vector for downstream purification of RamR and MarR via nickel-immobilised affinity chromatography. The His-tag located on the pTrc vector is not cleavable and the presence of these bulky amino acids can cause downstream problems in assays utilising the purified protein. Therefore, a thrombin cleavage site was introduced followed by an additional 6 x His-tag to allow for removal of these amino acids, if necessary.

RamR and MarR were amplified from the wild type and mutant strains (Figure 5.19) and introduced onto a linearized pTrcHis vector backbone by TA cloning. The recombinant vector was transformed into *E. coli* BL21 DE3, a strain of *E. coli* which is deficient for Lon and OmpT. pTrcHis was provided as a linear backbone and due to the nature of TA cloning this meant that the vector could not be circularised without introducing an insert with TA overhangs. Therefore, a PCR does not show a size difference between the empty and recombinant vector. Instead, to confirm successful cloning, *marR* and *ramR* were amplified from pTrcHis using primers that anneal upstream and downstream of the introduced gene to the vector backbone (Figure 5.20 and 5.21). DNA sequencing of the amplimers confirmed the successful introduction of wild type and mutant *marR* and *ramR* into pTrcHis (Figure 5.22).

Figure 5.19: Amplification of *ramR* (wild type and mutant) and *marR* (wild type and mutant) for cloning into pTrecHis.



Lane	Sample	Primer pair	Size (bp)
1	Nippon genetics 1kb ladder plus		
2	Contamination control primer set 1	2386 + 2387	
3	<i>ramR</i> wild type	2386 + 2387	582
4	<i>ramR</i> L158P	2386 + 2387	582
5	Contamination control primer set 2	2388 + 2389	
6	Contamination control primer set 3	2388 + 2390	
7	<i>marR</i> wild type	2388 + 2389	435
8	<i>marR</i> 141_142del	2388 + 2390	435
9	<i>marR</i> 105delC	2388 + 2389	433

Figure 5.20: Amplification of *ramR* WT and *ramR* L158P from the recombinant pTrc vector backbone.

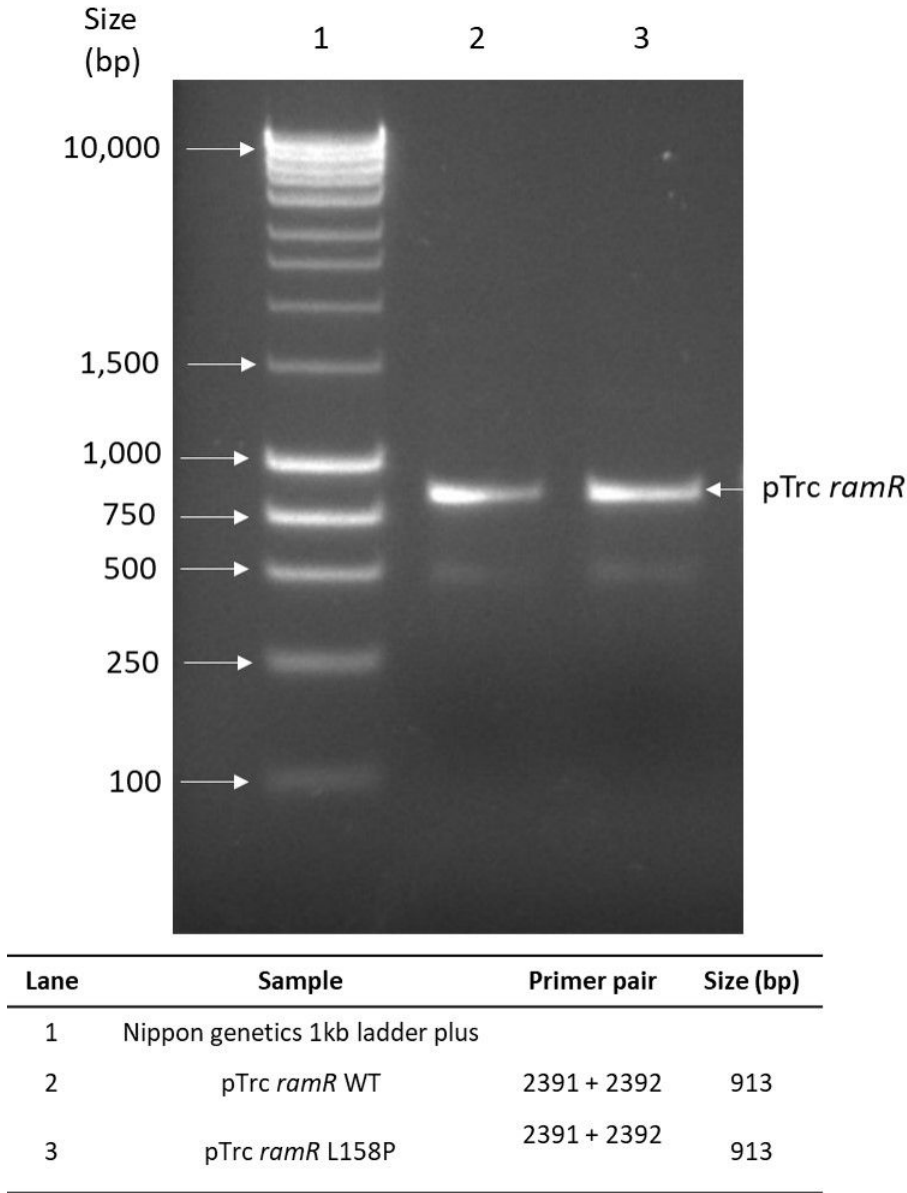


Figure 5.21: Amplification of *marR* WT, *marR* A105Rfs*114 and *marR* K141Sfs*150 from recombinant pTrc vector backbone.

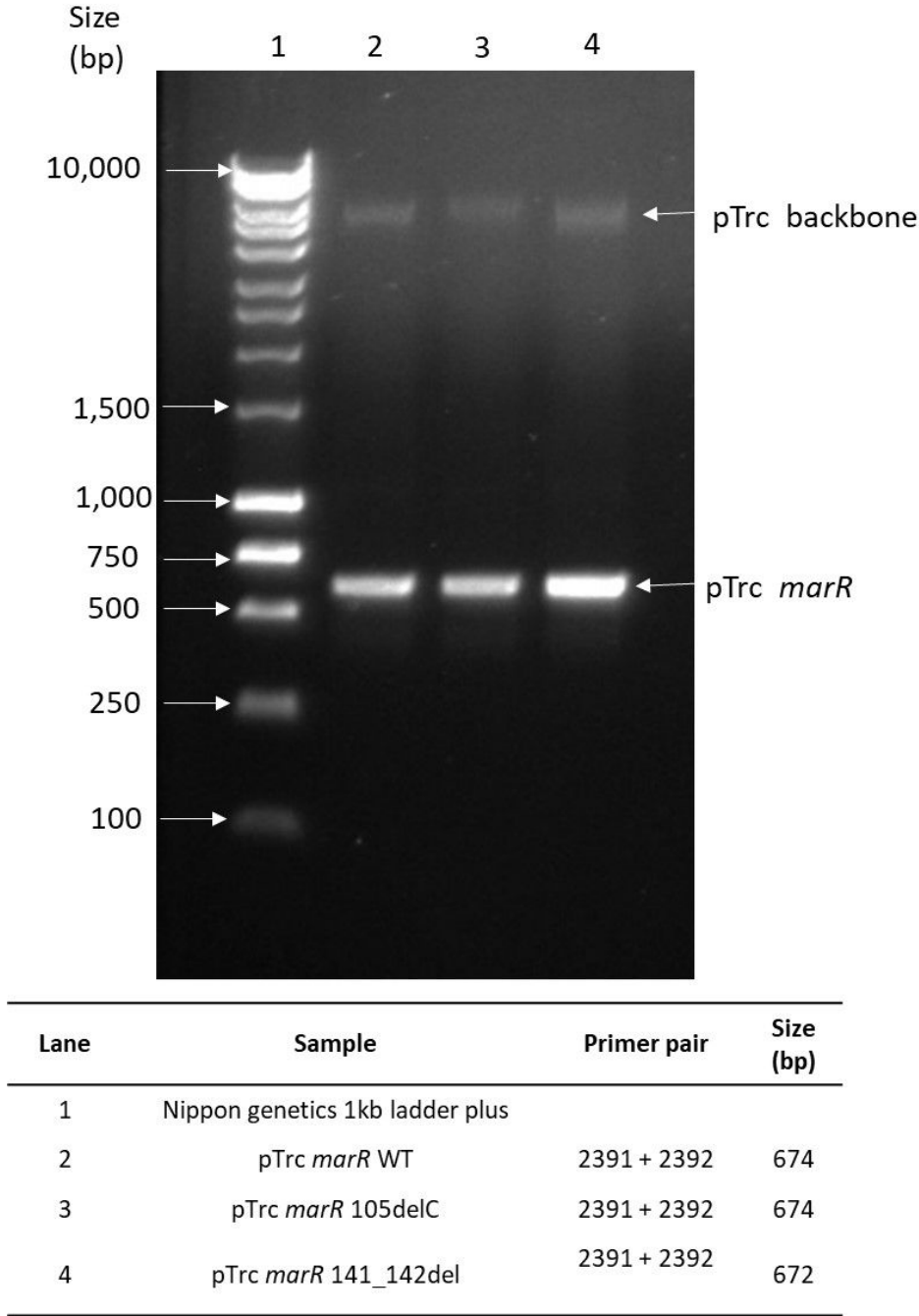


Figure 5.22: DNA sequencing to confirm correct cloning of wild type and mutant and *marR* and *ramR* into pTrcHis.

<i>E. coli</i> MG1655 <i>marR</i> wildtype	ACACTTGAGTATTTGGCTTAAGAAAAGTCTGCCGAAGGGCGAATTCGAAAGCTTACGTA
<i>E. coli</i> MG1655 <i>marR</i> K141Sfs*150	ACACTTGAGTATTTGGCTTA--AAAGTCTGCCGAAGGGCGAATTCGAAAGCTTACGTA

<i>E. coli</i> MG1655 <i>marR</i> wildtype	CAAGCGGCGGTACTGGTAAAACTTACCACCGGCGGCGGGCAATATGTGAACAAATG
<i>E. coli</i> MG1655 <i>marR</i> A105Rfs*114	CAAGCGGCGGTACTGGTAAAACTTACCACCGGCGGCGGGCAATATGTGAACAAATG

<i>S. Typhimurium</i> SL1344 <i>ramR</i> wildtype	GCGACGGCCTTTTCTGGCGCTGGCTGAAACAACAATGGATTCGCCGCGCGCGATC
<i>S. Typhimurium</i> SL1344 <i>ramR</i> L158P	GCGACGGCCTTTTCTGGCGCGGGCTGAAACAACAATGGATTCGCCGCGCGCGATC

The mutant sequences *marR* (K141Sfs*150), *marR* (A105Rfs*114) and *ramR* (L158P) were aligned against the pTrcHis *marR* and *ramR* wild type sequences. The mutation sites are displayed in red text.

5.12 Purification of wild type SL1344 RamR and SL1344 RamR L158P

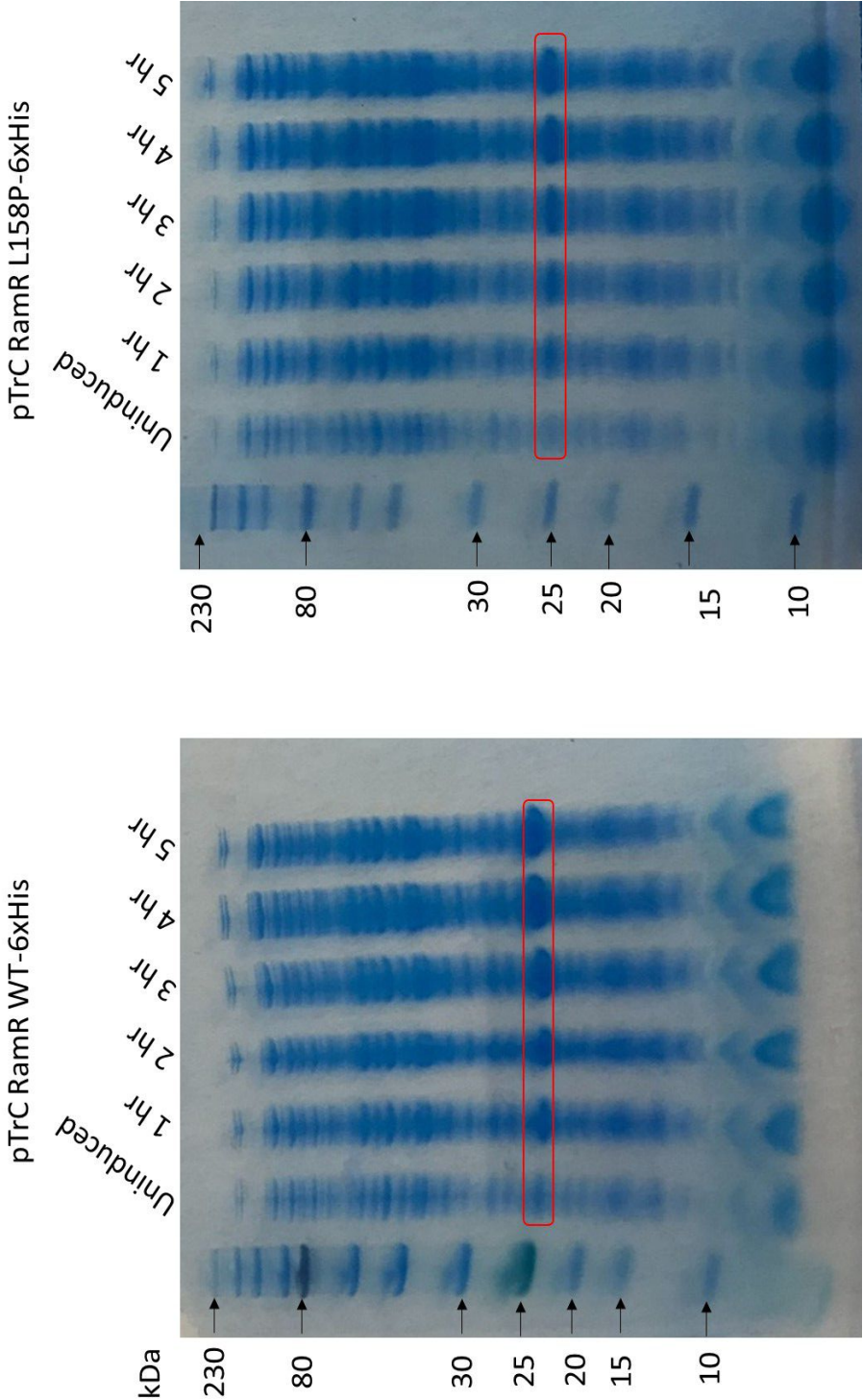
5.12.1 Determination of optimal expression conditions

To determine the induction conditions required for optimal protein yield, a pilot experiment was undertaken in which 10 ml of *E. coli* BL21 (DE3) cultures containing either pTrC RamR-6xHis wild type or RamR L158P-6xHis were grown to an OD₆₀₀ of 0.4, induced with 10 μ M of IPTG and growth continued at 37 °C for one, two, three, four and five hours post addition of IPTG. Following induction, the cells were disrupted by boiling at 100 °C and the samples were resolved by SDS-PAGE. Simply Blue Straining of the gels revealed the presence of both proteins at ~25kDa (Figure 5.23). The expected size of RamR-6xHis and RamR L158P-6xHis is 25.917 kDa. The intensity of the protein band increased over induction time and five hours was determined as the optimal period of induction for subsequent full expression.

5.12.2 Purification of RamR wild type and RamR L158P by nickel affinity chromatography

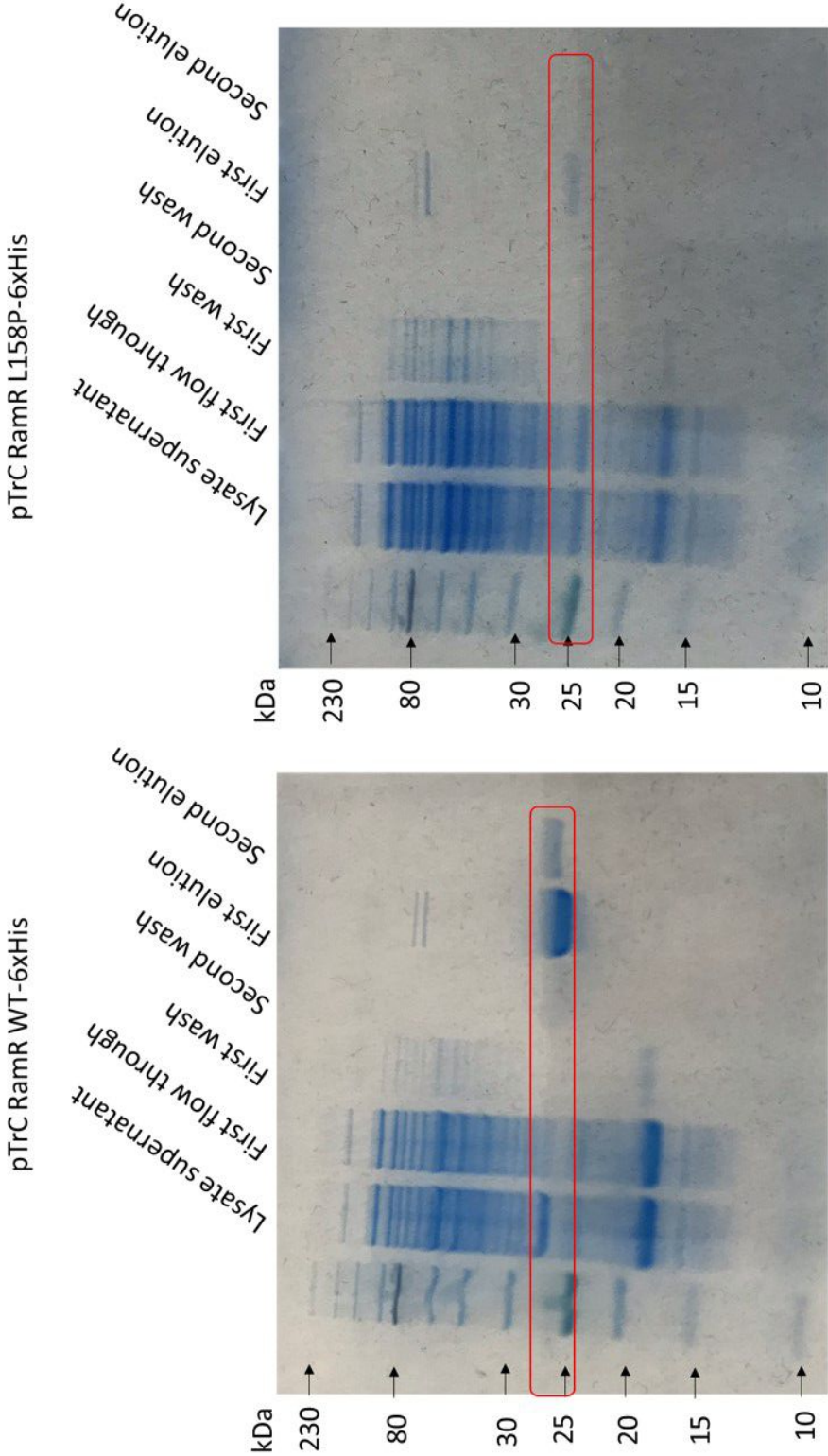
For full scale expression, 250 ml of *E. coli* BL21 (DE3) containing either pTrC RamR-6xHis wild type or RamR L158P-6xHis were grown to an OD₆₀₀ of 0.4, induced with 10 μ M of IPTG and growth continued at 37 °C for five hours post induction. Following expression, RamR WT-6xHis and RamR L158P-6xHis were purified by Ni-NTA affinity chromatography using QIAGEN Ni-NTA fast start columns. Fractions from each stage of purification were resolved by SDS-PAGE and the gels visualised by Simply Blue staining (Figure 5.24). The stained gels showed the presence of the desired protein at ~25 kDa. Accompanying both purified RamR WT-6xHis and RamR L158P-6xHis in the first elution was the presence of two single bands at ~80 kDa. Due to the ability of RamR to form multimeric structures, these secondary bands were presumed to be protein aggregates. A western blot performed

Figure 5.23: Coomassie staining of an SDS-PAGE gel containing pTrC RamR WT-6xHis and pTrC RamR L158P-6xHis samples post induction with 10 μ M IPTG at varying time points.



The samples were run against an NEB Pre-stained broad range (10-230 kDa) ladder. The molecular weights of the ladder are indicated and the desired protein is outlined with a red box. The calculated molecular weight of RamR WT-6xHis and RamR L158P-6xHis was 25.917 kDa.

Figure 5.24: Coomassie staining of an SDS-PAGE gel containing pTrC RamR WT-6xHis or pTrC RamR L158P-6xHis purified by nickel affinity chromatography.



The fractions from each stage of purification were run against an NEB Pre-stained broad range (10-230 kDa) ladder. The molecular weights of the ladder are indicated and the desired protein is outlined with a red box. Secondary products were observed at ~80kDa.

using Anti-His antibodies revealed the presence of protein at the desired size (~ 25 kDa) (Figure 5.25). The secondary bands were not visible by western blot. RamR L158P-6xHis was difficult to purify and less protein was produced. The concentration of purified RamR WT-6xHis and RamR L158P-6xHis was 1523 $\mu\text{g/ml}$ and 635 $\mu\text{g/ml}$, respectively.

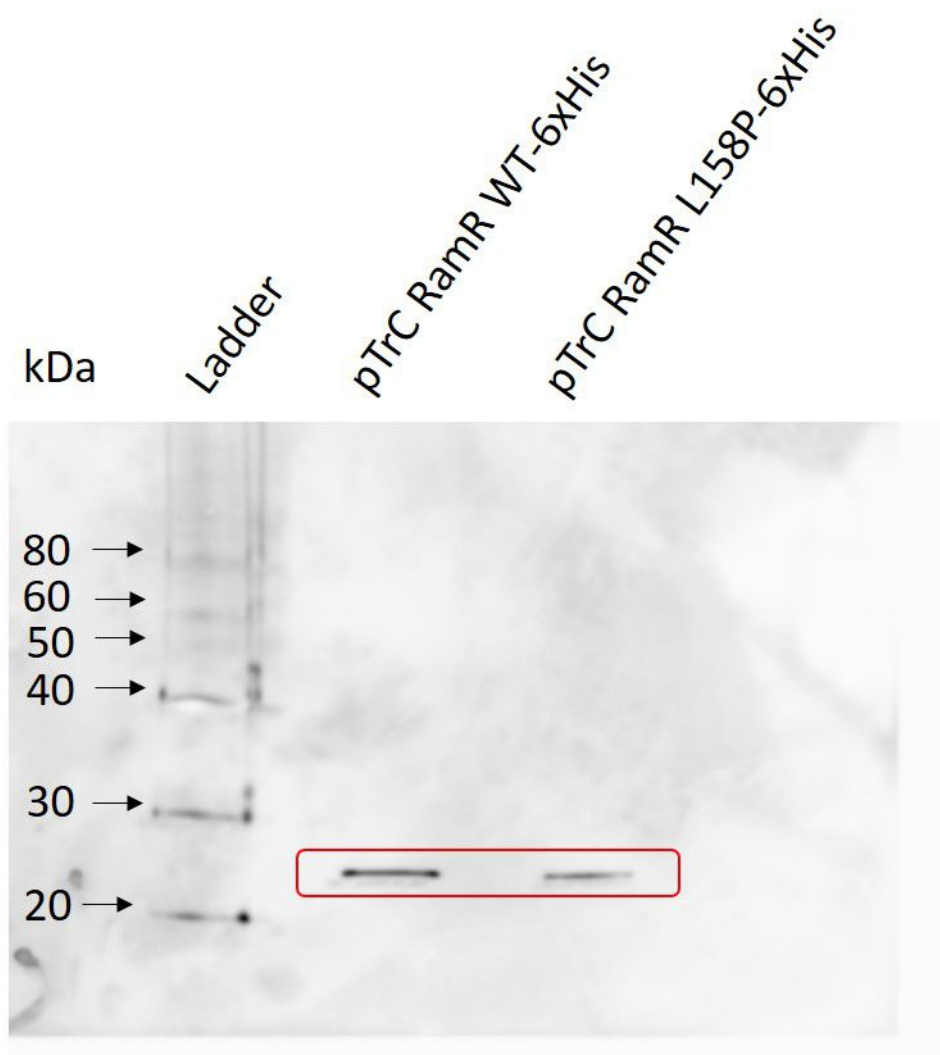
5.13 Binding to the *ramA* promoter is ablated in the RamR L158P-6xHis mutant

RamR has been previously shown by EMSA to bind to the promoter of *ramA* (*pramA*) from *S. Typhimurium* (Baucheron, Coste, et al., 2012). The L158P substitution is located within the dimerisation domain of RamR. Proline disrupts alpha helical structures (li et al 1996) and as such the L158P substitution was predicted to alter the secondary structure of RamR such that DNA binding is ablated.

To determine the interaction of SL1344 RamR and RamR L158P with *pramA*, an EMSA was performed with a 171-bp product (Figure 5.26) containing *pramA* in the presence and absence of RamR WT-6xHis and RamR L158P-6xHis. An EMSA in which DNA-protein binding is observed results in the shift of the free DNA band to higher up the gel matrix as a result of an increase in molecular mass upon protein binding. Here, a discreet shift was not observed (Figure 5.27). Instead, DNA-protein binding resulting in decreased mobility was indicated by a decrease in the intensity of the free DNA band, in the presence of protein, in comparison to the free DNA band in the absence of protein.

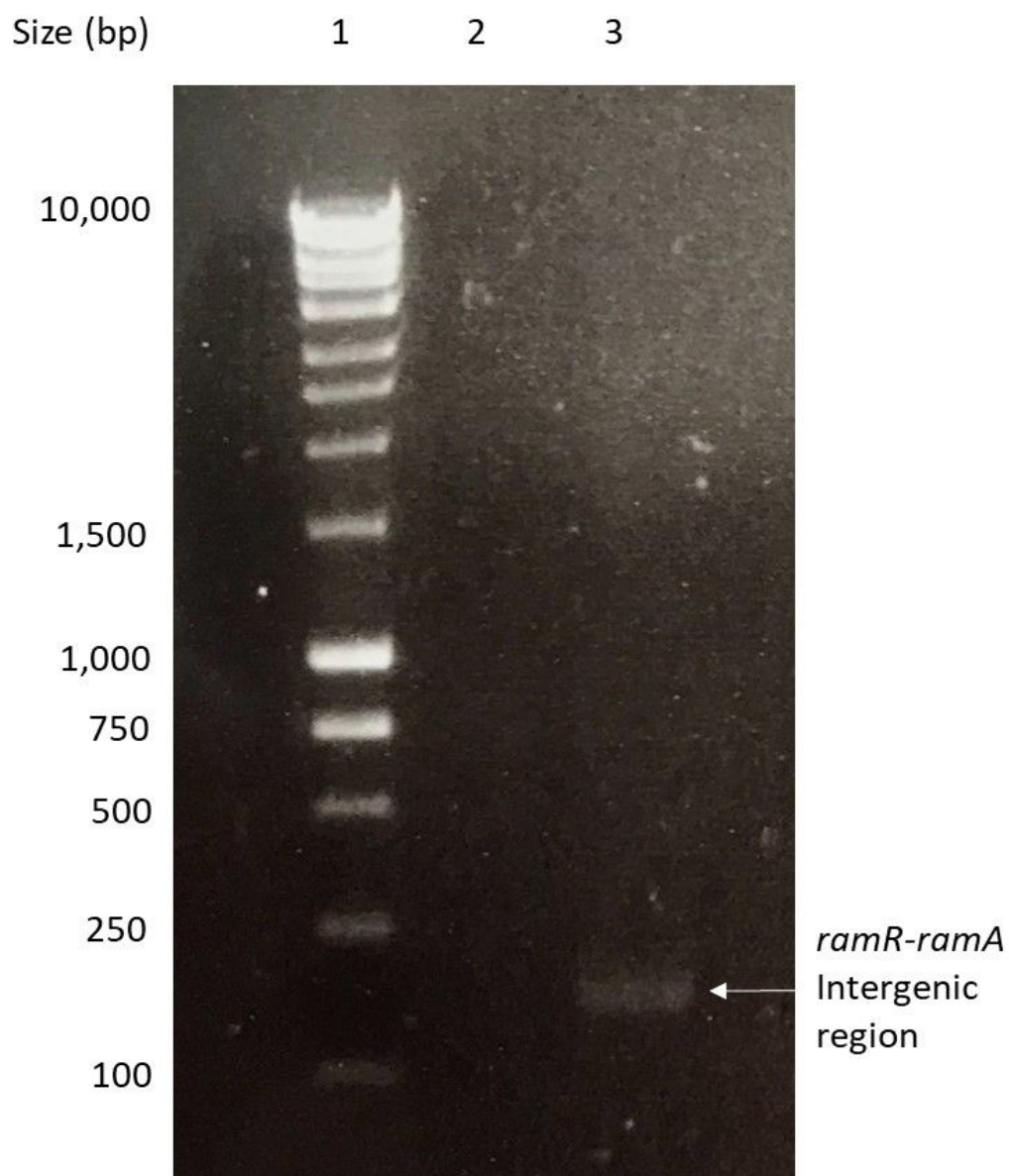
Addition of increasing concentrations of RamR WT-6xHis to the *pramA* reaction mixture resulted in decreased mobility of the DNA fragment. The intensity of the free DNA band decreased with increasing RamR concentration (Figure 5.27). The reduction in the intensity of the free DNA band was accompanied by the appearance of an additional band at the top of the gel matrix and a smeared migration of stained DNA down the gel matrix. In contrast to RamR WT-6xHis, for RamR L158P-6xHis no change in mobility or intensity

Figure 5.25: Western blot using anti-His antibodies of an SDS-PAGE gel containing pTrC RamR WT-6xHis or pTrC RamR L158P-6xHis purified by nickel affinity chromatography.



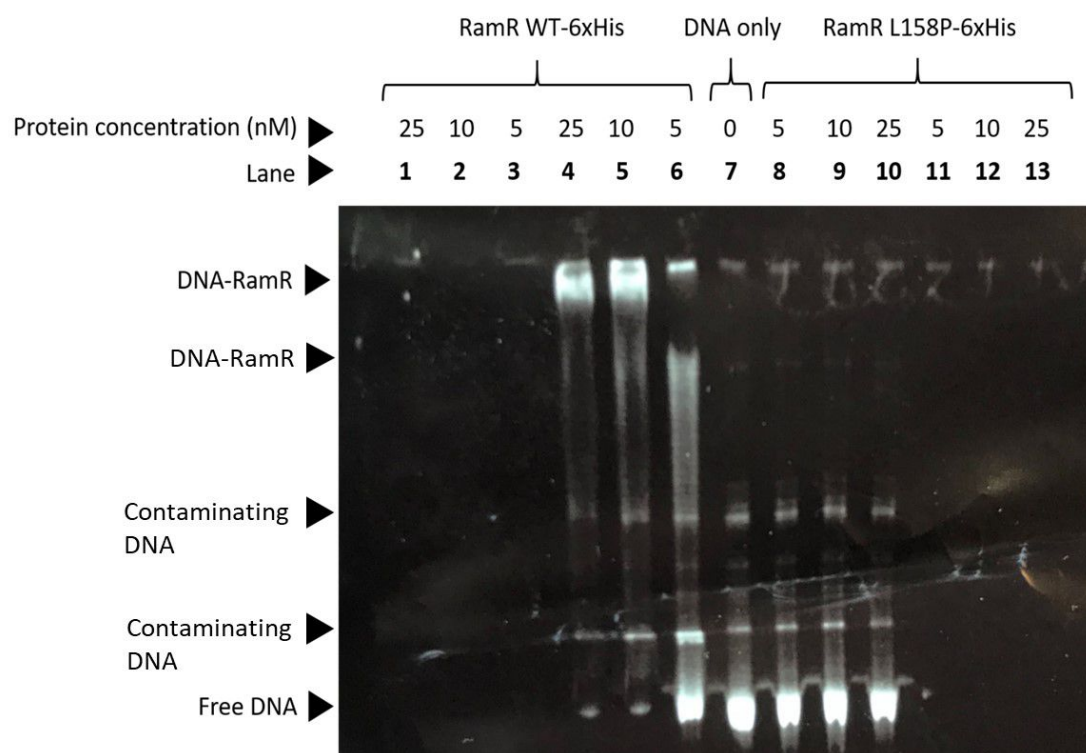
The proteins were run against an NEB Pre-stained broad range (10-230 kDa) ladder. The molecular weights of the ladder are indicated and the desired protein is outlined with a red box.

Figure 5.26: Amplification of *ramR-ramA* intergenic region from wild type *S.* Typhimurium SL1344.



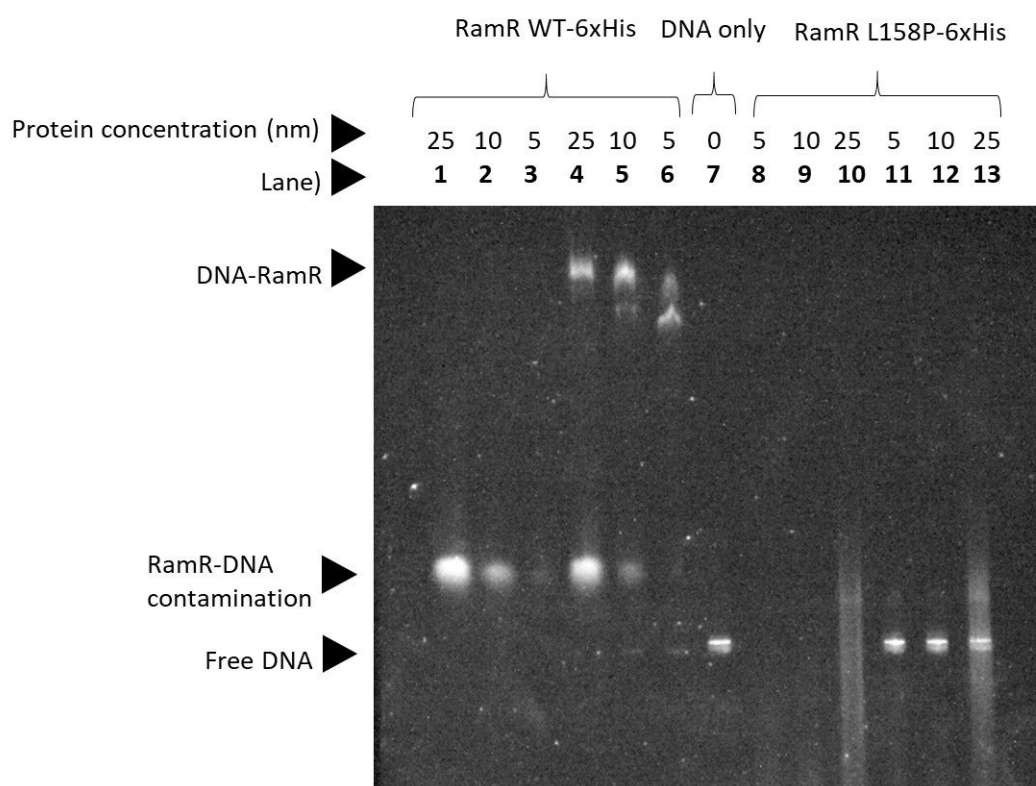
Lane	Sample	Primer pairs	Size (bp)
1	Nippon genetics 1kb ladder plus		
2	Contamination control primer	1233 + 1240	
3	<i>ramR-ramA</i> intergenic region	1233 + 1240	171

Figure 5.27: Electrophoretic mobility shift assay showing the interaction of RamR WT-6xHis and RamR L158P-6xHis with the *ramR-ramA* intergenic region including *pramA*.



Increasing concentrations of RamR WT-6xHis and RamR L158P-6xHis were incubated in presence and absence of a 171-bp fragment of free DNA containing *pramA*. Lanes 1-3 contain RamR WT-6xHis only at 25, 10 and 5 nmol. Lanes 4-6 contain RamR WT-6xHis at 25, 10 and 5 nmol + free DNA. Lane 7 contains free DNA only. Lanes 8-10 contain RamR L158P-6xHis only at 5, 10 and 25 nmol + free DNA. Lanes 11-13 contain RamR L158P-6xHis only at 5, 10 and 25 nmol.

Figure 5.28: Electrophoretic mobility shift assay, post gel extraction, showing the interaction of RamR WT-6xHis and RamR L158P-6xHis with the *ramR-ramA* intergenic region including *pramA*.



Increasing concentrations of RamR WT-6xHis and RamR L158P-6xHis were incubated in presence and absence of a 171-bp fragment of free DNA containing *pramA*. Lanes 1-3 contain RamR WT-6xHis only at 25, 10 and 5 nmol. Lanes 4-6 contain RamR WT-6xHis at 25, 10 and 5 nmol + free DNA. Lane 7 contains free DNA only. Lanes 8-10 contain RamR L158P-6xHis only at 5, 10 and 25 nmol + free DNA. Lanes 11-13 contain RamR L158P-6xHis only at 5, 10 and 25 nmol.

of the free DNA band was observed. Accompanying the free *pramA* DNA was multiple additional DNA bands, despite no observed extra DNA on an agarose gel (Figure 5.26). The EMSA assay was repeated with *pramA* DNA that had been run on a 1 % agarose gel and gel extracted four times. Once stained, the EMSA SDS-PAGE gel revealed a single free DNA band corresponding to *pramA* and a shift of the free DNA to higher up the gel matrix in the presence of RamR WT-6xHis (Figure 5.28). A shift that was not observed in the presence of RamR L158P-6xHis. Unfortunately, the RamR WT-6xHis appeared to be contaminated with unidentified DNA. Despite this, both these EMSA assays indicate that RamR WT-6xHis is able to bind to *pramA* resulting in a shift in free DNA, an ability that is ablated in RamR L158P-6xHis.

5.14 Discussion

In Chapter 3, it was shown that resistance of *S. Typhimurium* SL1344 and *E. coli* MG1655 to chlorpromazine was conferred by mutations with *ramR* and *marR*, respectively. RamR and MarR are DNA binding proteins that regulate the expression of AcrAB-TolC by binding to the promoter regions of the transcriptional activators *ramA* (*pramA*) and *marA* (*pmarA*), repressing their expression (Ricci, Busby, et al., 2012; Baucheron, Coste, et al., 2012; Martin, Rosner, et al., 1995; Alekshun and Levy, 1997; Yamasaki, Nikaido, et al., 2013a; Perera et al., 2010). Ligand binding to RamR and MarR alters their secondary structures ameliorating their ability to bind *pramA* and *pmarA*, resulting in the expression of *ramA* and *marA* and the consequent overexpression of *acrAB-tolC* (Perera et al., 2010; Yamasaki, Nikaido, et al., 2013a).

Given that the conformational changes that result from ligand binding are essential for de-repression of the AcrAB-TolC regulatory system it seems unlikely that the mode of action by which chlorpromazine elicits its efflux inhibitory activity is through interactions with RamR and MarR. Instead, it is proposed that chlorpromazine is a substrate of AcrB and that

alteration of RamR and MarR confers resistance to chlorpromazine through increased efflux by AcrAB-TolC as a result of overexpression of *ramA* and *marA*. These predicted phenotypic changes were hypothesised to result from conformational changes in the repressors protein structure that mimic ligand binding and prevent the interaction with *pramA* and *pmarA*.

In order to test this hypothesis the efflux phenotype of the mutants SL1344 RamR L158P, MG1655 MarR A105Rfs*114 and MG1655 MarR K141Sfs*150 were characterised and compared to wild type *S. Typhimurium* SL1344 and *E. coli* MG1655 by antibiotic susceptibility, gene reporting and AcrB substrate efflux/accumulation assays.

Here, promoter-GFP constructs, used to determine the activity of *ramA*, *marA* and *acrAB* in *S. Typhimurium* SL1344 and *E. coli* MG1655 show that the expression of *ramA* and *acrAB* in SL1344 RamR L158P and *marA* and *acrAB* in MG1655 MarR A105Rfs*114 and MG1655 MarR K141Sfs*150 was increased compared to their basal expression in the respective wild type strains. This increase in the expression of *ramA*, *marA* and *acrAB* indicates that MG1655 MarR A105Rfs*114, MG1655 MarR K141Sfs*150 and SL1344 RamR L158P are altered in their ability to repress *marA* and *ramA* leading to their overexpression.

Previously, Bailey et al., 2008 revealed that chlorpromazine induced the expression of *ramA*, in *S. Typhimurium*, but reduced the expression of *acrAB*. This was hypothesised to be a result of a negative feedback loop in which chlorpromazine repressed the expression of AcrB and a concomitant overexpression of *ramA* occurs to compensate for low *acrB* expression. As expected, induction of *ramA* and *acrAB* was observed upon addition of chlorpromazine in wild type *S. Typhimurium*. Known inducers of RamR have been found to bind the protein within the binding pocket resulting in an increase in the distance between the H-T-H motifs of the RamR dimer (Yamasaki, Nikaido, et al., 2013a; Yamasaki, Nakashima, et al., 2019). The resulting conformational changes in the dimerisation domain of RamR results in a reduced ability to bind DNA and derepression of *ramA*. The ability of chlorpromazine to

induce *ramA* and *acrAB* suggests this compound is able to directly bind RamR of wild type *S. Typhimurium*, an interaction that is ablated in RamR L158P. However, it is important to note that this derepression may be a direct reflection of the efflux inhibitory activity of chlorpromazine. In that *ramA* derepression is a result of a direct interaction of accumulated metabolites with RamR rather than the interaction of chlorpromazine with RamR. The expression of *ramA* and *acrAB* from SL1344 RamR L158P was not further induced by chlorpromazine. This indicates that the secondary structure of RamR L158P is altered such that *ramA* is completely derepressed.

Interestingly, in contrast with Bailey et al., 2008, here chlorpromazine did not decrease the expression of *acrAB* in *S. Typhimurium*. Instead, AcrB expression was increased. An RT-PCR revealed this discrepancy was due to differences in chlorpromazine concentration between these two studies. At 50 µg/ml, a relevant efflux inhibitory concentration, the expression of *acrB* was increased. However, at 200 µg/ml *acrB* expression was increased, consistent with Bailey et al., 2008.

The upregulation of *ramA* and *acrAB* that occurs in *S. Typhimurium* upon exposure to chlorpromazine is hypothesised to result from the role of chlorpromazine as a substrate of AcrB and as such is not reflective of the efflux inhibitory activity of this compound as previously suggested (Bailey et al., 2008). In addition, the mutant selection experiments have revealed a mechanism of resistance to chlorpromazine. As discussed, upon binding of inducers a conformational change within the dimerisation domain of RamR is triggered as a result of increases in the distance between H-T-H motifs (Yamasaki, Nikaido, et al., 2013a; Yamasaki, Nakashima, et al., 2019). Given that L158P is located within the dimerisation domain of RamR, just three amino acid outside of the known ligand binding residue Phe155, it is hypothesised that the RamR L158P substitution will largely mimic the conformational changes that occur upon ligand binding resulting in a reduction in DNA binding affinity and thus confer resistance through

increased gene expression and efflux activity. This hypothesis could be tested by comparing the structure of RamR L158P to the crystal structure of RamR that has been complexed with ligands including bile salts, berberine, crystal violet, dequalinium, ethidium bromide and rhodamine 6G (Yamasaki, Nikaido, et al., 2013a; Yamasaki, Nakashima, et al., 2019).

A similar mechanism of resistance to chlorpromazine is proposed in *E. coli*. Mutation of *marR* results in conformational changes in the structure of MarR reducing its affinity for DNA. Interestingly, chlorpromazine did not induce the expression of *marA* and *acrAB* in wild type MG1655. This suggests that this compound does not directly bind MarR and that upregulation of efflux does not occur in response to chlorpromazine. This evidence is at contrast with the hypothesis that chlorpromazine is a substrate of AcrB in *E. coli*. However, the fluorescence values produced by the pMW82 plasmid are very low in an *E. coli* background (~ 1000 units) compared with those seen in *Salmonella* ($\sim 10,000$). Therefore, small increases in expression may be hidden within the limitations of the method. It may be useful to quantify gene expression in these mutants in the presence and absence of chlorpromazine by quantitative PCR.

The expression of *marA* and *acrAB* was similar in MG1655 MarR A105Rfs*114, MG1655 MarR K141Sfs*150 and MG1655 *marR::aph* which suggests that, like *marR::aph*, MarR A105Rfs*114 and MarR K141Sfs*150 are completely non-functional in terms of their ability to repress *marA*. Unlike *E. coli*, in *S. Typhimurium*, although the level of *ramA* expression in RamR L158P and *ramR::aph* is similar, the level of *acrAB* expression in RamR L158P was much higher than *ramR::aph*. This was surprising as *ramR::aph* should be non-functional and thus would be expected to result in maximal de-repression of *ramA*. It is unknown why RamR L158P resulted in a higher expression of *acrAB* relative to *ramR::aph*. However, different mutations in RamR have been shown to de-repress *ramA* to varying degrees. However, even the so called 'super repressor' mutant RamR E118V did not derepress *ramA* more than *ramR::aph* (Ricci, Busby, et al., 2012). In addition, some genes are able to

self-regulate and there is evidence to suggest that RamA competes with RamR in terms of binding to *ramO* (a hypothetical operator sequence) and induces its own expression (Bailey et al., 2008). It could be hypothesised that the structure of RamR L158P is altered such that it behaves in a manner more similar to RamA and is able to further induce the expression of *ramA*, relative to *ramR::aph*.

The increase in the expression of *ramA* and *acrAB* by SL1344 RamR L158P and *marA* and *acrAB* by MG1655 MarR A105Rfs*114 and MG1655 MarR K141Sfs*150 was reflected by an increased efflux capability of these strains. SL1344 RamR L158P accumulated less H33342 and ethidium bromide, and MG1655 MarR A105Rfs*114 and MG1655 MarR K141Sfs*150 less H33342, relative to wild type SL1344 and MG1655. The extent of ethidium bromide accumulation of MG1655 MarR A105Rfs*114 and MG1655 MarR K141Sfs*150 was not increased relative to wild type MG1655. The high variability in the ethidium bromide efflux assay when performed in *E. coli* may suggest that ethidium bromide may not be a ‘good’ AcrB substrate in *E. coli*. Despite having increased *acrAB* expression relative to SL1344 *ramR::aph*, SL1344 RamR L158P accumulated the same level of H33342. However, the level of ethidium bromide accumulation was lower in SL1344 RamR L158P than *ramR::aph*, indicating a greater efflux of ethidium bromide reflecting the higher expression of *acrAB*. Of note, the mutations within *marR* and *ramR* did not ablate the ability of chlorpromazine and PaβN to inhibit the efflux activity of *E. coli* and *S. Typhimurium*. Both compounds were able to inhibit the efflux of H33342 from SL1344 RamR L158P, MG1655 MarR A105Rfs*114 and MG1655 MarR K141Sfs*150 to a similar extent as that against wild type SL1344 and MG1655. Therefore, a functional RamR and MarR are not required for the efflux inhibitory activity of chlorpromazine, as this compound clearly remains active against each mutant strain.

Data obtained herein confirm that the mechanism of resistance to chlorpromazine is not via a mutated binding site for this compound. Instead, rather than elucidating the

mode of action underlying the efflux inhibitory activity of chlorpromazine the mutant selections provided additional evidence to support that chlorpromazine is a substrate of the AcrB pump. And that mutation of the regulatory genes of AcrAB-TolC of *E. coli* and *S. Typhimurium* occurs to increase the export of chlorpromazine from these strains thus reducing the impact of its antibacterial and efflux inhibitory activity. Accumulation assays were performed with chlorpromazine (as the substrate) in order to determine the ability of wild type *S. Typhimurium* and *E. coli* to export this compound. Unfortunately, the background fluorescence level of chlorpromazine was too low for this experiment to be successfully performed. These experiments could be repeated with radiolabelled chlorpromazine. Alternatively, mass spectrometry of extracellular or intracellular bacterial suspensions, post exposure to chlorpromazine, could be performed to quantify the concentration of compound in each environment.

To confirm the hypothesis that the RamR L158P substitution alters protein structure and prevents its interactions with the target promoter, an EMSA was performed with purified wild type RamR and RamR L158P and the promoter region of *ramA*. This assay showed that while wild type RamR bound DNA as expected, RamR L158P was ablated in its ability to bind *pramA*. Thereby confirming the hypothesis that mutations within RamR alter the protein secondary structure in a way that mimics the changes observed upon ligand binding and results in derepression of *ramA*. It is important to note that, while this assay could be interpreted, there were problems in that initially, once stained, the DNA band representing *pramA* was accompanied by multiple additional DNA bands. This was despite the purified PCR product showing a single band on an agarose gel. Subsequently, the EMSA was repeated after multiple rounds of gel extraction and purification of the PCR product. While this revealed a single band representing *pramA*. the additional problem of DNA contamination of the purified protein unexpectedly arose. Due to time limitations, as a result of the COVID-19 pandemic, this problem could not be resolved.

In regards to the antibacterial activity of chlorpromazine, the impact of chlorpromazine on the membrane of *S. Typhimurium* SL1344 and *E. coli* MG1655 and their respective chlorpromazine resistant mutants was assessed. These assays revealed that although the impact of chlorpromazine was reduced compared to the wild type, this compound was still able to permeabilise the OM and depolarise the IM of SL1344 RamR L158P, MG1655 MarR A105Rfs*114 and MG1655 MarR K141Sfs*150. For SL1344 RamR L158P, this was despite not being able to potentiate the activity of the tested antibiotics in disk diffusion assays. Again, chlorpromazine is clearly active against the chlorpromazine-resistant mutants providing more support to the hypothesis that these mutations do not reflect the efflux inhibitory activity of chlorpromazine and instead have revealed chlorpromazine as a substrate of AcrB.

Disk diffusion assays revealed that SL1344 RamR L158P, MG1655 MarR A105Rfs*114 and MG1655 MarR K141Sfs*150 were less susceptible to AcrB substrates (nalidixic acid, chloramphenicol, ciprofloxacin and tetracycline) than the wild type strains. Interestingly, the presence of the RamR L158P substitution in *S. Typhimurium* ablated the ability of chlorpromazine to potentiate antibiotic activity. This result suggests that the ability of chlorpromazine to potentiate antibiotic activity was dependent on the presence of a functional RamR in *S. Typhimurium*. However, this hypothesis assumes RamR is the direct target site for chlorpromazine in *S. Typhimurium*. Which is unlikely considering the evidence presented thus far. Instead, it is proposed that the MIC of chlorpromazine was increased such that chlorpromazine is not able to potentiate antibiotic activity at the equivalent concentrations used for wild type SL1344. As such, it may be useful to repeat these disk diffusion assays with higher concentrations of chlorpromazine. Nonetheless, in order to explore this further it would be useful to undertake ligand binding experiments with chlorpromazine and both wild type and mutant RamR/MarR.

In contrast, in *E. coli*, chlorpromazine was able to potentiate the antibiotic activity

against MG1655 MarR A105Rfs*114 and MarR K141Sfs*150. Which shows chlorpromazine is able to interact with *E. coli* independent of MarR. Accompanied with the observation that MG1655 MarR A105Rfs*114 and MarR K141Sfs*150 only show small increases in *marA* expression and efflux activity relative to wild type MG1655 this suggests that the ability of chlorpromazine to potentiate antibiotic activity against *E. coli* may be influenced by its ability to damage the bacterial membrane.

5.15 Key findings

- SL1344 RamR L158P had increased expression of *ramA* and *acrAB* relative to wild type SL1344.
- Chlorpromazine increased the expression of *ramA* and *acrAB* in wild type SL1344 but not SL1344 RamR L158P.
- Chlorpromazine did not induce the expression of *marA* and *acrAB* from wild type MG1655, MG1655 MarR A105Rfs*114 or MG1655 MarR K141Sfs*150.
- MG1655 MarR A105Rfs*114 and MG1655 MarR K141Sfs*150 increased the expression of *marA* and *acrAB* relative to wild type MG1655.
- SL1344 RamR L158P effluxed more H33342 and ethidium bromide compared to wild type SL1344.
- MG1655 MarR A105Rfs*114 and MG1655 MarR K141Sfs*150 effluxed more H33342, but not ethidium bromide, compared to wild type MG1655.
- Chlorpromazine inhibited the efflux of H33342 from wild type SL1344 and MG1655 and their respective chlorpromazine-resistant mutants.
- Each chlorpromazine-resistant mutant was less susceptible to the antibiotic activity of AcrB substrates.

- Chlorpromazine potentiated the activity of antibiotics against MG1655 MarR A105Rfs*114 and MG1655 MarR K141Sfs*150 but not SL1344 L158P.
- Chlorpromazine permeabilised and depolarised the membranes of MG1655 MarR A105Rfs*114, MG1655 MarR K141Sfs*150 and SL1344 L158P. However, the extent to which the membrane was damaged was reduced compared to the wild type parental strains.
- RamR L158P-6xHis was ablated in terms of its ability to bind the *ramA* promoter region.

Chapter Six

Chlorpromazine and amitriptyline may elicit their activity through interactions with AcrB

6.1 Background

Thus far, the main observations are (i) Chlorpromazine was able to bind AcrB of *E. coli* and *S. Typhimurium* to the same locations as and clash with the binding of the AcrB substrates ethidium bromide and norfloxacin. (ii) Exposure to chlorpromazine resulted in the appearance of mutations within *ramR* and *marR*. The mutations confer chlorpromazine resistance to *S. Typhimurium* and *E. coli*, respectively, by increasing the efflux of AcrB substrates from these strains. The first observation provided evidence of competitive inhibition by chlorpromazine. And the second, evidence that chlorpromazine is an AcrB substrate. Together, the hypothesis that chlorpromazine is a competitive substrate of AcrB can be inferred.

However, chlorpromazine has off-target effects on the bacterial membrane and as such is hypothesised to have global cellular effects. Therefore, the mode of action of chlorpromazine, in terms of its efflux inhibitory and antimicrobial activities, may be multifaceted. The biological activity of antibiotics and antibiotic-adjuvants is largely understood by deciphering their primary molecular targets often by selecting for resistant

mutants. However, for chlorpromazine, mutant selection experiments revealed only the mechanism of resistance. Which although useful for inferring its role as an AcrB substrate, provided no information regarding its direct cellular targets. Therefore, experiments were designed to elucidate more about the global effects of chlorpromazine outside of its interactions with AcrB. These included mutant selections with chlorpromazine and strains of *S. Typhimurium* and *E. coli* lacking a functional AcrB pump and sequencing the RNA of *S. Typhimurium* exposed to chlorpromazine.

6.2 Hypothesis

- Exposure of *S. Typhimurium* SL1344 to chlorpromazine and Pa β N will result in a global stress response and upregulation of *acrAB-tolC* and its regulatory genes.
- The transcriptomic profile of *S. Typhimurium* SL1344 exposed to chlorpromazine will be similar to that of *S. Typhimurium* exposed to the competitive efflux inhibitor Pa β N.
- Mutant selection experiments with *S. Typhimurium* AcrB D408A and *E. coli* AcrB D408A, both lacking a functional AcrAB-TolC efflux pump, will reveal a different mechanism of chlorpromazine resistance compared to that revealed in mutants selected for wild type *S. Typhimurium* and *E. coli*.

6.3 Aims

- To analyse RNA-sequencing data to determine the transcriptomic changes in *S. Typhimurium* SL1344 that result from exposure to chlorpromazine at efflux inhibitory concentrations.
- Compare the transcriptomic changes that result from chlorpromazine exposure in *S. Typhimurium* against those that result from exposure to Pa β N.
- To design mutant selection experiments with *S. Typhimurium* SL1344 and *E. coli*

MG1655 AcrB D408A mutants to elucidate the molecular targets responsible for chlorpromazine resistance in the absence of a functional AcrAB-TolC efflux pump.

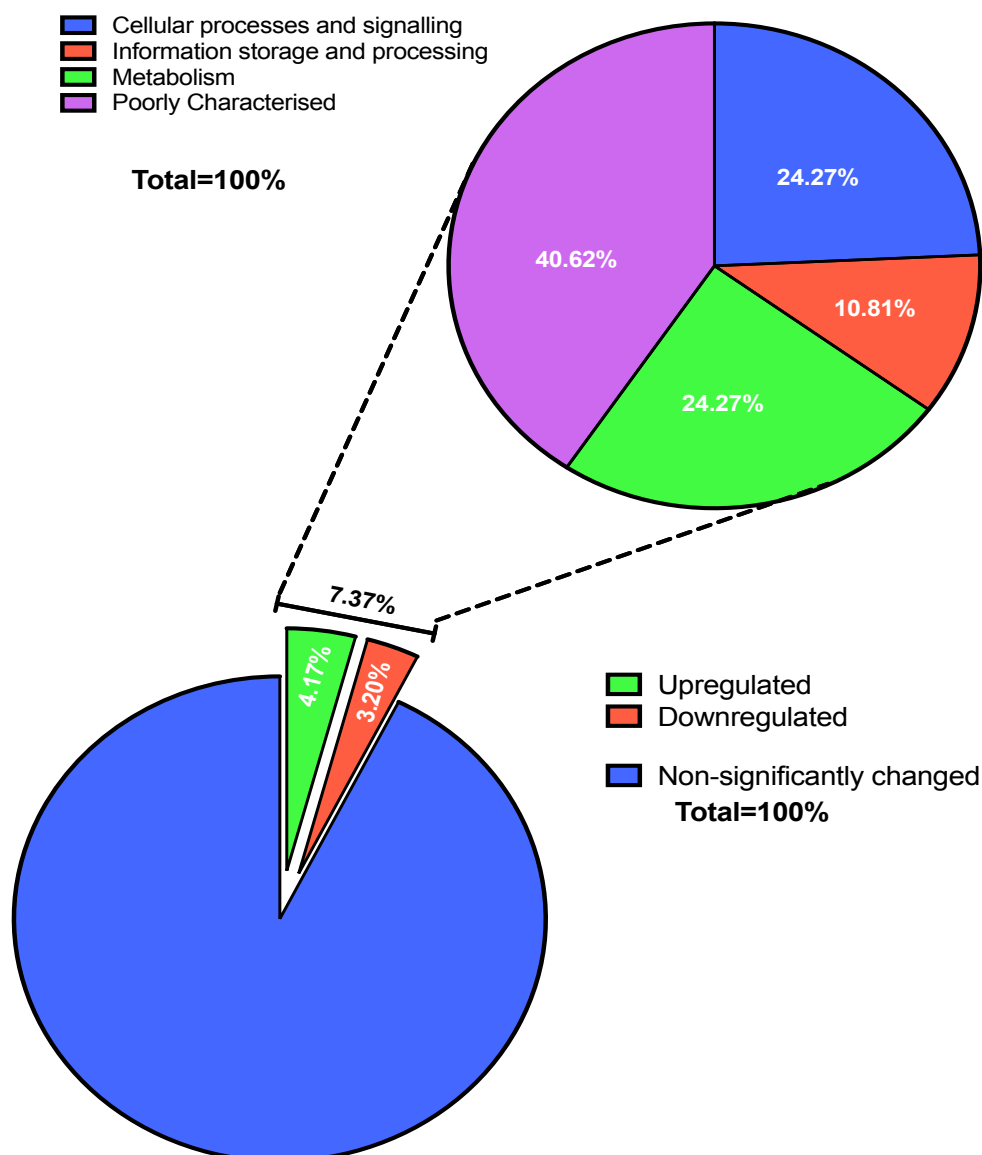
6.4 Impact of chlorpromazine on the transcriptomic profile of *S. Typhimurium* SL1344

To understand the physiological effects that occur upon exposure to efflux inhibitory concentrations of chlorpromazine (50 µg/ml) or PaβN (100 µg/ml), isolated RNA of *S. Typhimurium* SL1344 post 60 minute exposure to chlorpromazine/PaβN was sequenced. The paired-end RNA sequencing data for both chlorpromazine and PaβN was deposited in ArrayExpress on 12/06/2020 (accession no. E-MTAB-8190). Relative to the unexposed control strain, transcriptomic analysis revealed that in the presence of chlorpromazine 7.37% of the 5,225 genes in SL1344 were significantly ($\text{adjP} > 0.05$) altered in their transcription (Figure 6.1). The transcription of 56.62 % (218) was upregulated and of 43.38% (167) was downregulated.

The genes for which increased transcription were observed (Figure 6.2) included those encoding metabolic proteins (*treF*, *fumC*, *nfnB*, *acnA*, *yhbo* and *acs*), general stress response proteins (*asr*, *htrA*, *uspAB*, *cpxP*) membrane proteins (*ompC*, *ybdJ* and SL1344_3010), DNA repair proteins (*recA* and *recN*), fimbrial proteins (*fimCD*, *fimI*) transcriptional regulators (*ramA*, *ramR* and *yhjB*), SlsA encoded within *Salmonella* pathogenicity island (SPI) three and several conserved hypothetical proteins (*ybdF*, *tpeC*, *yhfG*, *yhcN*, *yddx*, *bssS*, *yacL*, *yaiB*). Importantly, the genes encoding AcrB, TolC, RamA, RamR, MarA and Lon were upregulated. Each of these genes are involved in the expression and regulation of the AcrAB-TolC multidrug efflux pump.

The genes for which decreased transcription was observed were primarily virulence and motility genes of the Type III secretion system (TTSS), which were either located

Figure 6.1: Percentage of *S. Typhimurium* SL1344 genes that were significantly changed upon exposure to chlorpromazine compared to unexposed SL1344 and classification of the significantly changed genes into COG categories.



The percentage is shown as the proportion of significantly altered genes that belong to each class; calculated by dividing the number of significantly altered genes by the total number of genes.

Chlorpromazine and amitriptyline may elicit their activity through interactions with AcrB

within SPI 1-5, or are effectors proteins transported via SPI TTSS but are encoded elsewhere on the chromosome. These include *sopE*, *sopE2*, *sptP*, *spaOPQRS*, *sipABCD*, *invABC*, *invEFGHIJKR*, *orgAB*, *hilA*, *hilC* and *rtsAB* of SPI-1 and *ssaBCDE*, *ssaGHIJKLMNOP*, *ssaRSTUV*, *sseABCDEF*, *sseIJKL*, *sscAB*, *sifA* and *srcA* of SPI-2 and *pipBC* of SPI-5. In addition, the genes encoding the type IV pilin family (*pilMNOPQRSTUV*) and OmpF were also downregulated.

To facilitate the interpretation of this data, the significantly altered genes were assigned to a COG class from the *Salmonella* SL1344 COG database. This database (4,615 genes) does not include RNA and plasmid encoded genes. The four COG categories (information, storage and process, cellular processes and signaling, metabolism and poorly characterized) are subdivided to give a total of 22 COG classes by which genes can be grouped with those that encode proteins with similar functions (Table 6.1).

Analysis of the COG classes revealed that the majority of significantly altered genes belonged to the following COG categories: “function unknown” (38.90 %), “intracellular trafficking, secretion and vesicular transport” (19.53 %), “cell motility” (10.74 %), “signal transduction mechanisms” (9.64 %) and “lipid transport and metabolism” (9.38 %). Analysis of the COG classifications confirmed that the majority of significantly upregulated genes upon exposure to chlorpromazine are confirmed or suggested to encode membrane proteins, transcriptional regulators or metabolic proteins (Figure 6.3). The COG classes with the greatest differential increase in transcription were “posttranslational modification and protein turnover” (7.64 %), “signal transduction mechanisms” (6.59 %), “cell wall/membrane/envelope biogenesis” (5.74 %), “carbohydrate transport and metabolism” (5.18 %), “energy production and conversion” (5.14 %), “inorganic ion transport and metabolism” (4.45 %) and “transcription” (4.20 %). Confirming the majority of downregulated genes are virulence genes located within SPI-1 and SPI-2 COG analysis revealed the COG classes with the greatest differential decrease in transcription were

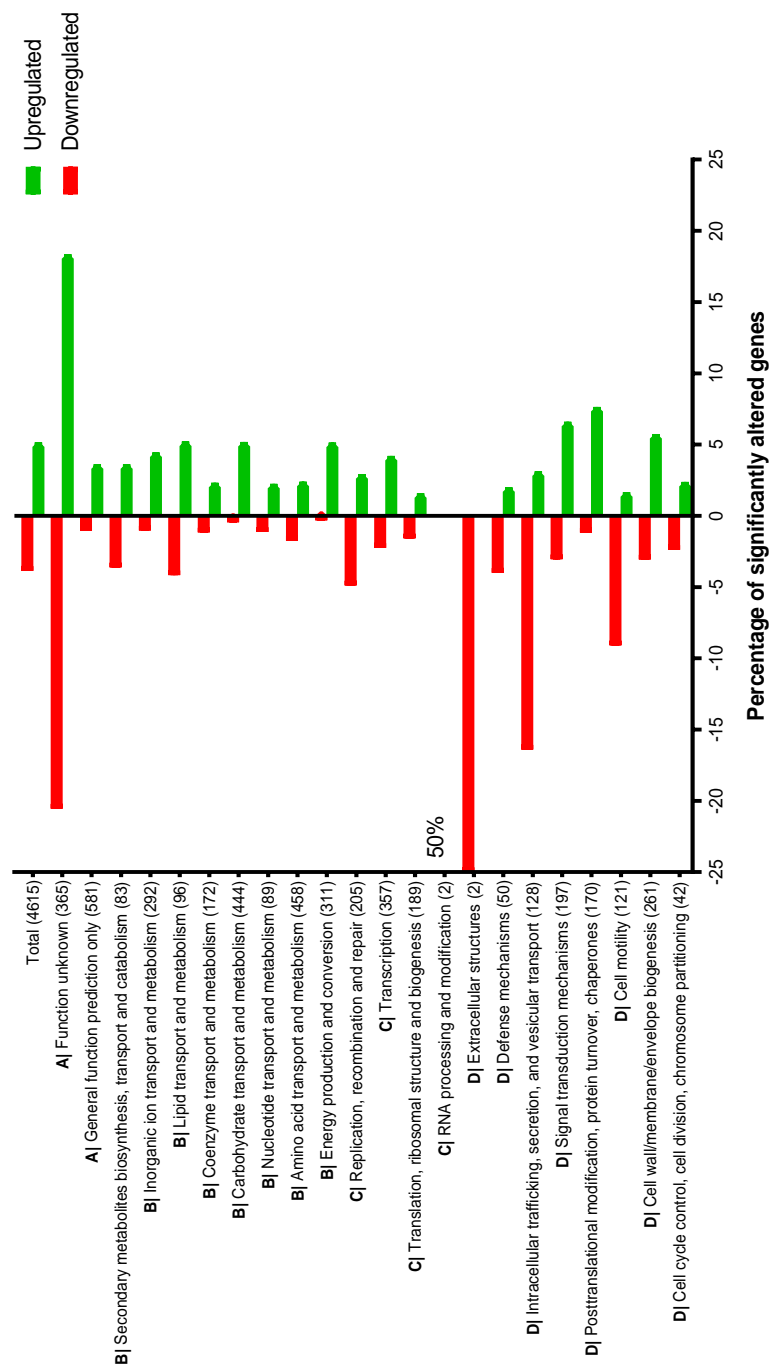
Chlorpromazine and amitriptyline may elicit their activity through interactions with AcrB

“intracellular trafficking, secretion and vesicular transport” (16.4 %) and “cell motility” (9.09%). The genes within the remaining COG classes were upregulated and downregulated in roughly equal proportion upon exposure to chlorpromazine.

Table 6.1 COG classes

COG category		COG class	Number of genes
A	Poorly characterised	Function unknown	365
		General function prediction only	581
		Energy production and conversion	311
		Amino acid transport and metabolism	458
		Nucleotide transport and metabolism	89
B	Metabolism	Carbohydrate transport and metabolism	444
		Coenzyme transport and metabolism	172
		Lipid transport and metabolism	96
		Inorganic ion transport and metabolism	292
		Secondary metabolites biosynthesis, transport and catabolism	83
		RNA processing and modification	2
C	Information storage and processing	Translation, ribosomal structure and biogenesis	189
		Transcription	357
		Replication, recombination and repair	205
		Cell cycle control, cell division, chromosome partitioning	42
		Cell wall/membrane/envelope biogenesis	261
		Cell motility	121
D	Cellular processing and signalling	Posttranslational modification, protein turnover, chaperones	170
		Signal transduction mechanisms	197
		Intracellular trafficking, secretion, and vesicular transport	128
		Defense mechanisms	50
		Extracellular structures	2

Figure 6.3: Percentage genes within each COG class that were significantly altered upon exposure to chlorpromazine.



The percentage of genes belonging to each class was calculated by the number of significantly altered genes divided by the total number of genes in a given class. COG classes are divided into categories as follows A; Poorly characterized . B; Metabolism. C; Information storage and processing. D; Cellular processes and signaling.

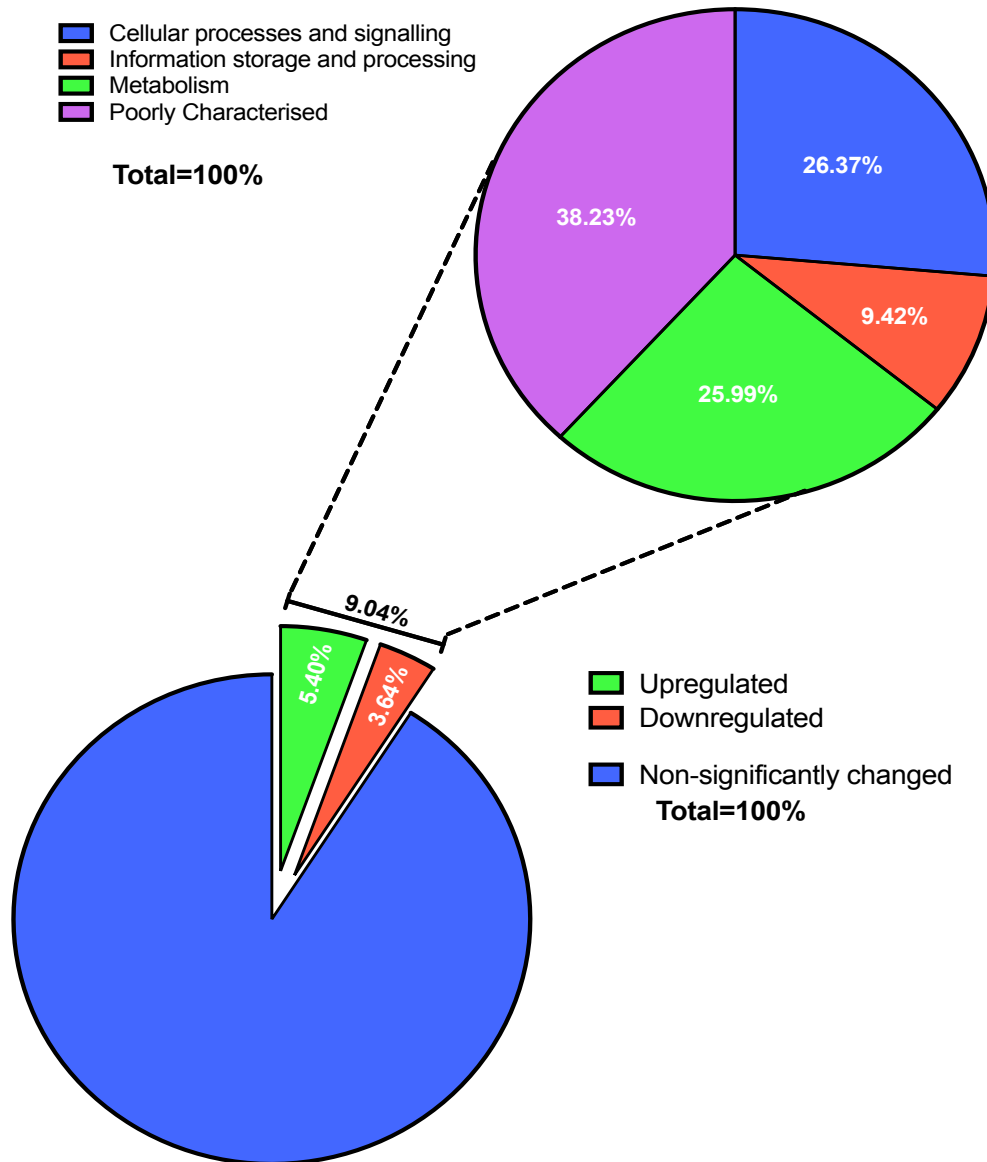
6.5 Impact of Pa β N on the transcriptomic profile of *S. Typhimurium* SL1344

Transcriptomic analysis revealed that, relative to the unexposed control strain, in the presence of Pa β N, 9.04% of the 5,225 genes in SL1344 were significantly (adjP >0.05) differentially transcribed (Figure 6.4 and 6.5). Of which the transcription of 59.75% (282) was upregulated and of 40.25 % (190) was downregulated.

The genes for which increased transcription was observed included those involved in the stress response (Figure 6.5). These included genes encoding DNA repair proteins (*umuD* and *recN*), metabolic proteins (*fkpA*, *bioAB*, *bioF* *yfcG*, *phoN*, *yecD* and *hypA*), membrane proteins (*yiaD* and *yeaY*), general stress response proteins (*htrA*, *asr* and *cutC*), the sigma factor *rpoE* and its regulatory proteins (*rseABC*), SlsA encoded within SPI three and several hypothetical proteins (*yggN*, *yaiB*, *ygbE*, *yncC*, *pagN*, *ybhB*, *ycfR* and *yjiS*). In addition, several non-coding RNA's (RyeF, RyeF_LT2, STnc1400_47 and *tisB-istR_TA*) were upregulated upon exposure to Pa β N.

Like chlorpromazine, the gene products for which decreased transcription was observed, upon exposure to Pa β N, were primarily virulence and motility genes found within, or transported by, SPI TTSS. These include: *sopAB* *sopE*, *sopE2*, *sptP*, *spaOPQRS*, *sipABCD*, *invABC*, *invEFGHIJKR*, *orgAB*, *hilA*, *hilC*, *hilD* and *rtsAB* of SPI-1, *siiA*, *siiDEF* of SPI-4 and *pipC* of SPI-5. In addition, the genes encoding the type IV pilin family (*pilMNOPQRSTUVWXYZ*), fimbriae proteins (*fimA*, *fimC*, *fimD*, *fimI*, *fimZ*, *stcA*, *pefA*, *traA*), flagellar proteins (*flgB*, *flgKLMN*. *fliBCD*, *fliM* *fliST*, *fliH*), chemotaxis proteins (*tsr*, *tcp*, *cheAB*, *cheM*, *cheR*, *cheW*, *cheYZ*) and OMP (*ompC*, *ompD*, *ompF* and *ompW*) were also downregulated.

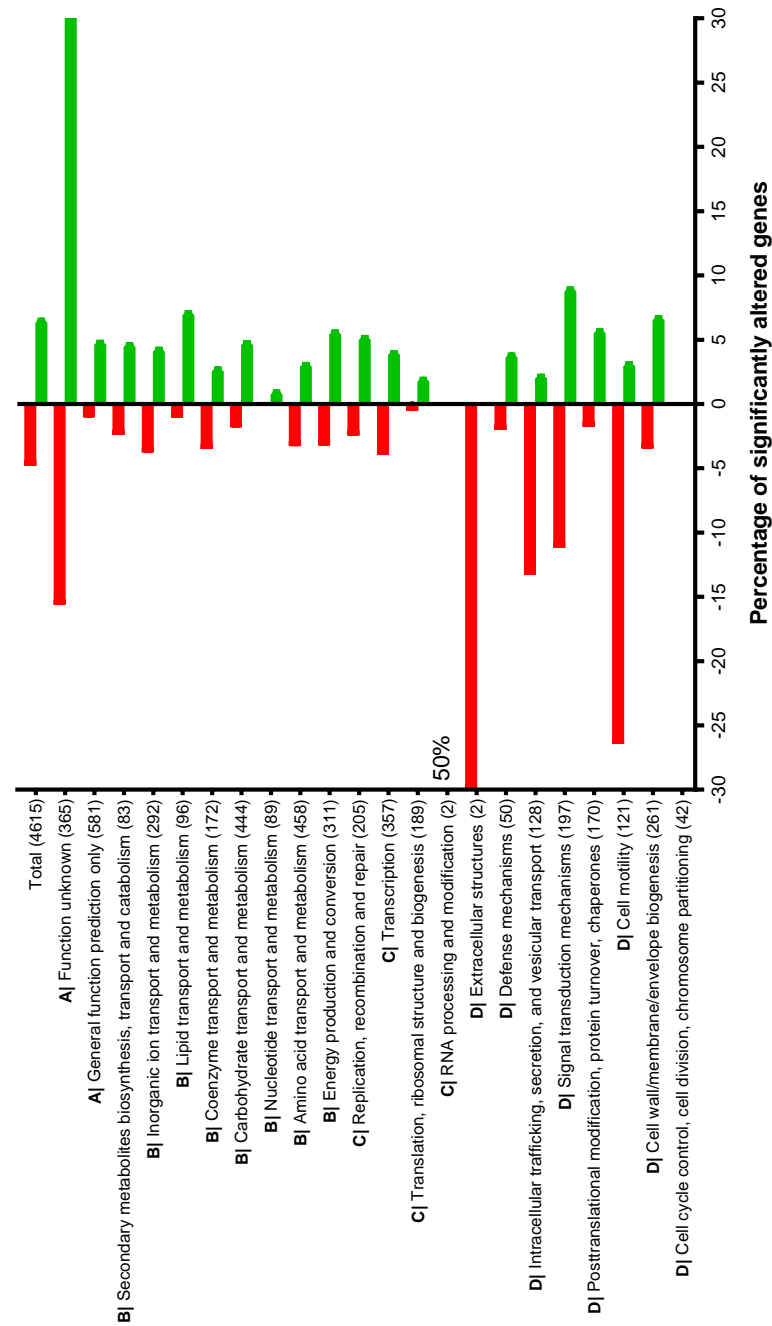
Figure 6.4: Percentage of *S. Typhimurium* SL1344 genes that were significantly changed upon exposure to Pa β N compared to unexposed SL1344 and classification of significantly changed genes into COG categories.



The percentage is shown as the proportion of significantly altered genes that belong to each class; calculated by dividing the number of significantly altered genes by the total number of genes.

Analysis of the COG classes revealed that the majority of differentially transcribed genes belonged to the following COG categories (Figure 6.6): “Function unknown” (46.03%), “cell motility” (29.7 %), “signal transduction mechanisms” (20.30 %), “intracellular trafficking, secretion and vesicular transport” (15.6%), “cell wall/membrane/envelope biogenesis” (10.34%) and energy production and conversion (9.00%). Those with the greatest differential increase in transcription were “lipid transport and metabolism” (7.29%), “cell wall/membrane/envelope biogenesis” (6.89%), “posttranslational modification and protein turnover” (5.88%), “energy production and conversion” (5.78%) and “replication, recombination and repair” (5.36%). Confirming the majority of downregulated genes are virulence genes located within SPI-1, COG analysis revealed the COG classes with the greatest differential decrease in transcription were “cell motility” (26.44%) and “intracellular trafficking, secretion and vesicular transport” (13.28%). The remaining COG classes were up or downregulated in equal proportion upon chlorpromazine exposure.

Figure 6.6: Percentage of genes within each COG class that were significantly altered upon exposure to Pa β N.



The percentage of genes belonging to each class was calculated by the number of significantly altered genes divided by the total number of genes in a given class. COG classes are divided into categories as follows A; Poorly characterized . B; Metabolism. C; Information storage and processing. D; Cellular processes and signaling.

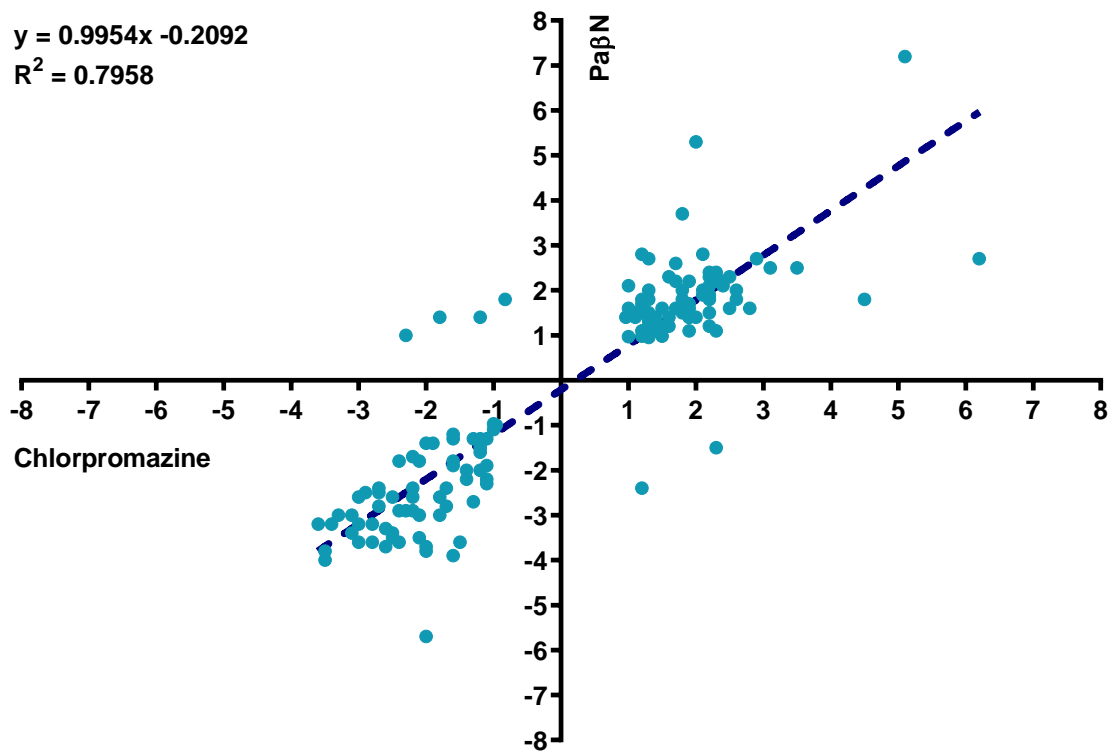
6.6 Comparison of the transcriptome of *S. Typhimurium* SL1344 post exposure to chlorpromazine and Pa β N

Chlorpromazine is hypothesised to be a competitive inhibitor of AcrB (Chapter 3). Therefore, to determine the activity of chlorpromazine in relation to a known competitive efflux inhibitor, the transcriptome of SL1344 exposed to chlorpromazine was compared against that of SL1344 exposed to Pa β N. In total, there were 710 genes that were significantly changed upon exposure to either chlorpromazine or Pa β N. Of these, 147 (20.70 %) were significantly changed in both conditions including 141 (95.92 %) which were changed in the same direction. A positive correlation between the two datasets was quantified by an R^2 value of 0.79 (Figure 6.7). In addition, comparison of the percentage of genes within each COG class that are significantly altered upon exposure to chlorpromazine or Pa β N showed the percentage of genes that were up/downregulated were similar for the majority of COG classes (Figure 6.8). Together, these data suggested these compounds behave in a similar manner.

6.7 Comparison of the transcriptome of *S. Typhimurium* SL1344 post exposure to chlorpromazine and Pa β N against *S. Typhimurium* SL1344 AcrB D408A.

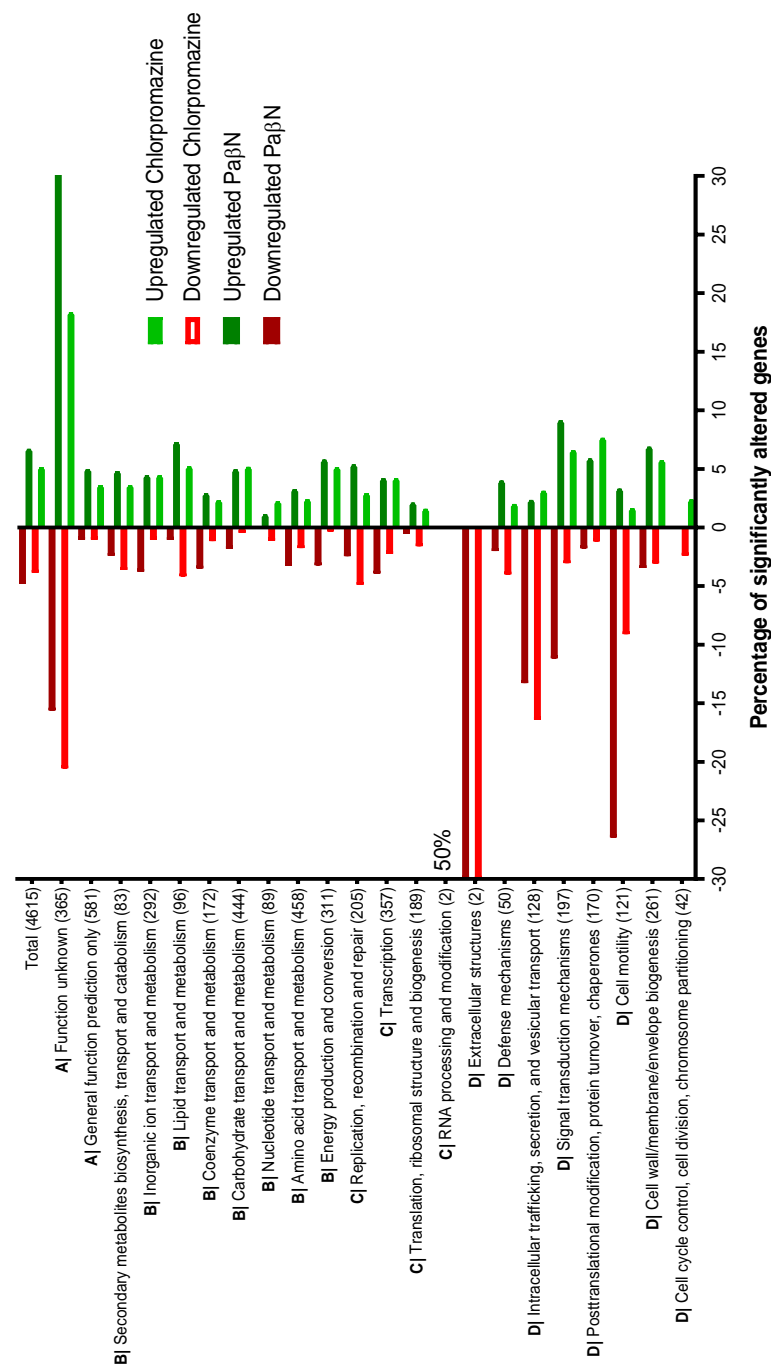
Chlorpromazine and Pa β N are suggested to elicit their activity as an efflux inhibitor through interactions with AcrB. Therefore, the transcriptome of SL1344 exposed to chlorpromazine and Pa β N was compared to the transcriptional landscape of SL1344 AcrB D408A, lacking a functional AcrB pump. When comparing SL1344 exposed to chlorpromazine and SL1344 AcrB D408A, in total, 82 genes were significantly altered relative to wild type SL1344 in both conditions. Of these, 54 (65.85%) were changed in the same direction. A very weak correlation was quantified by an R^2 value of 0.2497 (Figure 6.9).

Figure 6.7: Comparison of the Log2FC values between *S. Typhimurium* SL1344 exposed to chlorpromazine or PaβN for each significantly transcribed gene.



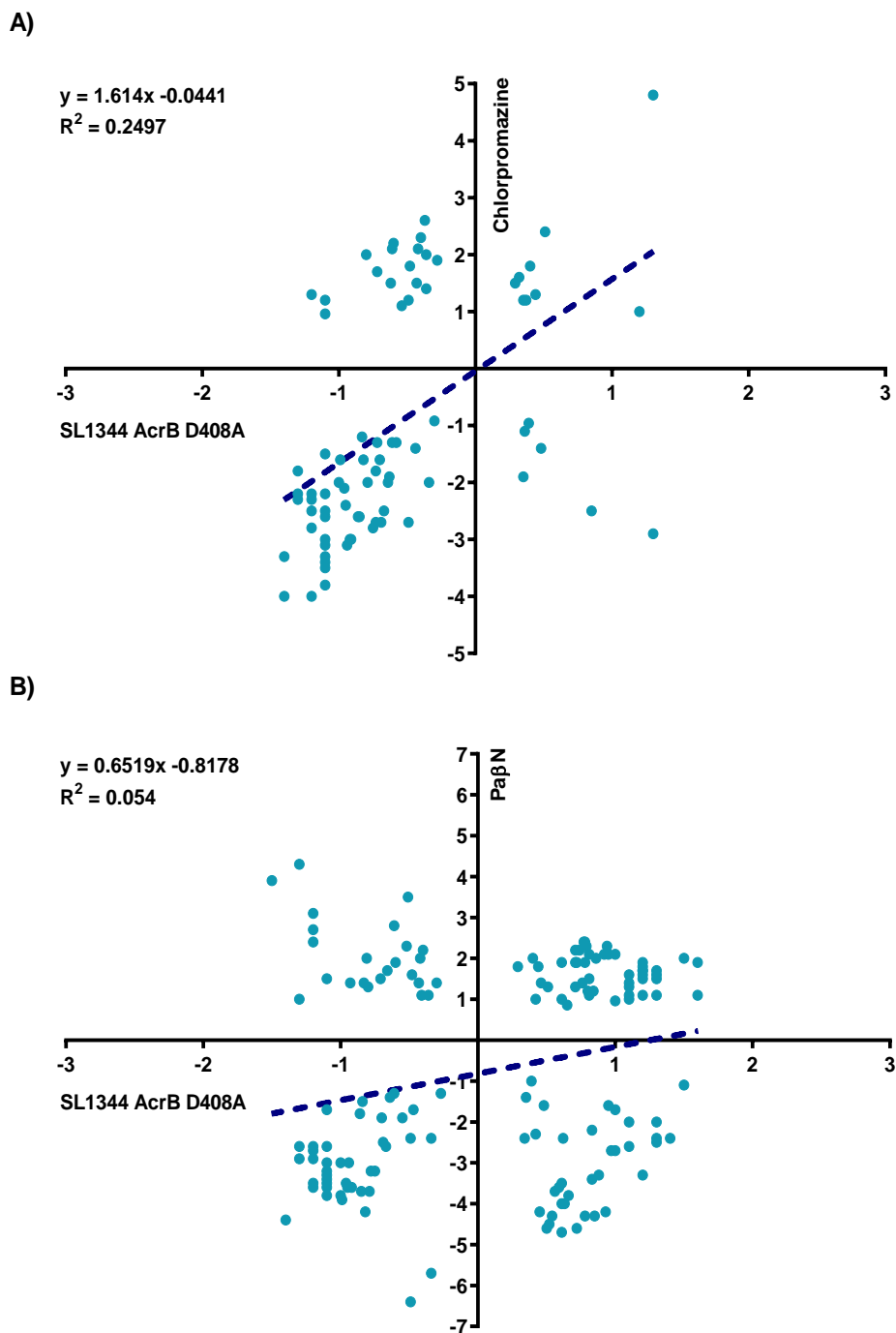
A Pearson's correlation was used to determine the R^2 value.

Figure 6.8: Comparison of the percentage of genes within each COG class for chlorpromazine and PaβN.



The percentage of genes belonging to each class was calculated by the number of significantly altered genes divided by the total number of genes in a given class. COG classes are divided into categories as follows A; Poorly characterized . B; Metabolism. C; Information storage and processing. D; Cellular processes and signaling.

Figure 6.9: Comparison of the Log2FC values of SL1344 exposed to (A) chlorpromazine or (B) PaβN for each significantly transcribed gene against SL1344 AcrB D408A.



A Pearson's correlation was used to determine the R^2 value.

For Pa β N vs SL1344 AcrB D408A, 154 genes were significantly altered in both conditions relative to wild type SL1344. Of these, 95 (61.69 %) were changed in the same direction. Linear regression analysis revealed an R^2 of 0.054 indicating no correlation between the two datasets (Figure 6.9).

6.8 Selection of chlorpromazine-resistant mutants for strains lacking a functional AcrB protein

In wild type *S. Typhimurium* SL1344 and *E. coli* MG1655, exposure to chlorpromazine resulted in the selection of mutants containing a substitution within RamR and frameshifts within MarR (Chapters 4 and 5). This evidence, alongside molecular dynamics simulations that show chlorpromazine is able to interact directly with the AcrB pump protein (Chapter 3), suggest that chlorpromazine may be a competitive substrate of AcrB. To elucidate if chlorpromazine has another mode of action independent of its ability to bind AcrB, mutant selection experiments were designed in which chlorpromazine resistance was selected in strains of *S. Typhimurium* SL1344 and *E. coli* MG1655 that contain a substitution within the proton relay network of AcrB (D408A) that renders this pump protein non-functional and unable to export AcrB substrates (Wang-Kan et al., 2017).

6.8.1 Chlorpromazine-resistant *S. Typhimurium* SL1344 AcrB D408A mutants were selected

S. Typhimurium SL1344 AcrB D408A chlorpromazine-resistant mutants were selected at 60 μ g/ml. The mutation frequency and rate was 2.79×10^{-11} CFU/ml and 3.44×10^{-10} CFU/ml, respectively. The MIC of chlorpromazine for each mutant was 256 μ g/ml; four doubling dilutions higher than the MIC of the parental strain. The MIC of SL1344 AcrB D408A and SL1344 AcrB WT were 64 μ g/ml and 256 μ g/ml, respectively (Table 6.2). In addition, relative to SL1344 AcrB D408A, the MICs of Pa β N, ciprofloxacin, nalidixic acid,

Chlorpromazine and amitriptyline may elicit their activity through interactions with AcrB

chloramphenicol, tetracycline and ethidium bromide, were increased for all mutants.

Table 6.2 Minimal inhibitory profiles (MIC) of chlorpromazine-resistant *S. Typhimurium* SL1344 AcrB D408A.

Strain	Selecting concentration ($\mu\text{g/ml}$)	MIC ($\mu\text{g/ml}$)						
		CPZ	Pa β N	CIP	CHL	TET	NAL	ETBR
SL1344 AcrB WT		256	512	0.03	4	2	8	1,024
SL1344 AcrB D408A		64	64	<0.008	1	1	2	256
1	60	256	>1,024	0.03	4	4	4	>1,024
2	60	256	1,024	0.03	4	4	4	>1,024
3	60	256	>1,024	0.06	8	8	8	>1,024
4	60	256	1,024	0.03	8	8	8	>1,024
5	60	256	1,024	0.03	4	4	4	>1,024
6	60	256	>1,024	0.03	4	4	4	>1,024

CPZ, chlorpromazine; Pa β N, phenylalanine-arginine beta-naphthylamide; CIP, ciprofloxacin; CHL, chloramphenicol; TET, tetracycline; NAL, nalidixic acid; ETBR, ethidium bromide. The wild type parental strains are shown in blue. A decrease in susceptibility is shown in red. The mode of three biological replicates is shown.

A single mutant (Strain 1) was sent for WGS by BGI genomics, Hong Kong. Analysis of the sequence revealed that the mutant did not contain the A→C SNP at nucleotide position 1,223/3,147 of *acrB* that confers the D408A substitution and instead possessed a wild type *acrB* gene. Mapping of the resistant mutant against the wild type SL1344 sequence revealed the absence of this SNP on the forward strand at position 503,622 of the chromosome (Figure 6.10). The reversion from the mutant C allele to the wild type A allele was confirmed by PCR of the *acrB* gene and DNA sequencing of the amplicons (Figure 6.10).

6.8.2 The mutated gene conferring AcrB D408A in *S. Typhimurium* consistently reverts to the wild type allele upon exposure to chlorpromazine and amitriptyline

In order to confirm that the observed reversions of *S. Typhimurium* SL1344 AcrB D408A to wild type SL1344 was a result of exposure to chlorpromazine, further mutant selection experiments were performed in which three biological replicates, each divided into 34 technical replicates, were plated onto LB agar containing 60 µg/ml of chlorpromazine. Each biological replicate was also plated onto an LB plate containing no selective pressure as a negative control. In total, 152 mutants were selected upon exposure to chlorpromazine across all 104 plates and each had a higher MIC compared to SL1344 AcrB D408A; the MIC of chlorpromazine for all mutants and the wild type SL1344 was 256 µg/ml. The mutation frequency and rate was 1.82×10^{-10} and 5.94×10^{-10} mutations per cell/per generation, respectively (Table 2).

To determine whether the mutants reverted to the wild type SL1344 *acrB* gene, an allelic specific real time PCR was used to identify the presence or absence of allele 1223C conferring the D408A substitution within *S. Typhimurium* SL1344. This method allows the detection of a single SNP by the use of two allele-specific primers that only amplify their complementary allele; one specific for the wild type allele (1223A) and one specific for the mutant allele (1223C). Real time PCR of 100 mutants from independent selective plates resulted in a binding curve for the wild type allele for all mutants with no accompanying curve for the mutant allele. This showed that 100% of the mutants had reverted from the mutant allele (1223C) to the wild type sequence (1223A) (Table 6.3). The wild type SL1344 negative controls (plated onto an LB plate with no selective pressure) produced a binding curve for the mutant but not the wild type allele. This confirmed no contamination of the culture with the wild type strain.

Table 6.3 Frequency and rate of mutation and reversion rate of the D408A mutation when *S. Typhimurium* AcrB (D408A) was exposed to chlorpromazine, amitriptyline, minocycline, spectinomycin and ethidium bromide.

Organism	Selecting drug	Selecting concentration (mg/ml)	Mutation frequency (CFU/ml)	Mutation rate (CFU/ml)	Total number of mutants	Reversion rate (%)
<i>S</i> <i>Typhimurium</i> SL1344 AcrB D408A	Chlorpromazine	60	1.82 x 10 ⁻¹⁰	5.94 x 10 ⁻¹⁰	152	100
	Amitriptyline	110	3.87 x 10 ⁻¹¹	1.44 x 10 ⁻¹⁰	43	100
	Minocycline	0.5	6.48 x 10 ⁻¹⁰	1.399 x 10 ⁻⁹	702	2
	Ethidium bromide	64	4.04 x 10 ⁻⁹	4.95 x 10 ⁻⁹	4,199	3
	Spectinomycin	128	5.46 x 10 ⁻¹⁰	1.34 x 10 ⁻⁹	459	0

Following the evidence that exposure of *S. Typhimurium* SL1344 AcrB D408A to chlorpromazine resulted in reversion to the wild type *acrB* sequence, the mutant selection experiment was repeated with amitriptyline. Given that amitriptyline also appears to possess efflux inhibitory properties through interactions with AcrB (Chapter 3), the use of this compound in this experiment was to determine whether reversion was specific to chlorpromazine exposure or is a feature of other tricyclic drugs capable of efflux inhibition. Consistent with chlorpromazine, of the 43 mutants selected upon exposure to amitriptyline (mutation frequency and rate 3.87×10^{-11} and 1.44×10^{-10} mutations per cell/per generation, respectively), in 100% of the mutants the *acrB* sequence reverted to the wild type sequence, with no accompanying reversion of the negative control (Table 2).

It was hypothesised that there would be no evolutionary benefit of reversion to the wild type *acrB* sequence if these compounds were not AcrB substrates thereby furthering the evidence that chlorpromazine and amitriptyline are substrates of AcrB. To test this hypothesis and determine if this a feature common amongst AcrB substrates or a feature unique to compounds with efflux inhibitory properties, the mutant selection experiment was repeated with the known AcrB substrates minocycline and ethidium bromide and, as a control, to a non-substrate, spectinomycin.

In total, 702, 4,199 and 459 mutants were selected with minocycline (mutation frequency and rate 6.48×10^{-10} and 1.399×10^{-9} mutations per cell/per generation, respectively), ethidium bromide (mutation frequency and rate 4.04×10^{-9} and 4.95×10^{-9} mutations per cell/per generation, respectively) and spectinomycin (mutation frequency and rate 5.46×10^{-10} and 1.34×10^{-9} mutations per cell/per generation, respectively). Real time PCR of 100 mutants revealed that only 2% of the minocycline-resistant mutants and 3% of the ethidium bromide-resistant mutants reverted to the wild type allele (Table 2). None of the mutants selected upon exposure to spectinomycin had reverted.

6.8.3 Exposure to chlorpromazine does not result in reversion of *E. coli* MG1655 D408A to the wild type sequence

To determine whether reversion of the D408A substitution to the wild type sequence upon exposure to chlorpromazine was a feature shared amongst other species of bacteria with an AcrAB-TolC efflux pump, mutant selection experiments to select for chlorpromazine resistance were repeated with *E. coli* MG1655 AcrB D408A. *E. coli* MG1655 AcrB D408A mutants resistant to chlorpromazine were selected at 70 µg/ml. The mutation frequency and rate was 1.33×10^{-9} CFU/ml and 6.87×10^{-9} CFU/ml, respectively. MIC determination of 10 mutants revealed that for six mutants the MIC of chlorpromazine was 2-4 doubling dilutions higher than the MIC of MG1655 AcrB D408A (64 µg/ml) (Table 6.4). In addition, cross resistance to PaβN, ciprofloxacin, nalidixic acid, chloramphenicol, tetracycline and/or ethidium bromide was observed for seven mutants. Due to the low number of mutants selected, to determine whether reversion of the AcrB D408A substitution had occurred in the presence of chlorpromazine, PCR amplification of the *acrB* gene of *E. coli* MG1655 and subsequent DNA sequencing of the amplicons was performed instead of an allelic specific real time PCR. DNA sequencing of the *acrB* gene of the six chlorpromazine-resistant mutants revealed that each mutant possessed the mutant allele (1223C) indicating no reversion.

To confirm the DNA sequencing and determine what alternative mechanism conferred chlorpromazine resistance to MG1655 AcrB D408A, a single mutant (Strain 1) was sent for WGS by BGI genomics, Hong Kong. Analysis of the sequence confirmed the presence of the C→A SNP at nucleotide position 1,223/3,147 of *acrB* that confers the D408A substitution (Figure 6.11). In addition, a SNP (C→T) at nucleotide position 113/1,497 within the phosphatase transporter *pitB* conferring an A38V substitution was observed. Mapping of the chlorpromazine-resistant mutant against the wild type MG1655 sequence confirmed the presence of the SNPs conferring the D408A mutation within AcrB

Chlorpromazine and amitriptyline may elicit their activity through interactions with AcrB

(Figure 6.11) and A38V within PitB (Figure 6.12) on the forward strand at chromosome positions 482181 and 3136257, respectively. Both mutations were confirmed by PCR and DNA sequencing of the amplimers (Figure 6.11 and Figure 6.12). For future work it would be useful to determine whether this mutation is present in all 10 mutants. Or whether resistance of *E. coli* AcrB D408A to chlorpromazine was conferred by other/additional mutations

Table 6.4 Minimal inhibitory profiles (MIC) of chlorpromazine-resistant *E. coli* MG1655 AcrB D408A.

Strain	Selecting concentration ($\mu\text{g/ml}$)	MIC ($\mu\text{g/ml}$)						
		CPZ	Pa β N	CIP	CHL	TET	NAL	ETBR
MG1655 AcrB WT		256	1,024	0.03	16	4	8	1,024
MG1655 AcrB D408A		64	64	<0.008	2	2	4	128
1	70	256	1,024	0.06	16	8	32	>1,024
2	70	256	1,024	0.06	16	8	32	>1,024
3	70	256	1,024	0.06	16	4	32	>1,024
4	70	128	512	0.015	2	1	4	512
5	70	128	512	0.015	2	1	4	>1,024
6	70	128	512	<0.008	2	1	8	>1,024
7	70	128	256	<0.008	2	1	4	128
8	70	64	256	<0.008	2	1	4	128
9	70	64	256	<0.008	2	1	4	128
10	70	64	256	<0.008	2	1	4	256

CPZ, chlorpromazine; Pa β N, phenylalanine-arginine beta-naphthylamide; CIP, ciprofloxacin; CHL, chloramphenicol; TET, tetracycline; NAL, nalidixic acid; ETBR, ethidium bromide. The wild type parental strains are shown in blue. A decrease in susceptibility is shown in red and an increase in susceptibility is shown in green. The mode of three biological replicates is shown.

6.9 Discussion

In Chapters 3, 4 and 5, evidence was presented to suggest that chlorpromazine is a competitive inhibitor and substrate of the AcrAB-TolC efflux pump. This was based on two main observations (i) Chlorpromazine was able to bind to the hydrophobic trap of AcrB within the distal binding pocket, a known substrate binding site and interact with residues that are important for substrate recognition and/or transport and may competitively inhibit the efflux of other substrates of AcrB. (ii) Mutant selection experiments revealed that while resistance to chlorpromazine was conferred by mutations within *ramR* and *marR* of *S. Typhimurium* and *E. coli*, respectively, the presence of these mutations did not ablate the efflux inhibitory activity of this compound. Instead, the appearance of mutations within *ramR* and *marR* were proposed to be reflective of its nature as an AcrB substrate; mutations within *ramR* and *marR* resulted in *ramA* and *marA* mediated overexpression of *acrAB-tolC* that increased the efflux activity of *S. Typhimurium* and *E. coli*. This mechanism of resistance was unlikely to confer resistance to a non-AcrB substrate.

Irrespective of data showing a mechanism of chlorpromazine resistance and corroborating molecular docking and dynamics simulations to suggest chlorpromazine is an AcrB substrate and competitive inhibitor, chlorpromazine has been shown to possess off target effects that contribute to its antimicrobial activity. Therefore, it was hypothesised that this compound has global cellular effects independent of inhibition of AcrB, and thus its mode of action may be multifaceted. To explore the physiological changes that occur upon exposure of *S. Typhimurium* to chlorpromazine and further elucidate the mechanism of action of this compound, RNA sequencing data was analysed and compared to the transcriptomic profile of *S. Typhimurium* exposed to Pa β N; a competitive efflux inhibitor.

Comparison of the transcriptome of *S. Typhimurium* SL1344 post-exposure to chlorpromazine vs post exposure to Pa β N revealed that 95.92 % of the genes that were

significantly altered in both the chlorpromazine and Pa β N datasets were changed in the same direction suggesting that these compounds behave in a very similar manner. Analysis of the COG classes indicated that exposure to chlorpromazine and Pa β N resulted in an induction of the stress response accompanied by large metabolic changes and a decrease in virulence in relation to unexposed SL1344. Typically, exposure of bacteria to sub-lethal concentrations of antibiotics results in the alteration of the expression of stress response genes via a variety of different mechanisms (Narimisa et al., 2020). Therefore, it was unsurprising that the majority of genes significantly altered in response to chlorpromazine and Pa β N are genes involved in the bacterial response to cellular stress.

The RNA sequencing data revealed that chlorpromazine and Pa β N induce an SOS response. This was evidenced by the upregulation of *recA* and *recN* and the downregulation of *recR* upon exposure to chlorpromazine and the upregulation of *umuC*, *umuD*, *recEb* and *recN* in response to Pa β N. Each of these genes are DNA repair genes involved in the SOS response to damaged DNA and arrested DNA replication (Baharoglu and Mazel, 2014). Some antibiotics including fluoroquinolones and trimetoprim induce the SOS response through replication arrest by inhibiting DNA gyrase (Pohlhaus et al., 2005) and purine/pyrimidine synthesis (Lewin et al., 1991), respectively. Although Pa β N has not been revealed to damage DNA, chlorpromazine is able to bind DNA either by intercalation with, or stacking on the DNA helix (Ben-Hur et al., 1980; De Mol, Posthuma, et al., 1983; De Mol and Busker, 1984; Viola et al., 2003) and dsDNA breaks occur upon the transfer of electrons between the DNA and the cations of chlorpromazine (Viola et al., 2003). In addition to direct DNA damage, the SOS response can also be activated by indirect damage to DNA as a result of the production of ROS by antibiotics (Baharoglu and Mazel, 2014). Considering their antibacterial activity, chlorpromazine and Pa β N may induce an SOS response through DNA damage mediated by direct interaction with DNA or the production of ROS.

Here, RNA sequencing revealed an induction of the Cpx pathway by chlorpromazine as

evidenced by a 4.8 fold increase in the expression of *cpxP*. Thereby suggesting that alongside an SOS response chlorpromazine induces an envelope stress response mediated through the Cpx pathway. The Cpx response is a widely conserved envelope stress response and regulation of the Cpx pathway is somewhat complex. Under no stress, CpxP behaves as a negative regulator and binds the sensor kinase CpxA preventing its activity (DiGiuseppe et al., 2003). Considering its role as a negative regulator, it was previously assumed that upon exposure to envelope stress, CpxP would dissociate from CpxA allowing phosphorylation of CpxR and the subsequent activation of the Cpx pathway. However, *cpxP* is the most highly induced gene of the Cpx regulon upon envelope stress (DiGiuseppe et al., 2003; Delhaye et al., 2016) and in the presence, absence and overexpression of *cpxP* the Cpx pathway can still be activated (DiGiuseppe et al., 2003; Raivio, Popkin, et al., 1999).

In addition to an induction of the SOS response, PaßN increased the expression of several sigma factors and sigma regulatory genes involved in stress resistance including the *rpoE-rseABC* operon and *rpoH*. *rpoE* encodes the sigma factor σ^E which is involved in the bacterial envelope stress response (Raivio and Silhavy, 2001; Rouviere et al., 1995); induced in response to osmotic stress and heat shock (Rouviere et al., 1995; Raina et al., 1995; Bianchi et al., 1999). *rpoE* is encoded alongside the regulatory genes *rseA*, *rseB* and *rseC*. In unstressed cells, σ^E is sequestered by RseA bound to RseB. Upon exposure to cell envelope stress, RseA is degraded and σ^E is able to interact with RNA polymerase and initiate transcription. RscC is a positive regulator of σ^E (Missiakas et al., 1997). Despite previous evidence showing that the overexpression of *rseA* and *rseB* is lethal to *E. coli*, the *rpoE-rseABC* operon is under the control of two promoters; one of which is dependent on σ^E (Miticka et al., 2003). Therefore, overexpression of *rpoE* results in the concomitant overexpression of *rseABC* to prevent an uncontrolled increase in the release of σ^E (Bianchi et al., 1999; Kabir et al., 2005; Price et al., 2009). In addition to an increase in the expression of the *rpoE-rseABC* operon, *htrA* and *fkpA* (both involved in the heat shock response) were

also upregulated upon exposure to Pa β N. Both *htrA* and *fkpA* are part of the σ^E regulon and are upregulated in response to increased expression of *rpoE* (Kabir et al., 2005).

Exposure to Pa β N also resulted in the increased expression of *rpoH*. *rpoH* encodes the sigma factor σ^S and a rapid increase in the expression of this gene is known to result from exposure to stress conditions including oxidative stress, heat shock and nutrient deprivation (Bang et al., 2005; Gunsekere et al., 2006). The role of *rpoH* indicates Pa β N may induce additional stress responses (e.g. heat shock or oxidative stress) in addition to causing envelope stress. However, induction of other response pathways may not be directly caused by Pa β N and instead a result of increased *rpoE* expression; one of the three promoters of *rpoH* is activated directly by σ^E (Bang et al., 2005).

Both chlorpromazine and Pa β N appear to induce an envelope stress response mediated by the Cpx or σ^E pathway, respectively. However, it is important to note that in addition to an envelope stress response, exposure to chlorpromazine and Pa β N appears to induce an SOS response and results in the upregulation of additional stress response genes including *asr*, an acid stress response gene upregulated in response to both compounds. Therefore, the stress response that is observed upon exposure to chlorpromazine and Pa β N appears to be multifaceted.

Although transcriptomics have not been previously performed with chlorpromazine, the transcriptomic landscape of *P. aeruginosa* exposed to Pa β N has been revealed. Unlike the data presented here no significant stress response was induced, this was due to the concentration of Pa β N used (Rampioni et al., 2017). The authors stated the concentration of Pa β N used (27 μ g) was considerably lower than that at which envelope damaging effects occur. Despite not observing the same stress response Pa β N did result in the downregulation of virulence and motility genes, consistent with the impact of chlorpromazine and Pa β N on *S. Typhimurium*. The authors linked the reduction in virulence of *P. aeruginosa* to the

Chlorpromazine and amitriptyline may elicit their activity through interactions with AcrB

downregulation of genes involved in iron and phosphate acquisition and nitrogen metabolism (Rampioni et al., 2017). However, this link is not consistent with the chlorpromazine and Pa β N datasets presented here instead the exposure of *S. Typhimurium* to chlorpromazine and Pa β N primarily result in the upregulation of metabolic genes and phosphate acquisition genes (*pstS*).

It was hypothesised that the transcriptomic profile of *S. Typhimurium* SL1344 exposed to an efflux inhibitor might be similar to a strain of *Salmonella* lacking a functional AcrB efflux pump. Therefore, the transcriptome of SL1344 exposed to chlorpromazine or Pa β N was compared against a strain of *S. Typhimurium* SL1344 which contained an amino acid substitution (D408A) within AcrB (Appendix Figure 6.2). A linear regression analysis revealed that very little correlation was observed between the chlorpromazine or Pa β N and the SL1344 AcrB D408A datasets. Although a higher degree of similarity to SL1344 AcrB D408A was noted for chlorpromazine compared to Pa β N. Overall, this result was surprising, indicating that the presence of an efflux inhibitor, at least in the absence of an antibiotic, does not mimic the transcriptomic phenotype of an AcrB-efflux deficient strain.

A similarity between all three datasets was the induction of a general stress response. Like, chlorpromazine and Pa β N, the lack of a functional efflux pump resulted in the upregulation of several stress response genes (Wang-Kan et al., 2017). The loss of AcrB activity has been suggested to result in an intracellular accumulation of toxic metabolites, many of which are proteotoxic resulting in the misfolding of proteins and the formation of dsDNA breaks (Gophna et al., 2003; Wang-Kan et al., 2017). This was supported by the observation that SL1344 AcrB D408A showed an increase in the expression of *recA* and *lexA* indicating induction of the SOS response (Wang-Kan et al., 2017). Genes belonging to metabolic COG classes were primarily downregulated in SL1344 AcrB D408A. This was hypothesised to be as a result of an accumulation of metabolic by-products in the absence

Chlorpromazine and amitriptyline may elicit their activity through interactions with AcrB

of a functional pump (Wang-Kan et al., 2017). In which the accumulation of metabolic end products in the absence of a functional efflux pump is sensed by the bacterial cell and repression of the metabolic genes of a biosynthetic pathway can occur in order to reduce the intracellular concentration of a toxic metabolite (Wang-Kan et al., 2017).

Although a reduction in the expression of genes belonging to the metabolic COG classes was observed in SL1344 AcrB D408A (Appendix Figure 6.2), analysis of the COG categories revealed that exposure to chlorpromazine and Pa β N predominantly resulted in the upregulation of genes involved in metabolism. Together, this suggests that although inhibition of efflux conferred by a non-functional AcrB pump decreases the expression of metabolic pathways, metabolism was increased as a response to efflux inhibitors. This discrepancy between the metabolic response may be a reflection of the mechanism by which Pa β N and chlorpromazine inhibit efflux; chlorpromazine and Pa β N are proposed to be competitive inhibitors of AcrB, inhibiting the efflux of substrates by interfering with their binding and extrusion to and from the transporter. This means that, unlike SL1344 AcrB D408A, wild type AcrB is likely still functional regardless of the presence of chlorpromazine and Pa β N. Therefore, in the absence of a substrate, of which chlorpromazine and Pa β N are able to outcompete, the pump is able to efflux other AcrB substrates which are not so readily outcompeted by these inhibitors (these may include metabolites). This is supported by the evidence that Pa β N is not so effective against all AcrB substrates (e.g. tetracycline and carbenicillin) due to differences in AcrB binding sites (Sharma, Gupta, et al., 2019). This means that unlike SL1344 AcrB D408A, chlorpromazine and Pa β N may not inhibit efflux of all AcrB substrates and as such may not confer the same metabolic consequences.

Instead, the increase in the metabolic activity of *Salmonella* upon exposure to chlorpromazine and Pa β N is consistent with a stress response similar to that observed in response to low antibiotic concentrations. Upon exposure to severe stress that results in a slowing or complete inhibition of bacterial growth, the primary response is a redirection of

Chlorpromazine and amitriptyline may elicit their activity through interactions with AcrB

energy to maintenance and repair processes (Mathieu et al., 2016). In contrast, upon exposure to sub-lethal concentrations of antibiotics an increase in the expression of metabolic genes is observed, alongside induction of the stress response, in order to maintain rapid bacterial growth (Mathieu et al., 2016).

Upregulation of *acrA*, *acrB*, *tolC* and *ramA* have been shown to occur upon exposure to certain AcrAB-TolC substrates in order to promote extrusion of a given antibiotic (Lawler et al., 2013; Nikaido, Yamaguchi, et al., 2008). The chlorpromazine-induced upregulation of each of these AcrAB-TolC efflux genes is further evidence to suggest that chlorpromazine may itself be a substrate of the AcrAB-TolC efflux pump. This is supported by previous observations that hypersusceptibility to chlorpromazine occurs in strains with deletions in efflux pump genes (*acrB*, *acrD*, *acrF* and, *tolC*) or regulatory genes (*marA* and *ramA*) (Bailey et al., 2008; Yamasaki, Fujioka, et al., 2016). The accompanying evidence that chlorpromazine does not cause upregulation of any genes involved in the activity or regulation of any additional efflux pumps suggests the activity of chlorpromazine may be selective for AcrAB-TolC. Interestingly, the exposure of *S. Typhimurium* to Pa β N did not result in the upregulation of *acrAB-tolC* or any of its regulatory genes. This suggests that, unlike chlorpromazine, Pa β N may not be a substrate of AcrAB-TolC, despite evidence to the contrary (Kinana et al., 2016) and therefore in the absence of an antibiotic substrate upregulation of genes involved in the activity or regulation of AcrAB-TolC would provide no fitness benefit. Hence why the same mechanism of Pa β N and chlorpromazine resistance were not observed. It is important to note that the hypothesis that compounds can be distinguished as 'substrates' and 'non substrates' on the basis of the upregulation of efflux pump genes needs to be carefully considered as Pa β N has been previously observed, by way of a nitrocefin hydrolysis assay, to be a 'good' substrate of AcrB (Kinana et al., 2016). Nonetheless, this discrepancy in the expression of AcrAB-TolC genes between chlorpromazine and Pa β N is an interesting

observation. Additionally, despite not overexpressing *acrAB-TolC*, PaβN did result in a small (0.98 fold) upregulation of *acrE* encoding the pump protein AcrE of the AcrEF-TolC efflux pump suggesting that PaβN may alter the activity of multiple efflux pumps of *S. Typhimurium*.

RNA sequencing revealed that, in the presence of chlorpromazine, upregulation of the transcriptional activator *ramA* occurred. Previously, upregulation of *ramA* has been linked to efflux inhibition; with chlorpromazine and amitriptyline resulting in the upregulation of *ramA* (Lawler et al., 2013). However, neither SL1344 AcrB D408A or exposure to PaβN resulted in the upregulation of *ramA*. This suggests that upregulation of *ramA* is not directly a consequence of loss of AcrB function or inhibition. Interestingly, while loss of AcrB function did not increase the expression of *ramA*, the complete loss of the AcrB protein (SL1344 Δ *acrB*) did (Wang-Kan et al., 2017). Previously, this was hypothesized to be a consequence of membrane instability resulting from the loss of a large membrane protein (Wang-Kan et al., 2017). However, both chlorpromazine and PaβN result in membrane instability (Lamers et al., 2013; De Filippi et al., 2007), but only chlorpromazine induced *ramA* expression and therefore is hypothesised that upregulation of this regulator in response to chlorpromazine simply reflects the property of chlorpromazine as a substrate of AcrB and was not a consequence of membrane instability.

In addition to the upregulation of *ramA*, exposure to chlorpromazine also increased the expression of *ramR*. Given that RamR binds the promoter of *ramA* preventing overexpression of *acrAB-tolC*, it was surprising that overexpression of *ramR* was observed alongside the increased expression of *ramA*. It is hypothesised that upregulation of this transcriptional repressor occurs as a part of a negative feedback loop to reduce the increased expression of AcrAB-TolC that occurs upon exposure to chlorpromazine.

Thus far, the RNA sequencing data suggests that PaβN and chlorpromazine behave

Chlorpromazine and amitriptyline may elicit their activity through interactions with AcrB

in a similar manner reflecting their shared antimicrobial activity and proposed role as competitive efflux inhibitors. Molecular dynamics simulations have shown that chlorpromazine is also able to bind to the same locations as other AcrB substrates and interfere with their binding. The additional evidence that exposure to chlorpromazine resulted in the upregulation of efflux pump genes, an observation common amongst AcrB substrates, shone light on its mechanism of competitive inhibition; preferential binding and extrusion. Chlorpromazine is hypothesised to be a preferential AcrB substrate, able to bind to and be extruded by AcrB before other less preferential substrates. Pa β N is proposed, by way of computational studies, to elicit its competitive action by binding to the hydrophobic trap at the same locations as AcrB substrates and by interfering with the functional rotation of the AcrB pump through interference with the G-loop thereby inhibiting the binding and extrusion of AcrB substrates (Sjuts et al., 2016; Vargiu and Nikaido, 2012; Nakashima, Sakurai, Yamasaki, Nishino, et al., 2011; Eicher, Cha, et al., 2012; Cha et al., 2014). A previous study has stated Pa β N is a 'good' substrate of AcrB. However, here Pa β N did not elicit a transcriptomic response that is indicative of an AcrB substrate. Therefore, at this stage, unlike chlorpromazine a distinction between its mode of competitive inhibition as a substrate of AcrB cannot be made.

An interesting observation is the differential transcription of OMP genes upon exposure to chlorpromazine and Pa β N. Chlorpromazine reduced the expression of *ompF* and increased the expression of *ompA*, *ompC* and *ompR*, while Pa β N reduced the expression of *ompA*, *ompC*, *ompD*, *ompF* and *ompW* and increased the expression of *ompR*. The downregulation of porin genes is frequently observed upon exposure to antibiotics in order to reduce the influx of these toxic compounds into the intracellular environment (Dupont et al., 2007; Fernández et al., 2012). Therefore, it is unsurprising that exposure to Pa β N resulted in a reduction in the expression of multiple porins. However, the response of the OM to chlorpromazine does not appear to be as severe

compared to that induced by Pa β N. This may be a function of the mechanism by which these compounds induce a stress response. As previously mentioned, it is proposed that Pa β N primarily induces a σ^E stress response while chlorpromazine induces the Cpx pathway. It is known that induction of a σ^E response results in a reduction in the expression of *ompF* and *ompC* (Batchelor et al., 2005) whereas induction of the Cpx pathway decreases *ompF* expression with concomitant overexpression of *ompC* (Batchelor et al., 2005). This differential expression is thought to be due to porin selectivity; not all solutes are able to pass through each porin. The compounds that induce the Cpx pathway have been suggested to pass primarily through *ompF* (Batchelor et al., 2005). If true, activation of *ompF* but not *ompC* through induction of the Cpx pathway is a simple mechanism by which to prevent the entry of chlorpromazine as opposed to downregulation of both *ompF* and *ompC*.

A theme that is consistent with SL1344 AcrB D408A, and upon exposure to chlorpromazine and Pa β N, is the attenuation of virulence genes. Unsurprising given that inactivation and deletion of *acrA* and *acrB* attenuate the virulence of *S. Typhimurium* through a *invF* mediated reduction in the expression of SPI-1 (Webber, Bailey, et al., 2009). This link between efflux and virulence is well documented for RND efflux pumps, other than AcrAB-TolC, across a variety of organisms including *P. aeruginosa* and *V. cholerae* (Rampioni et al., 2017; Bina et al., 2009). In addition, exposure to efflux pump inhibitors including NMP and Pa β N has been revealed to attenuate the virulence of *V. cholerae* and *P. aeruginosa*, respectively (Bina et al., 2009; Rampioni et al., 2017). Together, this data has allowed for the hypothesis that a downregulation of virulence may be a feature of efflux inhibition. It has previously been suggested that the decrease in the transcription of virulence genes observed in SL1344 AcrB D408A and an *acrB* deletion mutant may be as a result of a downregulation of the TCSS PhoPQ (Wang-Kan et al., 2017). If this is correct, the downregulation of virulence genes in response to chemical

inhibition of AcrB by chlorpromazine and Pa β N exposure, may occur, in part, as a result of a similar mechanism; an increase in the intracellular concentration of TCSS signaling molecules. However, the virulence response to chromosomal inactivation of AcrB and inhibition by chlorpromazine and Pa β N is likely to be complicated and multifaceted. Therefore, multiple hypotheses underlying the downregulation of virulence genes can be proposed.

The Cpx and σ^E pathways have been closely linked to virulence. In general, both pathways positively regulate the expression of virulence genes; deletion of *rpoE* and components of the Cpx pathway reduce the pathogenicity of *S. Typhimurium* (Humphreys, Stevenson, et al., 1999; Humphreys, Rowley, et al., 2004). However, both pathways are also able to negatively regulate virulence. For example, constitutive activation of the Cpx pathway, conferred by a mutation in *cpxA*, has been shown to reduce pathogenicity of *S. Typhimurium* through a reduction in its ability to adhere to eukaryotic cells (Humphreys, Rowley, et al., 2004). This reduction in pathogenicity has been suggested to be a result of the repression of *rpoE* expression that occurs upon induction of the Cpx pathway. Other genes that are negatively regulated by the Cpx pathway include *hilA* of SPI-1, *ssrB* of SPI-2 and *hilD* (able to activate both SPI-1 and SPI-1). Here, each of these genes and many of those located within their operons are downregulated in response to chlorpromazine; possibly as a result of induction of an envelope stress response. It is important to note that Pa β N also decreased the expression of *hilA* and *hilD*, despite not increasing the expression of *cpxP*. Although RpoE primarily positively regulates virulence genes, in *S. Typhimurium* activation of the σ^E stress response results in a downregulation of the Flh genes involved in flagellar synthesis (Spöring et al., 2018; Hews et al., 2019). Here, both *flhC* and *flhD* are downregulated upon exposure to Pa β N alongside other genes involved in the synthesis, regulation or functioning of *Salmonella* flagella (*flgKLMN* and *fliCDMSTZ*).

It is shown here that far more genes involved in bacterial virulence are downregulated than have been linked to the σ^E and Cpx stress responses. This leads to an alternative hypothesis based on analysis of COG classes; the observed reduction in the expression of virulence genes observed in SL1344 AcrB D408A and upon exposure to chlorpromazine and Pa β N is a result of a redirection of energy sources from less essential functions including virulence and motility to vital functions including general metabolism, cell wall biogenesis, replication and repair until a more favorable cellular environment is established. The differences between the profile of virulence genes that are downregulated in SL1344 D408A AcrB or upon exposure to chlorpromazine and Pa β N may be a result of differences in the mechanisms by which they induce stress responses, whether by increasing the intracellular concentration of metabolites as a result of efflux inhibition by chemical or chromosomal inactivation of AcrB, as a result of the intrinsic antibacterial activity of chlorpromazine and Pa β N, or from general cellular alterations resulting from the loss of a functioning AcrB protein.

One of the most highly upregulated genes upon exposure to both chlorpromazine and Pa β N was *slsA*, encoding a hydrolase. *slsA* is found within SPI-3 and has been shown to be involved in the colonization of calves and chicks by *S. Typhimurium* (Gan et al., 2011; Morgan et al., 2004). However, the role of *slsA* in virulence is not well understood and it is unknown why chlorpromazine and Pa β N induce high expression of this gene.

Another major discrepancy between the RNA sequencing of SL1344 containing AcrB D408A and that of SL1344 post exposure to chlorpromazine and Pa β N is the expression of genes belonging to the motility COG category. Motility genes are predominantly upregulated in SL1344 AcrB D408A and downregulated upon exposure to chlorpromazine and Pa β N. The upregulation of motility genes in SL1344 D408A was previously suggested to result from increased flagellar transcription to escape stress imposed by an increase in intracellular metabolites (Wang-Kan et al., 2017). Given this, it

was surprising that exposure to chlorpromazine and Pa β N, both of which induce a stress response, did not elicit the same response. However, Pa β N has been shown to induce the downregulation of motility genes in *P. aeruginosa* as a result of alterations in the metabolic pathways of *P. aeruginosa* (Bina et al., 2009). Here, it is proposed that chlorpromazine and Pa β N not only inhibit efflux but also possess antibacterial activity resulting from damage to the OM. This is likely to cause a more severe stress response that would trigger the additional downregulation of energetically costly flagellum synthesis to preserve energy required for more essential functions. In support of this is the evidence that downregulation of motility and flagella synthesis is observed in *S. Typhimurium* upon the sensing of cell envelope stress by chlorpromazine and Pa β N (Spöring et al., 2018).

In summary, RNA sequencing revealed that chlorpromazine behaves in a very similar manner to Pa β N and provides further support for the hypothesis that chlorpromazine is a competitive substrate of the AcrB pump. Interestingly, both chlorpromazine and Pa β N show distinct transcriptomic changes when compared to the transcriptional landscape of SL1344 AcrB D408A. This discrepancy may be representative of the different mechanisms of inhibition exhibited under these three conditions i.e chemical inhibition via competitive interactions with the AcrB pump vs chromosomal inactivation of the pump protein. In addition to this, it is important to note that SL1344 AcrB D408A has a non-functional AcrB pump with no external challenge from a toxic compound. Therefore, it is hypothesised that many of the discrepancies between the RNA sequencing datasets can be attributed to a more severe stress response resulting from the exposure of SL1344 to compounds with intrinsic antibacterial activity. In addition, as previously mentioned, given that chlorpromazine and Pa β N behave as competitive inhibitors, in the absence of an antibiotic substrate their efflux inhibitory activity may not be reflected and thus the same metabolic consequences as chromosomal inactivation of AcrB not observed. A transcriptomic profile more similar to that observed in SL1344 AcrB D408A may be

Chlorpromazine and amitriptyline may elicit their activity through interactions with AcrB

observed if these experiments were repeated with an antibiotic-efflux inhibitor combination. However, this may also suffer from the impact of the presence of toxic compounds.

The evidence thus far suggests that chlorpromazine elicits its efflux inhibitory activity through its role as a competitive substrate of AcrB; able to interact directly with the AcrB pump protein and interfere with the binding/extrusion of less preferential AcrB substrates. However, chlorpromazine appears to have multiple mode of actions that may be related not only to its intrinsic antibacterial activity but may also contribute to its efflux inhibitory activity. To elucidate the mechanism of activity of chlorpromazine, independent of its ability to bind AcrB mutant selection experiments were performed utilizing strains of *S. Typhimurium* and *E. coli* that each possess the previously described AcrB D408A substitution that renders the AcrB pump nonfunctional.

WGS of SL1344 AcrB D408A exposed to chlorpromazine revealed reversion of the D408A substitution to the parental wild type AcrB sequence. This provides further evidence to support that chlorpromazine is a substrate of AcrB and as such provides selective pressure to SL1344 AcrB D408A to result in reversion of the D408A substitution in order to restore the activity of AcrAB-TolC and increase the export of chlorpromazine by this pump. The AcrB D408A substitution incurs no fitness defects to *S. Typhimurium* (Wang-Kan et al., 2017), therefore if chlorpromazine were not a substrate of AcrB there would be no fitness benefit to this reversion.

To confirm this hypothesis, a mutation selection experiment was designed in which resistance to chlorpromazine, amitriptyline, minocycline and spectinomycin was selected in *S. Typhimurium* SL1344 AcrB D408A. The hypothesis was that exposure to an AcrB substrate would apply pressure that would select for ‘mutants’ with a wild-type sequence (revertants) and thus a functional AcrAB-TolC efflux pump. Exposure to chlorpromazine and amitriptyline resulted in the reversion of 100 % of *S. Typhimurium* D408A mutants

Chlorpromazine and amitriptyline may elicit their activity through interactions with AcrB

suggesting that these compounds are both substrates of AcrB. The observation that exposure to minocycline or ethidium bromide resulted in the reversion of 2 % and 3 % of *S. Typhimurium* D408A mutants, respectively, suggests that this may be a feature shared with well-characterized AcrB substrates. The evidence that exposure to spectinomycin, a non-AcrB substrate, does not induce reversion is further support that this genotypic change has the potential to identify AcrB substrates. However, it is important to note that the low reversion rate of minocycline and ethidium bromide mutants does limit its usefulness to identify all AcrB substrates. The discrepancy between the reversion rate for chlorpromazine and amitriptyline versus minocycline and ethidium bromide may be due to the AcrB-specific inhibitory properties of chlorpromazine and amitriptyline. Given this is a feature that appears to be selective for compounds with efflux inhibitory properties, there is the potential for this assay to be used to identify competitive substrates of AcrB for use as efflux inhibitors. However, there are severe limitations regarding the usefulness of this assay. For example, this assay may not identify true competitive inhibitors, but instead AcrB substrates that have less defined target sites, or target sites of which mutation would prove lethal. Therefore, further ligand binding studies would need to be used to characterize the strength of the interactions of each compound with AcrB in relation to their reversion rate. It is hypothesised that compounds in which a higher reversion rate is observed also bind more tightly to AcrB than those with a lower reversion rate and would thus be possible effective competitive efflux inhibitors of compounds with a lower reversion rate and affinity for AcrB.

Unlike *S. Typhimurium*, exposure of MG1655 AcrB D408A to chlorpromazine did not result in reversion of the D408A substitution. Instead, exposure of *E. coli* MG1655 AcrB D408A to chlorpromazine resulted in the selection of mutants each with a varying antibiotic susceptibility profile relative to MG1655 AcrB D408A. WGS of the most-resistant mutant revealed the presence of a single SNP within *pitB* encoding the phosphate transporter PitB.

E. coli possesses two main mechanisms for transporting inorganic phosphate (Pi); the Pst and the Pit systems. The Pst system is induced by the *pho* regulon and is the predominant system under conditions of phosphate starvation. Whereas when phosphate is plentiful the Pit system is the primary system by which Pi is uptaken (Rosenberg, Gerdes, et al., 1977; Harris et al., 2001; Willsky et al., 1980). The Pit system consists of the low-affinity transporters PitA and PitB; PitA is expressed constitutively and PitB repressed by the *pho* regulon under conditions of phosphate starvation (Harris et al., 2001).

A role for PitB in antibiotic resistance has not been elucidated and it is unknown why this mutation has been selected. However, based on what is known about *pitA* and *pitB* mutations and the impact of phosphate starvation on antibiotic resistance, several hypothesis are available. Mutation within *pitA* has been shown to increase tolerance of *S. aureus* to daptomycin. Characterisation of this mutant revealed increased intracellular levels of Pi (Mechler, Herbig, et al., 2015) which either directly or indirectly resulted in global transcriptional changes that cause daptomycin tolerance (Mechler, Bonetti, et al., 2016). In addition, the intracellular concentration of polyphosphate (polyP) was increased. PolyP has been revealed to play an important role in antibiotic resistance. PolyP stimulates the activity of the Lon protease which degrades components of the toxin-antitoxin system, allowing for bacterial persistence (Kuroda et al., 2001; Mechler, Herbig, et al., 2015). Very little is known about the role of *pitB*. However, it has been shown that that upon repression of *pitA*, mutation upstream of *pitB* occurs to alter the activity of PitB allowing it to behave more similarly to PitA (Hoffer et al., 2001).

In addition to antibiotic tolerance conferred by global transcriptomic changes and degradation of the anti-toxin system, another mechanism can be proposed for phosphate mediated antibiotic resistance: increases in intracellular Pi mediated by Pit mutations facilitates the generation of ATP enabling drug extrusion by ATP-dependent drug transporters.

Phosphate limitation activates the Pst system and concomitant repression of PitB through stimulation of the *pho* regulon. RNA sequencing shows that, at least in *S. Typhimurium*, *pstS* (a component of the Pst system) is one of the most highly expressed genes upon exposure to chlorpromazine indicating phosphate starvation. If chlorpromazine is also able to induce conditions of phosphate starvation in *E. coli*, the following can be proposed: chlorpromazine depletes the concentration of intracellular Pi activating the Pst system and repressing the activity of PitB. Mutation of *pitB* restores the intracellular levels of Pi by derepressing the activity of this transporter under conditions of phosphate limitation. The subsequent derepression of PitB confers antibiotic resistance by alterations in intracellular phosphate levels facilitating one or more of the following: global transcriptomic changes, degradation of toxin-antitoxin systems and increased drug efflux by ABC-transporters. This hypothesis could be investigated further by measuring the intracellular levels of both Pi and polyP. If altered, the hypothesis that these alter the activity of ABC-transporters and toxin-antitoxin system could be determined by measuring the efflux capability of drug transporters in *E. coli* other than AcrAB-TolC (e.g. MacAB and MsbA) and the degradation kinetics of the antitoxin proteins.

Pit transporters have been shown to efflux ions such as Zn^{2+} when their concentrations reach toxic levels. Therefore, in addition to responses to phosphate, mutation of *pitB* may have served the purpose to derepress the activity of PitB and facilitate the removal of toxic metabolites that accumulated upon combination of an efflux deficient strain (MG1655 AcrB D408A) with an efflux inhibitor (chlorpromazine). This mechanism of resistance to chlorpromazine may have had the secondary benefit of altering intracellular Pi leading to the described physiological changes that are hypothesised to contribute to drug resistance.

6.10 Key findings

- The transcriptomic profile of *S. Typhimurium* SL1344 exposed to chlorpromazine was similar to that of SL1344 exposed to Pa β N.
- Both chlorpromazine and Pa β N induced an envelope stress response. This response was primarily mediated by activation of the Cpx and σ^E pathways by chlorpromazine and Pa β N, respectively.
- The transcriptomic landscape of *S. Typhimurium* SL1344 exposed to chlorpromazine or Pa β N did not show a high degree of similarity compared to SL1344 AcrB D408A.
- Upregulation of *acrA*, *acrB*, *tolC* and *ramA* upon exposure to chlorpromazine provided further evidence to suggest this compound is a substrate of AcrB.
- Exposure of *S. Typhimurium* SL1344 AcrB D408A to chlorpromazine and known AcrB substrates resulted in the reversion of the D408A substitution to the wild type AcrB sequence.
- Exposure of *E. coli* MG1655 AcrB D408A to chlorpromazine did not result in reversion but instead selected for mutations within *pitB*.

Chapter Seven

Overall discussion and conclusions

Efflux pumps are a target for the discovery of inhibitors that can be developed into antimicrobial adjuvants that prevent the extrusion of antibiotics restoring their antimicrobial potency. The efflux inhibitory activity of the antipsychotics chlorpromazine and amitriptyline, against the AcrAB-TolC pump of *S. Typhimurium* has been described. This included evidence to show both compounds potentiated the antimicrobial activity of AcrB substrates (Bailey et al., 2008; Coutinho et al., 2009; Kristiansen, Hendricks, et al., 2007; Ying et al., 2007) and increased their intracellular concentrations (Bailey et al., 2008; Kaatz et al., 2003; Martins et al., 2011). Importantly, this activity was shown to be specific to AcrB; deletion of *acrB* in *S. Typhimurium* impaired the ability of chlorpromazine and amitriptyline to inhibit the efflux of ethidium bromide (Yamasaki, Nikaido, et al., 2013a; Bailey et al., 2008).

Despite the evidence to suggest that these compounds behave as efflux inhibitors, very little was known about the mechanism by which this occurs. In this thesis, experiments were designed to explore the mechanism of synergy of chlorpromazine with antimicrobials. Amitriptyline as an inhibitor of the AcrAB-TolC pump of *S. Typhimurium* and *E. coli* was also investigated. Pa β N, a known competitive inhibitor of AcrAB-TolC, was used for comparison throughout.

The ability of chlorpromazine and amitriptyline to potentiate the activity of antibiotics against *S. Typhimurium* was known, (Bailey et al., 2008; Coutinho et al., 2009; Kristiansen, Hendricks, et al., 2007; Ying et al., 2007). However, this activity was less well documented against *E. coli*, particularly for amitriptyline. Here, chlorpromazine and amitriptyline were revealed by chequerboard, disk diffusion and/or well diffusion assays to potentiate the activity of AcrB substrates against *S. Typhimurium* SL1344 *ramR::aph* and *E. coli* MG1655 *marR::aph*. In addition, chequerboard assays revealed a substrate-specific degree of antibiotic potentiation against *P. aeruginosa* K1454 and *A. baumannii* AB211. Neither of these strains possess an AcrAB-TolC pump but instead contain the homologous pumps MexAB-OprM (*P. aeruginosa*) and AdeABC (*A. baumannii*). This suggested a broader spectrum of activity of chlorpromazine and amitriptyline as potentiators of antibiotic activity.

In addition to potentiation of antibiotic activity, chlorpromazine and amitriptyline also inhibited the efflux of ethidium bromide, H33342 and norfloxacin by *S. Typhimurium* SL1344 *ramR::aph* and *E. coli* BW25113 *marR::aph*. The extent of this inhibition was concentration and strain-dependent. However, consistently, the data indicated that chlorpromazine was a more potent efflux inhibitor than amitriptyline. In addition, chlorpromazine and amitriptyline largely inhibited ethidium bromide and H33342 efflux to a greater extent in *E. coli* compared to *S. Typhimurium*. This suggested differences in the mechanism by which these compounds interact with *E. coli* and *S. Typhimurium*.

When considering their activity against strains containing AcrAB-TolC, it is important to note that the ability of chlorpromazine and amitriptyline to inhibit the efflux of ethidium bromide was consistently ablated in a strain of *S. Typhimurium* SL1344 in which *acrB* was deleted (Bailey et al., 2008; Yamasaki, Fujioka, et al., 2016). This indicated a mechanism of efflux inhibition specific to this protein for this species. In addition, other efflux inhibitors including MBX-3132, D13-9001 and Pa β N have been

shown, at least in part, to exert their activity as competitive inhibitors via interactions with the distal binding pocket of AcrB. Given this, it was decided to investigate whether the observed efflux inhibitory activity of chlorpromazine and amitriptyline could be rationalised by their binding to AcrB of *S. Typhimurium* and *E. coli* by molecular docking and molecular dynamics simulations. This was undertaken by Chiara Fais and Dr Attilio Vargiu as part of a collaboration with The University of Cagliari, Italy.

As found for MBX-3132, D13-9001 and Pa β N, chlorpromazine and amitriptyline bound to the distal pocket of AcrB_{EC} and AcrB_{ST} (Sjuts et al., 2016; Vargiu, Collu, et al., 2011; Vargiu, Ruggerone, et al., 2014; Vargiu, Ramaswamy, et al., 2018; Nakashima, Sakurai, Yamasaki, Hayashi, et al., 2013; Jewel et al., 2020; Tam et al., 2020). Specifically, both compounds interacted with a region of the distal pocket, known as the hydrophobic trap; a known AcrB substrate binding site. Importantly, binding of chlorpromazine and amitriptyline clashed with the binding of the AcrB substrates ethidium bromide and norfloxacin at the same binding site. This allowed the formation of the hypothesis that chlorpromazine and amitriptyline are competitive inhibitors that elicit their efflux inhibitory properties through direct interactions with AcrB. The increased efflux inhibitory activity of chlorpromazine in relation to amitriptyline was rationalised by (i) a larger number of interactions of chlorpromazine with the hydrophobic trap of both AcrB_{EC} and AcrB_{ST} and (ii) interactions with the CH3 entry gate of AcrB that are not observed with amitriptyline.

At this stage there were three mechanisms by which these interactions were proposed to inhibit the activity of AcrB. The first, is that binding by chlorpromazine and amitriptyline induces conformational changes that prevent substrate binding or extrusion. The second, is that chlorpromazine and amitriptyline are competitive inhibitors of AcrB that bind more tightly to the same locations as other AcrB substrates preventing their extrusion. The third, is that chlorpromazine and amitriptyline are themselves substrates of the pump and

as such they outcompete other AcrB substrates for binding sites and are therefore extruded first. Thus allowing for an increase in antibiotic accumulation and a restoration of antibiotic activity. Although these *in silico* investigations have shone some light on the interactions of chlorpromazine and amitriptyline with AcrB, it is important to consider the limitations discussed in Chapter 4 that accompany molecular docking and dynamic simulations.

The evidence that the inhibition of ethidium bromide efflux by chlorpromazine and amitriptyline is ablated in a strain of *S. Typhimurium* lacking *acrB* (Bailey et al., 2008; Yamasaki, Fujioka, et al., 2016) combined with the *in silico* investigations thus far suggested that chlorpromazine and amitriptyline exert their efflux inhibitory activities through interactions with AcrB. Therefore, it would seem sensible to undertake potentiation assays with a strain of *E. coli* and *S. Typhimurium* lacking *acrB*. Unfortunately, the MIC of chlorpromazine and amitriptyline is drastically reduced in *S. Typhimurium* and *E. coli* *acrB* deletion mutants (Bailey et al., 2008; Yamasaki, Nikaido, et al., 2013a). This means that the concentrations of chlorpromazine and amitriptyline used in potentiation assays cause slow growth and cell death. Interpretation of synergy assays relies on careful consideration of what is a synergistic vs an additive combination. Given the low concentrations at which antimicrobial activity is observed in an *acrB* deletion mutant, any potentiation is likely a result of additive effects rather than true synergy. As such, these experiments are not particularly helpful. It would be useful to determine the impact of chlorpromazine and amitriptyline on the efflux and accumulation of AcrB substrates in a cell free environment with protein alone. For example, reconstitution of AcrAB-TolC into proteoliposomes and X-ray crystallography or ligand binding studies of chlorpromazine with purified AcrB.

Antibiotic potentiation is often observed with compounds that cause damage to the bacterial membrane and this mechanism of antibiotic potentiation is a strong determinant as to a compounds cytotoxicity (Lomovskaya, Warren, et al., 2001; Lomovskaya and

Bostian, 2006). To determine whether the activity of chlorpromazine could also be due, in part, to interactions with the bacterial membrane, membrane permeabilisation and membrane potential assays were performed. Chlorpromazine damaged both the inner and the outer membrane of *S. Typhimurium* and *E. coli*. Membrane permeabilisation of both strains occurred at concentrations considerably higher than those at which efflux inhibition was observed. However, alterations to the membrane potential occurred at concentrations also associated with efflux inhibition. It was therefore hypothesised that chlorpromazine may elicit its efflux inhibitory activity, in part, by altering the PMF. While this does not necessarily preclude its use as an efflux inhibitor, it is a strong indicator that chlorpromazine may be cytotoxic to eukaryotic cells at concentrations that elicit efflux inhibition.

The data presented thus far suggested that chlorpromazine elicits its efflux inhibitory activity through direct interactions with AcrB. However, this did not preclude an additional mode of action as evidenced by the ability of chlorpromazine to damage both the inner and the outer membrane. Therefore, in order to further explore the mode of action of chlorpromazine, mutant selection experiments were designed to elucidate the molecular targets responsible for resistance of *S. Typhimurium* and *E. coli* to chlorpromazine. The rationale behind this experiment was that chlorpromazine resistance would be conferred by mutations within genes that encode the target protein.

Resistance of *S. Typhimurium* SL1344 and *E. coli* MG1655 to chlorpromazine were selected. WGS revealed that these mutants contained mutations within *ramR* (SL1344 RamR L158P) and *marR* (MG1655 A1504Rfs*114 and MG1655 K141Sfs*150) of *S. Typhimurium* and *E. coli*, respectively. The proteins encoded by these genes, RamR and MarR, are transcriptional repressors of the AcrAB-TolC efflux pump. In their resting state RamR and MarR bind the promoter regions of the transcriptional activators *ramA* and *marA* preventing their expression. Ligand binding to RamR and MarR drives

conformational changes that prevents their binding to DNA, allowing for expression of *ramA* and *marA* and the consequent overexpression of AcrAB-TolC. Given the biological role of RamR and MarR and the essentiality of ligand binding for its functionality, the hypothesis that these mutations occur directly in the chlorpromazine binding site of RamR and MarR was ruled out.

Instead, it was hypothesised that the observed substitutions and deletions result in conformational changes that prevent DNA binding. SL1344 RamR L158P is located within the dimerization domain of RamR. Substitutions within this region are known to result in structural changes as a result of disruptions to helical structures and a resultant reduction in the dimerization affinity of each monomer (Liu and Chen, 2017; Yamasaki, Nikaido, et al., 2013a). MG1655 MarR A105Rfs*114 and MG1655 MarR K141Sfs*150 are found within two distinct sites within MarR, the linker region (A105Rfs*114) and the C-terminus (K141Sfs*150). Not only does MarR A105Rfs*114 occur within the linker region that is essential for accommodating the structural changes that accompany ligand binding (Aleksun, Levy, et al., 2001; Duval et al., 2013), this mutation also results in the introduction of a premature stop codon at residue 113/145. This premature stop codon prevents the translation of the C-terminus that is essential for dimer formation and subsequent DNA binding. MarR K141Sfs*150 occurs within the C-terminus and like MarR A105Rfs*114 is predicted to be altered in its structure as a result of reduced dimerization.

As each mutation occurs within regions of RamR and MarR that are essential for its functionality, although not previously described, we can infer from what is known about RamR and MarR and the mutations that have been previously described to form the hypothesis that SL1344 RamR L158P, MG1655 MarR A105Rfs*114 and MG1655 MarR K141Sfs*150 are altered in their conformation such that they are unable to bind to the promoter regions of *ramA* and *marA*. The derepression of *ramA* and *marA* results in the subsequent overexpression of AcrAB-TolC and increased efflux activity. This hypothesis

was supported as SL1344 RamR L158P had increased expression of *ramA* and *acrAB* and MG1655 MarR A105Rfs*114 and MG1655 MarR K141Sfs*150 had increased expression of *marA* and *acrAB*. Chlorpromazine did not further increase the expression of *ramA* or *acrAB* from SL1344 RamR L158P, indicating that induction of both genes by this compound is entirely dependent on RamR.

In keeping with the increased expression of *ramA*, *marA* and *acrAB*, SL1344 RamR L158P, MG1655 MarR A105Rfs*114 and MG1655 MarR K141Sfs*150 each had an increase in their capability to efflux H33342, relative to their wild type parental strains. SL1344 RamR L158P was also increased in its ability to efflux ethidium bromide. Interestingly, both chlorpromazine and PaßN remained able to inhibit the efflux of H33342 from SL1344 RamR L158P, MG1655 MarR A105Rfs*114 and MG1655 MarR K141Sfs*150. These data suggest that a functional RamR and MarR protein are not required for the efflux inhibitory activity of chlorpromazine.

An EMSA assay with purified SL1344 wild type RamR and RamR L158P revealed that, in accordance with previous literature (Baucheron, Coste, et al., 2012), RamR wild type was able to bind to the promoter region of *ramA*. In contrast, RamR L158P was ablated in its ability to bind this DNA region. This experiment revealed that the increased expression of *ramA* and *acrAB* from SL1344 RamR L158P and its increased efflux activity was due to an inability of this mutant protein to bind the promoter of *ramA* resulting in derepression of this transcriptional activator.

It is important to note that the mutant selection experiments performed with chlorpromazine and the subsequent characterisation of the chlorpromazine-resistant mutants have revealed only the mechanism by which *S. Typhimurium* SL1344 and *E. coli* MG1655 evolve resistance to chlorpromazine. This mechanism does not appear to be directly reflective of the mechanism by which chlorpromazine elicits its antimicrobial or

efflux inhibitory activity. Instead, it is hypothesised that the mutations within *marR* and *ramR* reflect the role of chlorpromazine as an AcrB substrate, whereby mutation in these genes occurs in order to increase the expression of AcrAB-TolC and extrusion of chlorpromazine by this pump. This is a mechanism of resistance unlikely to occur for a non-AcrB substrate. Therefore, data arising from these experiments provide further support for the hypothesis that chlorpromazine interacts with and is extruded by AcrB.

The experimental and *in silico* evidence obtained suggested that the mechanism of action of chlorpromazine was likely to be multifaceted. Therefore, to understand more about activity of chlorpromazine, RNAseq was undertaken with samples of *S. Typhimurium* SL1344 exposed to chlorpromazine at a concentration at which efflux inhibition was observed. The data was compared in relation to unexposed and Pa β N treated *S. Typhimurium*. Analysis of the datasets revealed that there was a high degree of similarity between the transcriptomic landscapes of *S. Typhimurium* exposed to chlorpromazine and that exposed to Pa β N. Indicating these compounds behave in a very similar manner. Interestingly, comparison of these efflux inhibitor exposed datasets revealed very little correlation with that of *S. Typhimurium* AcrB D408A containing a non-functional AcrB protein. This suggests that the presence of an efflux inhibitor, in the absence of an antibiotic, does not mimic the transcriptomic phenotype of an efflux-deficient strain. These differences were largely a result of the differential transcription of metabolic and motility genes; exposure to chlorpromazine and Pa β N largely resulted in the upregulation of metabolic genes and downregulation of motility genes, while SL1344 AcrB D408A is largely downregulated for metabolic genes and upregulated for motility genes. This discrepancy was rationalised by differences between the mechanisms of inhibition of efflux i.e chemical inhibition vs chromosomal loss of efflux inhibition.

The antibacterial activity of chlorpromazine and Pa β N is attributed, at least in part, to their ability to damage the inner and outer bacterial membrane. Therefore, it was

unsurprising that a major similarity between the RNAseq datasets was the induction of general stress responses, in particular the induction of envelope stress pathways; primarily mediated through the Cpx and σ^E responses by chlorpromazine and Pa β N, respectively.

It should, however, be noted that there was an important distinction between the chlorpromazine and Pa β N RNAseq datasets. Expression of genes encoding AcrAB-TolC and its regulatory proteins was not the same in the two datasets; chlorpromazine, but not Pa β N, induced the upregulation of *acrA*, *acrB*, *tolC*, *ramA* and *ramR*. Upregulation of efflux genes has been commonly noted upon exposure to pump substrates (Lawler et al., 2013; Yamasaki, Fujioka, et al., 2016). As such, this observation provided further support to accompany the presented evidence that chlorpromazine is a substrate of AcrB and suggested that Pa β N, although a competitive inhibitor of AcrB, is unlikely to be a substrate. In terms of their mode of action as competitive efflux inhibitors, this allows a small but important distinction to be made. Pa β N is a competitive inhibitor of AcrB, able to bind to the same locations as AcrB substrates preventing their binding and subsequent extrusion possibly as a result of alterations in AcrB secondary structure. Chlorpromazine is a competitive substrate of AcrB, able to bind to and be extruded by AcrB before other less preferential substrates.

This work and hypothesis contradicts previous work that showed chlorpromazine induced the upregulation of *ramA*, but the downregulation of *acrB*. This was previously explained as a result of an interaction of chlorpromazine with AcrB causing downregulation of *acrB* and the establishment of a negative feedback loop that drove the upregulation of *ramA*. An RT-PCR performed in the research described here revealed this discrepancy was due to differences in chlorpromazine concentration. At the efflux inhibitory concentrations used here (50 μ g/ml, the expression of *acrB* was increased, whereas at 200 μ g/ml (used by (Bailey et al., 2008)), the expression of *acrB* was reduced.

Mutant selection experiments were designed to select for chlorpromazine resistance

using *S. Typhimurium* SL1344 AcrB D408A, which lacks a functional AcrB-TolC efflux pump. Instead of the intended aim of revealing the off-target activity of chlorpromazine in the absence of a functional AcrB protein, this experiment provided more support to the hypothesis that chlorpromazine is a substrate of AcrB. It was revealed that in the presence of chlorpromazine the D408A substitution reverted to the wild type allele, conferring a functional AcrAB-TolC efflux pump. Repetition of this experiment with amitriptyline showed that this was not a phenomenon exclusive to chlorpromazine. Furthermore, the observation that the AcrB substrates minocycline and ethidium bromide, but not the non-substrate spectinomycin, also result in SNP reversion to the wild type sequence identified this as an assay capable of discriminating between AcrB and non-AcrB substrates. Even more interestingly, it was observed that chlorpromazine and amitriptyline caused reversion at a rate of 100% while for ethidium bromide and minocycline this reversion rate was much lower at 2% and 3%. This feature of competitive inhibitors resulting in high reversion of the *acrB* SNP to wild type means that it may be possible to use this experimental approach to identify competitive substrates of AcrB, or at least to identify substrates that may be “better” substrates of AcrB. “Better” meaning that they bind tighter or are extruded more readily than other substrates. However, there are limitations when considering the usefulness of this assay. For example, this assay may not identify true competitive inhibitors, but instead AcrB substrates that have less defined target sites, or target sites of which mutation to confer resistance is accompanied by severe fitness costs.

Interestingly, this reversion phenotype appeared to be specific only to *S. Typhimurium*. Instead of reversion of the D408A substitution, resistance of *E. coli* MG1655 AcrB D408A to chlorpromazine was conferred by mutation of the phosphate transporter *pitB*. The role of this mutation in chlorpromazine resistance is unknown but hypothesised to be a response to phosphate depletion by chlorpromazine.

A key limitation of using mutant selection experiments to identify the target site of chlorpromazine is that in order to generate resistance to the inhibitor alone, chlorpromazine must be used at concentrations near to or at its MIC. This is more likely to elucidate mechanisms underlying its antimicrobial activity. Or in the case of chlorpromazine just provide information regarding the mechanism of resistance. Which in this study has been useful for identifying chlorpromazine as a substrate of AcrB and in combination with the other evidence for inferring its activity as a competitive substrate. However, these experiments were not useful for indicating its direct molecular target as an efflux inhibitor. Mutant selection experiments utilising a combination of an antibiotic with an inhibitor at concentrations at which efflux inhibition is observed was used as a strategy for identifying mutations that confer resistance to the combination. However, using this strategy, mutations in *gyrA* conferring resistance of *S. Typhimurium* to ciprofloxacin were isolated when used in combination with chlorpromazine or Pa β N. In the case of chlorpromazine, no additional mutations were observed and resistance was only conferred to ciprofloxacin. For Pa β N, the mutation in *gyrA* was accompanied by additional mutations within *recN* and *barA*. These mutations were very loosely hypothesised to be compensatory mutations that ameliorate the fitness costs that accompany a *gyrA* mutation, in the presence of the additional selective pressure provided by Pa β N.

During the course of this research, a target site for Pa β N (LpxM) was identified in the OM of *E. coli* (Schuster, Bohnert, et al., 2019). Consistent with this, the Pa β N resistance in *S. Typhimurium* observed in this study was conferred by mutations within *bamE* encoding the OMP BamE; a member of the BAM complex. These mutations were selected for at MIC concentrations of Pa β N and thus are likely a reflection of its antimicrobial activity as a membrane permeabiliser rather than elucidating the molecular targets of Pa β N as an efflux inhibitor.

In conclusion, the research described in this thesis has provided insight into the

mode of action of chlorpromazine as an efflux inhibitor; revealing this compound as a competitive substrate of AcrB. However, there remain unknowns including its direct molecular targets by which antimicrobial and efflux inhibitory activity is exerted. Furthermore, the clinical utility of this compound as an efflux inhibitor remains unexplored. Several questions arise from the use of chlorpromazine in psychiatry that could be useful for determining its clinical impact as an antibiotic adjuvant. For instance, are patients who receive phenothiazines less likely to have a bacterial infection or does phenothiazine administration improve the clinical outcome of patients with bacterial infections treated with antibiotics? In addition, given that the usefulness of efflux inhibitors will be limited if bacteria develop resistance to the adjuvant, does bacterial resistance to chlorpromazine occur in commensal organisms in patients administered this drug for its neuroleptic properties? Unfortunately, as of writing there were no published studies addressing these questions. Another question often raised about the use of these drug combinations is whether the drug-drug interactions of antibiotics and chlorpromazine limit their use in combination? Phenothiazines and many antibiotics share a similar organ distribution and very few antibiotics interact negatively with phenothiazines. However, there are no published studies showing that phenothiazines synergise with antibiotics *in vivo*. Drug interaction studies will need to be undertaken to determine whether phenothiazines can be co-administered with antibiotics. Finally, the concentrations at which phenothiazines can be administered therapeutically without cytotoxicity is $\sim 1,000$ fold lower than the concentration at which antibiotic-adjuvant activity is observed. Therefore, the clinical usefulness of these compounds may be limited. However, understanding the mode of action of phenothiazines as efflux-adjuvants may allow for the design of phenothiazine derivatives or novel compounds as efflux inhibitors without the accompanying cytotoxicity.

Publications resulting from this study

Chlorpromazine and amitriptyline and substrates and inhibitors of the AcrB multidrug efflux pump. Grimsey, E. M, Fais, C, Marshall, R. L, Ricci, V, Ciusa, M, Ivens, A, Malloci, G, Ruggerone, P, Vargiu, A. V, Piddock, L. J. V. (2020). MBio. 2020 Jun 2;11(3):e00465-20. doi: 10.1128/mBio.00465-20.

Perturbed structural dynamics underlie inhibition and altered efflux of the multidrug pump AcrB. Ahdash, Z, Reading, E. Wang Kan, X, Fais, C, Grimsey, E. M, Malloci, G, Lau, A. M, Findlay, H, Booth, P. J, Ruggerone, P, Vargiu, A. V, Piddock, L, J. V, Pollitis, A. (2020) Nat Commun. 2020 Nov 4;11(1):5565. doi: 10.1038/s41467-020-19397-2.

Overexpression of RamA, Which Regulates Production of the Multidrug Resistance Efflux Pump AcrAB-TolC, Increases Mutation Rate and Influences Drug Resistance Phenotype. Grimsey, E. M, Weston, N, Ricci, V, Stone, J. W, Piddock, L. J. V. Antimicrob Agents Chemother. 2020 Mar 24;64(4):e02460-19. doi: 10.1128/AAC.02460-19.

Conference presentations resulting from this study

Understanding the mode of action of compounds purported to possess efflux inhibitory properties. Elizabeth M. Grimsey and Laura J. V. Piddock at BSAC Antibiotic Resistance Mechanisms Workshop, 2018, Birmingham, UK.

Understanding the mode of action of compounds purported to possess efflux inhibitory properties. Elizabeth M. Grimsey and Laura J. V. Piddock at MRF National PhD Training Programme in AMR Research training Network Conference, 2018, Bristol, UK.

Chlorpromazine is a competitive substrate of the multidrug efflux pump AcrAB-TolC of *S. Typhimurium*. Elizabeth M. Grimsey, Chiara Fais, Robert L. Marshall, Vito Ricci, Maria Laura Ciusa, Giuliano Mallocci, Paolo Ruggerone, Attilio V. Vargiu and Laura J.V. Piddock at the Gordon Research Conference on Multi-Drug Efflux Systems, 2019, Lucca, Italy.

Chlorpromazine is a competitive substrate of the multidrug efflux pump AcrAB-TolC of *S. Typhimurium*. Elizabeth M. Grimsey, Chiara Fais, Robert L. Marshall, Vito Ricci, Maria Laura Ciusa, Giuliano Mallocci, Paolo Ruggerone, Attilio V. Vargiu and Laura J.V. Piddock at the 6th Midlands Molecular Microbiology Meeting, 2019, Nottingham, UK.

Chlorpromazine is a competitive substrate of the multidrug efflux pump AcrAB-TolC of *S. Typhimurium*. Elizabeth M. Grimsey, Chiara Fais, Robert L. Marshall, Vito Ricci, Maria Laura Ciusa, Giuliano Malloci, Paolo Ruggerone, Attilio V. Vargiu and Laura J.V. Piddock at BSAC Antibiotic Resistance Mechanisms Workshop, 2019, Birmingham, UK.

Appendices

Appendix Table 3.1. FIC of compounds +/- AMI against *S. Typhimurium* SL1344 *ramR::aph*, *E. coli* BW25113 *marR::aph*, *A. baumannii* AB211 and *P. aeruginosa* K1454.

Antibiotics	Amitriptyline (AMI) concentration	MIC (µg/ml)			
		SL1344 <i>ramR::aph</i>	BW25113 <i>marR::aph</i>	AB211	K1454
Chloramphenicol	No AMI				
	1/16 MIC AMI	0.56	1.06	1.08	0.56
	1/8 MIC AMI	0.38	1.13	1.63	0.63
	1/4 MIC AMI	0.38	0.75	0.5	0.75
Ciprofloxacin	No AMI				
	1/16 MIC AMI	0.56	8.06	1.08	1.06
	1/8 MIC AMI	0.63	2.13	1.13	1.13
	1/4 MIC AMI	0.31	1.25	1.25	0.75
Nalidixic acid	No AMI				
	1/16 MIC AMI	1.06	1.06	1.08	0.56
	1/8 MIC AMI	0.63	1.13	1.13	0.38
	1/4 MIC AMI	0.5	0.75	1.25	0.5
Tetracycline	No AMI				
	1/16 MIC AMI	0.56	1.06	1.08	1.06
	1/8 MIC AMI	0.38	1.13	1.13	1.13
	1/4 MIC AMI	0.38	0.75	1.25	0.75
Norfloxacin	No AMI				
	1/16 MIC AMI	0.54	2.06	1.08	1.06
	1/8 MIC AMI	1.13	1.13	1.13	1.13
	1/4 MIC AMI	1.13	1.25	1.25	1.25
Ethidium bromide	No AMI				
	1/16 MIC AMI	1.06	0.56	1.08	1.06
	1/8 MIC AMI	1.13	1.13	1.13	1.13
	1/4 MIC AMI	0.75	0.75	0.75	0.75

Bold font indicates a synergistic antibiotic-inhibitor interaction with an FIC value ≤ 0.5 . The MIC of amitriptyline was 888 µg/ml, 444 µg/ml, 222 µg/ml and 1,775 µg/ml against SL1344 *ramR::aph*, BW25113 *marR::aph*, AB211 and K1454, respectively.

Appendix Table 3.2 FIC of compounds +/- CPZ against *S. Typhimurium* SL1344 *ramR::aph*, *E. coli* BW25113 *marR::aph*, *A. baumannii* AB211 and *P. aeruginosa* K1454.

Antibiotics	Chlorpromazine (CPZ) concentration	MIC (µg/ml)			
		SL1344 <i>ramR::aph</i>	BW25113 <i>marR::aph</i>	AB211	K1454
Chloramphenicol	No CPZ				
	1/16 MIC CPZ	0.56	0.65	1.06	0.56
	1/8 MIC CPZ	0.38	0.63	1.13	0.38
	1/4 MIC CPZ	0.38	0.75	0.75	0.50
Ciprofloxacin	No CPZ				
	1/16 MIC CPZ	1.06	1.06	1.06	1.06
	1/8 MIC CPZ	0.64	1.13	1.13	1.13
	1/4 MIC CPZ	0.50	0.75	1.25	1.25
Nalidixic acid	No CPZ				
	1/16 MIC CPZ	0.56	0.56	1.06	0.31
	1/8 MIC CPZ	0.63	0.63	1.13	0.38
	1/4 MIC CPZ	0.31	0.75	1.25	0.38
Tetracycline	No CPZ				
	1/16 MIC CPZ	1.06	0.56	1.06	0.56
	1/8 MIC CPZ	0.63	0.63	0.63	0.38
	1/4 MIC CPZ	0.50	0.75	0.75	0.50
Norfloxacin	No CPZ				1
	1/16 MIC CPZ	2.06	1.10	1.06	1
	1/8 MIC CPZ	2.12	1.13	1.13	1
	1/4 MIC CPZ	2.25	1.25	0.75	1
Ethidium bromide	No CPZ				
	1/16 MIC CPZ	0.56	1.06	0.56	0.31
	1/8 MIC CPZ	0.63	0.63	0.63	0.38
	1/4 MIC CPZ	0.75	0.75	0.75	0.31

Bold font indicates a synergistic antibiotic-inhibitor interaction with an FIC value ≤ 0.5 . The MIC of chlorpromazine was 1,024 µg/ml, 256 µg/ml, 128 µg/ml and 2,048 µg/ml against SL1344 *ramR::aph*, BW25113 *marR::aph*, AB211 and K1454, respectively.

Appendix Table 3.3 FIC of compounds +/- PaβN against *S. Typhimurium* SL1344 *ramR::aph*, *E. coli* BW25113 *marR::aph*, *A. baumannii* AB211 and *P. aeruginosa* K1454.

Antibiotics	PaβN concentration	MIC (μg/ml)			
		SL1344 <i>ramR::aph</i>	BW25113 <i>marR::aph</i>	AB211	K1454
Chloramphenicol	No PaβN				
	1/16 MIC PaβN	0.13	N/D	0.14	0.04
	1/8 MIC PaβN	0.13	0.13	0.14	0.005
	1/4 MIC PaβN	0.06	0.13	0.07	0.005
Ciprofloxacin	No PaβN				
	1/16 MIC PaβN	0.25	N/D	1.25	0.48
	1/8 MIC PaβN	0.25	0.53	1.25	0.24
	1/4 MIC PaβN	0.07	0.53	0.63	0.24
Nalidixic acid	No PaβN				
	1/16 MIC PaβN	0.032	N/D	0.50	0.007
	1/8 MIC PaβN	0.032	0.13	0.50	0.004
	1/4 MIC PaβN	0.16	0.13	0.25	0.004
Tetracycline	No PaβN				
	1/16 MIC PaβN	0.501	N/D	1.5	0.53
	1/8 MIC PaβN	0.25	0.504	0.75	0.27
	1/4 MIC PaβN	0.13	0.504	0.36	0.07
Norfloxacin	No PaβN				
	1/16 MIC PaβN	1.0	1.0	1.25	1.0
	1/8 MIC PaβN	0.24	1.0	1.25	0.25
	1/4 MIC PaβN	0.06	0.501	0.03	0.03
Ethidium bromide	No PaβN				
	1/16 MIC PaβN	0.75	N/D	0.63	0.38
	1/8 MIC PaβN	0.375	1	0.31	0.38
	1/4 MIC PaβN	0.19	1	0.31	0.38

Bold font indicates a synergistic antibiotic-inhibitor interaction with an FIC value ≤ 0.5 . The MIC of PaβN was 1,024 μg/ml, 256 μg/ml, 1,024 μg/ml and 1,024 μg/ml against SL1344 *ramR::aph*, BW25113 *marR::aph*, AB211 and K1454, respectively.

Appendix Table A3.4 (Pseudo) binding free energies evaluated through the scoring function of AutoDock VINA for the top ranked poses of both amitriptyline and chlorpromazine on AcrB_{EC} and AcrB_{ST}.

Complex	ΔG_{max} (kcal/mol)
AMI - AcrB _{EC}	-11.6
AMI - AcrB _{ST}	-12.1
CPZ - AcrB _{EC}	-9.2
CPZ - AcrB _{ST}	-9.3

All corresponding poses are localized within the DP. Chlorpromazine; CPZ. Amitriptyline; AMI. Data provided by Attilio Vargiu. University of Cagliari, Italy.

Appendix Table A3.5 The residues of AcrB that interact with chlorpromazine and amitriptyline at their polar tail.

AMI - AcrB _{EC}	E130 (69.3%), Q176 (60.0%), water-mediated interactions (4.7%)
AMI - AcrB _{ST}	E130 (67.1%), Q176 (64.8%), water-mediated interactions (4.6%)
CPZ - AcrB _{EC}	S133 (82.7%), S134 (58.9%), water-mediated interactions (17.5%)
CPZ - AcrB _{ST}	S134 (52.0%), S135 (44.0%), F136 (10.0%), F617 (9.8%), water-mediated interactions (10.0%)

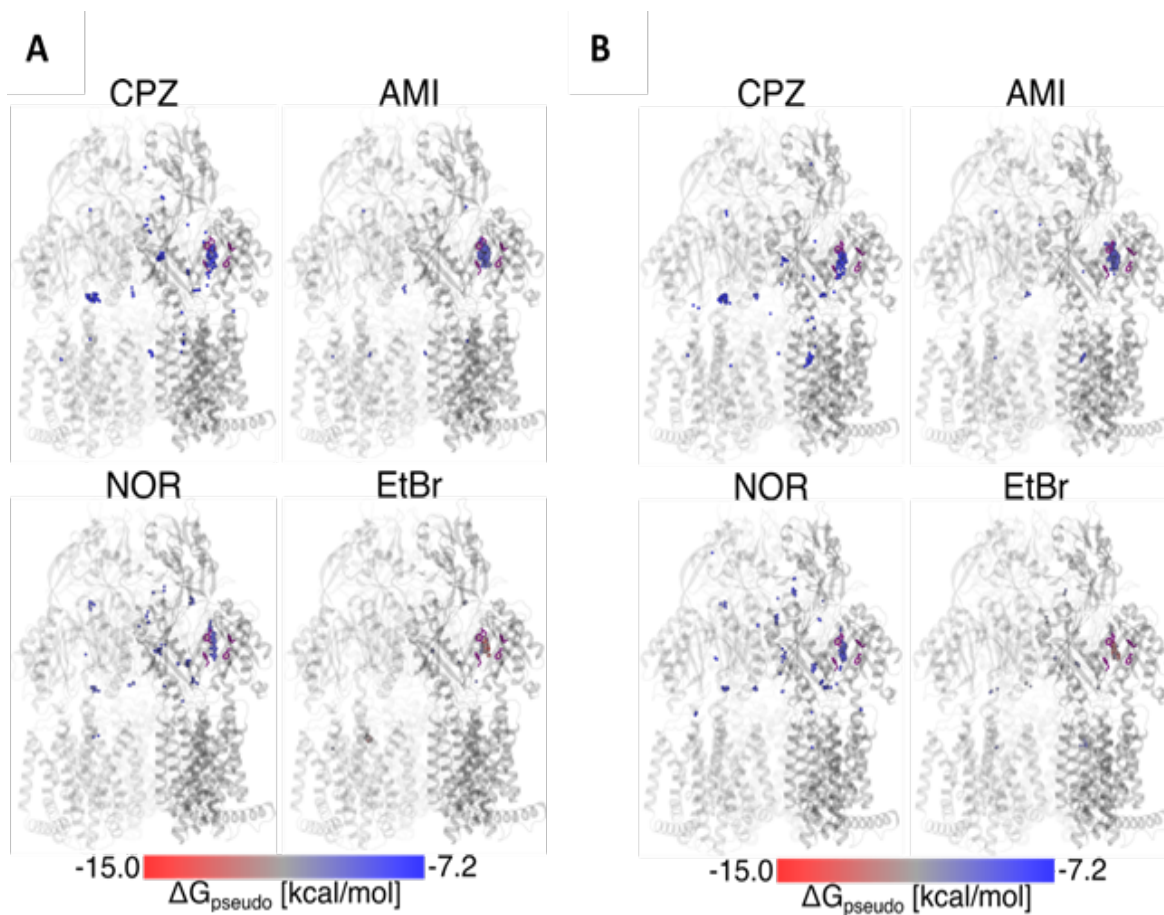
Chlorpromazine; CPZ. Amitriptyline; AMI. Data provided by Attilio Vargiu. University of Cagliari, Italy.

Appendix Table 3.6 Binding free energies (ΔG – Kcal/ml) of chlorpromazine (CPZ), amitriptyline (AMI), norfloxacin (NOR) and ethidium bromide (EtBr) to AcrB_{EC} and AcrB_{ST}.

	Compound	ΔG_b	DP	HT
<i>E. coli</i>	CPZ	-31.9 (4.0)	-13.9	-8.9
	AMI	-25.6 (3.4)	-9.1	-6.6
	NOR	-36.4 (5.2)	-10.0	-6.5
	EtBr	-43.5 (2.9)	-14.6	-10.9
<i>S. Typhimurium</i>	CPZ	-25.7 (3.1)	-10.3	-8.4
	AMI	-27.7 (3.2)	-10.8	-5.7
	NOR	-29.8 (3.3)	-12.7	-10.1
	EtBr	-34.8 (2.9)	-14.0	-8.7

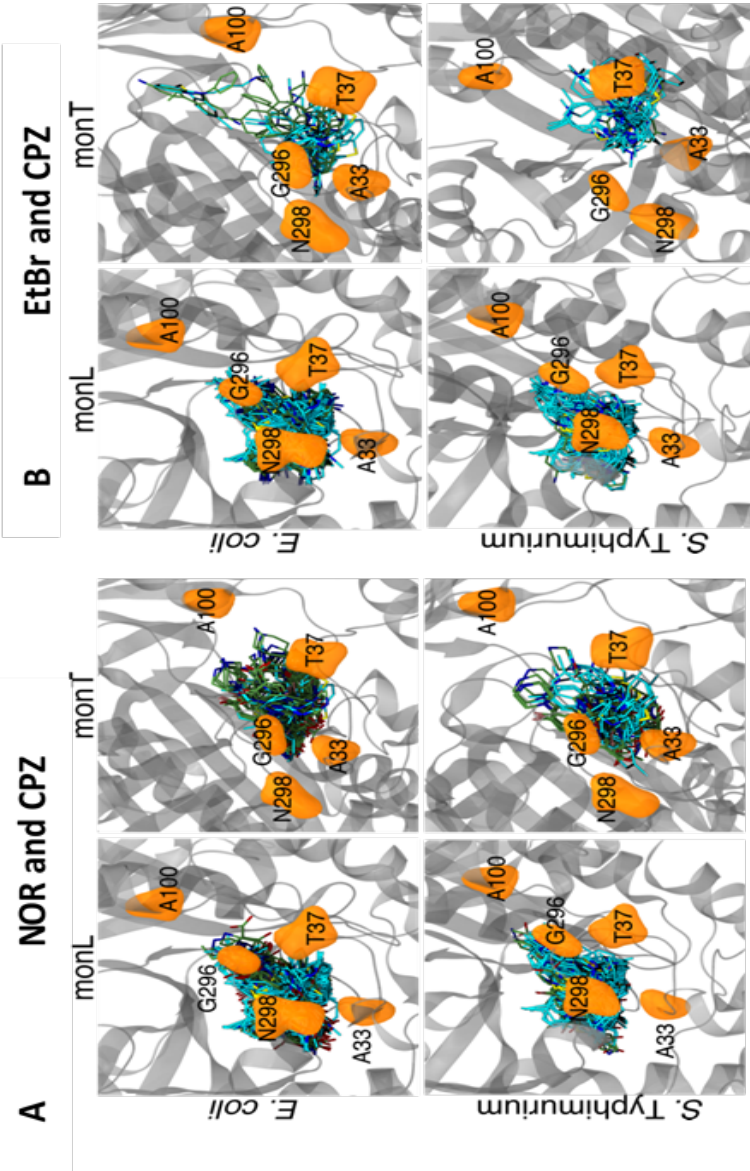
The standard error is shown in brackets. Data provided by Attilio Vargiu. University of Cagliari, Italy. Hydrophobic trap; HT. Distal pocket; DP.

Appendix Figure A3.1 Top docking poses of chlorpromazine, amitriptyline, norfloxacin and ethidium bromide with AcrB_{EC} (A) and AcrB_{ST} (B).

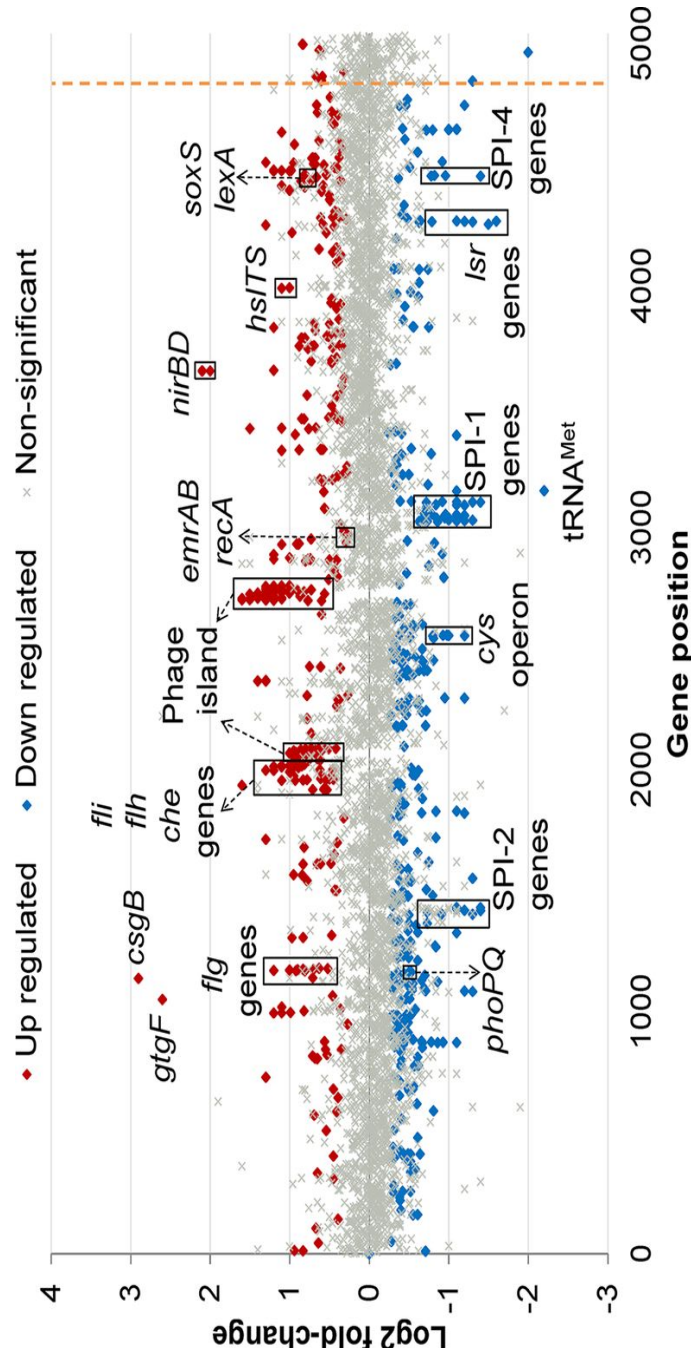


Each distribution pose (red-blue) was scored using AutoDock VINA (ΔG_{pseudo}). The protein is shown as transparent ribbons and the phenylalanines of the HT are displayed as magenta sticks. The transparency increases from Monomer T to L to P. Chlorpromazine; CPZ. Amitriptyline; AMI. Norfloxacin; NOR. Ethidium bromide; EtBr. Image provided by Attilio Vargiu. University of Cagliari, Italy.

Appendix Figure A3.2 Docking poses of chlorpromazine (CPZ) against norfloxacin (NOR) (A) and ethidium bromide (EtBr) (B) at the CH3 entry gate of AcrB_{EC} and AcrB_{ST} (monomers L and T).

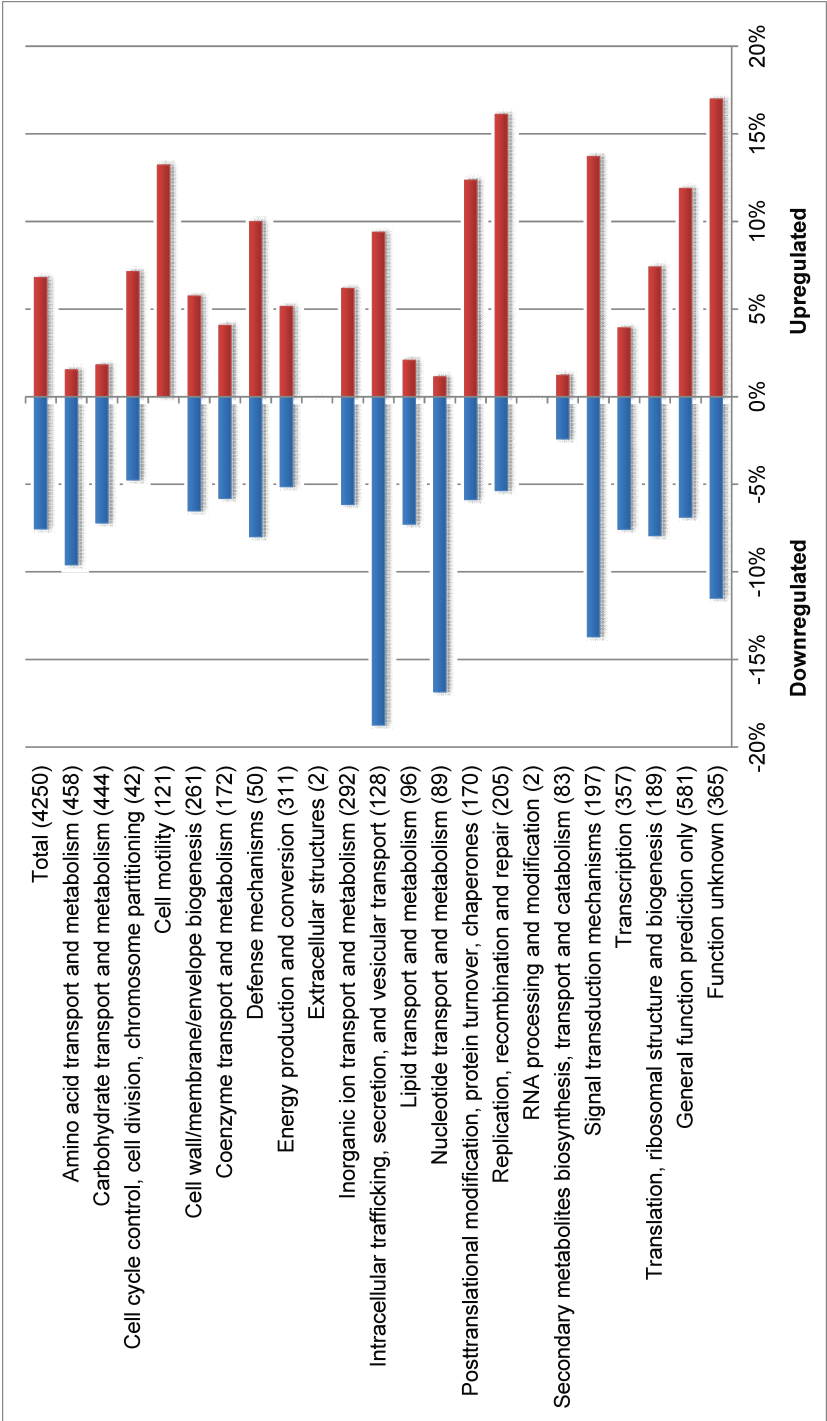


Appendix Figure A6.1 Transcriptional landscape of *S. Typhimurium* SL1344 AcrB D408A relative to wild type *S. Typhimurium* SL1344



The names of genes were displayed for those with ≥ 2.5 and ≤ -2.5 log2 fold change in expression relative to unexposed SL1344, for upregulated and downregulated genes, respectively. The grey shaded area represents those genes that lie outside these cutoff values.

Appendix Figure A6.2 Percentage of significantly altered genes of *S. Typhimurium* SL1344 AcrB D408A within each COG class



The percentage of genes belonging to each class was calculated by the number of significantly altered genes divided by the total number of genes in a given class. COG classes are divided into categories as follows A; Poorly characterized . B; Metabolism. C; Information storage and processing. D; Cellular processes and signaling.

References

- Abouzeed, Y. M. et al. (2008). “*ramR* Mutations Involved in Efflux-Mediated Multidrug Resistance in *Salmonella enterica* Serovar Typhimurium”. In: *Antimicrob Agents Chemother* 52.7, pp. 2428–2434. DOI: [10.1128/aac.00084-08](https://doi.org/10.1128/aac.00084-08).
- Aeschlimann, J. R. et al. (1999). “Effects of NorA inhibitors on *in vitro* antibacterial activities and postantibiotic effects of levofloxacin, ciprofloxacin, and norfloxacin in genetically related strains of *Staphylococcus aureus*.” In: *Antimicrobial agents and chemotherapy* 43.2, pp. 335–40. ISSN: 0066-4804.
- Aldridge, K. E. et al. (1986). “Variation in the potentiation of β -lactam antibiotic activity by clavulanic acid and sulbactam against multiply antibiotic-resistant bacteria | Journal of Antimicrobial Chemotherapy | Oxford Academic”. In: *J Antimicrob Chemother* 17.4, pp. 463–9.
- Alekshun, M. N., Kim, Y. S., et al. (2002). “Mutational analysis of MarR, the negative regulator of *marRAB* expression in *Escherichia coli*, suggests the presence of two regions required for DNA binding”. In: *Molecular Microbiology* 35.6, pp. 1394–1404. ISSN: 0950382X. DOI: [10.1046/j.1365-2958.2000.01802.x](https://doi.org/10.1046/j.1365-2958.2000.01802.x).
- Alekshun, M. N. and Levy, S. B. (1997). *Regulation of chromosomally mediated multiple antibiotic resistance: The mar regulon*. DOI: [10.1128/aac.41.10.2067](https://doi.org/10.1128/aac.41.10.2067).

- Alekshun, M. N. and Levy, S. B. (1999). “Characterization of *marr* superrepressor mutants”. In: *Journal of Bacteriology* 181.10, pp. 3303–3306. ISSN: 00219193. DOI: [10.1128/jb.181.10.3303-3306.1999](https://doi.org/10.1128/jb.181.10.3303-3306.1999).
- Alekshun, M. N., Levy, S. B., et al. (2001). “The crystal structure of MarR, a regulator of multiple antibiotic resistance, at 2.3 Å resolution”. In: *Nature Structural Biology* 8.8, pp. 710–714. ISSN: 10728368. DOI: [10.1038/90429](https://doi.org/10.1038/90429).
- Alm, E. et al. (2006). “The Evolution of Two-Component Systems in Bacteria Reveals Different Strategies for Niche Adaptation”. In: *PLoS Computational Biology* 2.11, e143. ISSN: 1553-734X. DOI: [10.1371/journal.pcbi.0020143](https://doi.org/10.1371/journal.pcbi.0020143).
- Altier, C. et al. (2000). “Characterization of two novel regulatory genes affecting *Salmonella* invasion gene expression”. In: *Molecular Microbiology* 35.3, pp. 635–646. ISSN: 0950382X. DOI: [10.1046/j.1365-2958.2000.01734.x](https://doi.org/10.1046/j.1365-2958.2000.01734.x).
- Alzrigat, L. P. et al. (2017). “Fitness cost constrains the spectrum of *marR* mutations in ciprofloxacin-resistant *Escherichia coli*”. In: *Journal of Antimicrobial Chemotherapy* 72.11, pp. 3016–3024. ISSN: 14602091. DOI: [10.1093/jac/dkx270](https://doi.org/10.1093/jac/dkx270).
- Amaral, L. and Lorian, V. (1991). “Effects of chlorpromazine on the cell envelope proteins of *Escherichia coli*”. In: 35.9, pp. 1923–1924. ISSN: 00664804. DOI: [10.1128/AAC.35.9.1923](https://doi.org/10.1128/AAC.35.9.1923).
- Amaral, L., Kristiansen, J. E., et al. (2000). “The effects of chlorpromazine on the outer cell wall of *Salmonella typhimurium* in ensuring resistance to the drug”. In: *International Journal of Antimicrobial Agents* 14.3, pp. 225–229. ISSN: 09248579. DOI: [10.1016/S0924-8579\(00\)00136-9](https://doi.org/10.1016/S0924-8579(00)00136-9).
- Ammeter, D. et al. (2019). “Development of a nebramine-cyclam conjugate as an antibacterial adjuvant to potentiate β -lactam antibiotics against multidrug-resistant *P. aeruginosa*”. In: *Journal of Antibiotics* 72.11, pp. 816–826. ISSN: 18811469. DOI: [10.1038/s41429-019-0221-9](https://doi.org/10.1038/s41429-019-0221-9).

- Andersen, C. et al. (2002). “An aspartate ring at the TolC tunnel entrance determines ion selectivity and presents a target for blocking by large cations”. In: *Molecular Microbiology* 44.5, pp. 1131–1139. ISSN: 0950382X. DOI: [10.1046/j.1365-2958.2002.02898.x](https://doi.org/10.1046/j.1365-2958.2002.02898.x).
- Andersson, D. I. et al. (2010). “Antibiotic resistance and its cost: Is it possible to reverse resistance?” In: *Nature Reviews Microbiology* 8.4, pp. 260–271. ISSN: 17401526. DOI: [10.1038/nrmicro2319](https://doi.org/10.1038/nrmicro2319).
- Andersson, D. I. et al. (2014). “Microbiological effects of sublethal levels of antibiotics”. In: *Nature Reviews Microbiology* 12.7, pp. 465–478. ISSN: 17401534. DOI: [10.1038/nrmicro3270](https://doi.org/10.1038/nrmicro3270).
- Andrews, J. M. (2001). “Determination of minimum inhibitory concentrations”. In: *Journal of Antimicrobial Chemotherapy* 48.suppl_1, pp. 5–16. ISSN: 1460-2091. DOI: [10.1093/jac/48.suppl_1.5](https://doi.org/10.1093/jac/48.suppl_1.5).
- Archer, J. S. et al. (1963). “Classifications of phenothiazine derivatives”. In: *British Journal of Anaesthesia* 35.7, p. 446. ISSN: 00070912. DOI: [10.1093/bja/35.7.446](https://doi.org/10.1093/bja/35.7.446).
- Aron, Z. et al. (2018). “The hydrophobic trap—the Achilles heel of RND efflux pumps”. In: *Research in Microbiology* 169.7-8, pp. 393–400. ISSN: 17697123. DOI: [10.1016/j.resmic.2017.11.001](https://doi.org/10.1016/j.resmic.2017.11.001).
- Baba, T. et al. (2006). “Construction of *Escherichia coli* K-12 in-frame, single-gene knockout mutants: The Keio collection”. In: *Molecular Systems Biology* 2.2006.0008. ISSN: 17444292. DOI: [10.1038/msb4100050](https://doi.org/10.1038/msb4100050).
- Baharoglu, Z., Krin, E., et al. (2013). “RpoS Plays a Central Role in the SOS Induction by Sub-Lethal Aminoglycoside Concentrations in *Vibrio cholerae*”. In: *PLoS Genetics* 9.4. ISSN: 15537390. DOI: [10.1371/journal.pgen.1003421](https://doi.org/10.1371/journal.pgen.1003421).
- Baharoglu, Z. and Mazel, D. (2014). “SOS, the formidable strategy of bacteria against aggressions”. In: *FEMS Microbiology Reviews* 38.6, pp. 1126–1145. ISSN: 15746976. DOI: [10.1111/1574-6976.12077](https://doi.org/10.1111/1574-6976.12077).

- Bailey, A. M. et al. (2008). “RamA confers multidrug resistance in *Salmonella enterica* via increased expression of *acrB*, which is inhibited by chlorpromazine”. In: *Antimicrobial Agents and Chemotherapy* 52.10, pp. 3604–3611. ISSN: 00664804. DOI: [10.1128/AAC.00661-08](https://doi.org/10.1128/AAC.00661-08).
- Baker, S. et al. (2013). “Fitness benefits in fluoroquinolone-resistant *Salmonella* Typhi in the absence of antimicrobial pressure”. In: *eLife* 2013.2, p. 1229. ISSN: 2050084X. DOI: [10.7554/eLife.01229.001](https://doi.org/10.7554/eLife.01229.001).
- Bang, I. S. et al. (2005). “Alternative sigma factor interactions in *Salmonella*: σ^E and σ^H promote antioxidant defences by enhancing σ^S levels”. In: *Molecular Microbiology* 56.3, pp. 811–823. ISSN: 0950382X. DOI: [10.1111/j.1365-2958.2005.04580.x](https://doi.org/10.1111/j.1365-2958.2005.04580.x).
- Barnard, F. M. et al. (2001). “Interaction between DNA gyrase and quinolones: Effects of alanine mutations at GyrA subunit residues Ser83 and Asp87”. In: *Antimicrobial Agents and Chemotherapy* 45.7, pp. 1994–2000. ISSN: 00664804. DOI: [10.1128/AAC.45.7.1994-2000.2001](https://doi.org/10.1128/AAC.45.7.1994-2000.2001).
- Batchelor, E. et al. (2005). “The *Escherichia coli* CpxA-CpxR envelope stress response system regulates expression of the porins OmpF and OmpC”. In: *Journal of Bacteriology* 187.16, pp. 5723–5731. ISSN: 00219193. DOI: [10.1128/JB.187.16.5723-5731.2005](https://doi.org/10.1128/JB.187.16.5723-5731.2005).
- Baucheron, S., Coste, F., et al. (2012). “Binding of the RamR repressor to wild-type and mutated promoters of the *ramA* gene involved in efflux-mediated multidrug resistance in *Salmonella enterica* serovar typhimurium”. In: *Antimicrobial Agents and Chemotherapy* 56.2, pp. 942–948. ISSN: 00664804. DOI: [10.1128/AAC.05444-11](https://doi.org/10.1128/AAC.05444-11).
- Baucheron, S., Tyler, S., et al. (2004). “AcrAB-TolC directs efflux-mediated multidrug resistance in *Salmonella enterica* serovar typhimurium DT104”. In: *Antimicrobial Agents and Chemotherapy* 48.10, pp. 3729–3735. ISSN: 00664804. DOI: [10.1128/AAC.48.10.3729-3735.2004](https://doi.org/10.1128/AAC.48.10.3729-3735.2004).

- Baugh, S. et al. (2012). “Loss of or inhibition of all multidrug resistance efflux pumps of *Salmonella enterica* serovar Typhimurium results in impaired ability to form a biofilm”. In: *Journal of Antimicrobial Chemotherapy* 67.10, pp. 2409–2417. ISSN: 03057453. DOI: [10.1093/jac/dks228](https://doi.org/10.1093/jac/dks228).
- Ben-Hur, E. et al. (1980). “pH dependence of the phototoxic and photomutagenic effects of chlorpromazine”. In: *Chemico-Biological Interactions* 29.2, pp. 223–233. ISSN: 00092797. DOI: [10.1016/0009-2797\(80\)90035-6](https://doi.org/10.1016/0009-2797(80)90035-6).
- Benarroch, J. M. et al. (2020). “The Microbiologist’s Guide to Membrane Potential Dynamics”. In: *Trends in Microbiology* 28.4, pp. 304–314.
- Bernthsen, A. et al. (1883). “Zur Kenntniss des Methylenblau und verwandter Farbstoffe”. en. In: *Berichte der deutschen chemischen Gesellschaft* 16.2, pp. 2896–2904. ISSN: 1099-0682. DOI: [10.1002/cber.188301602249](https://doi.org/10.1002/cber.188301602249).
- Bettencourt, M. V. et al. (2000). “Comparative *in vitro* activity of phenothiazines against multidrug-resistant *Mycobacterium tuberculosis*”. eng. In: *Int J Antimicrob Agents* 16.1, pp. 69–71. ISSN: 0924-8579 (Print)0924-8579.
- Bhattacharyya, D. et al. (1999). “The effect of binding of chlorpromazine and chloroquine to ion transporting ATPases”. In: *Molecular and Cellular Biochemistry* 198.1-2, pp. 179–185. ISSN: 03008177. DOI: [10.1023/A:1006902031255](https://doi.org/10.1023/A:1006902031255).
- Bianchi, A. A. et al. (1999). “Hyperosmotic shock induces the σ_{32} and σ_E stress regulons of *Escherichia coli*”. In: *Molecular Microbiology* 34.5, pp. 1029–1038. ISSN: 0950-382X. DOI: [10.1046/j.1365-2958.1999.01664.x](https://doi.org/10.1046/j.1365-2958.1999.01664.x).
- Bina, X. et al. (2009). “Effect of the efflux inhibitors 1-(1-naphthylmethyl)-piperazine and phenyl-arginine- β -naphthylamide on antimicrobial susceptibility and virulence factor production in *Vibrio cholerae*”. In: *J Antimicrob Chemo* 63.1, pp. 103–108.
- Björkman, J. and Andersson, D. I. (2000). “The cost of antibiotic resistance from a bacterial perspective”. In: *Drug Resistance Updates* 3.4, pp. 237–245. ISSN: 13687646. DOI: [10.1054/drup.2000.0147](https://doi.org/10.1054/drup.2000.0147).

- Björkman, J., Hughes, D., et al. (1998). “Virulence of antibiotic-resistant *Salmonella* typhimurium”. In: *Proceedings of the National Academy of Sciences of the United States of America* 95.7, pp. 3949–3953. ISSN: 00278424. DOI: [10.1073/pnas.95.7.3949](https://doi.org/10.1073/pnas.95.7.3949).
- Blair, J. M., Webber, M. A., et al. (2015). “Molecular mechanisms of antibiotic resistance”. eng. In: *Nat Rev Microbiol* 13.1, pp. 42–51. ISSN: 1740-1526. DOI: [10.1038/nrmicro3380](https://doi.org/10.1038/nrmicro3380).
- Blair, J. M. and Piddock, L. J. (2016). “How to measure export via bacterial multidrug resistance efflux pumps”. In: *mBio* 7.4, pp. 1–6. ISSN: 21507511. DOI: [10.1128/mBio.00840-16](https://doi.org/10.1128/mBio.00840-16).
- Blattner, F. R. et al. (1997). “The complete genome sequence of *Escherichia coli* K-12”. In: *Science* 277.5331, pp. 1453–1462. ISSN: 00368075. DOI: [10.1126/science.277.5331.1453](https://doi.org/10.1126/science.277.5331.1453).
- Bohnert, J. A. et al. (2008). “Site-directed mutagenesis reveals putative substrate binding residues in the *Escherichia coli* RND efflux pump AcrB”. In: *Journal of Bacteriology* 190.24, pp. 8225–8229. ISSN: 00219193. DOI: [10.1128/JB.00912-08](https://doi.org/10.1128/JB.00912-08).
- Bos, M. P. et al. (2007). “Biogenesis of the Gram-Negative Bacterial Outer Membrane”. In: *Annual Review of Microbiology* 61.1, pp. 191–214. ISSN: 0066-4227. DOI: [10.1146/annurev.micro.61.080706.093245](https://doi.org/10.1146/annurev.micro.61.080706.093245).
- Buchmeier, N. A. et al. (1993). “Recombination-deficient mutants of *Salmonella* Typhimurium are avirulent and sensitive to the oxidative burst of macrophages”. In: *Molecular Microbiology* 7.6, pp. 933–936. ISSN: 13652958. DOI: [10.1111/j.1365-2958.1993.tb01184.x](https://doi.org/10.1111/j.1365-2958.1993.tb01184.x).
- Buelow, D. R. et al. (2005). “Cpx signal transduction is influenced by a conserved N-terminal domain in the novel inhibitor CpxP and the periplasmic protease DegP”. In: *Journal of Bacteriology* 187.19, pp. 6622–6630. ISSN: 00219193. DOI: [10.1128/JB.187.19.6622-6630.2005](https://doi.org/10.1128/JB.187.19.6622-6630.2005).

- Bullough, D. A. et al. (1985). “The varied responses of different F1-ATPases to chlorpromazine”. In: *Archives of Biochemistry and Biophysics* 236.2, pp. 567–575. ISSN: 10960384. DOI: [10.1016/0003-9861\(85\)90660-5](https://doi.org/10.1016/0003-9861(85)90660-5).
- Bumann, D. et al. (2007). “Identification of host-induced pathogen genes by differential fluorescence induction reporter systems”. In: *Nature Protocols* 2.4, pp. 770–777. ISSN: 17542189. DOI: [10.1038/nprot.2007.78](https://doi.org/10.1038/nprot.2007.78).
- Cano, D. A. et al. (2002). “Role of the RecBCD recombination pathway in *Salmonella* virulence”. In: *Journal of Bacteriology* 184.2, pp. 592–595. ISSN: 00219193. DOI: [10.1128/JB.184.2.592-595.2002](https://doi.org/10.1128/JB.184.2.592-595.2002).
- Cha, H.J. et al. (2014). “Switch-loop flexibility affects transport of large drugs by the promiscuous AcrB multidrug efflux transporter”. In: *Antimicrobial Agents and Chemotherapy* 58.8, pp. 4767–4772. ISSN: 10986596. DOI: [10.1128/AAC.02733-13](https://doi.org/10.1128/AAC.02733-13).
- Champoux, J. J. (2001). “DNA Topoisomerases: Structure, Function, and Mechanism”. In: *Annual Review of Biochemistry* 70.1, pp. 369–413. ISSN: 0066-4154. DOI: [10.1146/annurev.biochem.70.1.369](https://doi.org/10.1146/annurev.biochem.70.1.369).
- Chan, W. et al. (2007). “A recombineering based approach for high-throughput conditional knockout targeting vector construction”. In: *Nucleic Acids Research* 35.8, e64. ISSN: 03051048. DOI: [10.1093/nar/gkm163](https://doi.org/10.1093/nar/gkm163).
- Charvalos, E. et al. (1995). “Evidence for an efflux pump in multidrug-resistant *Campylobacter jejuni*”. In: *Antimicrobial Agents and Chemotherapy* 39.9, pp. 2019–2022. ISSN: 00664804. DOI: [10.1128/AAC.39.9.2019](https://doi.org/10.1128/AAC.39.9.2019).
- Chavez, R. G. et al. (2010). “The physiological stimulus for the BarA sensor kinase”. In: *Journal of Bacteriology* 192.7, pp. 2009–2012. ISSN: 00219193. DOI: [10.1128/JB.01685-09](https://doi.org/10.1128/JB.01685-09).
- Cirz, R. T. et al. (2005). “Inhibition of mutation and combating the evolution of antibiotic resistance”. In: *PLoS Biology* 3.6, pp. 1024–1033. ISSN: 15457885. DOI: [10.1371/journal.pbio.0030176](https://doi.org/10.1371/journal.pbio.0030176).

- Coelho, T. et al. (2015). “Enhancement of antibiotic activity by efflux inhibitors against multidrug resistant *Mycobacterium tuberculosis* clinical isolates from Brazil”. In: *Frontiers in Microbiology* 6.APR. ISSN: 1664302X. DOI: [10.3389/fmicb.2015.00330](https://doi.org/10.3389/fmicb.2015.00330).
- Cohen, S. P., Hachler, H., et al. (1993). “Genetic and functional analysis of the multiple antibiotic resistance (*mar*) locus in *Escherichia coli*”. In: *Journal of Bacteriology* 175.5, pp. 1484–1492. ISSN: 00219193. DOI: [10.1128/jb.175.5.1484-1492.1993](https://doi.org/10.1128/jb.175.5.1484-1492.1993).
- Cohen, S. P., McMurry, L. M., et al. (1988). “*marA* locus causes decreased expression of OmpF porin in multiple-antibiotic-resistant (Mar) mutants of *Escherichia coli*”. In: *Journal of Bacteriology* 170.12, pp. 5416–5422. ISSN: 00219193. DOI: [10.1128/jb.170.12.5416-5422.1988](https://doi.org/10.1128/jb.170.12.5416-5422.1988).
- Coldham, N. G. et al. (2010). “A 96-well plate fluorescence assay for assessment of cellular permeability and active efflux in *Salmonella enterica* serovar Typhimurium and *Escherichia coli*”. In: *The Journal of antimicrobial chemotherapy* 65.8, pp. 1655–63. ISSN: 1460-2091. DOI: [10.1093/jac/dkq169](https://doi.org/10.1093/jac/dkq169).
- Corbett, D., Wise, A., et al. (2017). “Potentiation of antibiotic activity by a novel cationic peptide: Potency and spectrum of activity of SPR741”. In: *Antimicrobial Agents and Chemotherapy* 61.8. ISSN: 10986596. DOI: [10.1128/AAC.00200-17](https://doi.org/10.1128/AAC.00200-17).
- Corbett, K. D. and Berger, J. M. (2004). “Structure, Molecular Mechanisms, and Evolutionary Relationships in DNA Topoisomerases”. In: *Annual Review of Biophysics and Biomolecular Structure* 33.1, pp. 95–118. ISSN: 1056-8700. DOI: [10.1146/annurev.biophys.33.110502.140357](https://doi.org/10.1146/annurev.biophys.33.110502.140357).
- Courtney, C. M. et al. (2017). “Potentiating antibiotics in drug-resistant clinical isolates via stimuli-activated superoxide generation”. In: *Science Advances* 3.10. ISSN: 23752548. DOI: [10.1126/sciadv.1701776](https://doi.org/10.1126/sciadv.1701776).
- Coutinho, H. D. et al. (2009). “Herbal therapy associated with antibiotic therapy: Potentiation of the antibiotic activity against methicillin - Resistant *Staphylococcus*

- aureus* by *Turnera ulmifolia* L". In: *BMC Complementary and Alternative Medicine* 9. ISSN: 14726882. DOI: [10.1186/1472-6882-9-13](https://doi.org/10.1186/1472-6882-9-13).
- Cowperthwaite, M. C. et al. (2006). "From bad to good: Fitness reversals and the ascent of deleterious mutations". In: *PLoS Computational Biology* 2.10, pp. 1292–1300. ISSN: 1553734X. DOI: [10.1371/journal.pcbi.0020141](https://doi.org/10.1371/journal.pcbi.0020141).
- Dabbeni-Sala, F. et al. (1990). "Mechanism of local anesthetic effect. Involvement of F₀ in the inhibition of mitochondrial ATP synthase by phenothiazines". eng. In: *Biochim Biophys Acta* 1015.2, pp. 248–252. ISSN: 0006-3002 (Print)0006-3002.
- Das, D. et al. (2007). "Crystal structure of the multidrug efflux transporter AcrB at 3.1 Å resolution reveals the N-terminal region with conserved amino acids". In: *Journal of Structural Biology* 158.3, pp. 494–502. ISSN: 10478477. DOI: [10.1016/j.jsb.2006.12.004](https://doi.org/10.1016/j.jsb.2006.12.004).
- Dastidar, S. G., Chaudhury, A., et al. (1995). "*In vitro* and *in vivo* antimicrobial action of fluphenazine". eng. In: *J Chemother* 7.3, pp. 201–206. ISSN: 1120-009X (Print)1120-009x. DOI: [10.1179/joc.1995.7.3.201](https://doi.org/10.1179/joc.1995.7.3.201).
- Dastidar, S. G., Kristiansen, J. E., et al. (2013). "Role of Phenothiazines and Structurally Similar Compounds of Plant Origin in the Fight against Infections by Drug Resistant Bacteria". eng. In: *Antibiotics (Basel)* 2.1, pp. 58–72. ISSN: 2079-6382 (Print)2079-6382. DOI: [10.3390/antibiotics2010058](https://doi.org/10.3390/antibiotics2010058).
- Davis, R. et al. (1996). "Ciprofloxacin. An updated review of its pharmacology, therapeutic efficacy and tolerability." In: *Drugs* 51.6, pp. 1019–1074. ISSN: 0012-6667. DOI: [10.2165/00003495-199651060-00010](https://doi.org/10.2165/00003495-199651060-00010).
- De Filippi, L. et al. (2007). "Membrane stress is coupled to a rapid translational control of gene expression in chlorpromazine-treated cells". In: *Current Genetics* 52.3-4, pp. 171–185. ISSN: 01728083. DOI: [10.1007/s00294-007-0151-0](https://doi.org/10.1007/s00294-007-0151-0).
- De Mol, N. J. and Busker, R. W. (1984). "Irreversible binding of the chlorpromazine radical cation and of photoactivated chlorpromazine to biological macromolecules".

- In: *Chemico-Biological Interactions* 52.1, pp. 79–92. ISSN: 00092797. DOI: [10.1016/0009-2797\(84\)90084-X](https://doi.org/10.1016/0009-2797(84)90084-X).
- De Mol, N. J., Posthuma, R. M., et al. (1983). “Induction of repairable DNA damage in *Escherichia coli* and interaction with DNA *in vitro* by the radical cation of chlorpromazine”. In: *Chemico-Biological Interactions* 47.2, pp. 223–237. ISSN: 00092797. DOI: [10.1016/0009-2797\(83\)90159-X](https://doi.org/10.1016/0009-2797(83)90159-X).
- de Rautlin de la Roy, Y. et al. (1991). “Kinetics of bactericidal activity of antibiotics measured by luciferin-luciferase assay”. In: *Journal of Bioluminescence and Chemiluminescence* 6.3, pp. 193–201. ISSN: 0884-3996. DOI: [10.1002/bio.1170060310](https://doi.org/10.1002/bio.1170060310).
- Deeds, F. et al. (1939). “Studies on phenothiazine VIII. Aniseptic value of phenothiazine in urinary tract infections”. en. In: *The Journal of Pharmacological and Experimental Therapeutics* 65.4, pp. 353–371.
- Deguchi, T. et al. (1997). “*In vivo* selection of *Klebsiella pneumoniae* strains with enhanced quinolone resistance during fluoroquinolone treatment of urinary tract infections.” In: *Antimicrobial agents and chemotherapy* 41.7, pp. 1609–11. ISSN: 0066-4804.
- Delhaye, A. et al. (2016). “Fine-tuning of the Cpx envelope stress response is required for cell wall homeostasis in *Escherichia coli*”. In: *mBio* 7.1, pp. 47–63. ISSN: 21507511. DOI: [10.1128/mBio.00047-16](https://doi.org/10.1128/mBio.00047-16).
- DiGiuseppe, P. A. et al. (2003). “Signal detection and target gene induction by the CpxRA two-component system”. In: *Journal of Bacteriology* 185.8, pp. 2432–2440. ISSN: 00219193. DOI: [10.1128/JB.185.8.2432-2440.2003](https://doi.org/10.1128/JB.185.8.2432-2440.2003).
- Dillingham, M. S. et al. (2008). “RecBCD Enzyme and the Repair of Double-Stranded DNA Breaks”. In: *Microbiology and Molecular Biology Reviews* 72.4, pp. 642–671. ISSN: 1092-2172. DOI: [10.1128/mmbr.00020-08](https://doi.org/10.1128/mmbr.00020-08).
- Do Thi, T. et al. (2011). “Effect of *recA* inactivation on mutagenesis of *Escherichia coli* exposed to sublethal concentrations of antimicrobials”. In: *Journal of Antimicrobial Chemotherapy* 66.3, pp. 531–538. ISSN: 03057453. DOI: [10.1093/jac/dkq496](https://doi.org/10.1093/jac/dkq496).

- Drlica, K. (2003). “The mutant selection window and antimicrobial resistance”. In: *Journal of Antimicrobial Chemotherapy* 52.1, pp. 11–17. ISSN: 0305-7453. DOI: [10.1093/jac/dkg269](https://doi.org/10.1093/jac/dkg269).
- Du, D. et al. (2014). “Structure of the AcrAB-TolC multidrug efflux pump”. In: *Nature* 509.7501, pp. 512–515. ISSN: 14764687. DOI: [10.1038/nature13205](https://doi.org/10.1038/nature13205).
- Dupont, M. et al. (2007). “An early response to environmental stress involves regulation of OmpX and OmpF, two *enterobacterial* outer membrane pore-forming proteins”. In: *Antimicrobial Agents and Chemotherapy* 51.9, pp. 3190–3198. ISSN: 00664804. DOI: [10.1128/AAC.01481-06](https://doi.org/10.1128/AAC.01481-06).
- Durão, P. et al. (2018). “Evolutionary Mechanisms Shaping the Maintenance of Antibiotic Resistance”. In: *Trends in Microbiology* 26.8, pp. 677–691. ISSN: 18784380. DOI: [10.1016/j.tim.2018.01.005](https://doi.org/10.1016/j.tim.2018.01.005).
- Durrant, J. D. et al. (2011). “Molecular dynamics simulations and drug discovery”. In: *BMC Biology* 9, p. 71. ISSN: 17417007. DOI: [10.1186/1741-7007-9-71](https://doi.org/10.1186/1741-7007-9-71).
- Duval, V. et al. (2013). “Mutational analysis of the multiple-antibiotic resistance regulator *marR* reveals a ligand binding pocket at the interface between the dimerization and DNA binding domains”. In: *Journal of Bacteriology* 195.15, pp. 3341–3351. ISSN: 00219193. DOI: [10.1128/JB.02224-12](https://doi.org/10.1128/JB.02224-12).
- Eaves, D. J. et al. (2004). “Prevalence of mutations within the quinolone resistance-determining region of *gyrA*, *gyrB*, *parC*, and *parE* and association with antibiotic resistance in quinolone-resistant *Salmonella enterica*”. In: *Antimicrobial Agents and Chemotherapy* 48.10, pp. 4012–4015. ISSN: 00664804. DOI: [10.1128/AAC.48.10.4012-4015.2004](https://doi.org/10.1128/AAC.48.10.4012-4015.2004).
- Edwards, A. N., Patterson-Fortin, L. M., et al. (2011). “Circuitry linking the Csr and stringent response global regulatory systems”. In: *Molecular Microbiology* 80.6, pp. 1561–1580. ISSN: 0950382X. DOI: [10.1111/j.1365-2958.2011.07663.x](https://doi.org/10.1111/j.1365-2958.2011.07663.x).

- Edwards, S., Morel, C., et al. (2018). “Combatting Antibiotic Resistance Together: How Can We Enlist the Help of Industry?” In: *Antibiotics* 7.4, p. 111. ISSN: 2079-6382. DOI: [10.3390/antibiotics7040111](https://doi.org/10.3390/antibiotics7040111).
- Eicher, T., Seeger, M., et al. (2014). “Coupling of remote alternating-access transport mechanisms for protons and substrates in the multidrug efflux pump AcrB”. In: *eLife* 3.e03145.
- Eicher, T., Cha, H.-j., et al. (2012). “Transport of drugs by the multidrug transporter AcrB involves an access and a deep binding pocket that are separated by a switch-loop”. en. In: *Proceedings of the National Academy of Sciences of the United States of America* 109.5, pp. 5656–5687. DOI: [10.1073/pnas.1114944109](https://doi.org/10.1073/pnas.1114944109).
- Eilam, Y. (1983). “Membrane effects of phenothiazines in yeasts. I. Stimulation of calcium and potassium fluxes”. eng. In: *Biochim Biophys Acta* 733.2, pp. 242–248. ISSN: 0006-3002 (Print)0006-3002.
- Eilam, Y. (1984). “Effects of phenothiazines on inhibition of plasma membrane ATPase and hyperpolarization of cell membranes in the yeast *Saccharomyces cerevisiae*”. In: *BBA - Biomembranes* 769.3, pp. 601–610. ISSN: 00052736. DOI: [10.1016/0005-2736\(84\)90059-2](https://doi.org/10.1016/0005-2736(84)90059-2).
- Eisenberg, S. et al. (2008). “Differential interference of chlorpromazine with the membrane interactions of oncogenic K-ras and its effects on cell growth”. In: *Journal of Biological Chemistry* 283.40, pp. 27279–27288. ISSN: 00219258. DOI: [10.1074/jbc.M804589200](https://doi.org/10.1074/jbc.M804589200).
- El Mouali, Y. et al. (2018). “CRP-cAMP mediates silencing of *Salmonella* virulence at the post-transcriptional level”. In: *PLoS Genetics* 14.6. ISSN: 15537404. DOI: [10.1371/journal.pgen.1007401](https://doi.org/10.1371/journal.pgen.1007401).
- Elkes, J. et al. (1954). “Effect of chlorpromazine on the behavior of chronically overactive psychotic patients”. eng. In: *Br Med J* 2.4887, pp. 560–565. ISSN: 0007-1447 (Print)0007-1447.

- Elkins, C. A. et al. (2002). “Substrate Specificity of the RND-Type Multidrug Efflux Pumps AcrB and AcrD of *Escherichia coli* Is Determined Predominately by Two Large Periplasmic Loops”. In: *Journal of Bacteriology* 184.23, p. 6490. DOI: [10.1128/JB.184.23.6490-6498.2002](https://doi.org/10.1128/JB.184.23.6490-6498.2002).
- Fange, D. et al. (2009). “Drug efflux pump deficiency and drug target resistance masking in growing bacteria”. In: *Proceedings of the National Academy of Sciences of the United States of America* 106.20, pp. 8215–8220. ISSN: 00278424. DOI: [10.1073/pnas.0811514106](https://doi.org/10.1073/pnas.0811514106).
- Fardini, Y. et al. (2009). “Investigation of the role of the BAM complex and SurA chaperone in outer-membrane protein biogenesis and type III secretion system expression in *Salmonella*”. In: *Microbiology* 155.5, pp. 1613–1622. ISSN: 13500872. DOI: [10.1099/mic.0.025155-0](https://doi.org/10.1099/mic.0.025155-0).
- Farha, M. A. et al. (2013). “Collapsing the proton motive force to identify synergistic combinations against *staphylococcus aureus*”. In: *Chemistry and Biology* 20.9, pp. 1168–1178. ISSN: 10745521. DOI: [10.1016/j.chembiol.2013.07.006](https://doi.org/10.1016/j.chembiol.2013.07.006).
- Faria, P. A. de et al. (2015). “Cytotoxicity of phenothiazine derivatives associated with mitochondrial dysfunction: A structure-activity investigation”. In: *Toxicology* 330, pp. 44–54. ISSN: 18793185. DOI: [10.1016/j.tox.2015.02.004](https://doi.org/10.1016/j.tox.2015.02.004).
- Fernández, L. et al. (2012). “Adaptive and mutational resistance: Role of porins and efflux pumps in drug resistance”. In: *Clinical Microbiology Reviews* 25.4, pp. 661–681. ISSN: 08938512. DOI: [10.1128/CMR.00043-12](https://doi.org/10.1128/CMR.00043-12).
- Ferrer-Espada, R. et al. (2019). “A permeability-increasing drug synergizes with bacterial efflux pump inhibitors and restores susceptibility to antibiotics in multi-drug resistant *Pseudomonas aeruginosa* strains”. In: *Scientific Reports* 9.1. ISSN: 20452322. DOI: [10.1038/s41598-019-39659-4](https://doi.org/10.1038/s41598-019-39659-4).
- Fortune, D. R. et al. (2006). “Identification of CsrC and characterization of its role in epithelial cell invasion in *Salmonella enterica* serovar typhimurium”. In: *Infection*

- and Immunity* 74.1, pp. 331–339. ISSN: 00199567. DOI: [10.1128/IAI.74.1.331-339.2006](https://doi.org/10.1128/IAI.74.1.331-339.2006).
- Foster, P. L. (2006). “Methods for Determining Spontaneous Mutation Rates”. In: *Methods in Enzymology* 409, pp. 195–213. ISSN: 00766879. DOI: [10.1016/S0076-6879\(05\)09012-9](https://doi.org/10.1016/S0076-6879(05)09012-9).
- Gan, E. et al. (2011). “Phenotypic and molecular characterization of *Salmonella enterica* serovar Sofia, an avirulent species in Australian poultry”. In: *Microbiology* 157.4, pp. 1056–1065. ISSN: 13500872. DOI: [10.1099/mic.0.047001-0](https://doi.org/10.1099/mic.0.047001-0).
- Gellert, M. et al. (1976). “DNA gyrase: an enzyme that introduces superhelical turns into DNA”. In: *Proceedings of the National Academy of Sciences of the United States of America* 73.11, pp. 3872–3876. ISSN: 00278424. DOI: [10.1073/pnas.73.11.3872](https://doi.org/10.1073/pnas.73.11.3872).
- Gerrish, P. J. et al. (1998). “The fate of competing beneficial mutations in an asexual population”. In: *Genetica* 102, p. 127.
- Ghosh, A. S. et al. (1998). “Involvement of an efflux system in high-level fluoroquinolone resistance of *Shigella dysenteriae*.” In: *Biochemical and biophysical research communications* 242.1, pp. 54–6. ISSN: 0006-291X. DOI: [10.1006/bbrc.1997.7902](https://doi.org/10.1006/bbrc.1997.7902).
- Gillette, W. K. et al. (2000). “Probing the *Escherichia coli* transcriptional activator MarA using alanine-scanning mutagenesis: Residues important for DNA binding and activation”. In: *Journal of Molecular Biology* 299.5, pp. 1245–1255. ISSN: 00222836. DOI: [10.1006/jmbi.2000.3827](https://doi.org/10.1006/jmbi.2000.3827).
- Giraud, E., Cloeckert, A., Kerboeuf, D., et al. (2000). “Evidence for active efflux as the primary mechanism of resistance to ciprofloxacin in *Salmonella enterica* serovar Typhimurium.” In: *Antimicrobial agents and chemotherapy* 44.5, pp. 1223–8. ISSN: 0066-4804. DOI: [10.1128/aac.44.5.1223-1228.2000](https://doi.org/10.1128/aac.44.5.1223-1228.2000).
- Giraud, E., Cloeckert, A., Baucheron, S., et al. (2003). “Fitness cost of fluoroquinolone resistance in *Salmonella enterica* serovar Typhimurium”. In: *Journal of Medical Microbiology* 52.8, pp. 697–703. ISSN: 00222615. DOI: [10.1099/jmm.0.05178-0](https://doi.org/10.1099/jmm.0.05178-0).

- Gophna, U. et al. (2003). *Virulence and the heat shock response*. DOI: [10.1078/1438-4221-00230](https://doi.org/10.1078/1438-4221-00230).
- Goswami, M., Mangoli, S. H., et al. (2006). “Involvement of reactive oxygen species in the action of ciprofloxacin against *Escherichia coli*”. In: *Antimicrobial Agents and Chemotherapy* 50.3, pp. 949–954. ISSN: 00664804. DOI: [10.1128/AAC.50.3.949-954.2006](https://doi.org/10.1128/AAC.50.3.949-954.2006).
- Goswami, M. and Narayana Rao, A. V. S. S. (2018). “Transcriptome Profiling Reveals Interplay of Multifaceted Stress Response in *Escherichia coli* on Exposure to Glutathione and Ciprofloxacin”. In: *mSystems* 3.1, pp. 1–18. ISSN: 2379-5077. DOI: [10.1128/msystems.00001-18](https://doi.org/10.1128/msystems.00001-18).
- Goswami, M., Subramanian, M., et al. (2016). “Involvement of antibiotic efflux machinery in glutathione-mediated decreased ciprofloxacin activity in *Escherichia coli*”. In: *Antimicrobial Agents and Chemotherapy* 60.7, pp. 4369–4374. ISSN: 10986596. DOI: [10.1128/AAC.00414-16](https://doi.org/10.1128/AAC.00414-16).
- Gotoh, N. et al. (1999). “Topological analysis of an RND family transporter, MexD of *Pseudomonas aeruginosa*”. In: *FEBS Letters* 458.1, pp. 32–36. ISSN: 00145793. DOI: [10.1016/S0014-5793\(99\)01116-3](https://doi.org/10.1016/S0014-5793(99)01116-3).
- Green, A. T. et al. (2020). “Discovery of multidrug efflux pump inhibitors with a novel chemical scaffold”. In: *Biochimica et Biophysica Acta (BBA) - General Subjects* 1864.6, p. 129546. ISSN: 03044165. DOI: [10.1016/j.bbagen.2020.129546](https://doi.org/10.1016/j.bbagen.2020.129546).
- Guan, L. et al. (2001). “Identification of essential charged residues in transmembrane segments of the multidrug transporter MexB of *Pseudomonas aeruginosa*”. In: *Journal of Bacteriology* 183.5, pp. 1734–1739. ISSN: 00219193. DOI: [10.1128/JB.183.5.1734-1739.2001](https://doi.org/10.1128/JB.183.5.1734-1739.2001).
- Guedes, I. A. et al. (2018). “Empirical scoring functions for structure-based virtual screening: Applications, critical aspects, and challenges”. In: *Frontiers in Pharmacology* 9.SEP. ISSN: 16639812. DOI: [10.3389/fphar.2018.01089](https://doi.org/10.3389/fphar.2018.01089).

- Gullberg, E. et al. (2011). “Selection of resistant bacteria at very low antibiotic concentrations”. In: *PLoS Pathogens* 7.7. ISSN: 15537366. DOI: [10.1371/journal.ppat.1002158](https://doi.org/10.1371/journal.ppat.1002158).
- Gunesekere, I. C. et al. (2006). “Comparison of the RpoH-dependent regulon and general stress response in *Neisseria gonorrhoeae*”. In: *Journal of Bacteriology* 188.13, pp. 4769–4776. ISSN: 00219193. DOI: [10.1128/JB.01807-05](https://doi.org/10.1128/JB.01807-05).
- Gupta, R. C. et al. (1997). “Activities of human recombination protein Rad51”. In: *Proceedings of the National Academy of Sciences of the United States of America* 94.2, pp. 463–468. ISSN: 00278424. DOI: [10.1073/pnas.94.2.463](https://doi.org/10.1073/pnas.94.2.463).
- Gutierrez, A. et al. (2013). “ β -lactam antibiotics promote bacterial mutagenesis via an RpoS-mediated reduction in replication fidelity”. In: *Nature Communications* 4. ISSN: 20411723. DOI: [10.1038/ncomms2607](https://doi.org/10.1038/ncomms2607).
- Hall, A. R., Griffiths, V. F., et al. (2010). “Mutational neighbourhood and mutation supply rate constrain adaptation in *Pseudomonas aeruginosa*”. In: *Proceedings of the Royal Society B: Biological Sciences* 277.1681, pp. 643–650. ISSN: 14712970. DOI: [10.1098/rspb.2009.1630](https://doi.org/10.1098/rspb.2009.1630).
- Hall, M. J., Middleton, R. F., et al. (1983). “fractional inhibitory concentration (FIC) index as a measure of synergy | Journal of Antimicrobial Chemotherapy | Oxford Academic”. In: *Journal of Antimicrobial Chemotherapy* 11.5, pp. 427–433.
- Händel, N. et al. (2013). “Compensation of the metabolic costs of antibiotic resistance by physiological adaptation in *escherichia coli*”. In: *Antimicrobial Agents and Chemotherapy* 57.8, pp. 3752–3762. ISSN: 00664804. DOI: [10.1128/AAC.02096-12](https://doi.org/10.1128/AAC.02096-12).
- Hansen, H. et al. (2003). “Topoisomerase IV mutations in quinolone-resistant *salmonellae* selected *in vitro*”. In: *Microbial Drug Resistance* 9.1, pp. 25–32. ISSN: 10766294. DOI: [10.1089/107662903764736319](https://doi.org/10.1089/107662903764736319).

- Harris, R. M. et al. (2001). “Characterization of PitA and PitB from *Escherichia coli*”. In: *Journal of Bacteriology* 183.17, pp. 5008–5014. ISSN: 00219193. DOI: [10.1128/JB.183.17.5008-5014.2001](https://doi.org/10.1128/JB.183.17.5008-5014.2001).
- Heesterbeek, D. A. et al. (2019). “Complement-dependent outer membrane perturbation sensitizes Gram-negative bacteria to Gram-positive specific antibiotics”. In: *Scientific Reports* 9.1, pp. 1–10. ISSN: 20452322. DOI: [10.1038/s41598-019-38577-9](https://doi.org/10.1038/s41598-019-38577-9).
- Heinrichs, D. E. et al. (1998). “Molecular basis for structural diversity in the core regions of the lipopolysaccharides of *Escherichia coli* and *Salmonella enterica*”. In: *Molecular Microbiology* 30.2, pp. 221–232. ISSN: 0950382X.
- Heisig, P. (1996). “Genetic evidence for a role of *parC* mutations in development of high-level fluoroquinolone resistance in *Escherichia coli*”. In: *Antimicrobial Agents and Chemotherapy* 40.4, pp. 879–885. ISSN: 00664804. DOI: [10.1128/aac.40.4.879](https://doi.org/10.1128/aac.40.4.879).
- Heller, A. A. et al. (2019). “A rapid method for post-antibiotic bacterial susceptibility testing”. In: *PLoS ONE* 14.1. ISSN: 19326203. DOI: [10.1371/journal.pone.0210534](https://doi.org/10.1371/journal.pone.0210534).
- Herrera, G. (1993). “Quinolone action in *Escherichia coli* cells carrying *gyrA* and *gyrB* mutations”. In: *FEMS Microbiology Letters* 106.2, pp. 187–191. ISSN: 03781097. DOI: [10.1016/0378-1097\(93\)90079-h](https://doi.org/10.1016/0378-1097(93)90079-h).
- Hews, C. L. et al. (2019). “Maintaining Integrity Under Stress: Envelope Stress Response Regulation of Pathogenesis in Gram-Negative Bacteria”. In: *Frontiers in Cellular and Infection Microbiology* 9, p. 313. ISSN: 22352988. DOI: [10.3389/fcimb.2019.00313](https://doi.org/10.3389/fcimb.2019.00313).
- Hilpert, K. et al. (2010). “Short cationic antimicrobial peptides interact with ATP”. In: *Antimicrobial Agents and Chemotherapy* 54.10, pp. 4480–4483. ISSN: 00664804. DOI: [10.1128/AAC.01664-09](https://doi.org/10.1128/AAC.01664-09).
- Hoffer, S. M. et al. (2001). “Activation by gene amplification of *pitB*, encoding a third phosphate transporter of *Escherichia coli* K-12”. In: *Journal of Bacteriology* 183.15, pp. 4659–4663. ISSN: 00219193. DOI: [10.1128/JB.183.15.4659-4663.2001](https://doi.org/10.1128/JB.183.15.4659-4663.2001).

- Horiyama, T. et al. (2010). “TolC dependency of multidrug efflux systems in *Salmonella enterica* serovar Typhimurium”. In: *Journal of Antimicrobial Chemotherapy* 65.7, pp. 1372–1376. ISSN: 1460-2091. DOI: [10.1093/jac/dkq160](https://doi.org/10.1093/jac/dkq160).
- Hornsey, M. et al. (2011). “Whole-genome comparison of two *Acinetobacter baumannii* isolates from a single patient, where resistance developed during tigecycline therapy”. In: *Journal of Antimicrobial Chemotherapy* 66.7, pp. 1499–1503. ISSN: 03057453. DOI: [10.1093/jac/dkr168](https://doi.org/10.1093/jac/dkr168).
- Hughes, D. et al. (2017). “Evolutionary Trajectories to Antibiotic Resistance”. In: *Annual Review of Microbiology* 71.1, pp. 579–596. ISSN: 0066-4227. DOI: [10.1146/annurev-micro-090816-093813](https://doi.org/10.1146/annurev-micro-090816-093813).
- Humphreys, S., Rowley, G., et al. (2004). “Role of the two-component regulator CpxAR in the virulence of *Salmonella enterica* serotype Typhimurium”. In: *Infection and Immunity* 72.8, pp. 4654–4661. ISSN: 00199567. DOI: [10.1128/IAI.72.8.4654-4661.2004](https://doi.org/10.1128/IAI.72.8.4654-4661.2004).
- Humphreys, S., Stevenson, A., et al. (1999). “The alternative sigma factor, $\sigma(E)$, is critically important for the virulence of *Salmonella typhimurium*”. In: *Infection and Immunity* 67.4, pp. 1560–1568. ISSN: 00199567. DOI: [10.1128/iai.67.4.1560-1568.1999](https://doi.org/10.1128/iai.67.4.1560-1568.1999).
- Jaszczyszyn, A. et al. (2012). “Chemical structure of phenothiazines and their biological activity”. In: 64.1, pp. 16–23. ISSN: 17341140. DOI: [10.1016/S1734-1140\(12\)70726-0](https://doi.org/10.1016/S1734-1140(12)70726-0).
- Jewel, Y. et al. (2020). “Substrate-dependent transport mechanism in AcrB of multidrug resistant bacteria”. In: *Proteins: Structure, Function and Bioinformatics*, prot.25877. ISSN: 10970134. DOI: [10.1002/prot.25877](https://doi.org/10.1002/prot.25877).
- Jiang, Y. W. et al. (2017). “Fluorescence studies on the interaction between chlorpromazine and model cell membranes”. In: *New Journal of Chemistry* 41.10, pp. 4048–4057. ISSN: 13699261. DOI: [10.1039/c7nj00037e](https://doi.org/10.1039/c7nj00037e).
- Johnning, A. et al. (2015). “Resistance Mutations in *gyrA* and *parC* are Common in *Escherichia* Communities of both Fluoroquinolone-Polluted and Uncontaminated

- Aquatic Environments". In: *Frontiers in Microbiology* 6.DEC, p. 1355. ISSN: 1664-302X. DOI: [10.3389/fmicb.2015.01355](https://doi.org/10.3389/fmicb.2015.01355).
- Kaatz, G. W. et al. (2003). "Phenothiazines and Thioxanthenes Inhibit Multidrug Efflux Pump Activity in *Staphylococcus aureus*". eng. In: *Antimicrob Agents Chemother* 47.2, pp. 719–726. ISSN: 0066-4804 (Print)1098-6596 (Electronic). DOI: [10.1128/aac.47.2.719-726.2003](https://doi.org/10.1128/aac.47.2.719-726.2003).
- Kabir, M. S. et al. (2005). "Cell lysis directed by σ E in early stationary phase and effect of induction of the *rpoE* gene on global gene expression in *Escherichia coli*". In: *Microbiology* 151.8, pp. 2721–2735. ISSN: 13500872. DOI: [10.1099/mic.0.28004-0](https://doi.org/10.1099/mic.0.28004-0).
- Katju, V. et al. (2019). "Old trade, new tricks: Insights into the spontaneous mutation process from the partnering of classical mutation accumulation experiments with high-throughput genomic approaches". In: *Genome Biology and Evolution* 11.1, pp. 136–165. ISSN: 17596653. DOI: [10.1093/gbe/evy252](https://doi.org/10.1093/gbe/evy252).
- Kern, W. V. et al. (2006). "Effect of 1-(1-naphthylmethyl)-piperazine, a novel putative efflux pump inhibitor, on antimicrobial drug susceptibility in clinical isolates of *Escherichia coli*". In: *Journal of Antimicrobial Chemotherapy* 57.2, pp. 339–343. ISSN: 03057453. DOI: [10.1093/jac/dki445](https://doi.org/10.1093/jac/dki445).
- Keyamura, K. et al. (2013). "RecA protein recruits structural maintenance of chromosomes (SMC)-like RecN protein to DNA double-strand breaks". In: *Journal of Biological Chemistry* 288.41, pp. 29229–29237. ISSN: 00219258. DOI: [10.1074/jbc.M113.485474](https://doi.org/10.1074/jbc.M113.485474).
- Kinana, A. D. et al. (2016). "Aminoacyl β -naphthylamides as substrates and modulators of AcrB multidrug efflux pump". In: *Proceedings of the National Academy of Sciences of the United States of America* 113.5, pp. 1405–1410. ISSN: 10916490. DOI: [10.1073/pnas.1525143113](https://doi.org/10.1073/pnas.1525143113).
- King, D. E. et al. (2000). "New Classification and Update on the Quinolone Antibiotics". In: *American Family Physician* 61.9, pp. 2741–2748. ISSN: 0002-838X.

- Knopp, M. et al. (2018). “Predictable phenotypes of antibiotic resistance mutations”. In: *mBio* 9.3. ISSN: 21507511. DOI: [10.1128/mBio.00770-18](https://doi.org/10.1128/mBio.00770-18).
- Knopp, M. et al. (2015). “Amelioration of the Fitness Costs of Antibiotic Resistance Due To Reduced Outer Membrane Permeability by Upregulation of Alternative Porins.” In: *Molecular biology and evolution* 32.12, pp. 3252–63. ISSN: 1537-1719. DOI: [10.1093/molbev/msv195](https://doi.org/10.1093/molbev/msv195).
- Kobylka, J. et al. (2020). “AcrB: a mean, keen, drug efflux machine”. In: 1459.1, pp. 38–68. ISSN: 17496632. DOI: [10.1111/nyas.14239](https://doi.org/10.1111/nyas.14239).
- Komatsu, N. et al. (1997). “Induction of a protective immunity in mice against *Escherichia coli* by phenothiazines, 10-[n-(phthalimido)alkyl]-2-substituted-10H-phenothiazines and 1-(2-chloroethyl)-3-(2-substituted-10H-phenothiazines-10-yl)alkyl-1 -ureas .” In: *In vivo (Athens, Greece)* 11.1, pp. 13–6. ISSN: 0258-851X.
- Koronakis, V., Eswaran, J., et al. (2004). “Structure and Function of TolC: The Bacterial Exit Duct for Proteins and Drugs”. In: *Annual Review of Biochemistry* 73.1, pp. 467–489. ISSN: 0066-4154. DOI: [10.1146/annurev.biochem.73.011303.074104](https://doi.org/10.1146/annurev.biochem.73.011303.074104).
- Koronakis, V., Sharff, A., et al. (2000). “Crystal structure of the bacterial membrane protein TolC central to multidrug efflux and protein export”. In: *Nature* 405.6789, pp. 914–919. ISSN: 00280836. DOI: [10.1038/35016007](https://doi.org/10.1038/35016007).
- Kowalczykowski, S. C. (2000). “Initiation of genetic recombination and recombination-dependent replication”. In: 25.4, pp. 156–165. ISSN: 09680004. DOI: [10.1016/S0968-0004\(00\)01569-3](https://doi.org/10.1016/S0968-0004(00)01569-3).
- Kraker, M. E. A. de et al. (2016). “Will 10 Million People Die a Year due to Antimicrobial Resistance by 2050?” In: *PLoS medicine* 13.11, e1002184. ISSN: 1549-1676. DOI: [10.1371/journal.pmed.1002184](https://doi.org/10.1371/journal.pmed.1002184).
- Kristiansen, J. E. and Blom, J. (1981). “Effect of chlorpromazine on the ultrastructure of *Staphylococcus aureus*.” In: *Acta pathologica et microbiologica Scandinavica. Section B, Microbiology* 89.6, pp. 399–405. ISSN: 0105-0656.

- Kristiansen, J. E. H., Mortensen, I., et al. (1982). “Membrane stabilizers inhibit potassium efflux from *Staphylococcus aureus* strain No. U2275”. In: *BBA - Biomembranes* 685.3, pp. 379–382. ISSN: 00052736. DOI: [10.1016/0005-2736\(82\)90079-7](https://doi.org/10.1016/0005-2736(82)90079-7).
- Kristiansen, J. E., Hendricks, O., et al. (2007). “Reversal of resistance in microorganisms by help of non-antibiotics.” In: *The Journal of antimicrobial chemotherapy* 59.6, pp. 1271–9. ISSN: 0305-7453. DOI: [10.1093/jac/dkm071](https://doi.org/10.1093/jac/dkm071).
- Kristiansen, J. E. (1979). “Experiments to Illustrate The Effect Of Chlorpromazine On The Permeability Of The Bacterial Cell Wall”. In: *Acta Pathologica Microbiologica Scandinavica Section B Microbiology* 87 B.1-6, pp. 317–319. ISSN: 16000463. DOI: [10.1111/j.1699-0463.1979.tb02445.x](https://doi.org/10.1111/j.1699-0463.1979.tb02445.x).
- Krulwich, T. A. et al. (2011). “Molecular aspects of bacterial pH sensing and homeostasis”. In: *Nature Reviews Microbiology* 9.5, pp. 330–343. ISSN: 17401526. DOI: [10.1038/nrmicro2549](https://doi.org/10.1038/nrmicro2549).
- Kuroda, A. et al. (2001). “Role of inorganic polyphosphate in promoting ribosomal protein degradation by the Lon protease in *E. coli*”. In: *Science* 293.5530, pp. 705–708. ISSN: 00368075. DOI: [10.1126/science.1061315](https://doi.org/10.1126/science.1061315).
- Labedan, B. (1988). “Increase in permeability of *Escherichia coli* outer membrane by local anesthetics and penetration of antibiotics”. In: *Antimicrobial Agents and Chemotherapy* 32.1, pp. 153–155. ISSN: 00664804. DOI: [10.1128/AAC.32.1.153](https://doi.org/10.1128/AAC.32.1.153).
- Lamers, R. P. et al. (2013). “The efflux inhibitor phenylalanine-arginine beta-naphthylamide (PAβN) permeabilizes the outer membrane of gram-negative bacteria”. eng. In: *PLoS One* 8.3, e60666. ISSN: 1932-6203. DOI: [10.1371/journal.pone.0060666](https://doi.org/10.1371/journal.pone.0060666).
- Lamut, A. et al. (2019). “Efflux pump inhibitors of clinically relevant multidrug resistant bacteria”. In: *Medicinal Research Reviews* 39.6, pp. 2460–2504. ISSN: 0198-6325. DOI: [10.1002/med.21591](https://doi.org/10.1002/med.21591).

- Laudy, A. E. et al. (2017). “The impact of efflux pump inhibitors on the activity of selected non-antibiotic medicinal products against gram-negative bacteria”. In: *Molecules* 22.1. ISSN: 14203049. DOI: [10.3390/molecules22010114](https://doi.org/10.3390/molecules22010114).
- Lawler, A. J. et al. (2013). “Genetic inactivation of *acrAB* or inhibition of efflux induces expression of *ramA*”. In: *Journal of Antimicrobial Chemotherapy* 68.7, pp. 1551–1557. ISSN: 0305-7453. DOI: [10.1093/jac/dkt069](https://doi.org/10.1093/jac/dkt069).
- Lee, C.-R. et al. (2013). “Strategies to minimize antibiotic resistance.” In: *International journal of environmental research and public health* 10.9, pp. 4274–305. ISSN: 1660-4601. DOI: [10.3390/ijerph10094274](https://doi.org/10.3390/ijerph10094274).
- Lewin, C. S. et al. (1991). “The role of the SOS response in bacteria exposed to zidovudine or trimethoprim”. In: *Journal of Medical Microbiology* 34.6, pp. 329–332. ISSN: 00222615. DOI: [10.1099/00222615-34-6-329](https://doi.org/10.1099/00222615-34-6-329).
- Lewis, C. et al. (2008). “Small outer-membrane lipoprotein, SmpA, is regulated by σ E and has a role in cell envelope integrity and virulence of *Salmonella enterica* serovar Typhimurium”. In: *Microbiology* 154.3, pp. 979–988. ISSN: 13500872. DOI: [10.1099/mic.0.2007/011999-0](https://doi.org/10.1099/mic.0.2007/011999-0).
- Li, S. C., Goto, N. K., et al. (1996). “ α -Helical, but not β -sheet, propensity of proline is determined by peptide environment”. In: *Proceedings of the National Academy of Sciences of the United States of America* 93.13, pp. 6676–6681. ISSN: 00278424. DOI: [10.1073/pnas.93.13.6676](https://doi.org/10.1073/pnas.93.13.6676).
- Li, X. Z. and Nikaido, H. (2009). “Efflux-mediated drug resistance in bacteria: An update”. In: *Drugs* 69.12, pp. 1555–1623. ISSN: 00126667. DOI: [10.2165/11317030-000000000-00000](https://doi.org/10.2165/11317030-000000000-00000).
- Lim, S. P. et al. (2010). “Kinetic parameters of efflux of penicillins by the multidrug efflux transporter AcrAB-TolC of *Escherichia coli*”. In: *Antimicrobial Agents and Chemotherapy* 54.5, pp. 1800–1806. ISSN: 00664804. DOI: [10.1128/AAC.01714-09](https://doi.org/10.1128/AAC.01714-09).

- Linde, H. J. et al. (2000). “*In vivo* increase in resistance to ciprofloxacin in *Escherichia coli* associated with deletion of the C-terminal part of *marR*”. In: *Antimicrobial Agents and Chemotherapy* 44.7, pp. 1865–1868. ISSN: 00664804. DOI: [10.1128/AAC.44.7.1865-1868.2000](https://doi.org/10.1128/AAC.44.7.1865-1868.2000).
- Lindgren, P. K. et al. (2005). “Biological cost of single and multiple norfloxacin resistance mutations in *Escherichia coli* implicated in urinary tract infections”. In: *Antimicrobial Agents and Chemotherapy* 49.6, pp. 2343–2351. ISSN: 00664804. DOI: [10.1128/AAC.49.6.2343-2351.2005](https://doi.org/10.1128/AAC.49.6.2343-2351.2005).
- Lindstedt, B. A. et al. (2004). “Geographically dependent distribution of *gyrA* gene mutations at codons 83 and 87 in *Salmonella* Hadar, and a novel codon 81 Gly to His mutation in *Salmonella* Enteritidis”. In: *APMIS* 112.3, pp. 165–171. ISSN: 09034641. DOI: [10.1111/j.1600-0463.2004.apm1120302.x](https://doi.org/10.1111/j.1600-0463.2004.apm1120302.x).
- Ling, J. M. et al. (2003). “Mutations in Topoisomerase Genes of Fluoroquinolone-Resistant *Salmonellae* in Hong Kong”. In: *Antimicrobial Agents and Chemotherapy* 47.11, pp. 3567–3573. ISSN: 00664804. DOI: [10.1128/AAC.47.11.3567-3573.2003](https://doi.org/10.1128/AAC.47.11.3567-3573.2003).
- Liu, A., Fong, A., et al. (2011). “Selective advantage of resistant strains at trace levels of antibiotics: A simple and ultrasensitive color test for detection of antibiotics and genotoxic agents”. In: *Antimicrobial Agents and Chemotherapy* 55.3, pp. 1204–1210. ISSN: 00664804. DOI: [10.1128/AAC.01182-10](https://doi.org/10.1128/AAC.01182-10).
- Liu, B. T., Liao, X. P., et al. (2012). “Detection of mutations in the *gyrA* and *parC* genes in *Escherichia coli* isolates carrying plasmid-mediated quinolone resistance genes from diseased food-producing animals”. In: *Journal of Medical Microbiology* 61.PART 11, pp. 1591–1599. ISSN: 00222615. DOI: [10.1099/jmm.0.043307-0](https://doi.org/10.1099/jmm.0.043307-0).
- Liu, Y. Y. and Chen, C. C. (2017). “Computational analysis of the molecular mechanism of RamR mutations contributing to antimicrobial resistance in *salmonella enterica*”. In: *Scientific Reports* 7.1, pp. 1–9. ISSN: 20452322. DOI: [10.1038/s41598-017-14008-5](https://doi.org/10.1038/s41598-017-14008-5).

- Lobanovska, M. et al. (2017). “Penicillin’s discovery and antibiotic resistance: Lessons for the future?” In: *Yale Journal of Biology and Medicine* 90.1, pp. 135–145. ISSN: 00440086.
- Lodish, H. et al. (2000). “Electron Transport and Oxidative Phosphorylation”. In:
- Lomovskaya, O. and Bostian, K. A. (2006). “Practical applications and feasibility of efflux pump inhibitors in the clinic - A vision for applied use”. In: *Biochemical Pharmacology* 71.7, pp. 910–918. ISSN: 00062952. DOI: [10.1016/j.bcp.2005.12.008](https://doi.org/10.1016/j.bcp.2005.12.008).
- Lomovskaya, O., Warren, M. S., et al. (2001). “Identification and characterization of inhibitors of multidrug resistance efflux pumps in *Pseudomonas aeruginosa*: Novel agents for combination therapy”. In: *Antimicrobial Agents and Chemotherapy* 45.1, pp. 105–116. ISSN: 00664804. DOI: [10.1128/AAC.45.1.105-116.2001](https://doi.org/10.1128/AAC.45.1.105-116.2001).
- Lou, L. et al. (2019). “*Salmonella* Pathogenicity Island 1 (SPI-1) and Its Complex Regulatory Network”. In: *Frontiers in Cellular and Infection Microbiology* 9, p. 270. ISSN: 22352988. DOI: [10.3389/fcimb.2019.00270](https://doi.org/10.3389/fcimb.2019.00270).
- Luria, S. E. et al. (1943). “Mutations of Bacteria from Virus Sensitivity to Virus Resistance.” In: *Genetics* 28.6, pp. 491–511. ISSN: 0016-6731.
- Ma, D., Cook, D. N., et al. (1993). “Molecular cloning and characterization of *acrA* and *acrE* genes of *Escherichia coli*.” In: *Journal of bacteriology* 175.19, pp. 6299–313. ISSN: 0021-9193.
- Ma, D., Alberti, M., et al. (1996). “The local repressor AcrR plays a modulating role in the regulation of *acrAB* genes of *Escherichia coli* by global stress signals”. In: *Molecular Microbiology* 19.1, pp. 101–112. ISSN: 0950382X. DOI: [10.1046/j.1365-2958.1996.357881.x](https://doi.org/10.1046/j.1365-2958.1996.357881.x).
- Machuca, J. et al. (2014). “Interplay between plasmid-mediated and chromosomal-mediated fluoroquinolone resistance and bacterial fitness in *Escherichia coli*”. In: *Journal of Antimicrobial Chemotherapy* 69.12, pp. 3203–3215. ISSN: 14602091. DOI: [10.1093/jac/dku308](https://doi.org/10.1093/jac/dku308).

- MacPhee, D. G. et al. (1996). “Spontaneous mutations in bacteria: chance or necessity?” In: *Genetica* 97.1, pp. 87–101. ISSN: 0016-6707. DOI: [10.1007/bf00132585](https://doi.org/10.1007/bf00132585).
- Magiorakos, A. P. et al. (2012). “Multidrug-resistant, extensively drug-resistant and pandrug-resistant bacteria: An international expert proposal for interim standard definitions for acquired resistance”. In: *Clinical Microbiology and Infection* 18.3, pp. 268–281. ISSN: 14690691. DOI: [10.1111/j.1469-0691.2011.03570.x](https://doi.org/10.1111/j.1469-0691.2011.03570.x).
- Magnet, S. et al. (2001). “Resistance-nodulation-cell division-type efflux pump involved in aminoglycoside resistance in *Acinetobacter baumannii* strain BM4454.” In: *Antimicrobial agents and chemotherapy* 45.12, pp. 3375–80. ISSN: 0066-4804. DOI: [10.1128/AAC.45.12.3375-3380.2001](https://doi.org/10.1128/AAC.45.12.3375-3380.2001).
- Maldonado, R. F. et al. (2016). “Lipopolysaccharide modification in gram-negative bacteria during chronic infection”. In: *FEMS Microbiology Reviews* 40.4, pp. 480–493. ISSN: 15746976. DOI: [10.1093/femsre/fuw007](https://doi.org/10.1093/femsre/fuw007).
- Mándi, Y. et al. (1975). “Efficient curing of an *Escherichia coli* F-prime plasmid by phenothiazines”. In: *Genetical Research* 26.1, pp. 109–111. ISSN: 14695073. DOI: [10.1017/S0016672300015895](https://doi.org/10.1017/S0016672300015895).
- Manion, R. E. et al. (1969). “Retardation of the Emergence of Isoniazid-Resistant *Mycobacteria* by Phenothiazines and Quinacrine”. In: *Proceedings of the Society for Experimental Biology and Medicine* 130.1, pp. 206–209. ISSN: 15353699. DOI: [10.3181/00379727-130-33522](https://doi.org/10.3181/00379727-130-33522).
- Manson, M. D. et al. (1977). “A protonmotive force drives bacterial flagella”. In: *Proceedings of the National Academy of Sciences of the United States of America* 74.7, pp. 3060–3064. ISSN: 00278424. DOI: [10.1073/pnas.74.7.3060](https://doi.org/10.1073/pnas.74.7.3060).
- Marcusson, L. L. et al. (2009). “Interplay in the Selection of Fluoroquinolone Resistance and Bacterial Fitness”. In: *PLoS Pathogens* 5.8. Ed. by B. R. Levin, e1000541. ISSN: 1553-7374. DOI: [10.1371/journal.ppat.1000541](https://doi.org/10.1371/journal.ppat.1000541).

- Markham, P. N. et al. (1999). “Multiple novel inhibitors of the NorA multidrug transporter of *Staphylococcus aureus*”. In: *Antimicrobial Agents and Chemotherapy* 43.10, pp. 2404–2408. ISSN: 00664804. DOI: [10.1128/aac.43.10.2404](https://doi.org/10.1128/aac.43.10.2404).
- Marquez, B. (2005). “Bacterial efflux systems and efflux pumps inhibitors”. In: *Biochimie* 87.12, pp. 1137–1147. ISSN: 61831638. DOI: [10.1016/j.biochi.2005.04.012](https://doi.org/10.1016/j.biochi.2005.04.012).
- Martin, R. G., Rosner, J. L., et al. (1995). “Binding of purified multiple antibiotic-resistance repressor protein (MarR) to *mar* operator sequences”. In: *Biochemistry* 92, pp. 5456–5460.
- Martin, R. G., Jair, K. W., et al. (1996). “Autoactivation of the *marRAB* multiple antibiotic resistance operon by the *marA* transcriptional activator in *Escherichia coli*”. In: *Journal of Bacteriology* 178.8, pp. 2216–2223. ISSN: 00219193. DOI: [10.1128/jb.178.8.2216-2223.1996](https://doi.org/10.1128/jb.178.8.2216-2223.1996).
- Martinez, J. L. et al. (2000). “Mutation frequencies and antibiotic resistance”. In: *Antimicrobial Agents and Chemotherapy* 44.7, pp. 1771–1777. ISSN: 00664804. DOI: [10.1128/AAC.44.7.1771-1777.2000](https://doi.org/10.1128/AAC.44.7.1771-1777.2000).
- Martínez, L. C. et al. (2014). “*In silico* identification and experimental characterization of regulatory elements controlling the expression of the *Salmonella csrB* and *csrC* genes”. In: *Journal of Bacteriology* 196.2, pp. 325–336. ISSN: 00219193. DOI: [10.1128/JB.00806-13](https://doi.org/10.1128/JB.00806-13).
- Martins, A. et al. (2011). “Role of calcium in the efflux system of *Escherichia coli*”. In: *International Journal of Antimicrobial Agents* 37.5, pp. 410–414. ISSN: 09248579. DOI: [10.1016/j.ijantimicag.2011.01.010](https://doi.org/10.1016/j.ijantimicag.2011.01.010).
- Mathieu, A. et al. (2016). “Discovery and Function of a General Core Hormetic Stress Response in *E. coli* Induced by Sublethal Concentrations of Antibiotics”. In: *Cell Reports* 17.1, pp. 46–57. ISSN: 22111247. DOI: [10.1016/j.celrep.2016.09.001](https://doi.org/10.1016/j.celrep.2016.09.001).
- Matsunaga, Y. et al. (2018). “Energetics and conformational pathways of functional rotation in the multidrug transporter AcrB”. In: *eLife* 7.e31715.

- Matter, H. et al. (2009). “Evidence for C-Cl/C-Br... π interactions as an important contribution to protein-ligand binding affinity”. In: *Angewandte Chemie - International Edition* 48.16, pp. 2911–2916. ISSN: 14337851. DOI: [10.1002/anie.200806219](https://doi.org/10.1002/anie.200806219).
- May, K. L. et al. (2017). “Making a membrane on the other side of the wall”. In: *Biochimica et Biophysica Acta - Molecular and Cell Biology of Lipids* 1862.11, pp. 1386–1393. ISSN: 18792618. DOI: [10.1016/j.bbalip.2016.10.004](https://doi.org/10.1016/j.bbalip.2016.10.004).
- Mazumder, R. et al. (2001). “Trifluoperazine: a broad spectrum bactericide especially active on *staphylococci* and *vibrios*”. eng. In: *Int J Antimicrob Agents* 18.4, pp. 403–406. ISSN: 0924-8579 (Print)0924-8579.
- Mazzariol, A. et al. (2000). “High-level fluoroquinolone-resistant clinical isolates of *Escherichia coli* overproduce multidrug efflux protein AcrA.” In: *Antimicrobial agents and chemotherapy* 44.12, pp. 3441–3. ISSN: 0066-4804. DOI: [10.1128/aac.44.12.3441-3443.2000](https://doi.org/10.1128/aac.44.12.3441-3443.2000).
- Mcmurry, L. M. et al. (2013). “Amino acid residues involved in inactivation of the *Escherichia coli* multidrug resistance repressor MarR by salicylate, 2,4-dinitrophenol, and plumbagin”. In: *FEMS Microbiology Letters* 349.1, pp. 16–24. ISSN: 03781097. DOI: [10.1111/1574-6968.12291](https://doi.org/10.1111/1574-6968.12291).
- Mechler, L., Bonetti, E. J., et al. (2016). “Daptomycin tolerance in the *Staphylococcus aureus* *pitA6* mutant is due to upregulation of the *dlt* operon”. In: *Antimicrobial Agents and Chemotherapy* 60.5, pp. 2684–2691. ISSN: 10986596. DOI: [10.1128/AAC.03022-15](https://doi.org/10.1128/AAC.03022-15).
- Mechler, L., Herbig, A., et al. (2015). “A novel point mutation promotes growth phase-dependent daptomycin tolerance in *Staphylococcus aureus*”. In: *Antimicrobial Agents and Chemotherapy* 59.9, pp. 5366–5376. ISSN: 10986596. DOI: [10.1128/AAC.00643-15](https://doi.org/10.1128/AAC.00643-15).
- Meddows, T. R. et al. (2005). “RecN protein and transcription factor DksA combine to promote faithful recombinational repair of DNA double-strand breaks”. In: *Molecular*

- Microbiology* 57.1, pp. 97–110. ISSN: 0950382X. DOI: [10.1111/j.1365-2958.2005.04677.x](https://doi.org/10.1111/j.1365-2958.2005.04677.x).
- Melnyk, A. H. et al. (2015). “The fitness costs of antibiotic resistance mutations”. In: *Evolutionary Applications* 8.3, pp. 273–283. ISSN: 17524571. DOI: [10.1111/eva.12196](https://doi.org/10.1111/eva.12196).
- Mikolosko, J. et al. (2006). “Conformational flexibility in the multidrug efflux system protein AcrA”. In: *Structure* 14.3, pp. 577–587. ISSN: 09692126. DOI: [10.1016/j.str.2005.11.015](https://doi.org/10.1016/j.str.2005.11.015).
- Miller, J. H. (1996). “Spontaneous mutators in bacteria: insights into pathways of mutagenesis and repair.” In: *Annual Review of Microbiology* 50.625, pp. 625–643.
- Misra, R. et al. (2015). “Importance of real-time assays to distinguish multidrug efflux pump-inhibiting and outer membrane-destabilizing activities in *Escherichia coli*”. In: *Journal of Bacteriology* 197.15, pp. 2479–2488. ISSN: 10985530. DOI: [10.1128/JB.02456-14](https://doi.org/10.1128/JB.02456-14).
- Missiakas, D. et al. (1997). “Modulation of the *Escherichia coli* $\sigma(E)$ (RpoE) heat-shock transcription-factor activity by the RseA, RseB and RseC proteins”. In: *Molecular Microbiology* 24.2, pp. 355–371. ISSN: 0950382X. DOI: [10.1046/j.1365-2958.1997.3601713.x](https://doi.org/10.1046/j.1365-2958.1997.3601713.x).
- Miticka, H. et al. (2003). “Transcriptional analysis of the *rpoE* gene encoding extracytoplasmic stress response sigma factor E in *Salmonella enterica* serovar Typhimurium”. In: *FEMS Microbiology Letters* 226.2, pp. 307–314. ISSN: 03781097. DOI: [10.1016/S0378-1097\(03\)00600-1](https://doi.org/10.1016/S0378-1097(03)00600-1).
- Moreno, A. J. et al. (2015). “Measuring mitochondrial membrane potential with a tetraphenylphosphonium-selective electrode”. In: *Current Protocols in Toxicology* 2015, pp. 25.5.1–25.5.16. ISSN: 19349262. DOI: [10.1002/0471140856.tx2505s65](https://doi.org/10.1002/0471140856.tx2505s65).
- Morgan, E. et al. (2004). “Identification of host-specific colonization factors of *Salmonella enterica* serovar Typhimurium”. In: *Molecular Microbiology* 54.4, pp. 994–1010. ISSN: 0950382X. DOI: [10.1111/j.1365-2958.2004.04323.x](https://doi.org/10.1111/j.1365-2958.2004.04323.x).

- Mortimer, P. G. et al. (1993). “The accumulation of five antibacterial agents in porin-deficient mutants of *Escherichia coli*.” In: *The Journal of antimicrobial chemotherapy* 32.2, pp. 195–213. ISSN: 0305-7453. DOI: [10.1093/jac/32.2.195](https://doi.org/10.1093/jac/32.2.195).
- Mowla, R. et al. (2018). “Kinetic analysis of the inhibition of the drug efflux protein AcrB using surface plasmon resonance”. In: *Biochimica et Biophysica Acta - Biomembranes* 1860.4, pp. 878–886. ISSN: 18792642. DOI: [10.1016/j.bbamem.2017.08.024](https://doi.org/10.1016/j.bbamem.2017.08.024).
- Muheim, C. et al. (2017). “Increasing the permeability of *Escherichia coli* using MAC13243”. In: *Scientific Reports* 7.1, pp. 1–11. ISSN: 20452322. DOI: [10.1038/s41598-017-17772-6](https://doi.org/10.1038/s41598-017-17772-6).
- Munita, J. M. et al. (2016). “Mechanisms of Antibiotic Resistance”. eng. In: *Microbiol Spectr* 4.2, pp. 1–37. ISSN: 2165-0497 (Electronic). DOI: [10.1128/microbiolspec.VMBF-0016-2015](https://doi.org/10.1128/microbiolspec.VMBF-0016-2015).
- Murakami, S., Nakashima, R., Yamashita, E., Matsumoto, T., et al. (2006). “Crystal structures of a multidrug transporter reveal a functionally rotating mechanism”. In: *Nature* 443.7108, pp. 173–179. ISSN: 14764687. DOI: [10.1038/nature05076](https://doi.org/10.1038/nature05076).
- Murakami, S., Nakashima, R., Yamashita, E., and Yamaguchi, A. (2002). “Crystal structure of bacterial multidrug efflux transporter AcrB”. In: *Nature* 419.6907, pp. 587–593. ISSN: 00280836. DOI: [10.1038/nature01050](https://doi.org/10.1038/nature01050).
- Murínová, S. et al. (2014). “Response Mechanisms of Bacterial Degraders to Environmental Contaminants on the Level of Cell Walls and Cytoplasmic Membrane”. In: *International Journal of Microbiology* 2014. DOI: [10.1155/2014/873081](https://doi.org/10.1155/2014/873081).
- Nagano, K. et al. (2009). “Kinetic behavior of the major multidrug efflux pump AcrB of *Escherichia coli*”. In: *Proceedings of the National Academy of Sciences of the United States of America* 106.14, pp. 5854–5858. ISSN: 00278424. DOI: [10.1073/pnas.0901695106](https://doi.org/10.1073/pnas.0901695106).
- Nakamura, S. et al. (1989). “*gyrA* and *gyrB* mutations in quinolone-resistant strains of *Escherichia coli*”. In: *Antimicrobial Agents and Chemotherapy* 33.2, pp. 254–255. ISSN: 00664804. DOI: [10.1128/AAC.33.2.254](https://doi.org/10.1128/AAC.33.2.254).

- Nakashima, R., Sakurai, K., Yamasaki, S., Hayashi, K., et al. (2013). “Structural basis for the inhibition of bacterial multidrug exporters”. In: *Nature* 500.7460, pp. 102–106. ISSN: 00280836. DOI: [10.1038/nature12300](https://doi.org/10.1038/nature12300).
- Nakashima, R., Sakurai, K., Yamasaki, S., Nishino, K., et al. (2011). “Structures of the multidrug exporter AcrB reveal a proximal multisite drug-binding pocket”. In: *Nature* 480.7378, pp. 565–569. ISSN: 00280836. DOI: [10.1038/nature10641](https://doi.org/10.1038/nature10641).
- Narimisa, N. et al. (2020). “Effects of sub-inhibitory concentrations of antibiotics and oxidative stress on the expression of type II toxin-antitoxin system genes in *Klebsiella pneumoniae*”. In: *Journal of Global Antimicrobial Resistance* 21, pp. 51–56. ISSN: 22137173. DOI: [10.1016/j.jgar.2019.09.005](https://doi.org/10.1016/j.jgar.2019.09.005).
- Nehme, H. et al. (2018). “Antibacterial activity of antipsychotic agents, their association with lipid nanocapsules and its impact on the properties of the nanocarriers and on antibacterial activity”. eng. In: *PLoS One* 13.1, e0189950. ISSN: 1932-6203. DOI: [10.1371/journal.pone.0189950](https://doi.org/10.1371/journal.pone.0189950).
- Ng, E. Y. et al. (1994). “Quinolone resistance mediated by *norA*: physiologic characterization and relationship to *flqB*, a quinolone resistance locus on the *Staphylococcus aureus* chromosome.” In: *Antimicrobial agents and chemotherapy* 38.6, pp. 1345–55. ISSN: 0066-4804. DOI: [10.1128/aac.38.6.1345](https://doi.org/10.1128/aac.38.6.1345).
- Nguyen, S. T. et al. (2015). “Structure-activity relationships of a novel pyranopyridine series of Gram-negative bacterial efflux pump inhibitors”. In: *Bioorganic and Medicinal Chemistry* 23.9, pp. 2024–2034. ISSN: 14643391. DOI: [10.1016/j.bmc.2015.03.016](https://doi.org/10.1016/j.bmc.2015.03.016).
- Nikaido, E., Yamaguchi, A., et al. (2008). “AcrAB Multidrug Efflux Pump Regulation in *Salmonella enterica* serovar Typhimurium by RamA in Response to Environmental Signals”. In: *J Biol Chem* 283.35, pp. 24245–53. DOI: [10.1074/jbc.M804544200](https://doi.org/10.1074/jbc.M804544200).

- Nikaido, H., Basina, M., et al. (1998). "Multidrug efflux pump AcrAB of *Salmonella typhimurium* excretes only those beta-lactam antibiotics containing lipophilic side chains." In: *Journal of bacteriology* 180.17, pp. 4686–92. ISSN: 0021-9193.
- Nikaido, H. (2003). "Molecular Basis of Bacterial Outer Membrane Permeability Revisited". In: *Microbiology and Molecular Biology Reviews* 67.4, pp. 593–656. ISSN: 1092-2172. DOI: [10.1128/mmbr.67.4.593-656.2003](https://doi.org/10.1128/mmbr.67.4.593-656.2003).
- Nikaido, H. (1996). "Multidrug efflux pumps of gram-negative bacteria". In: *Journal of Bacteriology* 178.20, pp. 5853–5859. ISSN: 00219193. DOI: [10.1128/jb.178.20.5853-5859.1996](https://doi.org/10.1128/jb.178.20.5853-5859.1996).
- Nikaido, H. and Takatsuka, Y. (2009). "Mechanisms of RND multidrug efflux pumps". In: *Biochimica et Biophysica Acta - Proteins and Proteomics* 1794.5, pp. 769–781. ISSN: 15709639. DOI: [10.1016/j.bbapap.2008.10.004](https://doi.org/10.1016/j.bbapap.2008.10.004).
- Norrande, J. et al. (1983). "Construction of improved M13 vectors using oligodeoxynucleotide-directed mutagenesis". In: *Gene* 26.1, pp. 101–106. ISSN: 03781119. DOI: [10.1016/0378-1119\(83\)90040-9](https://doi.org/10.1016/0378-1119(83)90040-9).
- Notka, F. et al. (2002). "A C-terminal 18 amino acid deletion in MarR in a clinical isolate of *Escherichia coli* reduces MarR binding properties and increases the MIC of ciprofloxacin". In: *Journal of Antimicrobial Chemotherapy* 49.1, pp. 41–47. ISSN: 03057453. DOI: [10.1093/jac/49.1.41](https://doi.org/10.1093/jac/49.1.41).
- Nunoshima, T. et al. (1992). "Two-stage control of an oxidative stress regulon: The *Escherichia coli* SoxR protein triggers redox-inducible expression of the *soxS* regulatory gene". In: *Journal of Bacteriology* 174.19, pp. 6054–6060. ISSN: 00219193. DOI: [10.1128/jb.174.19.6054-6060.1992](https://doi.org/10.1128/jb.174.19.6054-6060.1992).
- O'Neill, A. J. et al. (2004). "Comparison of assays for detection of agents causing membrane damage in *Staphylococcus aureus*". In: *Journal of Antimicrobial Chemotherapy* 54.6, pp. 1127–1129.

- O'Neill, J. (2016). "Tackling drug-resistant infections globally: final report and recommendations". In: *The Review on Antimicrobial Resistance* 5, p. 84. ISSN: 0042-9686. DOI: [10.1016/j.jpha.2015.11.005](https://doi.org/10.1016/j.jpha.2015.11.005).
- O'Rourke, A. et al. (2020). "Mechanism-of-action classification of antibiotics by global transcriptome profiling". In: *Antimicrobial Agents and Chemotherapy* 64.3. ISSN: 10986596. DOI: [10.1128/AAC.01207-19](https://doi.org/10.1128/AAC.01207-19).
- Olson, E. R. (1993). "Influence of pH on bacterial gene expression". In: *Molecular Microbiology* 8.1, pp. 5–14. ISSN: 0950-382X. DOI: [10.1111/j.1365-2958.1993.tb01198.x](https://doi.org/10.1111/j.1365-2958.1993.tb01198.x).
- Opperman, T. J., Kwasny, S. M., et al. (2014). "Characterization of a novel pyranopyridine inhibitor of the AcrAB efflux pump of *Escherichia coli*". In: *Antimicrobial Agents and Chemotherapy* 58.2, pp. 722–733. ISSN: 00664804. DOI: [10.1128/AAC.01866-13](https://doi.org/10.1128/AAC.01866-13).
- Opperman, T. J. and Nguyen, S. T. (2015). "Recent advances toward a molecular mechanism of efflux pump inhibition". In: *Frontiers in Microbiology* 6.421, pp. 1–16. ISSN: 1664302X. DOI: [10.3389/fmicb.2015.00421](https://doi.org/10.3389/fmicb.2015.00421).
- Ouabdesselam, S. et al. (1995). "Detection of *gyrA* and *gyrB* mutations in quinolone-resistant clinical isolates of *Escherichia coli* by single-strand conformational polymorphism analysis and determination of levels of resistance conferred by two different single *gyrA* mutations". In: *Antimicrobial Agents and Chemotherapy* 39.8, pp. 1667–1670. ISSN: 00664804. DOI: [10.1128/AAC.39.8.1667](https://doi.org/10.1128/AAC.39.8.1667).
- Paixão, L. et al. (2009). "Fluorometric determination of ethidium bromide efflux kinetics in *Escherichia coli*". In: *Journal of Biological Engineering* 3, p. 18. ISSN: 17541611. DOI: [10.1186/1754-1611-3-18](https://doi.org/10.1186/1754-1611-3-18).
- Parker, C. T. et al. (1992). "Role of the *rfaG* and *rfaP* genes in determining the lipopolysaccharide core structure and cell surface properties of *Escherichia coli* K-12." In: *Journal of bacteriology* 174.8, pp. 2525–38. ISSN: 0021-9193. DOI: [10.1128/jb.174.8.2525-2538.1992](https://doi.org/10.1128/jb.174.8.2525-2538.1992).

- Paulsen, I. T. et al. (1996). “Proton-dependent multidrug efflux systems”. In: *Microbiological Reviews* 60.4, pp. 575–608. ISSN: 01460749. DOI: [10.1128/mmbr.60.4.575-608.1996](https://doi.org/10.1128/mmbr.60.4.575-608.1996).
- Perera, I. C. et al. (2010). “Molecular mechanisms of ligand-mediated attenuation of DNA binding by MarR family transcriptional regulators”. In: *Journal of Molecular Cell Biology* 2.5, pp. 243–254. ISSN: 16742788. DOI: [10.1093/jmcb/mjq021](https://doi.org/10.1093/jmcb/mjq021).
- Pérez, A. et al. (2012). “Effect of transcriptional activators SoxS, RobA, and RamA on expression of multidrug efflux pump AcrAB-TolC in *Enterobacter cloacae*”. In: *Antimicrobial Agents and Chemotherapy* 56.12, pp. 6256–6266. ISSN: 00664804. DOI: [10.1128/AAC.01085-12](https://doi.org/10.1128/AAC.01085-12).
- Pernestig, A. K. et al. (2001). “Identification of UvrY as the cognate response regulator for the BarA sensor kinase in *Escherichia coli*”. In: *Journal of Biological Chemistry* 276.1, pp. 225–231. ISSN: 00219258. DOI: [10.1074/jbc.M001550200](https://doi.org/10.1074/jbc.M001550200).
- Perron, G. G. et al. (2010). “Hypermutable and compensatory adaptation in antibiotic-resistant bacteria”. In: *American Naturalist* 176.3, pp. 303–311. ISSN: 00030147. DOI: [10.1086/655217](https://doi.org/10.1086/655217).
- Pfaffl, M. W. (2001). “A new mathematical model for relative quantification in real-time RT-PCR”. In: *Nucleic Acids Research* 29.9, 45e–45. ISSN: 1362-4962. DOI: [10.1093/nar/29.9.e45](https://doi.org/10.1093/nar/29.9.e45).
- Picksley, S. M. et al. (1984). “Repair of DNA double-strand breaks in *Escherichia coli* K12 requires a functional recN product”. In: *MGG Molecular & General Genetics* 195.1-2, pp. 267–274. ISSN: 00268925. DOI: [10.1007/BF00332758](https://doi.org/10.1007/BF00332758).
- Piddock, L. J. et al. (2000). “Evidence for an efflux pump mediating multiple antibiotic resistance in *Salmonella enterica* serovar Typhimurium.” In: *Antimicrobial agents and chemotherapy* 44.11, pp. 3118–21. ISSN: 0066-4804. DOI: [10.1128/aac.44.11.3118-3121.2000](https://doi.org/10.1128/aac.44.11.3118-3121.2000).
- Piddock, L. J. V. (2012). “The crisis of no new antibiotics-what is the way forward?” In: 12.3, pp. 249–253. ISSN: 14733099. DOI: [10.1016/S1473-3099\(11\)70316-4](https://doi.org/10.1016/S1473-3099(11)70316-4).

- Piddock, L. J. (2002). “Fluoroquinolone resistance in *Salmonella* serovars isolated from humans and food animals”. In: *FEMS Microbiology Reviews* 26.1, pp. 3–16. ISSN: 0168-6445. DOI: [10.1111/j.1574-6976.2002.tb00596.x](https://doi.org/10.1111/j.1574-6976.2002.tb00596.x).
- Pinzi, L. et al. (2019). “Molecular docking: Shifting paradigms in drug discovery”. In: *International Journal of Molecular Sciences* 20.18. ISSN: 14220067. DOI: [10.3390/ijms20184331](https://doi.org/10.3390/ijms20184331).
- Plenge-Tellechea, F. et al. (2018). “Chlorpromazine and dimethyl sulfoxide modulate the catalytic activity of the plasma membrane Ca²⁺-ATPase from human erythrocyte”. In: *Journal of Bioenergetics and Biomembranes* 50.1, pp. 59–69. ISSN: 15736881. DOI: [10.1007/s10863-017-9741-9](https://doi.org/10.1007/s10863-017-9741-9).
- Pohlhaus, J. R. et al. (2005). “Norfloxacin-induced DNA gyrase cleavage complexes block *Escherichia coli* replication forks, causing double-stranded breaks *in vivo*”. In: *Molecular Microbiology* 56.6, pp. 1416–1429. ISSN: 0950382X. DOI: [10.1111/j.1365-2958.2005.04638.x](https://doi.org/10.1111/j.1365-2958.2005.04638.x).
- Pope, C. F. et al. (2008). “A practical guide to measuring mutation rates in antibiotic resistance”. In: *Antimicrobial Agents and Chemotherapy* 52.4, pp. 1209–1214. ISSN: 00664804. DOI: [10.1128/AAC.01152-07](https://doi.org/10.1128/AAC.01152-07).
- Pos, K. M. (2009). “Drug transport mechanism of the AcrB efflux pump”. In: *Biochimica et Biophysica Acta - Proteins and Proteomics* 1794.5, pp. 782–793. ISSN: 15709639. DOI: [10.1016/j.bbapap.2008.12.015](https://doi.org/10.1016/j.bbapap.2008.12.015).
- Potts, A. H., Guo, Y., et al. (2019). “Role of CsrA in stress responses and metabolism important for *Salmonella* virulence revealed by integrated transcriptomics”. In: *PLoS ONE* 14.1. ISSN: 19326203. DOI: [10.1371/journal.pone.0211430](https://doi.org/10.1371/journal.pone.0211430).
- Potts, A. H., Vakulskas, C. A., et al. (2017). “Global role of the bacterial post-transcriptional regulator CsrA revealed by integrated transcriptomics”. In: *Nature Communications* 8.1. ISSN: 20411723. DOI: [10.1038/s41467-017-01613-1](https://doi.org/10.1038/s41467-017-01613-1).

- Prajapat, M. K. et al. (2015). “Control of MarRAB operon in *Escherichia coli* via autoactivation and autorepression”. In: *Biophysical Journal* 109.7, pp. 1497–1508. ISSN: 15420086. DOI: [10.1016/j.bpj.2015.08.017](https://doi.org/10.1016/j.bpj.2015.08.017).
- Price, N. L. et al. (2009). “Characterization of the Cpx regulon in *Escherichia coli* strain MC4100”. In: *Journal of Bacteriology* 191.6, pp. 1798–1815. ISSN: 00219193. DOI: [10.1128/JB.00798-08](https://doi.org/10.1128/JB.00798-08).
- Qin, T. T. et al. (2015). *SOS response and its regulation on the fluoroquinolone resistance*. DOI: [10.3978/j.issn.2305-5839.2015.12.09](https://doi.org/10.3978/j.issn.2305-5839.2015.12.09).
- Raetz, C. R. H. et al. (2002). “Lipopolysaccharide Endotoxins”. In: *Annual Review of Biochemistry* 71.1, pp. 635–700. ISSN: 0066-4154. DOI: [10.1146/annurev.biochem.71.110601.135414](https://doi.org/10.1146/annurev.biochem.71.110601.135414).
- Raina, S. et al. (1995). “The *rpoE* gene encoding the σ^E (σ^{24}) heat shock sigma factor of *Escherichia coli*.” In: *The EMBO Journal* 14.5, pp. 1043–1055. ISSN: 02614189. DOI: [10.1002/j.1460-2075.1995.tb07085.x](https://doi.org/10.1002/j.1460-2075.1995.tb07085.x).
- Raivio, T. L. and Silhavy, T. J. (2001). “Periplasmic stress and ECF sigma factors”. In: *Annual Review of Microbiology* 55, pp. 591–624. ISSN: 00664227. DOI: [10.1146/annurev.micro.55.1.591](https://doi.org/10.1146/annurev.micro.55.1.591).
- Raivio, T. L., Popkin, D. L., et al. (1999). “The Cpx envelope stress response is controlled by amplification and feedback inhibition”. In: *Journal of Bacteriology* 181.17, pp. 5263–5272. ISSN: 00219193. DOI: [10.1128/jb.181.17.5263-5272.1999](https://doi.org/10.1128/jb.181.17.5263-5272.1999).
- Ramaswamy, V. K. et al. (2017). “Molecular Rationale behind the Differential Substrate Specificity of Bacterial RND Multi-Drug Transporters”. In: *Scientific Reports* 7.1. ISSN: 20452322. DOI: [10.1038/s41598-017-08747-8](https://doi.org/10.1038/s41598-017-08747-8).
- Ramirez, M. S. et al. (2010). “Aminoglycoside modifying enzymes.” In: *Drug resistance updates : reviews and commentaries in antimicrobial and anticancer chemotherapy* 13.6, pp. 151–71. ISSN: 1532-2084. DOI: [10.1016/j.drug.2010.08.003](https://doi.org/10.1016/j.drug.2010.08.003).

- Rampioni, G. et al. (2017). “Effect of efflux pump inhibition on *Pseudomonas aeruginosa* transcriptome and virulence”. In: *Sci Rep* 7.11392.
- Randall, L. P. et al. (2005). “Detection of Mutations in *Salmonella* Enterica *gyrA*, *gyrB*, *parC* and *parE* Genes by Denaturing High Performance Liquid Chromatography (DHPLC) Using Standard HPLC Instrumentation”. In: *J Antimicrob Chemother* 56.4, pp. 619–623.
- Reens, A. L. et al. (2018). “A cell-based infection assay identifies efflux pump modulators that reduce bacterial intracellular load”. In: *PLoS Pathogens* 14.6, e1007115. ISSN: 15537374. DOI: [10.1371/journal.ppat.1007115](https://doi.org/10.1371/journal.ppat.1007115).
- Reyes, E. D. et al. (2010). “RecN is a cohesin-like protein that stimulates intermolecular DNA interactions *in vitro*”. In: *Journal of Biological Chemistry* 285.22, pp. 16521–16529. ISSN: 00219258. DOI: [10.1074/jbc.M110.119164](https://doi.org/10.1074/jbc.M110.119164).
- Rgen, J. et al. (2011). “Efflux inhibition by selective serotonin reuptake inhibitors in *Escherichia coli*”. In: *J Antimicrob Chemother* 66.9, pp. 2057–60. DOI: [10.1093/jac/dkr258](https://doi.org/10.1093/jac/dkr258).
- Ricci, V., Blair, J. M. A., et al. (2014). “RamA, which controls expression of the MDR efflux pump AcrAB-TolC, is regulated by the Lon protease”. eng. In: *J Antimicrob Chemother* 69.3, pp. 643–650. ISSN: 0305-7453 (Print)1460-2091 (Electronic). DOI: [10.1093/jac/dkt432](https://doi.org/10.1093/jac/dkt432).
- Ricci, V., Attah, V., et al. (2017). “CsrA maximizes expression of the AcrAB multidrug resistance transporter”. In: *Nucleic Acids Research* 45.22, pp. 12798–12807. ISSN: 13624962. DOI: [10.1093/nar/gkx929](https://doi.org/10.1093/nar/gkx929).
- Ricci, V., Busby, S. J., et al. (2012). “Regulation of RamA by RamR in *Salmonella enterica* serovar Typhimurium: Isolation of a RamR superrepressor”. In: *Antimicrobial Agents and Chemotherapy* 56.11, pp. 6037–6040. ISSN: 00664804. DOI: [10.1128/AAC.01320-12](https://doi.org/10.1128/AAC.01320-12).

- Ricci, V., Tzakas, P., et al. (2006). “Ciprofloxacin-resistant *Salmonella enterica* serovar typhimurium strains are difficult to select in the absence of AcrB and TolC”. In: *Antimicrobial Agents and Chemotherapy* 50.1, pp. 38–42. ISSN: 00664804. DOI: [10.1128/AAC.50.1.38-42.2006](https://doi.org/10.1128/AAC.50.1.38-42.2006).
- Roe, A. J. et al. (1998). “Perturbation of anion balance during inhibition of growth of *Escherichia coli* by weak acids”. In: *Journal of Bacteriology* 180.4, pp. 767–772. ISSN: 00219193. DOI: [10.1128/jb.180.4.767-772.1998](https://doi.org/10.1128/jb.180.4.767-772.1998).
- Romeo, T. et al. (2013). “Post-transcriptional regulation on a global scale: Form and function of Csr/Rsm systems”. In: *Environmental Microbiology* 15.2, pp. 313–324. ISSN: 14622912. DOI: [10.1111/j.1462-2920.2012.02794.x](https://doi.org/10.1111/j.1462-2920.2012.02794.x).
- Rosche, W. A. et al. (2000). “Determining mutation rates in bacterial populations”. In: *Methods* 20.1, pp. 4–17. ISSN: 10462023. DOI: [10.1006/meth.1999.0901](https://doi.org/10.1006/meth.1999.0901).
- Rosenberg, E. Y., Bertenthal, D., et al. (2003). “Bile salts and fatty acids induce the expression of *Escherichia coli* AcrAB multidrug efflux pump through their interaction with Rob regulatory protein”. In: *Molecular Microbiology* 48.6, pp. 1609–1619. ISSN: 0950382X. DOI: [10.1046/j.1365-2958.2003.03531.x](https://doi.org/10.1046/j.1365-2958.2003.03531.x).
- Rosenberg, H., Gerdes, R. G., et al. (1977). “Two systems for the uptake of phosphate in *Escherichia coli*.” In: *Journal of Bacteriology* 131.2, pp. 505–511. ISSN: 00219193. DOI: [10.1128/jb.131.2.505-511.1977](https://doi.org/10.1128/jb.131.2.505-511.1977).
- Rossiter, A. E. et al. (2011). “The essential β -barrel assembly machinery complex components *bamd* and *bama* are required for autotransporter biogenesis”. In: *Journal of Bacteriology* 193.16, pp. 4250–4253. ISSN: 00219193. DOI: [10.1128/JB.00192-11](https://doi.org/10.1128/JB.00192-11).
- Rouviere, P. E. et al. (1995). “*rpoE*, the gene encoding the second heat-shock sigma factor, $\sigma(E)$, in *Escherichia coli*”. In: *EMBO Journal* 14.5, pp. 1032–1042. ISSN: 02614189. DOI: [10.1002/j.1460-2075.1995.tb07084.x](https://doi.org/10.1002/j.1460-2075.1995.tb07084.x).

- Rozen, D. E. et al. (2007). “Fitness costs of fluoroquinolone resistance in *Streptococcus pneumoniae*”. In: *Antimicrobial Agents and Chemotherapy* 51.2, pp. 412–416. ISSN: 00664804. DOI: [10.1128/AAC.01161-06](https://doi.org/10.1128/AAC.01161-06).
- Ruggerone, P. et al. (2013). “Molecular dynamics computer simulations of multidrug RND efflux pumps”. In: 5.6, e201302008. ISSN: 20010370. DOI: [10.5936/csbj.201302008](https://doi.org/10.5936/csbj.201302008).
- Ruiz, C. et al. (2014). “Regulation of *acrAB* expression by cellular metabolites in *Escherichia coli*”. In: *Journal of Antimicrobial Chemotherapy* 69.2, pp. 390–399. ISSN: 0305-7453. DOI: [10.1093/jac/dkt352](https://doi.org/10.1093/jac/dkt352).
- Saier, M. H., Tam, R., et al. (1994). “Two novel families of bacterial membrane proteins concerned with nodulation, cell division and transport”. In: *Molecular Microbiology* 11.5, pp. 841–847. ISSN: 13652958. DOI: [10.1111/j.1365-2958.1994.tb00362.x](https://doi.org/10.1111/j.1365-2958.1994.tb00362.x).
- Saier, M. H., Paulsen, I. T., et al. (1998). “Evolutionary origins of multidrug and drug-specific efflux pumps in bacteria”. In: *FASEB Journal* 12.3, pp. 265–274. ISSN: 08926638. DOI: [10.1096/fasebj.12.3.265](https://doi.org/10.1096/fasebj.12.3.265).
- Salmaso, V. et al. (2018). “Bridging molecular docking to molecular dynamics in exploring ligand-protein recognition process: An overview”. In: *Frontiers in Pharmacology* 9.AUG, p. 923. ISSN: 16639812. DOI: [10.3389/fphar.2018.00923](https://doi.org/10.3389/fphar.2018.00923).
- Sanchez, H., Kidane, D., et al. (2006). “Recruitment of *Bacillus subtilis* RecN to DNA double-strand breaks in the absence of DNA end processing”. In: *Journal of Bacteriology* 188.2, pp. 353–360. ISSN: 00219193. DOI: [10.1128/JB.188.2.353-360.2006](https://doi.org/10.1128/JB.188.2.353-360.2006).
- Sanchez, L., Pan, W., et al. (1997). “The *acrAB* homolog of *Haemophilus influenzae* codes for a functional multidrug efflux pump”. In: *Journal of Bacteriology* 179.21, pp. 6855–6857. ISSN: 00219193. DOI: [10.1128/jb.179.21.6855-6857.1997](https://doi.org/10.1128/jb.179.21.6855-6857.1997).
- Santos, L. H. et al. (2019). “Integrating molecular docking and molecular dynamics simulations”. In: *Methods in Molecular Biology* 2053, pp. 13–34. ISSN: 19406029. DOI: [10.1007/978-1-4939-9752-7_2](https://doi.org/10.1007/978-1-4939-9752-7_2).

- Sanz-García, F. et al. (2018). “Mutation-driven evolution of *Pseudomonas aeruginosa* in the presence of either ceftazidime or ceftazidime-avibactam”. In: *Antimicrobial Agents and Chemotherapy* 62.10. ISSN: 10986596. DOI: [10.1128/AAC.01379-18](https://doi.org/10.1128/AAC.01379-18).
- Sargentini, N. J. et al. (1986). “Quantitation of the involvement of the *recA*, *recB*, *recC*, *recF*, *recJ*, *recN*, *IexA*, *radA*, *radB*, *uvrD*, and *umuC* genes in the repair of X-ray-induced DNA double-strand breaks in *Escherichia coli*”. In: *Radiation Research* 107.1, pp. 58–72. ISSN: 00337587. DOI: [10.2307/3576850](https://doi.org/10.2307/3576850).
- Schuster, S., Vavra, M., et al. (2016). “Evidence of a Substrate-Discriminating Entrance Channel in the Lower Porter Domain of the Multidrug Resistance Efflux Pump AcrB”. In: *Antimicrobial Agents and Chemotherapy* 60.7, pp. 4315–4323.
- Schuster, S., Bohnert, J. A., et al. (2019). “Proof of an outer membrane target of the efflux inhibitor phe-Arg- β -naphthylamide from random mutagenesis”. In: *Molecules* 24.3. ISSN: 14203049. DOI: [10.3390/molecules24030470](https://doi.org/10.3390/molecules24030470).
- Schuster, S., Kohler, S., et al. (2014). “Random mutagenesis of the multidrug transporter AcrB from *Escherichia coli* for identification of putative target residues of efflux pump inhibitors”. In: *Antimicrobial Agents and Chemotherapy* 58.11, pp. 6870–6878. ISSN: 10986596. DOI: [10.1128/AAC.03775-14](https://doi.org/10.1128/AAC.03775-14).
- Seeger, M. A. et al. (2006). “Structural asymmetry of AcrB trimer suggests a peristaltic pump mechanism”. In: *Science* 313.5791, pp. 1295–1298. ISSN: 00368075. DOI: [10.1126/science.1131542](https://doi.org/10.1126/science.1131542).
- Seigel, G. M. et al. (2004). “High-throughput microtiter assay for Hoechst 33342 dye uptake”. In: *Cytotechnology* 45.3, pp. 155–160. ISSN: 09209069. DOI: [10.1007/s10616-004-7256-9](https://doi.org/10.1007/s10616-004-7256-9).
- Sennhauser, G. et al. (2007). “Drug export pathway of multidrug exporter AcrB revealed by DARPin inhibitors”. In: *PLoS Biology* 5.1, pp. 0106–0113. ISSN: 15449173. DOI: [10.1371/journal.pbio.0050007](https://doi.org/10.1371/journal.pbio.0050007).

- Seoane, A. S. et al. (1995). “Characterization of MarR, the repressor of the multiple antibiotic resistance (*mar*) operon in *Escherichia coli*”. In: *Journal of Bacteriology* 177.12, pp. 3414–3419. ISSN: 00219193. DOI: [10.1128/jb.177.12.3414-3419.1995](https://doi.org/10.1128/jb.177.12.3414-3419.1995).
- Seukep, A. J. et al. (2020). “Plant-derived secondary metabolites as the main source of efflux pump inhibitors and methods for identification”. In: *Journal of Pharmaceutical Analysis*. ISSN: 20951779. DOI: [10.1016/j.jpha.2019.11.002](https://doi.org/10.1016/j.jpha.2019.11.002).
- Shapiro, R. S. (2015). “Antimicrobial-Induced DNA Damage and Genomic Instability in Microbial Pathogens”. In: *PLOS Pathogens* 11.3. Ed. by D. A. Hogan, e1004678. ISSN: 1553-7374. DOI: [10.1371/journal.ppat.1004678](https://doi.org/10.1371/journal.ppat.1004678).
- Sharma, A., Gupta, V. K., et al. (2019). “Efflux pump inhibitors for bacterial pathogens: From bench to bedside”. In: *Indian Journal of Medical Research* 149.2, pp. 129–145. ISSN: 09715916. DOI: [10.4103/ijmr.IJMR_2079_17](https://doi.org/10.4103/ijmr.IJMR_2079_17).
- Sharma, D., Patel, R. P., et al. (2017). “Interplay of the quality of ciprofloxacin and antibiotic resistance in developing countries”. In: *Frontiers in Pharmacology* 8.AUG, p. 546. ISSN: 16639812. DOI: [10.3389/fphar.2017.00546](https://doi.org/10.3389/fphar.2017.00546).
- Sharma, S., Kaur, H., et al. (2006). “Cell cycle effects of the phenothiazines: trifluoperazine and chlorpromazine in *Candida albicans*”. In: *FEMS Microbiology Letters* 199.2, pp. 185–190. DOI: [10.1111/j.1574-6968.2001.tb10672.x](https://doi.org/10.1111/j.1574-6968.2001.tb10672.x).
- Shi, X. et al. (2019). “*In situ* structure and assembly of the multidrug efflux pump AcrAB-TolC”. In: *Nature Communications* 10.1. ISSN: 20411723. DOI: [10.1038/s41467-019-10512-6](https://doi.org/10.1038/s41467-019-10512-6).
- Silhavy, T. J., Kahne, D., et al. (2010). “The bacterial cell envelope.” In: *Cold Spring Harbor perspectives in biology* 2.5. ISSN: 19430264. DOI: [10.1101/cshperspect.a000414](https://doi.org/10.1101/cshperspect.a000414).
- Silhavy, T. J. and Malinverni, J. C. (2011). “Assembly of Outer Membrane β -Barrel Proteins: the Bam Complex”. In: *EcoSal Plus* 4.2. ISSN: 2324-6200. DOI: [10.1128/ecosalplus.4.3.8](https://doi.org/10.1128/ecosalplus.4.3.8).

- Sjuts, H. et al. (2016). “Molecular basis for inhibition of AcrB multidrug efflux pump by novel and powerful pyranopyridine derivatives”. en. In: *Proceedings of the National Academy of Sciences of the United States of America* 113.13, pp. 3509–3514. DOI: [10.1073/pnas.1602472113](https://doi.org/10.1073/pnas.1602472113).
- Sklar, J. G. et al. (2007). “Lipoprotein SmpA is a component of the YaeT complex that assembles outer membrane proteins in *Escherichia coli*”. In: *Proceedings of the National Academy of Sciences of the United States of America* 104.15, pp. 6400–6405. ISSN: 00278424. DOI: [10.1073/pnas.0701579104](https://doi.org/10.1073/pnas.0701579104).
- Sorlozano, A. et al. (2007). “Contribution of a new mutation in *parE* to quinolone resistance in extended-spectrum- β -lactamase-producing *Escherichia coli* isolates”. In: *Journal of Clinical Microbiology* 45.8, pp. 2740–2742. ISSN: 00951137. DOI: [10.1128/JCM.01093-07](https://doi.org/10.1128/JCM.01093-07).
- Spengler, G. et al. (2003). “Enhancement of plasmid curing by 9-aminoacridine and two phenothiazines in the presence of proton pump inhibitor 1-(2-benzoxazolyl)-3,3,3-trifluoro-2-propanone”. eng. In: *Int J Antimicrob Agents* 22.3, pp. 223–227. ISSN: 0924-8579 (Print)0924-8579.
- Spindler, E. C. et al. (2011). “Deciphering the mode of action of the synthetic antimicrobial peptide bac8c”. In: *Antimicrobial Agents and Chemotherapy* 55.4, pp. 1706–1716. ISSN: 00664804. DOI: [10.1128/AAC.01053-10](https://doi.org/10.1128/AAC.01053-10).
- Spöring, I. et al. (2018). “Regulation of flagellum biosynthesis in response to cell envelope stress in *salmonella enterica* serovar Typhimurium”. In: *mBio* 9.3. ISSN: 21507511. DOI: [10.1128/mBio.00736-17](https://doi.org/10.1128/mBio.00736-17).
- Srikumar, R. et al. (2000). “Influence of mutations in the *mexR* repressor gene on expression of the MexA-MexB-OprM multidrug efflux system of *Pseudomonas aeruginosa*”. In: *Journal of Bacteriology* 182.5, pp. 1410–1414. ISSN: 00219193. DOI: [10.1128/JB.182.5.1410-1414.2000](https://doi.org/10.1128/JB.182.5.1410-1414.2000).

- Stock, J. B. et al. (1977). “Periplasmic space in *Salmonella typhimurium* and *Escherichia coli*”. In: *J Biol Chem*, pp. 7850–7861.
- Strahl, H. et al. (2010). “Membrane potential is important for bacterial cell division”. In: *Proceedings of the National Academy of Sciences of the United States of America* 107.27, pp. 12281–12286. ISSN: 00278424. DOI: [10.1073/pnas.1005485107](https://doi.org/10.1073/pnas.1005485107).
- Su, C. C., Li, M., et al. (2006). “Conformation of the AcrB multidrug efflux pump in mutants of the putative proton relay pathway”. In: *Journal of Bacteriology* 188.20, pp. 7290–7296. ISSN: 00219193. DOI: [10.1128/JB.00684-06](https://doi.org/10.1128/JB.00684-06).
- Su, C. C., Rutherford, D. J., et al. (2007). “Characterization of the multidrug efflux regulator AcrR from *Escherichia coli*”. In: *Biochemical and Biophysical Research Communications* 361.1, pp. 85–90. ISSN: 0006291X. DOI: [10.1016/j.bbrc.2007.06.175](https://doi.org/10.1016/j.bbrc.2007.06.175).
- Su, L.-H., Chiu, C.-H., et al. (2004). “Antimicrobial Resistance in Nontyphoid *Salmonella* Serotypes: A Global Challenge”. In: *Clinical Infectious Diseases* 39.4, pp. 546–551. ISSN: 1058-4838. DOI: [10.1086/422726](https://doi.org/10.1086/422726).
- Suzuki, K. et al. (2002). “Regulatory circuitry of the CsrA/CsrB and BarA/UvrY systems of *Escherichia coli*”. In: *Journal of Bacteriology* 184.18, pp. 5130–5140. ISSN: 00219193. DOI: [10.1128/JB.184.18.5130-5140.2002](https://doi.org/10.1128/JB.184.18.5130-5140.2002).
- Takatsuka, Y., Chen, C., et al. (2010). “Mechanism of recognition of compounds of diverse structures by the multidrug efflux pump AcrB of *Escherichia coli*”. In: *Proceedings of the National Academy of Sciences of the United States of America* 107.15, pp. 6559–6565. ISSN: 00278424. DOI: [10.1073/pnas.1001460107](https://doi.org/10.1073/pnas.1001460107).
- Takatsuka, Y. and Nikaido, H. (2006). “Threonine-978 in the transmembrane segment of the multidrug efflux pump AcrB of *Escherichia coli* is crucial for drug transport as a probable component of the proton relay network”. In: *Journal of Bacteriology* 188.20, pp. 7284–7289. ISSN: 00219193. DOI: [10.1128/JB.00683-06](https://doi.org/10.1128/JB.00683-06).

- Tam, H. K. et al. (2020). “Binding and Transport of Carboxylated Drugs by the Multidrug Transporter AcrB”. In: *Journal of Molecular Biology* 432.4, pp. 861–877. ISSN: 10898638. DOI: [10.1016/j.jmb.2019.12.025](https://doi.org/10.1016/j.jmb.2019.12.025).
- Tanaka, K. J. et al. (2018). “Selective substrate uptake: The role of ATP-binding cassette (ABC) importers in pathogenesis”. In: *Biochimica et Biophysica Acta - Biomembranes* 1860.4, pp. 868–877. ISSN: 18792642. DOI: [10.1016/j.bbamem.2017.08.011](https://doi.org/10.1016/j.bbamem.2017.08.011).
- Taurand, G. (2000). “Phenothiazine and Derivatives”. en. In: *Ullmans Encyclopedia of Industrial Chemistry* 26, pp. 601–615. ISSN: 9783527306732. DOI: [10.1002/14356007.a19_387](https://doi.org/10.1002/14356007.a19_387).
- Te Dorsthorst, D. T. et al. (2002). “Comparison of fractional inhibitory concentration index with response surface modeling for characterization of *in vitro* interaction of antifungals against itraconazole-susceptible and -resistant *Aspergillus fumigatus* isolates”. In: *Antimicrobial Agents and Chemotherapy* 46.3, pp. 702–707. ISSN: 00664804. DOI: [10.1128/AAC.46.3.702-707.2002](https://doi.org/10.1128/AAC.46.3.702-707.2002).
- Tenover, F. C. (2006). “Mechanisms of antimicrobial resistance in bacteria”. In: *American Journal of Infection Control* 34.5 SUPPL. S3–S10. ISSN: 01966553. DOI: [10.1016/j.ajic.2006.05.219](https://doi.org/10.1016/j.ajic.2006.05.219).
- Teplitski, M. et al. (2003). “Pathways Leading from BarA/SirA to Motility and Virulence Gene Expression in *Salmonella*”. In: *Journal of Bacteriology* 185.24, pp. 7257–7265. ISSN: 00219193. DOI: [10.1128/JB.185.24.7257-7265.2003](https://doi.org/10.1128/JB.185.24.7257-7265.2003).
- Thede, G. L. et al. (2011). “Structure of the periplasmic stress response protein CpxP”. In: *Journal of Bacteriology* 193.9, pp. 2149–2157. ISSN: 00219193. DOI: [10.1128/JB.01296-10](https://doi.org/10.1128/JB.01296-10).
- Tikhonova, E. B. et al. (2004). “AcrA, AcrB, and TolC of *Escherichia coli* form a stable intermembrane multidrug efflux complex”. In: *Journal of Biological Chemistry* 279.31, pp. 32116–32124. ISSN: 00219258. DOI: [10.1074/jbc.M402230200](https://doi.org/10.1074/jbc.M402230200).

- Tillotson, G. S. (1996). “Quinolones: Structure-activity relationships and future predictions”. In: *Journal of Medical Microbiology* 44.5, pp. 320–324. DOI: [10.1099/00222615-44-5-320](https://doi.org/10.1099/00222615-44-5-320).
- Tillotson, G. S. (2017). “Keeping the faith—reporting on antimicrobial resistance in an era of fake news”. In: *The Lancet Infectious Diseases* 17.5, pp. 473–474. ISSN: 14744457. DOI: [10.1016/S1473-3099\(17\)30181-0](https://doi.org/10.1016/S1473-3099(17)30181-0).
- Tiwari, S. et al. (2017). “Two-Component Signal Transduction Systems of Pathogenic Bacteria As Targets for Antimicrobial Therapy: An Overview”. In: *Frontiers in Microbiology* 8.OCT, p. 1878. ISSN: 1664-302X. DOI: [10.3389/fmicb.2017.01878](https://doi.org/10.3389/fmicb.2017.01878).
- Touzé, T. et al. (2004). “Interactions underlying assembly of the *Escherichia coli* AcrAB-TolC multidrug efflux system”. In: *Molecular Microbiology* 53.2, pp. 697–706. ISSN: 0950382X. DOI: [10.1111/j.1365-2958.2004.04158.x](https://doi.org/10.1111/j.1365-2958.2004.04158.x).
- Tseng, T. T. et al. (1999). “The RND permease superfamily: An ancient, ubiquitous and diverse family that includes human disease and development proteins”. In: *Journal of Molecular Microbiology and Biotechnology* 1.1, pp. 107–125. ISSN: 14641801.
- Uranga, L. A. et al. (2017). “The cohesin-like RecN protein stimulates RecA-mediated recombinational repair of DNA double-strand breaks”. In: *Nature Communications* 8.1, pp. 1–11. ISSN: 20411723. DOI: [10.1038/ncomms15282](https://doi.org/10.1038/ncomms15282).
- Urios, A. et al. (1991). “Influence of *recA* mutations on *gyrA* dependent quinolone resistance”. In: *Biochimie* 73.4, pp. 519–521. ISSN: 61831638. DOI: [10.1016/0300-9084\(91\)90123-I](https://doi.org/10.1016/0300-9084(91)90123-I).
- Vaara, M. (1992). “Agents that increase the permeability of the outer membrane”. In: *Microbiol Rev* 56.3, pp. 395–411.
- Vakulskas, C. A. et al. (2015). “Regulation of Bacterial Virulence by Csr (Rsm) Systems”. In: *Microbiology and Molecular Biology Reviews* 79.2, pp. 193–224. ISSN: 1092-2172. DOI: [10.1128/mmb.00052-14](https://doi.org/10.1128/mmb.00052-14).

- Van Amsterdam, K. et al. (2005). “A *Helicobacter pylori* TolC efflux pump confers resistance to metronidazole”. In: *Antimicrobial Agents and Chemotherapy* 49.4, pp. 1477–1482. ISSN: 00664804. DOI: [10.1128/AAC.49.4.1477-1482.2005](https://doi.org/10.1128/AAC.49.4.1477-1482.2005).
- Van Dijk, T. et al. (2017). “Mutation supply and the repeatability of selection for antibiotic resistance”. In: *Physical Biology* 14.5. ISSN: 14783975. DOI: [10.1088/1478-3975/aa7f36](https://doi.org/10.1088/1478-3975/aa7f36). arXiv: [1703.01896](https://arxiv.org/abs/1703.01896).
- Varga, B. et al. (2017). “Possible Biological and Clinical Applications of Phenothiazines”. eng. In: *Anticancer Res* 37.11, pp. 5983–5993. ISSN: 0250-7005. DOI: [10.21873/anticancerres.12045](https://doi.org/10.21873/anticancerres.12045).
- Vargiu, A. V., Ruggerone, P., et al. (2014). “Molecular Mechanism of MBX2319 Inhibition of *Escherichia coli* AcrB Multidrug Efflux Pump and Comparison with Other Inhibitors”. eng. In: *Antimicrob Agents Chemother* 58.10, pp. 6224–6234. ISSN: 0066-4804 (Print)1098-6596 (Electronic). DOI: [10.1128/aac.03283-14](https://doi.org/10.1128/aac.03283-14).
- Vargiu, A. V., Collu, F., et al. (2011). “Effect of the F610A mutation on substrate extrusion in the AcrB transporter: Explanation and rationale by molecular dynamics simulations”. In: *Journal of the American Chemical Society* 133.28, pp. 10704–10707. ISSN: 00027863. DOI: [10.1021/ja202666x](https://doi.org/10.1021/ja202666x).
- Vargiu, A. V. and Nikaido, H. (2012). “Multidrug binding properties of the AcrB efflux pump characterized by molecular dynamics simulations”. In: *Proceedings of the National Academy of Sciences of the United States of America* 109.50, pp. 20637–20642. ISSN: 10916490. DOI: [10.1073/pnas.1218348109](https://doi.org/10.1073/pnas.1218348109).
- Vargiu, A. V., Ramaswamy, V. K., et al. (2018). “Computer simulations of the activity of RND efflux pumps”. In: *Research in Microbiology* 169.7-8, pp. 384–392. ISSN: 17697123. DOI: [10.1016/j.resmic.2017.12.001](https://doi.org/10.1016/j.resmic.2017.12.001).
- Venter, H. et al. (2015). “RND-type drug efflux pumps from Gram-negative bacteria: molecular mechanism and inhibition”. eng. In: *Front Microbiol* 6.377, pp. 1–11. ISSN: 1664-302X (Print)1664-302x. DOI: [10.3389/fmicb.2015.00377](https://doi.org/10.3389/fmicb.2015.00377).

- Vila, J. et al. (1996). “Detection of mutations in *parC* in quinolone-resistant clinical isolates of *Escherichia coli*”. In: *Antimicrobial Agents and Chemotherapy* 40.2, pp. 491–493. ISSN: 00664804. DOI: [10.1128/aac.40.2.491](https://doi.org/10.1128/aac.40.2.491).
- Vinué, L. et al. (2016). “Mutations that enhance the ciprofloxacin resistance of *Escherichia coli* with *qnrA1*”. In: *Antimicrobial Agents and Chemotherapy* 60.3, pp. 1537–1545. ISSN: 10986596. DOI: [10.1128/AAC.02167-15](https://doi.org/10.1128/AAC.02167-15).
- Viola, G. et al. (2003). “Photosensitization of DNA strand breaks by three phenothiazine derivatives”. In: *Chemical Research in Toxicology* 16.5, pp. 644–651. ISSN: 0893228X. DOI: [10.1021/tx025680t](https://doi.org/10.1021/tx025680t).
- Viveiros, M. et al. (2005). “Inducement and reversal of tetracycline resistance in *Escherichia coli* K-12 and expression of proton gradient-dependent multidrug efflux pump genes”. In: *Antimicrobial Agents and Chemotherapy* 49.8, pp. 3578–3582. ISSN: 00664804. DOI: [10.1128/AAC.49.8.3578-3582.2005](https://doi.org/10.1128/AAC.49.8.3578-3582.2005).
- Wang, H., Dzik-Fox, J. L., et al. (2001). “Genetic characterization of highly fluoroquinolone-resistant clinical *Escherichia coli* strains from China: Role of *acrR* mutations”. In: *Antimicrobial Agents and Chemotherapy* 45.5, pp. 1515–1521. ISSN: 00664804. DOI: [10.1128/AAC.45.5.1515-1521.2001](https://doi.org/10.1128/AAC.45.5.1515-1521.2001).
- Wang, Z., Fan, G., et al. (2017). “An allosteric transport mechanism for the AcrAB-TolC multidrug efflux pump”. In: *eLife* 6. ISSN: 2050084X. DOI: [10.7554/eLife.24905](https://doi.org/10.7554/eLife.24905).
- Wang-Kan, X. et al. (2017). “Lack of AcrB Efflux Function Confers Loss of Virulence on *Salmonella enterica* Serovar Typhimurium”. eng. In: *mBio* 8.4, e00968–17. ISSN: 2150-7511 (Electronic). DOI: [10.1128/mBio.00968-17](https://doi.org/10.1128/mBio.00968-17).
- Warr, A. R. et al. (2019). “Protease-deficient SOS constitutive cells have RecN-dependent cell division phenotypes”. In: *Molecular Microbiology* 111.2, pp. 405–422. ISSN: 0950382X. DOI: [10.1111/mmi.14162](https://doi.org/10.1111/mmi.14162).

- Watanabe, R. et al. (2012). “Contributions of mutations in *acrR* and *marR* genes to organic solvent tolerance in *Escherichia coli*”. In: *AMB Express* 2.1, pp. 1–11. ISSN: 21910855. DOI: [10.1186/2191-0855-2-58](https://doi.org/10.1186/2191-0855-2-58).
- Webber, M., Bailey, A., et al. (2009). “The Global Consequence of Disruption of the AcrAB-TolC Efflux Pump in *Salmonella enterica* Includes Reduced Expression of SPI-1 and Other Attributes Required To Infect the Host”. In: *Journal of Bacteriology* 191.13, pp. 4276–85.
- Webber, M. A., Ricci, V., et al. (2013). “Clinically relevant mutant DNA gyrase alters supercoiling, changes the transcriptome, and confers multidrug resistance”. In: *mBio* 4.4. ISSN: 21507511. DOI: [10.1128/mBio.00273-13](https://doi.org/10.1128/mBio.00273-13).
- Whittle, E. E. et al. (2019). “Flow Cytometric Analysis of Efflux by Dye Accumulation”. In: *Frontiers in Microbiology* 10, p. 2319. ISSN: 1664-302X. DOI: [10.3389/fmicb.2019.02319](https://doi.org/10.3389/fmicb.2019.02319).
- Williams, R. J. et al. (1984). “Mechanisms of beta-lactam resistance in British isolates of *Pseudomonas aeruginosa*.” In: *Journal of medical microbiology* 17.3, pp. 283–93. ISSN: 0022-2615. DOI: [10.1099/00222615-17-3-283](https://doi.org/10.1099/00222615-17-3-283).
- Willsky, G. R. et al. (1980). “Characterization of two genetically separable inorganic phosphate transport systems in *Escherichia coli*”. In: *Journal of Bacteriology* 144.1, pp. 356–365. ISSN: 00219193. DOI: [10.1128/jb.144.1.356-365.1980](https://doi.org/10.1128/jb.144.1.356-365.1980).
- Wistrand-Yuen, E. et al. (2018). “Evolution of high-level resistance during low-level antibiotic exposure”. In: *Nature Communications* 9.1. ISSN: 20411723. DOI: [10.1038/s41467-018-04059-1](https://doi.org/10.1038/s41467-018-04059-1).
- Wray, C. et al. (1978). “Experimental *Salmonella* Typhimurium infection in calves.” In: *Research in Veterinary Science* 25.2, pp. 139–143. ISSN: 00345288. DOI: [10.1016/s0034-5288\(18\)32968-0](https://doi.org/10.1016/s0034-5288(18)32968-0).

- Wu, J. et al. (1991). “Two divergently transcribed genes, *soxR* and *soxS*, control a superoxide response regulon of *Escherichia coli*”. In: *Journal of Bacteriology* 173.9, pp. 2864–2871. ISSN: 00219193. DOI: [10.1128/jb.173.9.2864-2871.1991](https://doi.org/10.1128/jb.173.9.2864-2871.1991).
- Yamagishi, J.-i. et al. (1986). “Nalidixic acid-resistant mutations of the *gyrB* gene of *Escherichia coli*”. In: *Mol Gen Genet* 204, pp. 367–373.
- Yamasaki, S., Nakashima, R., et al. (2019). “Crystal structure of the multidrug resistance regulator RamR complexed with bile acids”. In: *Sci Rep* 9.177.
- Yamasaki, S., Fujioka, T., et al. (2016). “Phenotype microarray analysis of the drug efflux systems in *Salmonella enterica* serovar Typhimurium”. In: *Journal of Infection and Chemotherapy* 22.11, pp. 780–784. ISSN: 14377780. DOI: [10.1016/j.jiac.2016.03.015](https://doi.org/10.1016/j.jiac.2016.03.015).
- Yamasaki, S., Nikaido, E., et al. (2013a). “The crystal structure of multidrug-resistance regulator RamR with multiple drugs”. en. In: *Nature Communications* 4. ISSN: 2041-1723. DOI: [doi:10.1038/ncomms3078](https://doi.org/10.1038/ncomms3078).
- Yamasaki, S., Nikaido, E., et al. (2013b). “The crystal structure of multidrug-resistance regulator RamR with multiple drugs”. In: *Nature Communications* 4.1, pp. 1–7. ISSN: 20411723. DOI: [10.1038/ncomms3078](https://doi.org/10.1038/ncomms3078).
- Yang, N. J. et al. (2015). “Getting across the cell membrane: an overview for small molecules, peptides, and proteins”. In: 1266, pp. 29–53. ISSN: 19406029. DOI: [10.1007/978-1-4939-2272-7_3](https://doi.org/10.1007/978-1-4939-2272-7_3).
- Yasir, M. et al. (2019). “Comparative mode of action of the antimicrobial peptide melimine and its derivative Mel4 against *Pseudomonas aeruginosa*”. In: *Scientific Reports* 9.1. ISSN: 20452322. DOI: [10.1038/s41598-019-42440-2](https://doi.org/10.1038/s41598-019-42440-2).
- Ying, Y. C. et al. (2007). “Synergistic interaction between phenothiazines and antimicrobial agents against *Burkholderia pseudomallei*”. In: *Antimicrobial Agents and Chemotherapy* 51.2, pp. 623–630. ISSN: 00664804. DOI: [10.1128/AAC.01033-06](https://doi.org/10.1128/AAC.01033-06).
- Yoshida, K. ichi et al. (2007). “MexAB-OprM specific efflux pump inhibitors in *Pseudomonas aeruginosa*. Part 7: Highly soluble and *in vivo* active quaternary ammonium analogue

- D13-9001, a potential preclinical candidate”. In: *Bioorganic and Medicinal Chemistry* 15.22, pp. 7087–7097. ISSN: 09680896. DOI: [10.1016/j.bmc.2007.07.039](https://doi.org/10.1016/j.bmc.2007.07.039).
- Youssef, M. M. et al. (2014). “Genetic characterization of *Escherichia coli* RecN protein as a member of SMC family of proteins”. In: *Arabian Journal of Chemistry* 7.3, pp. 327–334. ISSN: 18785352. DOI: [10.1016/j.arabjc.2011.02.001](https://doi.org/10.1016/j.arabjc.2011.02.001).
- Yu, E. W. et al. (2003). “Structural basis of multiple drug-binding capacity of the AcrB multidrug efflux pump”. In: *Science* 300.5621, pp. 976–980. ISSN: 00368075. DOI: [10.1126/science.1083137](https://doi.org/10.1126/science.1083137).
- Zere, T. R. et al. (2015). “Genomic Targets and Features of BarA-UvrY (-SirA) Signal Transduction Systems”. In: *PLOS ONE* 10.12. Ed. by I. Biswas, e0145035. ISSN: 1932-6203. DOI: [10.1371/journal.pone.0145035](https://doi.org/10.1371/journal.pone.0145035).
- Zgurskaya, H. I. et al. (1999). “AcrA is a highly asymmetric protein capable of spanning the periplasm”. In: *Journal of Molecular Biology* 285.1, pp. 409–420. ISSN: 00222836. DOI: [10.1006/jmbi.1998.2313](https://doi.org/10.1006/jmbi.1998.2313).
- Zgurskaya, H. I. et al. (2000). “Multidrug resistance mechanisms: Drug efflux across two membranes”. In: *Molecular Microbiology* 37.2, pp. 219–225. ISSN: 0950382X. DOI: [10.1046/j.1365-2958.2000.01926.x](https://doi.org/10.1046/j.1365-2958.2000.01926.x).
- Zhang, X. et al. (2017). “Energy coupling mechanisms of AcrB-like RND transporters”. In: *Biophys Rep* 3.4, pp. 73–84.
- Zilberstein, D., Agmon, V., et al. (1984). “*Escherichia coli* intracellular pH, membrane potential, and cell growth”. In: *Journal of Bacteriology* 158.1, pp. 246–252. ISSN: 00219193. DOI: [10.1128/jb.158.1.246-252.1984](https://doi.org/10.1128/jb.158.1.246-252.1984).
- Zilberstein, D., Liveanu, V., et al. (1990). “Tricyclic drugs reduce proton motive force in *leishmania donovani* promastigotes”. In: *Biochemical Pharmacology* 39.5, pp. 935–940. ISSN: 00062952. DOI: [10.1016/0006-2952\(90\)90210-C](https://doi.org/10.1016/0006-2952(90)90210-C).

Zwama, M. et al. (2018). “Multiple entry pathways within the efflux transporter AcrB contribute to multidrug recognition”. In: *Nature Communications* 9.1, pp. 1–9. ISSN: 20411723. DOI: [10.1038/s41467-017-02493-1](https://doi.org/10.1038/s41467-017-02493-1).